

FINAL REPORTGTI PROJECT NUMBER 20385

Plastic Pipe Failure, Risk, and Threat Analysis

DOT Project# 194

Contract Number: DTPH56-06-T-0004

Reporting Period:

May 1, 2006 through January 31, 2009

Report Issued:

March 31, 2009

Revised:

April 29, 2009

Revision No.:

01

Prepared For:Ms. Terri Binns
Senior Engineer
PHMSA
713-272-2825
Terri.J.Binns@dot.gov**Prepared By:**Gas Technology Institute
Ms. Julie Maupin
Dr. Michael Mamoun**Gas Technology Institute**1700 S. Mount Prospect Rd.
Des Plaines, Illinois 60018
www.gastechnology.org

This research was funded in part under the Department of Transportation, Pipeline and Hazardous Materials Safety Administration's Pipeline Safety Research and Development Program. The views and conclusions contained in this document are those of the authors and should not be interpreted as representing the official policies, either expressed or implied, of the Pipeline and Hazardous Materials Safety Administration, or the U.S. Government

Signature Page

<i>Print or typed First M. Last</i>	<i>Signature</i>	<i>Date</i>
AUTHOR:	Michael M. Mamoun	March 31, 2009
	<i>Title:</i> <u>Senior Institute Engineer</u>	
AUTHOR:	Julie K. Maupin	March 31, 2009
	<i>Title:</i> <u>Engineer</u>	
AUTHOR:	Michael J. Miller	March 31, 2009
	<i>Title:</i> <u>Engineer</u>	

Legal Notice

This information was prepared by Gas Technology Institute (“GTI”) for the U.S. Department of Transportation, Pipeline and Hazardous Materials Safety Administration (“DOT/PHMSA”) (Contract Number: DTPH56-06-T-0004).

Neither GTI, the members of GTI, the Sponsor(s), nor any person acting on behalf of any of them:

a. Makes any warranty or representation, express or implied with respect to the accuracy, completeness, or usefulness of the information contained in this report, or that the use of any information, apparatus, method, or process disclosed in this report may not infringe privately-owned rights. Inasmuch as this project is experimental in nature, the technical information, results, or conclusions cannot be predicted. Conclusions and analysis of results by GTI represent GTI's opinion based on inferences from measurements and empirical relationships, which inferences and assumptions are not infallible, and with respect to which competent specialists may differ.

b. Assumes any liability with respect to the use of, or for any and all damages resulting from the use of, any information, apparatus, method, or process disclosed in this report; any other use of, or reliance on, this report by any third party is at the third party's sole risk.

c. The results within this report relate only to the items tested.

Table of Contents

Signature Page	i
Legal Notice	ii
Table of Contents.....	iii
Table of Figures	xi
List of Tables.....	xxi
Abstract.....	1
Executive Summary	2
Introduction	3
Classification of Failures and Their Causes.....	6
Ductile Rupture Failure Mechanism	6
Slow Crack Growth Failure Mechanism	7
Rapid Crack Propagation (RCP) Failure Mechanism.....	8
Types of PE Failures	9
Project Structure	10
Literature Review on Severity and Frequency of Plastic Pipe Failures	11
DOT/PHMSA Natural Gas Distribution Incident Data Discussion	11
Severity of Failures	11
Frequency of Failures	19
Susceptibility of PE to Slow Crack Growth Failures.....	26
Objective	26
Types of PE Gas Pipe Materials in GTI Database.....	26
Detailed List of PE Resin and Pipe Manufacturers	26
Visual and Optical Examinations of Slow Crack Growth Failures.....	26
SCG Failures Due to Rock Impingement Loads	27
SCG Failures Due to Squeeze-Off Operations	30
Short-Term Laboratory Tests.....	33
Melt Index.....	33
ALDYL-A Melt Index and Density Data (1965 – 1992).....	33
Tensile Strength	35
Quick Burst.....	36
PENT.....	36
Bend Back.....	45

Bend-Back Test Conducted on a LDIW Material from February 1971	46
Bend-Back Test Conducted on a LDIW Material from March 1971	46
Bend-Back Tests Conducted on Non-LDIW Materials (1970, 1972-1993).....	47
Accelerated Long Term Hydrostatic Stress-Rupture (LTHS) Tests	52
Accelerated LTHS Tests with Secondary Stresses.....	52
Squeeze-Off	52
Rock Impingement	53
Bending	54
Transverse Deflections or Soil Loads	54
GTI Database on Accelerated LTHS Tests.....	55
Stresses that Drive Crack Initiation and Growth through Pipe Walls	56
Effects of Elevated Test Temperatures.....	58
Engineering Methods to Predict Life Expectancy	61
Original Bi-Directional Shift Functions Model.....	62
Modified Bi-Directional Shift Functions Equations	62
Original Three-Coefficient Rate Process Method.....	63
Modified Three-Coefficient Rate Process Method	63
Sample Set on the Predicted Remaining Life Expectancy.....	64
Secondary Stress Effects.....	66
Field Temperature Effects.....	67
Slow Crack Growth Conclusion	69
Root Cause Analysis of Field Failures	71
Failure Categories.....	71
Laboratory Field Failure Analysis Procedure	72
Impingement – #602533	72
Visual Examination.....	73
Density	77
Melt Flow.....	77
Thermal Analysis.....	78
Infrared Analysis	79
Conclusions.....	81
Research Approach	81
Material Failures	82
Tap Tee – #678156.....	82
Visual Examination.....	83

Density	88
Melt Flow.....	88
Thermal Analysis.....	88
Infrared Analysis	90
Conclusions.....	91
Impingement - #00590	92
Visual Examination.....	93
Density and Melt Flow.....	95
Conclusions.....	95
Impingement - #04020731	96
Visual Examination.....	97
External Loading - #26020806	98
Visual Examination.....	99
Tee Caps.....	101
Cap –#50020726.....	101
Visual Examination.....	102
Infrared Analysis	104
Differential Scanning Calorimetry.....	105
Thermogravimetric Analysis and Energy Dispersive X-ray	105
Conclusions.....	107
Cap - #20020447	108
Visual Examination.....	109
Cap - #21020739	110
Visual Examination.....	111
Cap - #22020733	112
Visual Examination.....	113
Cap - #23020464	114
Visual Examination.....	115
Cap - #24020499	116
Visual Examination.....	117
Caps - #25020718 and #49020718.....	118
Visual Examination.....	119
Cap - #31020649	120
Visual Examination.....	121
Thread Inserts	122

Service Tee Threads - #15020650.....	122
Visual Examination.....	122
Service Tee Threads - #29020510.....	124
Visual Examination.....	125
Socket Couplings	126
Socket Coupling - #30020542.....	126
Visual Examination.....	127
Socket Coupling - #35020485.....	128
Visual Examination.....	129
Socket Coupling - #39020605.....	131
Visual Examination.....	132
Socket Tees	133
Socket Tee - #19020414.....	133
Visual Examination.....	134
Socket Tee - #33020602.....	135
Visual Examination.....	136
Supplemental Inspection.....	136
Socket Tee - #34020623.....	137
Visual Examination.....	138
Supplemental Inspection.....	139
Procedural Failures.....	140
High Volume Tapping Tee - #00632	140
Visual Examination.....	141
Density	145
Melt Flow.....	145
Thermal Analysis.....	145
Infrared Analysis	148
Conclusions.....	151
Butt Fusions	152
Butt Fusion - #060204100.....	152
Visual Examination.....	153
Butt Fusion - #07020714.....	155
Visual Examination.....	156
Butt Fusion - #08020601	157
Visual Examination.....	158

Butt Fusion - #09020552.....	159
Visual Examination.....	160
Butt Fusion - #10020477.....	161
Visual Examination.....	162
Butt Fusion - #11020511.....	163
Visual Examination.....	164
Butt Fusion - #12020550.....	166
Visual Examination.....	167
Butt Fusion - #13020706.....	168
Visual Examination.....	169
Butt Fusion - #45020551.....	170
Visual Examination.....	171
Multiple Fusion Joints - #40020413.....	173
Visual Examination.....	174
Socket Couplings.....	176
Socket Coupling - #16020611.....	176
Visual Examination.....	177
Socket Coupling - #31020649.....	178
Visual Examination.....	179
Socket Tees.....	180
Socket Tee - #36020713.....	180
Visual Examination.....	181
Socket Tee - #47020565.....	182
Visual Examination.....	183
Squeeze-offs.....	185
Squeeze-Off - #02020717.....	185
Visual Examination.....	186
Squeeze-off - #03020647.....	187
Visual Examination.....	188
Squeeze-off - #05020548.....	189
Visual Examination.....	190
Tap Tees.....	192
Tap Tee - #28020502.....	192
Visual Examination.....	193
Tap Tee - #42020711.....	195

Visual Examination.....	196
Tap Tee - #43020555.....	198
Visual Examination.....	199
Tap Tee - #44020539.....	200
Visual Examination.....	201
Tap Tee – Socket Fusion - #32020543.....	202
Visual Examination.....	203
Transition Fitting.....	204
Transition Fitting - #18020538	204
Visual Examination.....	205
Quality Control Problems	206
3" Elbow - #675540	206
Visual Examination.....	207
Density	213
Melt Flow.....	214
Thermal Analysis- Pipe Wall	214
Thermal Analysis - Elbow.....	214
Infrared Analysis	217
Conclusions.....	220
¾" Valve – #642535	221
Visual Examination.....	222
Infrared Analysis and Hardness Testing	227
Conclusions.....	228
Miscellaneous Problems	229
Charred Pipe – #01020436	229
Visual Examination.....	230
Tap Tee – #642909.....	231
Visual Examination.....	232
Density	237
Melt Flow.....	237
Thermal Analysis.....	237
Infrared Analysis	239
Conclusions.....	241
Electrofusion Tee – #642430	242
Visual Examination.....	243

Thermal Analysis.....	243
Infrared Analysis	247
Conclusions.....	249
Material / Quality.....	250
Compression Fitting - #17020701	250
Visual Examination.....	251
Procedural / Material.....	252
Mechanical Fitting - #41020409	252
Visual Examination.....	253
Tap Tee - #27020640.....	254
Visual Examination.....	255
Bolt-on Tap Tee - #14020742	256
Visual Examination.....	257
Root Cause Failure Results	258
Characterizing the Resistance of PE to RCP through S-4 Testing	267
Rapid Crack Propagation.....	267
S-4 Background	270
Test Requirements.....	270
Full-Scale RCP Field Tests	270
S-4 Testing.....	271
ISO Specification (ISO 13477)	272
Initiation Tests.....	272
Critical Pressure Testing.....	273
Correlation of the S-4 Critical Pressure to the Full-Scale Field Test.....	273
Critical Temperature Testing.....	274
GTI S-4 Test Apparatus.....	275
Shaft, Anvil, Baffles and Pipe Assembly	275
External Containment Cage and Frame.....	278
Striking Blade Assembly	280
PE Materials Subjected to S-4 Test s	281
6 Inch MDPE – Critical Pressure and Critical Temperature	282
6” Inch HDPE Critical Pressure and Critical Temperature	287
6” PE100 Critical Pressure and Critical Temperature	292
8” MDPE Critical Pressure	297
8” PE100 Critical Pressure.....	300

12" MDPE Critical Pressure	303
RCP Results, Correlations, and Conclusions	306
Conclusion	307
Recommendations	308
References.....	309
List of Acronyms	313

Table of Figures

	Page
Figure 1. Percentage of Miles of Main, 1995	3
Figure 2. Percentage of Miles of Main, 2006	4
Figure 3. Percentage of Services, 1995.....	4
Figure 4. Percentage of Services, 2006.....	5
Figure 5. Comparison of Total Services, Plastic Services, and PE Services in 2005.....	5
Figure 6. Ductile Failure Resulting From a Quick Burst Test.....	6
Figure 7. Ductile Failure Resulting From a Quick Burst Test.....	7
Figure 8. SCG Failure Morphology	8
Figure 9. RCP Rupture in a PE Pipe Subjected To a Small-Scale Steady State (S-4) Test.....	8
Figure 10. Cost of damages categorized by cause from 1984 - March 2004	14
Figure 11. Cost of Outside Force Damages by Secondary Cause from 1984 - March 2004.....	14
Figure 12. Cost of Damages Categorized By Cause from March 2004 - 2006.....	15
Figure 13. Cost of Excavation Damages by Secondary Cause from March 2004 - 2006.....	15
Figure 14. Fatalities by Primary Cause As Reported From 1984 - March 2004	16
Figure 15. Fatalities by Primary Cause As Reported From March 2004 - 2006	17
Figure 16. Injuries by Primary Cause As Reported From 1984 - March 2004	18
Figure 17. Injuries by Primary Cause As Reported From March 2004 - 2006	18
Figure 18. Total Cost of Reported Incidents for Each Data Period.....	19
Figure 19. Frequency of Failures by Cause from 1984 - March 2004.....	20
Figure 20. Frequency of Failures by Cause from March 2004 - 2006.....	20
Figure 21. Frequency of Failures by Type of PE and Cause for 1984 - 2004.....	21
Figure 22. Frequency of Failures by Type of PE and Cause for 2004 - 2006.....	22
Figure 23. Frequency of Incidents by Manufacturer and Cause for 1984 - March 2004.....	23
Figure 24. Frequency of Incidents by Manufacturer and Cause for March 2004 - 2006.....	24
Figure 25. Frequency of Plastic Incidents by Time of Day from 1984 - March 2004	25
Figure 26. Frequency of Plastic Incidents by Time of Day from March 2004 – 2006.....	25
Figure 27. Pipe Exhibited Through Wall Axial Slit While Under Internal Pressure.....	27
Figure 28. Rock Impingement Failure	28
Figure 29. Off-Axis Slit Failure that Initiated on the ID Due to an Impinging Rock.....	28
Figure 30. Rock Impingement Failure Induced in Field Service	29
Figure 31. Micrograph of the SCG Fracture Surface of a Rock Impingement Failure	29

Figure 32. Failure of an Aldyl-A Pipe at Squeeze Ears.....	30
Figure 33. Inner Surface of an Aldyl-A Pipe Subjected to About 15% Squeeze	30
Figure 34. MDPE Pipe that Failed in Field Service Due to a Squeeze-Off	31
Figure 35. End View Depicting Large-Scale Deformations Due to a Squeeze-Off	31
Figure 36. Pipe ID with Axial Slit at the Ears of Pipe Shown in Figure 34	32
Figure 37. Schematic Illustration of the Rectangular PENT Test Specimen.....	37
Figure 38. Notched MDPE Test Specimens	37
Figure 39. Brittle SCG Failure of a PLEXCO MDPE 2406 PENT Test Specimen	38
Figure 40. Brittle SCG Failure of HDPE Performance Pipe PENT Test Specimen.....	39
Figure 41. Ring Sector Specimen Before and After the Bend Back Test	45
Figure 42. Bend-Back Test Exhibiting LDIW Surface Features	46
Figure 43. Bend-Back Test Exhibiting LDIW Surface Features	47
Figure 44. Bend Back Test of a 1970 Aldyl-A Material	47
Figure 45. Bend Back Test of a 1972 Aldyl-A Material (During and After).....	48
Figure 46. Bend Back Test of a 1973 Aldyl-A Material (During and After).....	48
Figure 47. Bend Back Test of a 1974 Aldyl-A Material	49
Figure 48. Bend Back Test of a 1976 Aldyl-A Material	49
Figure 49. Bend Back Test of a 1986 Aldyl-A Material	50
Figure 50. Bend Back Test of a 1991 Aldyl-A Material	50
Figure 51. Bend Back Test of a 1993 Aldyl-A Material	51
Figure 52. Double Bar Squeeze-Off Tool.....	52
Figure 53. Rock Impingement Loading Fixture	53
Figure 54. Indentation unto the Pipe Using Ball Bearing	53
Figure 55. Pipe Bending Fixture	54
Figure 56. PE Pipe Test Specimens Installed in Earth Load Fixtures	55
Figure 57. Circumferential Residual Stress Component as a Function of the Wall Depth.....	57
Figure 58. Effect of Test Temperature and Time on Residual Hoop Stress Component.....	58
Figure 59. Predicted Remaining Life Expectancy of an Older Aldyl-A Pipe.....	67
Figure 60. Predicted Remaining Life Expectancy as a Function of Temperature.....	68
Figure 61. As Received Sample with Attached 4" X 2" Electrofusion Tapping Tee	72
Figure 62. Slit Failure Growing Away From Impingement Point	73
Figure 63. View of the Slit from the Inner Wall.....	74
Figure 64. Pipe Was Force Fractured to Reveal the Fracture Faces.....	74
Figure 65. Close Up View of the Fracture Faces	75
Figure 66. Microscopy.....	76

Figure 67. Differential Scanning Calorimetry	78
Figure 68. Oxidative Induction Time	79
Figure 69. FT-IR Outer Wall.....	80
Figure 70. FT-IR Middle Wall	80
Figure 71. FT-IR Inner Wall	81
Figure 72. As Received Sample with Two Tees. Leak Occurred At Untapped Tee, Left.....	82
Figure 73. Untapped Tee with Circumferential Slit	82
Figure 74. Underwater Leak Test Revealing Leak Location	84
Figure 75. Sample Was Cut to Show Inner Pipe Wall	84
Figure 76. Close Up of the Circumferential Slit on the Inner Wall.....	85
Figure 77. Length of Fracture Faces Identified with Red Marker.....	85
Figure 78. Close up of the Fracture Face Away from the Tee	86
Figure 79. Close up of the Fracture Face towards the Tee with Area of Interest Identified.....	86
Figure 80. Microscopy of the Fracture Face Away From the Tee	87
Figure 81. Microscopy of the Fracture Face towards the Tee	87
Figure 82. Differential Scanning Calorimetry	89
Figure 83. Oxidative Induction Time	89
Figure 84. FT-IR Outer Wall.....	90
Figure 85. FT-IR Middle Wall	91
Figure 86. FT-IR Inner Wall	91
Figure 87. As Received Condition	92
Figure 88. Crack on Outer Wall	93
Figure 89. Close Up, Dimple and Crack	93
Figure 90. Crack As Seen On Inner Wall.....	94
Figure 91. Fracture Origin.....	94
Figure 92. Composite Photo, Fracture Surface - Outer Wall at Top	95
Figure 93. Bottom Side of as Received Sample	96
Figure 94. Axial Slit on Outer Wall	97
Figure 95. Axial Slit on Inner Pipe Wall.....	97
Figure 96. As Received Sample	98
Figure 97. Side and Bottom View of Sample	99
Figure 98. Slit on Outer Wall.....	100
Figure 99. Slit on Inner Wall.....	100
Figure 100. As Received Cap	101
Figure 101. Topside Fracture Surface	102

Figure 102. Bottom Side Fracture Surface	103
Figure 103. Cap Threads	103
Figure 104. Topside Fracture Surface	104
Figure 105. FT-IR Spectrum of the Cap Material	104
Figure 106. DSC Thermogram of the Cap Material	105
Figure 107. TGA Plot	106
Figure 108. EDX Spectrum of the Cap Material Ash	106
Figure 109. As Received Cap	108
Figure 110. Crack Seen Inside the Cap	109
Figure 111. As Received Cap	110
Figure 112. Soil on Interior Surface	111
Figure 113. As Received Cap	112
Figure 114. Dirty Interior Surface	113
Figure 115. As Received Cap	114
Figure 116. Cracked Cap with Wrench Marks	115
Figure 117. As Received Cap	116
Figure 118. Yellow Tee Visible Through the Crack	117
Figure 119. As Received Service Tee with Broken Cap	118
Figure 120. Fracture Surfaces of Cap	119
Figure 121. Fracture Surface of the Top of the Cap	119
Figure 122. As Received Cap	120
Figure 123. Cap, Underside Left and Topside Right	121
Figure 124. Internal Threads of the Saddle Tee	121
Figure 125. As Received Tee	122
Figure 126. Close-up View of Thread Insert	123
Figure 127. As Received Tee	124
Figure 128. Close up of Severed Insert	125
Figure 129. Cap with Insert Attached	125
Figure 130. As Received	126
Figure 131. Severed Coupling	127
Figure 132. Fracture Face	127
Figure 133. As Received Service Tee with Socket Coupling	128
Figure 134. Side View	129
Figure 135. Bottom View	129
Figure 136. 1 - 3/4" Circumferential Slit on Underside of Coupling	130

Figure 137. As Received Coupling	131
Figure 138. Crack in Pipe Wall on ID	132
Figure 139. Side View of Socket Fusion	132
Figure 140. As Received Socket Tee	133
Figure 141. Circumferential Slit in Fitting	134
Figure 142. As Received Socket Tee	135
Figure 143. Circumferential Slit in Socket	136
Figure 144. As Received Socket Tee	137
Figure 145. Crack on Socket Surface	138
Figure 146. Features on ID	138
Figure 147: Photograph of Tee Showing Location of Leak.....	139
Figure 148. Close-up of Pipe Section with Tee as Seen in the Field.....	140
Figure 149. Left Side with No Bead Rollback and Right Side with Uneven Bead Rollback.....	141
Figure 150. Close-up of Gap between Pipe Surface and Fitting.....	141
Figure 151. Pressure Test to Identify Leak Location	142
Figure 152. Pipe Segment Surface from Under the Tee on the Side Containing the Leak	143
Figure 153. Mating Surfaces of the Tee and Pipe	144
Figure 154. OIT and DSC – Outer Wall – Pipe	146
Figure 155. OIT and DSC – Middle Wall – Pipe	146
Figure 156. OIT and DSC – Inner Wall – Pipe.....	147
Figure 157. FT-IR - Outer Wall – Pipe	148
Figure 158. FT-IR - Middle Wall – Pipe.....	149
Figure 159. FT-IR - Inner Wall – Pipe	149
Figure 160. FT-IR – Good Fusion Area	150
Figure 161. FT-IR - Poor Fusion Area	150
Figure 162. As Received Butt Fusion	152
Figure 163. Side View of Butt Fusion.....	153
Figure 164. Fusion Faces	154
Figure 165. Inside Bead on One Side of Fusion	154
Figure 166. As Received Butt Fusion	155
Figure 167. Incomplete Bead Rollover.....	156
Figure 168. As Received Butt Fusion	157
Figure 169. Fusion Faces Showing Cold Fusion Area.....	158
Figure 170. As Received Butt Fusion	159
Figure 171. Uneven Rollback.....	160

Figure 172. Side of Bead	160
Figure 173. As Received.....	161
Figure 174. Area of Cold Fusion	162
Figure 175. Fusion Faces	162
Figure 176. As Received Butt Fusion	163
Figure 177. Leak Location at the Bead Weld.....	164
Figure 178. View down the Inside of the Pipe Section.....	164
Figure 179. Close-up of the Inner Weld Bead.....	165
Figure 180. As Received.....	166
Figure 181. Weld Separation along ~3" Arc Length.....	167
Figure 182. Uneven Beads	167
Figure 183. As Received.....	168
Figure 184. Fusion Faces	169
Figure 185. As Received 6" Butt Fusion	170
Figure 186. Fusion Face, Valve	171
Figure 187. Fusion Face, Pipe.....	172
Figure 188. As Received.....	173
Figure 189. Close Up View of Specimen	174
Figure 190. Misalignment and Poor Bead Rollover at the Reducing Coupling	175
Figure 191. Back to Back Couplings.....	175
Figure 192. As Received.....	176
Figure 193. Leak Location	177
Figure 194. As Received.....	178
Figure 195. End View of Pipe	179
Figure 196. Leak Location as Identified by Utility	179
Figure 197. As Received.....	180
Figure 198. Leak Location as Identified by Utility	181
Figure 199. End View on Leak Side.....	181
Figure 200. As Received Socket Tee	182
Figure 201. Radial Distortion	183
Figure 202. Leak at Pipe/Socket Interface.....	184
Figure 203. Close up of Pipe/Socket Interface	184
Figure 204. Top and Side View of as Received Squeeze-off	185
Figure 205. End View Showing Deformation	186
Figure 206. Slit as Viewed from Inner Wall.....	186

Figure 207. Top and Side View of as Received Sample.....	187
Figure 208. Dimpling and Buckling	188
Figure 209. Two of Three Squeeze Points Visible on the Inner Wall.....	188
Figure 210. As Received Squeeze-off Sample	189
Figure 211. Top and Sides of Squeeze Location	190
Figure 212. Cavity and Deformation on Inner Wall	191
Figure 213. As Received Tap Tee	192
Figure 214. Underside of the Pipe and Saddle	193
Figure 215. Side View of the Saddle.....	194
Figure 216. Leak Location	194
Figure 217. As Received Tap Tee	195
Figure 218. Backside of Saddle Tee.....	196
Figure 219. Close-up of Backside of Tee.....	197
Figure 220. Side of Tee	197
Figure 221. As Received Tap Tee	198
Figure 222. Saddle Face.....	199
Figure 223. Pipe Surface	199
Figure 224. As Received Tap Tee	200
Figure 225. Backside of Tee	201
Figure 226. As Received Tap Tee	202
Figure 227. Socket of Tee, Side View.....	203
Figure 228. Ductile Tearing.....	203
Figure 229. As Received.....	204
Figure 230. Side and Bottom View of Transition.....	205
Figure 231. As Received Sample - 3" Elbow	206
Figure 232. Leak Location As Identified By a Soap Solution	207
Figure 233. Cut Sample to Expose Inner Wall.....	208
Figure 234. Portion of Elbow Containing Leak.....	208
Figure 235. Inner Fusion Interface with Area of Observed Lack of Fusion	209
Figure 236. Fusion Interface	209
Figure 237. Force Fracture of the Sample, Showing Area of Observed Lack of Fusion.....	210
Figure 238. Fractured Sample with the Elbow Side, Top, and Pipe Side, Bottom.	210
Figure 239. Close up of the Fracture Faces with the Elbow Side on the Right.....	211
Figure 240. Fracture Face on the Elbow Side. Ductile Failure Region	211
Figure 241. Close up of the Fracture Face on the Pipe Side.....	212

Figure 242. Fracture Face on the Pipe Side with an Area of Interest Identified.....	212
Figure 243. Microscopy - Fracture Face of Elbow – Toward the Elbow Side	213
Figure 244. Microscopy – Fracture Face of Elbow – Toward the Pipe Side	213
Figure 245. Differential Scanning Calorimetry – Pipe	215
Figure 246. Oxidative Induction Time – Pipe	215
Figure 247. Differential Scanning Calorimetry - Elbow	216
Figure 248. Oxidative Induction Time - Elbow	216
Figure 249. FT-IR Outer Wall – Pipe	217
Figure 250. FT-IR Middle Wall – Pipe	218
Figure 251. FT-IR Inner Wall – Pipe	218
Figure 252. FT-IR - Outer Wall - Elbow	219
Figure 253. FT-IR - Middle Wall - Elbow	219
Figure 254. FT-IR - Inner Wall - Elbow	220
Figure 255. As Received Sample Shown Leaking from Under the Cap	221
Figure 256. Valve with Leak Pinpointed.....	222
Figure 257. Valve Was Halved to Help Expose O-Ring.....	223
Figure 258. Close up of the Core and Seal.....	223
Figure 259. Valve Core with Indexing Marks	224
Figure 260. Valve Core Removed from Housing	224
Figure 261. Valve Core. Lower O-Ring Bottom	225
Figure 262. O-Ring Damage. Upper O-Ring, Foreground. Lower O-Ring, Background.....	225
Figure 263. Imbedded Fragment Between Upper O-Ring and Core Land.	226
Figure 264. O-Ring Fragment Removed from the Upper O-ring Land Area.	226
Figure 265. Higher Magnification of Figure 264.....	227
Figure 266. FT-IR - Lower O-Ring Nitrile Rubber	227
Figure 267. FT-IR - Upper O-Ring Nitrile Rubber	228
Figure 268. As Received.....	229
Figure 269. Up Close View of Damaged Pipe Section	230
Figure 270. As Received Sample of a Leaking Tee.....	231
Figure 271. Circumferential Slit on the Backside of the Tee.....	231
Figure 272. Pipe Was Cut Away to Reveal the Inner Pipe Wall	233
Figure 273. Damage on the Inner Wall	233
Figure 274. Damage on the Inner Wall	234
Figure 275. Tee Separated from Pipe during Force Fracture	234
Figure 276. Fracture Face on the Pipe No Longer Attached to the Tee	235

Figure 277. Opposing Fracture Face	235
Figure 278. Fracture Face Microscopy on the Pipe No Longer Attached to the Tee	236
Figure 279. Opposing Fracture Face Microscopy	236
Figure 280. Differential Scanning Calorimetry	238
Figure 281. Oxidative Induction Time	238
Figure 282. FT-IR - Outer Wall	239
Figure 283. FT-IR - Middle Wall	240
Figure 284. FT-IR - Inner Wall	240
Figure 285. As Received Sample	242
Figure 286. Brittle Plastic Seepage from the Tee	242
Figure 287. Oxidative Induction Time - Pipe	244
Figure 288. Oxidative Induction Time - Tee	244
Figure 289. Oxidative Induction Time - Seepage Material	245
Figure 290. Differential Scanning Calorimetry – Pipe	245
Figure 291. Differential Scanning Calorimetry – Tee	246
Figure 292. Differential Scanning Calorimetry – Seepage Material	246
Figure 293. FT-IR Spectrum – Pipe Material	247
Figure 294. FT-IR Spectrum – Tee Material	248
Figure 295. FT-IR Spectrum – Seepage Material: Note ketone absorbance	248
Figure 296. As Received Fitting	250
Figure 297. Slit at Knit Line	251
Figure 298. As Received Sample	252
Figure 299. Close up View of AMP Fitting	253
Figure 300. As Received Sample	254
Figure 301. Socket Joint	255
Figure 302. Area Identified as Leaking	255
Figure 303. As Received Tee	256
Figure 304. Side View of Mechanical Tee	257
Figure 305: Schematic of Growing RCP Crack. (Kanninen, Et Al., 1997)	268
Figure 306: Full Scale RCP Testing Result (Kanninen Et Al., 1997)	271
Figure 307: S-4 Crack Initiation Result	273
Figure 308: GTI's S-4 Testing Apparatus	275
Figure 309: End Cap Contains a Port to Fill/Monitor Pipe Specimen.	276
Figure 310: Assembly Anvil Prevents Excessive Pipe Wall Deformation during Impact.....	277
Figure 311: Schematic of Pipe Assembly Used at GTI	277

Figure 312: Baffles and Anvil That Are Contained Within the Pipe Specimen.....278

Figure 313: FET Analysis Showing the Extensive Deformation of a Pipe during RCP.....279

Figure 314: External Cage279

Figure 315: Blade Resting in the Crack It Initiated.....280

Figure 316: 6" MDPE Critical Pressure Test Results: Critical Pressure: 15.5 Psig.....283

Figure 317: 6" MDPE Critical Temperature Test Results: Critical Temperature: 65.5 °F.....285

Figure 318: 6" MDPE S-4 Tests: Left, Crack Arrest; Right, Crack Propagation.....286

Figure 319: 6" HDPE Critical Pressure Test Results: Critical Pressure: 17.0 Psig.....288

Figure 320: 6" HDPE Critical Temperature Test Results: Critical Temperature: 50.8 °F291

Figure 321: 6"HDPE S-4 Tests: Left, an Insufficient Crack Length; Right, Crack Propagation.291

Figure 322: 6" PE100 Critical Pressure Test Results: Critical Pressure: 27.6 Psig293

Figure 323: 6" PE 100 Critical Temperature Test Results: Critical Temperature: 36.9 °F295

Figure 324: 6"PE100 S-4 Tests: Left, Initiation Test; Right, Crack Propagation.....296

Figure 325: 8" MDPE Critical Pressure Test Results: Critical Pressure: 11.5 Psig.....298

Figure 326: 8" MDPE S-4 Tests: Left, Crack Arrest; Right, Crack Propagation.....299

Figure 327: 8" PE 100 Critical Pressure Test Results: Critical Pressure: 27.0 Psig301

Figure 328: 8" PE 100 S-4 Tests: Left, Crack Arrest; Right, Crack Propagation302

Figure 329: 12" MDPE Critical Pressure Test Results: Critical Pressure: 18.5 Psig.....304

Figure 330: 12" MDPE S-4 Tests: Left, Crack Arrest; Right, Crack Propagation.....305

List of Tables

Table 1. NTSB Reported Brittle-Like Cracking Incidents	12
Table 2. Aldyl-A Melt Index Data 1965 - 1992 (DuPont)	33
Table 3. Aldyl-A Density Data, 1965 -1992 (unconfirmed by DuPont)	33
Table 4. Comparative of Melt Index Test Data	34
Table 5. Comparative of Average Tensile Strength Test Data	35
Table 6. Comparative of Average Quick Burst Pressure Test Data.....	36
Table 7. PENT Test Failure Time of Aldyl-A Pipe Lots (1973 - 1975)	40
Table 8. PENT Test Failure Time of Aldyl-A Pipe Lots (1976 – 1979).....	41
Table 9. PENT Test Failure Time of Aldyl-A Pipe Lots (1979 – 1982).....	42
Table 10. PENT Test Failure Time of Aldyl-A Pipe Lots (1983 – 1985).....	43
Table 11. PENT Test Failure Times for Polypipe 4810 and Driscopipe 8100.....	44
Table 12. Test Data for a 2 Inch Aldyl-A Pipe Manufactured In 1973 and Removed From Gas Service in 1983.	59
Table 13. Predicted remaining life expectancy for PE gas pipe.....	65
Table 14. Impingement Background	73
Table 15: Test Methods Used in Root-Cause Evaluation	77
Table 16: Melt Flow Measurements	77
Table 17. Tap Tee Background	83
Table 18: Melt Flow Measurements - Pipe	88
Table 19. Impingement Background	92
Table 20. Slit Failure Background.....	96
Table 21. External Loading Background.....	98
Table 22. Cap Background	108
Table 23. Cap Background	110
Table 24. Cap Background	112
Table 25. Cap Background	114
Table 26. Cap Background	116
Table 27. Cap Background	118
Table 28. Cap Background	120
Table 29. Service Tee Threads Background	124
Table 30. Coupling Background.....	126
Table 31. Socket Coupling Background.....	128
Table 32. Socket Coupling Background.....	131

Table 33. Socket Tee Background.....	133
Table 34. Socket Tee Background.....	135
Table 35. Socket Tee Background.....	137
Table 36. 4" x 2" HVTT Background	140
Table 37: Melt Flow Measurements - Pipe	145
Table 38: Melt Flow Measurements - Tee	145
Table 39. 2" Butt Fusion Background	152
Table 40. 4" Butt Fusion Background	155
Table 41. 3" Butt Fusion Background	157
Table 42. 2" Butt Fusion Background	159
Table 43. 4" Butt Fusion Background	161
Table 44. 4" Butt Fusion Background	163
Table 45. 4" Butt Fusion Background	166
Table 46. 4" Butt Fusion Background	168
Table 47. Poly Valve Butt Fusion Background.....	170
Table 48. Multiple Fusion Joints Background	173
Table 49. Socket Fusion Coupling Background.....	176
Table 50. Coupling Background.....	178
Table 51. Socket Tee Background.....	180
Table 52. Socket Tee Background.....	182
Table 53. 4" Single Bar Squeeze-off Background.....	185
Table 54. 2" Squeeze-off Background	187
Table 55. Squeeze-off Background	189
Table 56. 1 – ¼" x 1" Tap Tee Background	192
Table 57. 2" x 3/4" Tap Tee Background	195
Table 58. 2" x 3/4" Tap Tee Background	198
Table 59. 1 – ¼" x 1" Tap Tee Background	200
Table 60. 2" x ½" Tap Tee - Socket Fusion Background	202
Table 61. Transition Fitting Background	204
Table 62. 3" Elbow Background.....	206
Table 63: Melt Flow Measurements - Pipe	214
Table 64: Melt Flow Measurements - Elbow	214
Table 65. ¾" Valve Background.....	221
Table 66. Charred ¾" Pipe Background	229
Table 67. 1 - Tap Tee Background	232

Table 68: Melt Flow Measurements	237
Table 69. 4" x 4" Electrofusion Tee Background.....	243
Table 70. 1 – ¼" Amp Fitting Background	250
Table 71. 1 – ¼" x 1" Fitting Background	252
Table 72. Tap Tee Background	254
Table 73. Bolt-on Tap Tee Background	256
Table 74. Material Failures	258
Table 75. Procedural Failures.....	260
Table 76. Quality Control Failures	261
Table 77. Miscellaneous Failures	261
Table 78. Other Failures	261
Table 79. All Failures	262
Table 80. Received Failures	266
Table 81: Pipe Materials Used For the S-4 Testing	281
Table 82: 6" MDPE Critical Pressure Test Results	282
Table 83: 6" MDPE: Critical Temperature Test Results.....	284
Table 84: 6" IPS HDPE Critical Pressure Test Results.....	287
Table 85: 6" HDPE Critical Temperature Test Results	289
Table 86: 6" PE100 Critical Pressure Test Results	292
Table 87: 6" HDPE Critical Temperature Test Results	294
Table 88: 8' MDPE Critical Pressure Test Results.....	297
Table 89: 8" PE 100 Critical Pressure Test Results.....	300
Table 90: 12" MDPE Critical Pressure Test Results	303
Table 91: Summary of S-4 Test Results	306

Abstract

The three primary failure modes that may be exhibited by polyethylene (PE) gas pipe materials were described in detail. The modes are: ductile rupture, slow crack growth (SCG), and rapid crack propagation (RCP). Short term mechanical tests were evaluated for usefulness in determining the relative resistance of PE materials to SCG failures. Long-term hydrostatic stress-rupture test data was used with various models to predict the remaining life expectancy of a few older PE materials under specific field conditions. More than 50 field failures were classified by cause. Small scale steady state (S-4) testing was conducted on six large diameter PE materials to determine the critical pressure and/or the critical temperature.

Executive Summary

Reports, publications, papers, and databases were reviewed to better define risks and threats to plastic gas distribution piping. Failure modes were described for plastic PE piping with the most significant being slow crack growth (SCG). Short-term mechanical tests such as tensile, quick burst, melt index, and density tests did not show correlation with a material's susceptibility to SCG failure. The bend-back test was able to visually identify 1971 low-ductile inner wall materials. PENT test failure times were reported for materials manufactured during the period 1972-1985. The PENT test did not show correlations with the material's susceptibility to SCG failure for these materials.

Life expectancy was determined to be a key measure of the susceptibility of PE gas pipe materials to SCG field failures. Long term hydrostatic stress-rupture data combined with the Rate Process Method or with the Bi-Directional Shift Functions predicted the remaining life expectancy of several PE materials at 60°F average field temperature under varying loading conditions. Data showed rock impingement loads and pipe squeeze offs can result in the greatest reduction in remaining life expectancy. Lower operating field temperatures and pressures significantly increased the predicted remaining life expectancy of PE materials.

Fifty-five PE pipe samples that failed in field service were examined in the laboratory to identify the root cause of the failures. Eight of the samples underwent in-depth analysis, which included density and melt index tests and differential scanning calorimetry, infrared spectroscopy, and microscopic examination of the fracture surfaces. The samples were combined with another set of additional data resulting in 45 material, 36 procedural, 12 quality control, and 7 miscellaneous failures. A separate categorization method attributed a total of 321 failures to their respective pipe/component, with most occurring at joints.

RCP in large diameter PE materials was investigated through laboratory testing. Critical pressure was determined for 6 pipe materials. Critical temperature was determined for 3 materials.

Introduction

Statistics from the United States Department of Transportation (DOT) show more than 619,000 miles of plastic gas mains were in service at the end of 2006, up 75% since 1995. Of these plastic pipes, polyethylene (PE) makes up nearly 97% and polyvinyl chloride (PVC) and acrylonitrile butadiene styrene (ABS) make up the other 3%. In 1995, plastic pipe accounted for just 35% of the total mileage of gas distribution mains. In 2006 that number grew to more than 50%. The percent contribution of each material to the total number of miles in the U.S. distribution system is shown in Figure 1 and Figure 2 for 1995 and 2006 respectively. Comparison of the data show that the increase in system size is largely due to plastic pipe installations. The decline in steel and cast iron indicates these mains are being removed from service and are being replaced by plastic materials.

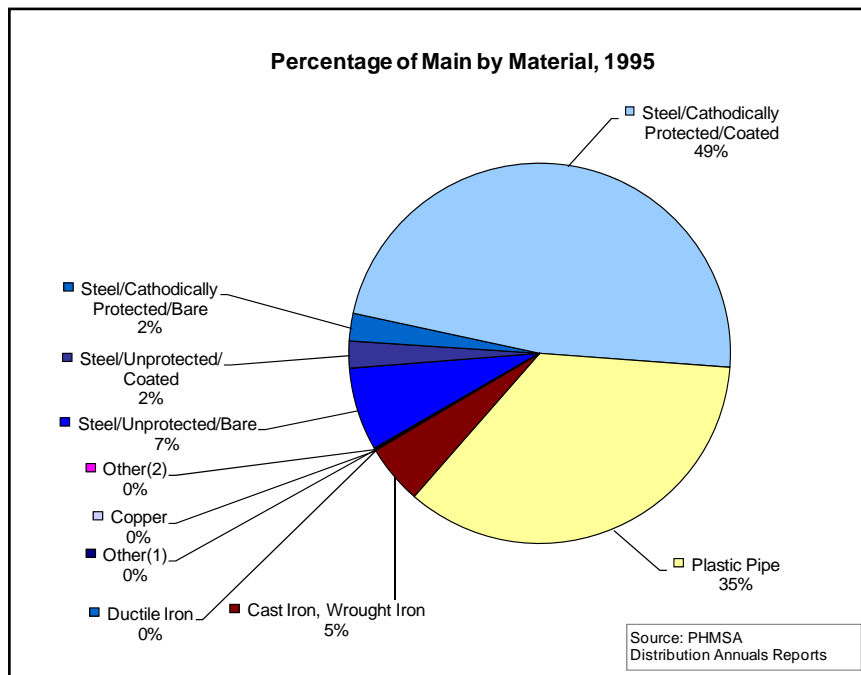


Figure 1. Percentage of Miles of Main, 1995

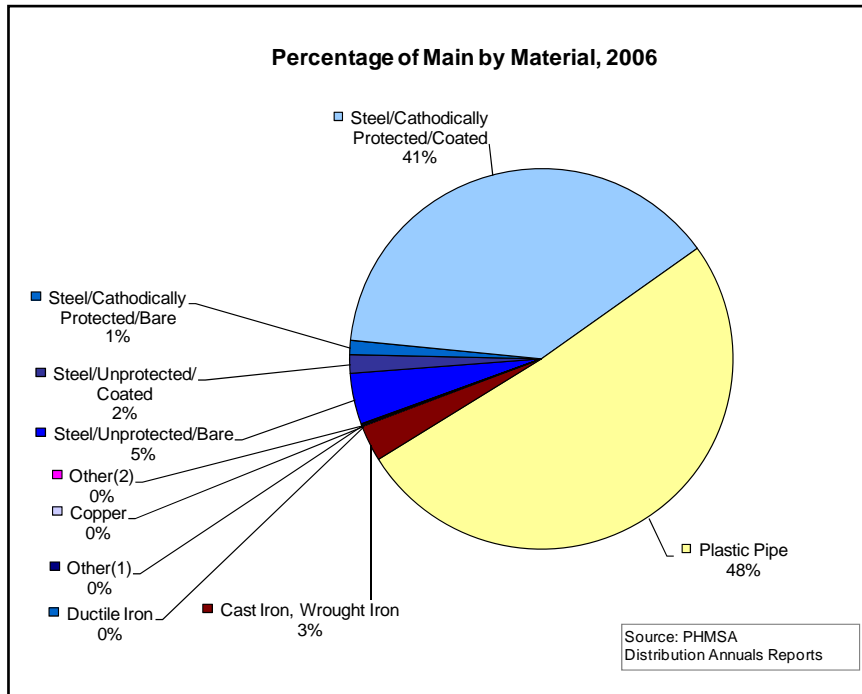


Figure 2. Percentage of Miles of Main, 2006

From 1995 to 2006, the number of services in the U.S. grew by 8M to a total of 63.5M. In 1995, there were 26M plastic services. That number rose to 39.6M by the end of 2006. In terms of the market share, plastic services represented ~48% of the total in 1995 as seen in Figure 3 and 61% of the total in 2006 as seen in Figure 4. PE makes up the majority of plastic services at 99.38%.

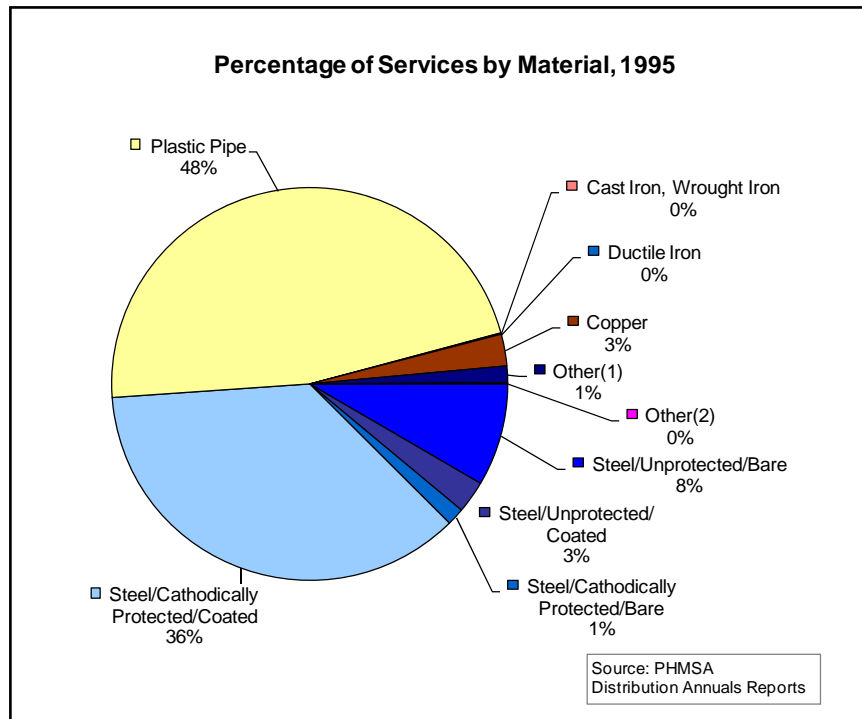


Figure 3. Percentage of Services, 1995

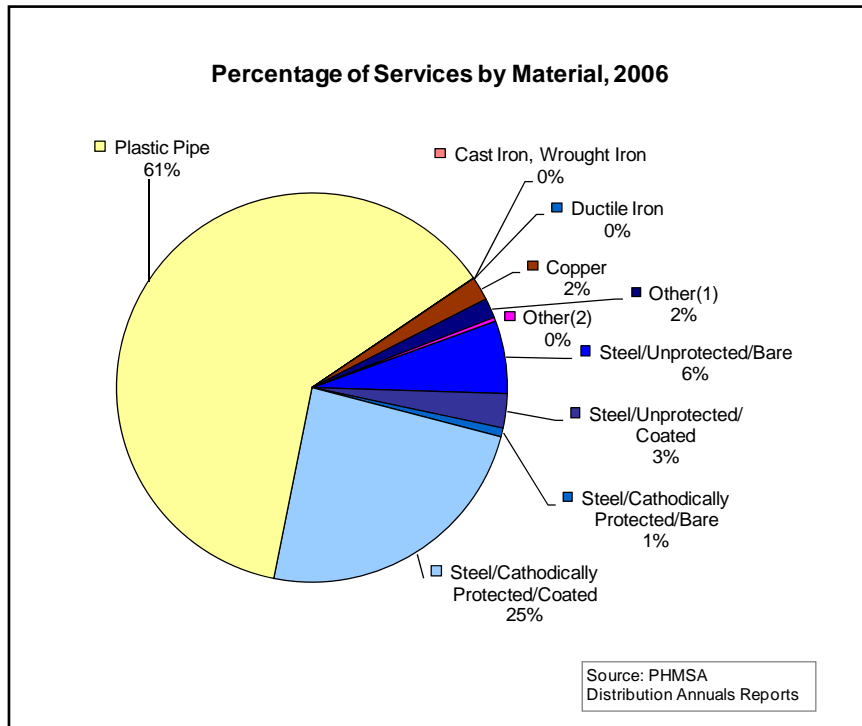


Figure 4. Percentage of Services, 2006

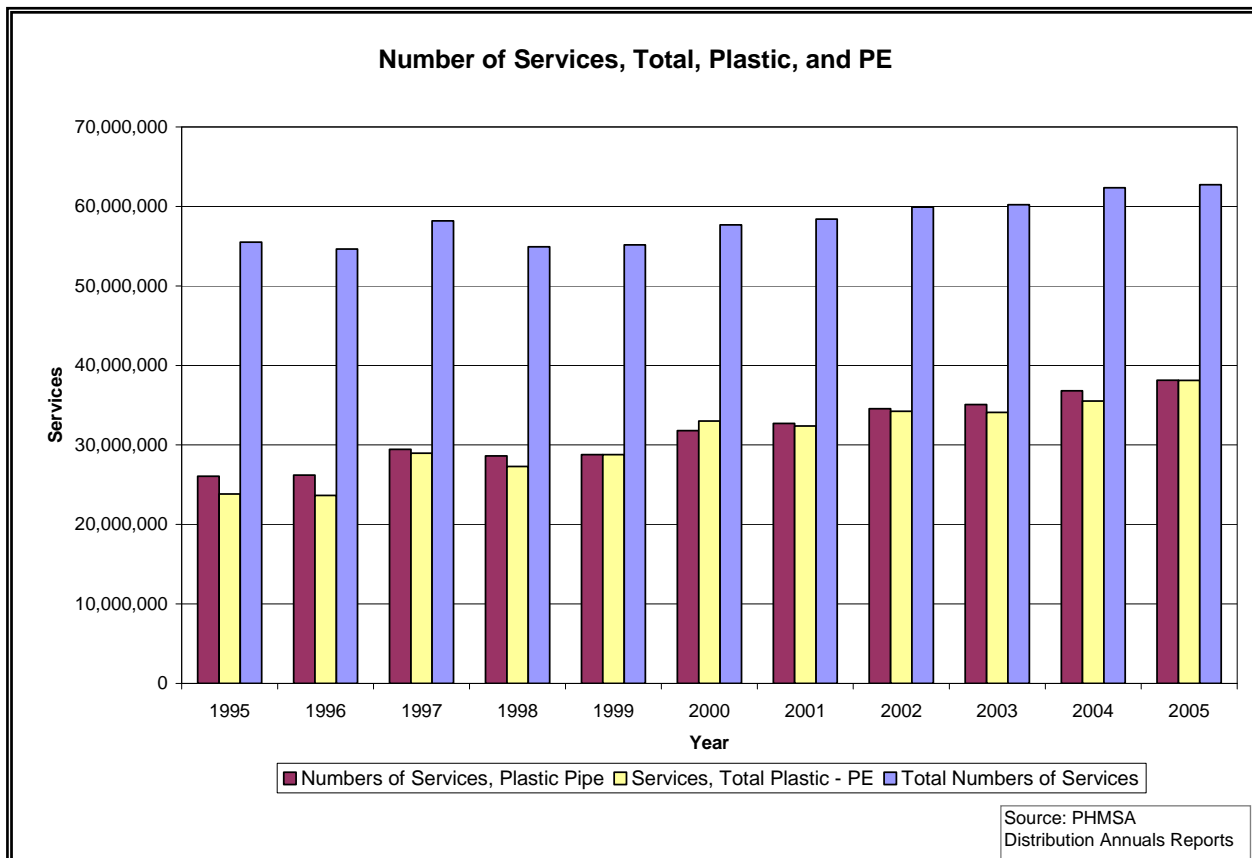


Figure 5. Comparison of Total Services, Plastic Services, and PE Services in 2005

The large magnitude of polyethylene pipes in the gas distribution system is undeniable. The low life cycle cost and reliability will continue to encourage the installation of polyethylene mains and services. In order to continue providing safe and reliable energy to gas distribution customers, the failures, risks, and threats associated with polyethylene piping must be well understood and that information needs to be available to gas distribution providers. Continued laboratory testing of failures and material properties should provide additional benefits. The findings must influence the pursuit to improve methods, procedures, and practices as they have in the past.

Classification of Failures and Their Causes

Many published reports and surveys estimated that about 65% of all failures in PE gas pipes are due to excavation damage. Outside of excavation damage, evaluations and laboratory analyses have shown that plastic polyethylene (PE) gas pipe materials fail by one of three modes. These modes are ductile rupture, brittle-like slow crack growth (SCG) failures, or rapid crack propagation (RCP) failures. The majority of plastic PE pipe in-field failures are typically the result of slow crack growth. About 1% of failures are ductile ruptures resulting from pipe over-pressurization.

Ductile Rupture Failure Mechanism

Plastic pipes experience ductile rupture failures due to the presence of high internal pressures. The failure mode is manifested in large localized plastic permanent deformations of the pipe wall. For PE pipes, they occur as a result of increasing pressure to levels greater than 400psig. Increasing pressures cause the pipe to undergo large diametric expansions typically resulting in wall thinning and stretching until a point where the remaining wall ligament is not sufficiently large to withstand the induced high circumferential hoop stresses. Figure 6 and Figure 7 show typical ductile failures in PE gas pipe materials subjected to high pressures.



Figure 6. Ductile Failure Resulting From a Quick Burst Test



Figure 7. Ductile Failure Resulting From a Quick Burst Test

Slow Crack Growth Failure Mechanism

Slow crack growth (SCG) failures occur over long periods of time at relatively low loads below the yield point of the material and are characterized by brittle (slit) fractures which exhibit very little material flow or deformation. Using high-magnification scanning electron microscopy, surface morphology of an SCG fracture can be characterized. Examinations show cracks initiate and radiate from an initiation point. Initiation points are stress risers caused by inclusions, contaminants, scratches, defects, cavities, dimples, high stress risers, etc. SCG failures grow stepwise and are associated with the sequential formation and fracture of the craze damage zone formed ahead of the crack tip. The damage zone consists of a main craze with a continuous membrane at the crack tip. The duration of each craze corresponds to arrest periods for the developed craze. At the end of an arrest period, the main part of the craze fractures. After a period of time following the craze fracture, the membrane ruptures and leaves fibrils creating visible and prominent striations indicative of the advancing crack front. The number of striations formed during the SCG process corresponds to the number of step jumps in the progressive craze formation and fracture process. Newer PE materials that are more resistant to SCG will show many more striations as the process of craze formation and fracture occurs repeatedly until the crack grows through the pipe wall.

Figure 8 shows an optical micrograph of the SCG failure process in the PE pipe specimen. The SCG failure initiated on the inner diameter (ID) and grew in a SCG manner along the axial direction and through the pipe wall to the outer diameter (OD) surface. The observed step-wise growth of the SCG process, exhibited in the form of striation marks (or tidal waves) from ID to OD, is typical of the SCG failure morphology observed for most of the PE gas pipe materials that fail in service.

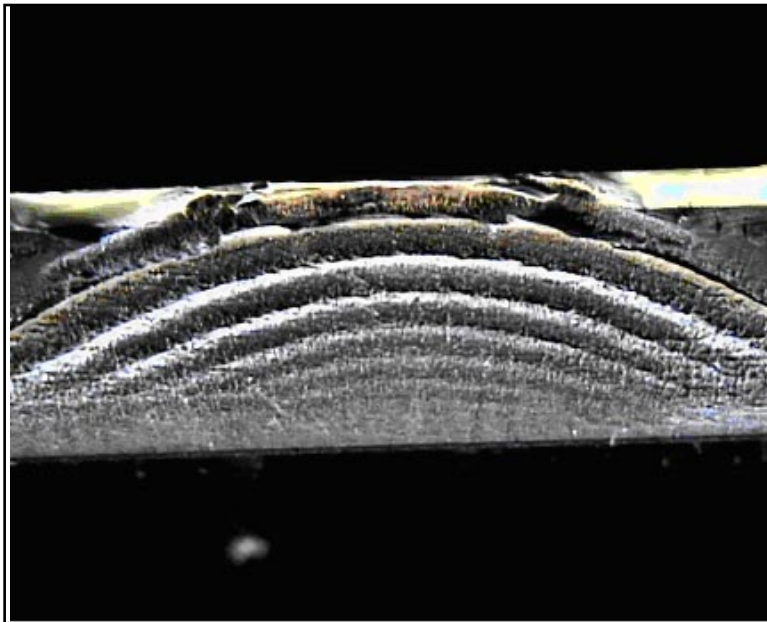


Figure 8. SCG Failure Morphology

Rapid Crack Propagation (RCP) Failure Mechanism

RCP failures are manifested in the form of a large-scale brittle crack that propagates at high speeds exceeding 300 ft/sec over a long span of polyethylene pipe. RCP failures could be catastrophic due to the rapid release of high volumes of gas over long spans. In order for RCP to occur, a “critical” initial axial notch must exist in the pipe wall and the driving force has to exceed the dynamic fracture resistance of the material. The dynamic fracture resistance decreases with decreasing temperatures making PE materials more susceptible to RCP ruptures at lower field temperatures. The susceptibility to RCP also increases with increasing field service pressure, increasing pipe diameter, increasing dimension ratio, SDR, and decreasing modulus of elasticity of the PE. Figure 9 shows an RCP rupture induced in a Small-Scale Steady State S-4 test.



Figure 9. RCP Rupture in a PE Pipe Subjected To a Small-Scale Steady State (S-4) Test

Types of PE Failures

Failure types in PE gas pipe materials that are relevant to the project are:

- Internal Pressure – The pipe ruptures (ductile) from inability to sustain the internal pressure.
- Plow-in, Insert Renewal, Installation Related – A failure of this sort may result from high tensile pull loads exceeding the yield strength; excessive pipe bending; deep surface scratches; or degradation due to excessive weathering, thermal degradation, and/or absorption of hydrocarbons.
- Squeeze Off – Pipes damaged in squeeze-off operations can be attributed to very high localized plastic deformations and cold-flow resulting from “over-squeezing”. Brittle slit failures occur in the axial direction and usually initiate in the “ears” of the squeeze-off at the inner pipe wall as micro-cracks before propagating through the wall.
- Bending – The pipe experiences high bending stresses; a crack initiates on the outer pipe wall at the section subjected to a maximum bending moment and grows through the wall resulting in a circumferential slit.
- Earth Settlement – Transverse loads due to earth settlement can cause axial slow crack growth slit failures to initiate along the axial direction on the inner pipe wall. These slit failures grow through the wall and longitudinally.
- Rock Impingement – Impinging rocks induce high localized stresses leading to slit SCG failures that initiate on the inner pipe surface and grow through the wall along an off-axis direction.
- Material: Quality Control, Other Defects – Quality control issues include the presence of inclusions, dimples, and cavities, etc. in the pipe wall; these defects act as initiation sites for SCG failures.
- Butt Fusion – Lack of fusion or partial lack of fusion penetration is generally the primary cause of failures in butt fusion joints. Inadequate fusion practices including low heater temperature, insufficient heating time, low interfacial pressure, improper squaring or misalignment of the pipe ends, contaminants, smudges, or lack of cleaning can all cause failures within a butt fused joint.
- Mechanical Fitting Failures – Ground movement, improper installations, and deterioration of components, e.g. gaskets can contribute to failures within mechanical saddles and sockets. Seasonal temperature changes causing high tensile thermal stresses may lead to pull-out failures.
- Fusion Fitting Failures – In general, the main reason for failures in fittings installed using fusion methods are attributable to improper fusion conditions such as low heater temperature, insufficient heating time, low interfacial pressure, inclusions, dimples, cavities, contaminants, finger smudges, or lack of proper cleaning. These causes can result in cold joints and lack of bonding.

- End Caps and Tapping Tee Caps – End cap failures result from improper bonding or material quality control defects within the cap. Tapping Tee caps sometimes suffer from leaking o-rings, fracture of the cap at the threads, or material quality control defects in the cap.
- Tees and Ells – Tees and ells generally fail from lack of bonding. Tees may also fail from large external secondary stresses due to excessive bending and high soil/earth loads. Manufacturing and material quality control defects could also cause failures in both types of fittings.
- Socket Fusion – Lack of proper fusion bonding combined with excessive external loads result in slit failures at the socket / pipe interface. Quality control defects within the socket can cause failures.
- Saddle Fusion – Saddle fusions can suffer separation and/or blow out. Quality control defects and improper fusion practices causing lack of fusion can both contribute to failures in saddle fusion joints.

Project Structure

The project activities were performed under four major tasks. The task titles and major objectives are:

- Literature Search – identify types, causes, frequency, and severity of plastic pipe failures
- Slow Crack Growth – characterize SCG and predict remaining life expectancy of materials and joints susceptible to premature SCG failures
- Root Cause Analysis – conduct laboratory examinations on field failures to determine failure mode and identify cause
- S-4 RCP Testing – evaluate susceptibility of large diameter PE pipes to RCP failure by performing S-4 tests

Literature Review on Severity and Frequency of Plastic Pipe Failures

GTI performed a literature search of available publications to classify the frequency and consequences associated with plastic pipe failures. The consequence of a plastic pipe failure can range from a small amount of lost gas to substantial property damages or loss of life. Many failures result in leaks that are so small they can go without repair and not pose a threat. There was a lack of publically available data to classify these low consequence failures. Other failures can cause explosions and fires which can result in serious events. Events resulting in loss of life or \$50,000 in property damages are reported in PHMSA's "Natural Gas Distribution Incident Data". GTI obtained and analyzed the incident dataset from PHMSA's "FOIA On-Line Library" located at the website: <http://ops.dot.gov/stats/IA98.htm>.

DOT/PHMSA Natural Gas Distribution Incident Data Discussion

All records classified as "Other" for material type were reviewed for any information that would justify changing the material type. For example, if the material was "other" and the material specification was "PE2306" or "2306", the material would be reclassified as polyethylene. The remainder of "other" was left alone. Primary and secondary cause categories were also reclassified if assumptions could be inferred. Usually, the records lacked enough useful information to determine them to be anything but what they were: "Unknown" or "No Data".

Another difficulty of analyzing the data is the change in the reporting requirements in March 2004. The data from 1984 to 2004 had 5 primary cause categories. They are: Corrosion, Damage by Outside Forces, Construction/Operating Error, Accidentally Caused by Operator, and Other. The introduction of the new reporting format expands the primary cause to 7 categories, each with sub-level or secondary causes. The major categories are: Corrosion, Natural Forces, Excavation, Other Outside Force Damage, Materials or Welds, Equipment or Operations, and Other. Some of the secondary causes have sub-causes. Without having the actual reports, it is impossible to reclassify the old incidents into the new categories. A study done by Allegro Energy Consulting actually used the operator's reports to reclassify all the incidents from 1999 to 2003 to the new format. Incidents previously classified as "Damage by Outside Forces" were reassigned into 5 of 7 of the new categories. "Other/No data" incidents fell into 6 of 7 of the new categories.

The dataset for March 2004 to 2006 was a huge improvement over the previous years but with less than 2 years of data, the sample of incidents is not large enough to deduce much. From 1984 to early 2004, more than 700 incidents involving plastic pipe were reported. More than 200 (nearly 30%) incidents were recorded as being of "Unknown" cause. Only 6% of the 2004 to 2006 data was reported as "Unknown." It is unclear why some of the incidents had even been reported as a number of records reported no injuries, loss of life, or property damages. A few of the records were removed from the dataset because they were erroneous.

Severity of Failures

Some of the most significant incidents resulting from plastic pipe failures have been attributed to brittle-like cracking. The National Transportation Safety Board published a Special Investigation Report titled "Brittle-like Cracking in Plastic Pipe for Gas Service" in 1998. The

Safety Board found the occurrence of slow crack growth (SCG) was second only to excavation damage for older plastic pipe materials. A number of the incidents mentioned in the report are shown in Table 1. The date, location, number of deaths and injuries, pipe manufacturer, and the cause of the cracking are noted.

Table 1. NTSB Reported Brittle-Like Cracking Incidents

Date	Location	Deaths	Injuries	Manufacturer	Cause
10/94	Waterloo, IA	6	7	Century	Stress intensification
11/96	San Juan, Puerto Rico	33	69	DuPont	Inadequate support
08/97	Lake Dallas, TX			Nipak	Loading by metal pipe
'71	TX		1	Not Specified	Loading on a connection
'73	MD	3	1	Not Specified	Occluded particle
'75	NC			Not Specified	Concrete drain resting on service
'78	AZ	1	5	Not Specified	
'78	NE		1	Century	Inadequate support at a fitting
12/81	AZ		3	Not Specified	At a fitting
07/82	CA			Not Specified	Not Specified
09/83	MN		5	Century	Rock Impingement
12/83	TX	1	1	Not Specified	Squeeze
'78, '79, '83	IL, IL, IA		5	Century	Not Specified
'95	MI			Century	Not Specified

In December 2002, the U.S. Department of Transportation issued an Advisory Bulletin titled “Notification of the Susceptibility to Premature Brittle-Like Cracking of Older Plastic Pipe.” The older polyethylene piping materials identified as being susceptible to premature SCG were:

- Century Utility Products, Inc. products.
- Low-ductile inner wall “Aldyl A” piping manufactured by DuPont Company before 1973.
- Polyethylene gas pipe designated PE 3306.

Another significant pipeline accident involving plastic piping occurred in DuBois, Pennsylvania in August of 2004. It was investigated and subsequently, an NTSB report (PAB-06-01) was issued. The leak, explosion, and fire resulted in \$800,000 in property damages and 2 fatalities. Excavation of the 2-inch main uncovered a faulty butt-fusion joint with mitering of the pipe ends. Further examination indicated the fracture initiation site was consistent with inadequate fusion. As a result of the investigation, the NTSB recommended butt-fusion procedures to “include a requirement for the avoidance of mitering” and the distribution company to revise butt-fusion procedures and qualification procedures.

An NTSB report (PAR-01-01), “Pipeline Accident Report: Natural Gas Explosion and Fire, South Riding, Virginia, July 7, 1998” documents an explosion and fire that killed one person, seriously injured another, leveled two houses, and damaged four other houses. The cause of the failed gas pipe was determined to be heat damage from an electrical service. The gas company has since revised their standards for minimum separation of PE pipes and electrical facilities to be 12 inches. The report also referred to two other incidents involving electric line failures. In Georgia in 1998, a 2-inch PE pipe was melted supposedly by a failed splice connector. During an excavation of the pipe, the gas ignited and burned an employee. The other accident occurred in Illinois in 1999. A fault in the electric cable supposedly melted a hole in the PE service. Fortunately, nobody was injured but the sustained damages totaled \$250,000.

“Pipeline Accident Report: Natural Gas Pipeline Rupture and Subsequent Explosion” authored by the NTSB details an accident involving third party damage. A communications network installation crew unintentionally cut a 1”, high pressure plastic gas service. Within 40 minutes of striking the line, an explosion occurred. There were 4 deaths and 11 injuries, including 1 serious. Six buildings were obliterated. The estimated property damages totaled \$399,000.

Despite reports of failures attributed to materials or procedures, statistics show that the number one cause of failures in plastic materials is caused by excavation damage. Excavation damage is the largest contributor to the cost of damages, fatalities, and injuries as reported in DOT/PHMSA natural gas distribution incident data. The same is true for steel materials. Failures that could be considered plastic pipe failures as a result of material or components cost the industry less than \$5M from 1984 to 2006. Figure 10 and Figure 12 break down the cost of damages by the primary cause of the incident for various material types. Third party damage is considered a secondary cause and is categorized under “Damage by Outside Forces” in the 1984 dataset and “Excavation” in the 2004 dataset. Figure 11 and Figure 13 show the cost of third party damages by material. In the last 22 years, third party damages cost the industry more than \$49M for plastic pipe and \$79M for steel. These costs are only those associated with reportable incidents and the actual total cost of third party damages would be larger if non-reportable damages were counted.

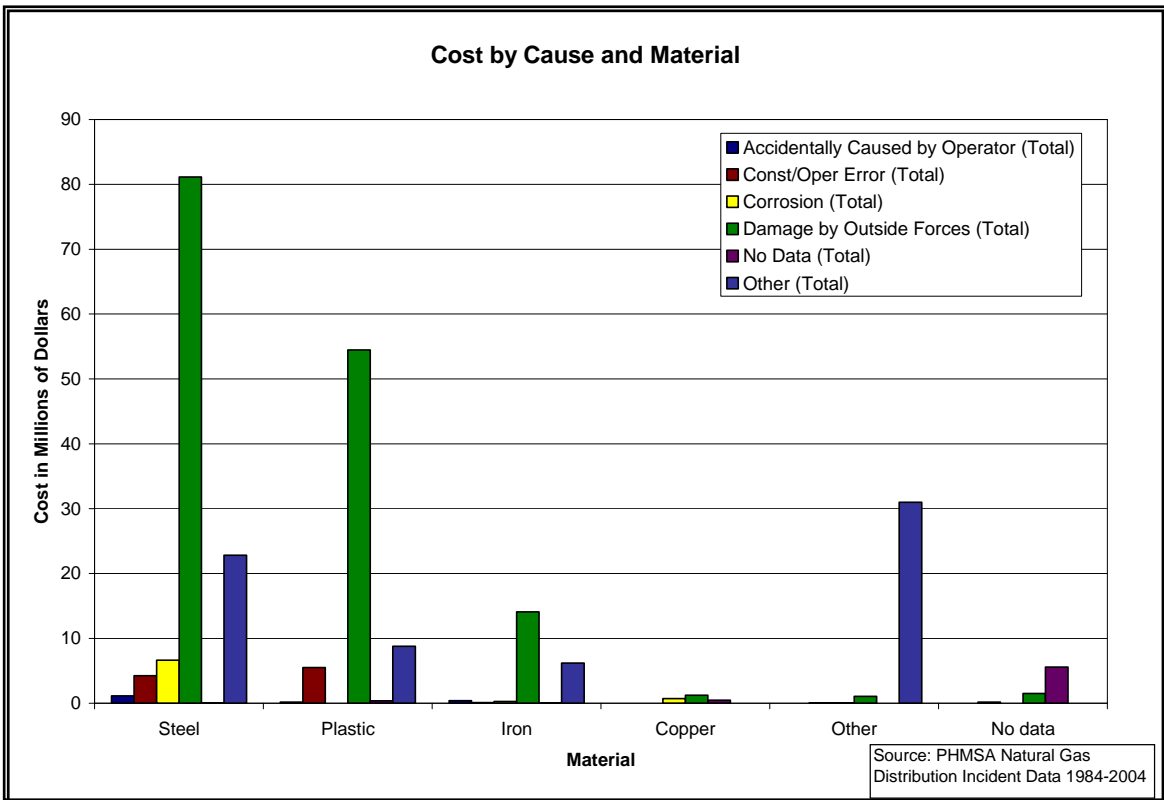


Figure 10. Cost of damages categorized by cause from 1984 - March 2004

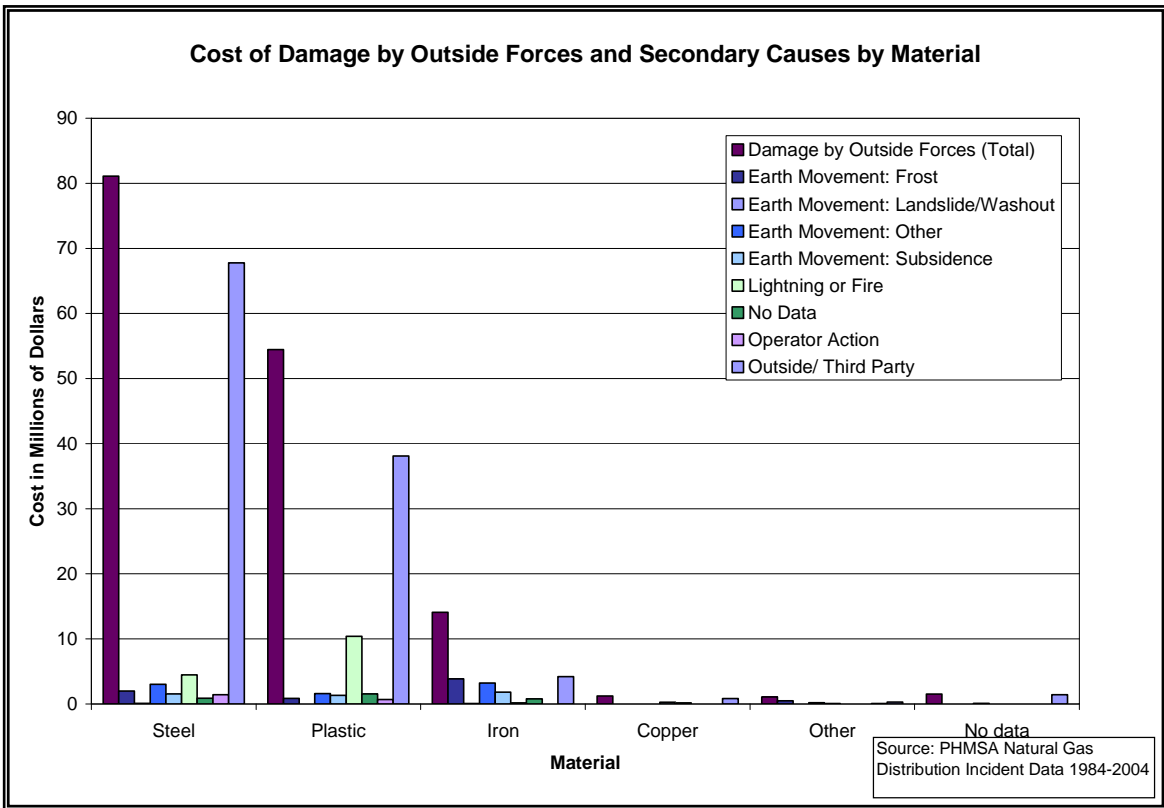


Figure 11. Cost of Outside Force Damages by Secondary Cause from 1984 - March 2004

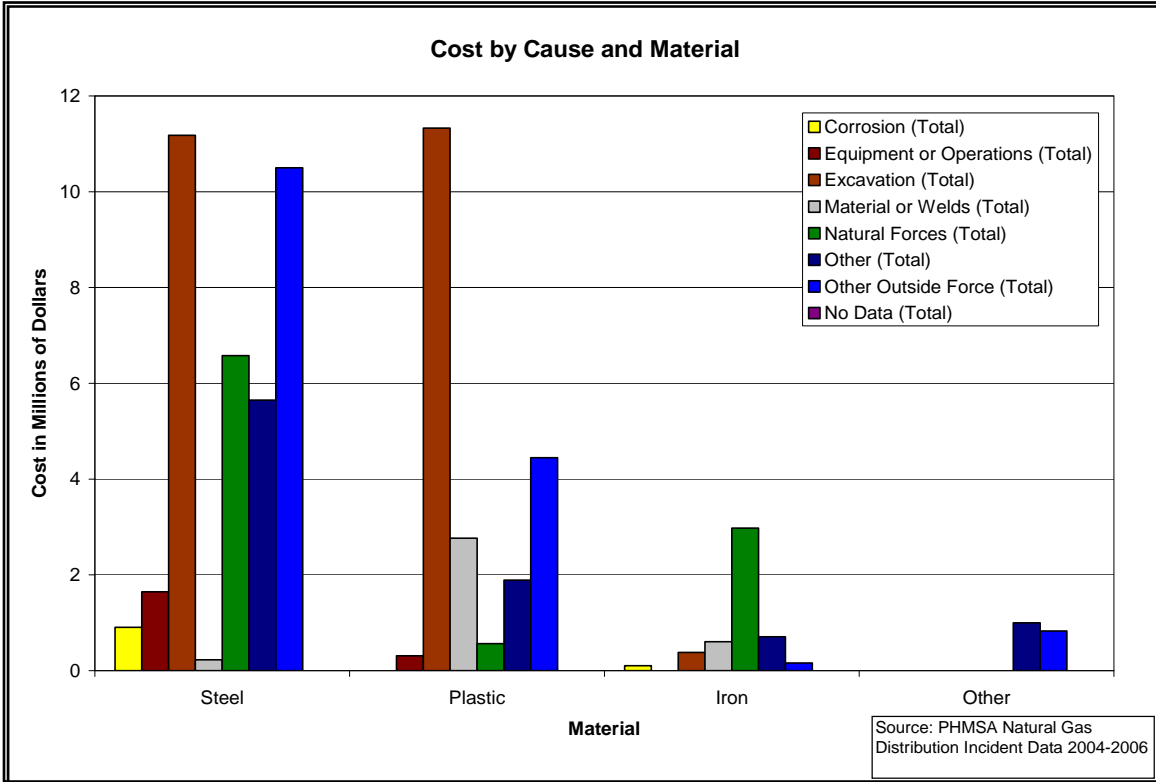


Figure 12. Cost of Damages Categorized By Cause from March 2004 - 2006

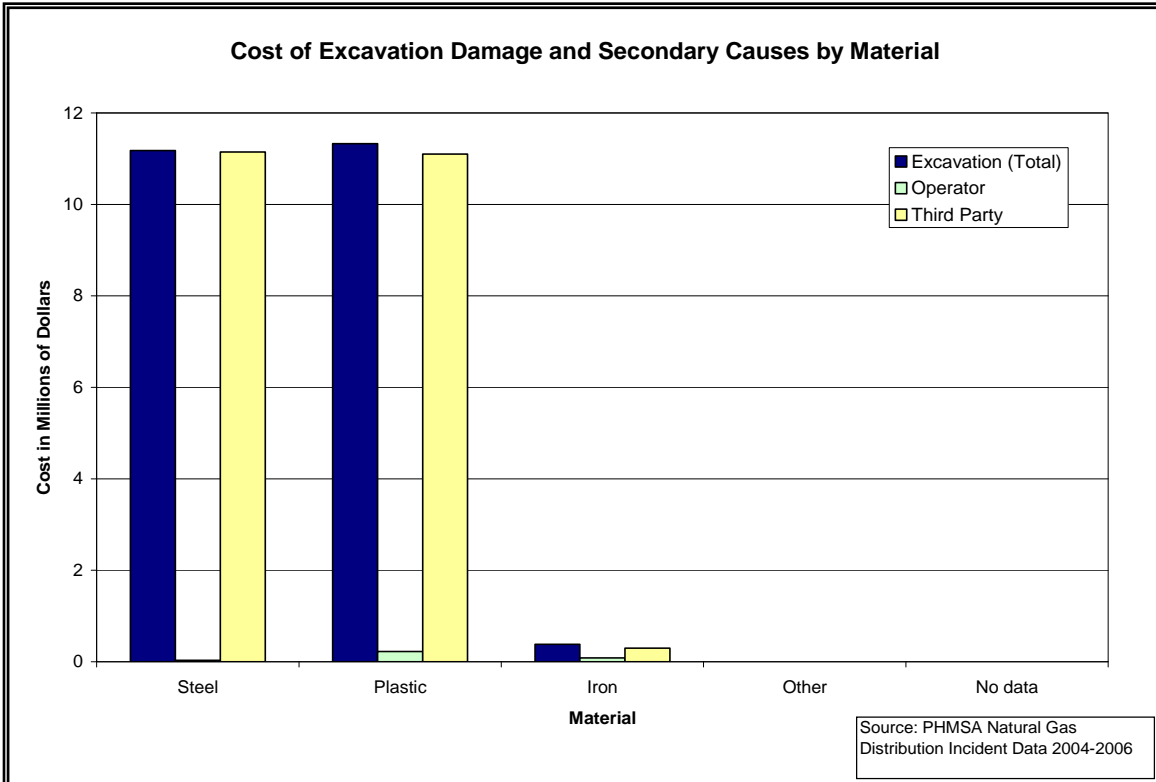


Figure 13. Cost of Excavation Damages by Secondary Cause from March 2004 - 2006

Figure 14 through Figure 17 show the total number of deaths and injuries reported to DOT since 1984. Figure 14 and Figure 15 demonstrate the number of fatalities reported by primary cause and material. Third party damage caused more than 60 deaths involving steel piping and about 40 deaths in plastic. Figure 15 shows 7 deaths with “Natural Forces” as the primary cause. Four of these fatalities occurred because of lightning. The other three fatalities were related to temperature or frost/thaw cycles. In both incidents, there was ignition and explosion. Only a handful of fatalities were caused by a compromised plastic pipe segment, joint, or component. “Other” is the second largest category, especially from the 1984 to 2004 dataset. A discussion of the datasets follows Figure 18.

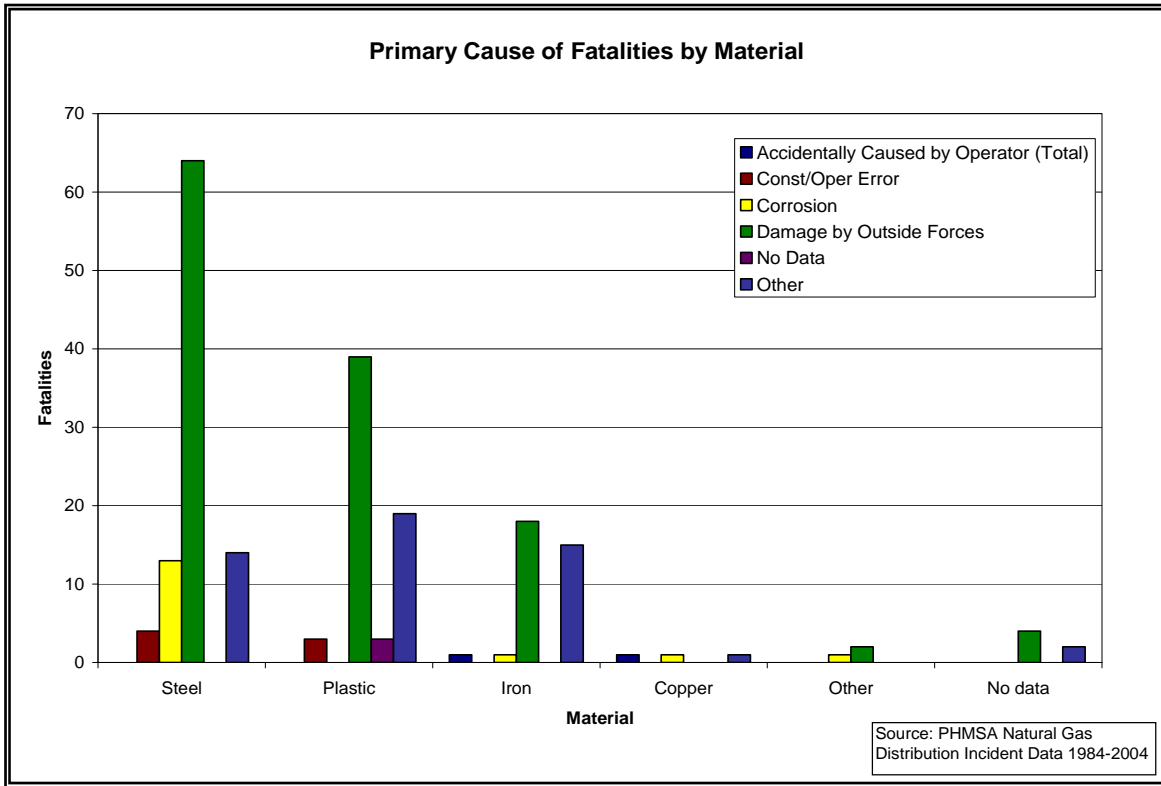


Figure 14. Fatalities by Primary Cause As Reported From 1984 - March 2004

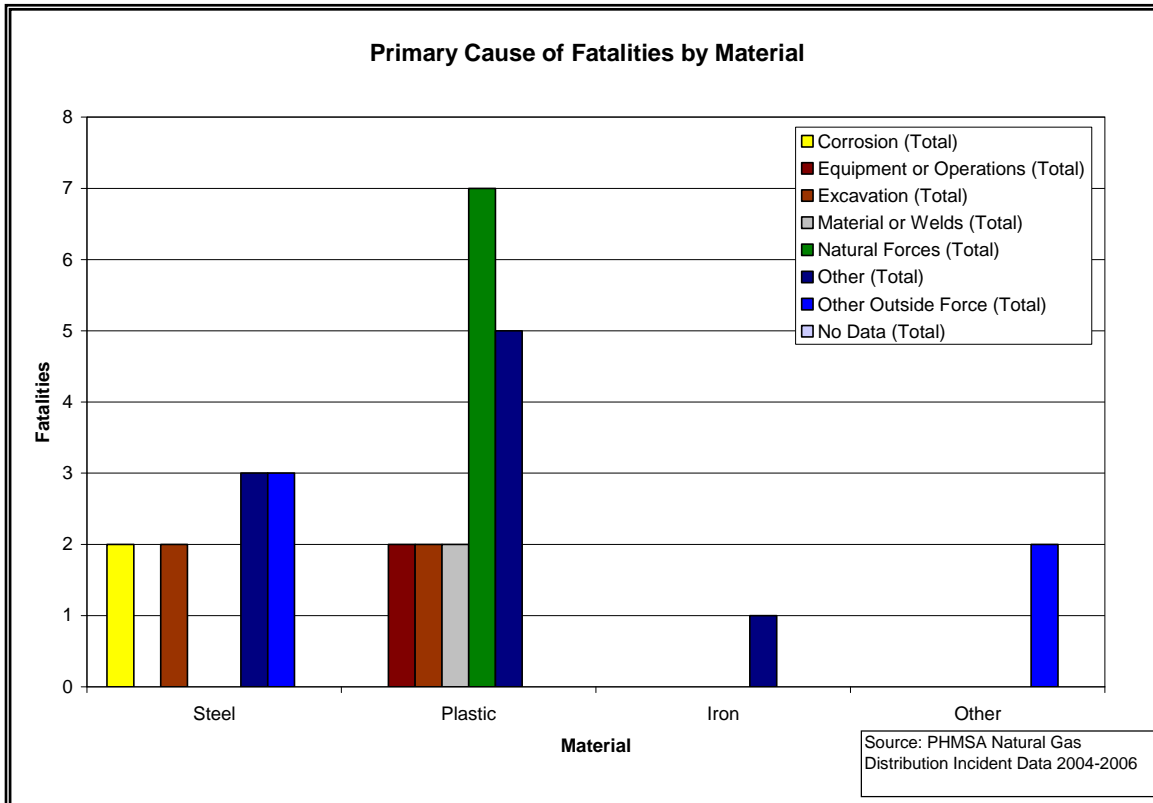


Figure 15. Fatalities by Primary Cause As Reported From March 2004 - 2006

Figure 16 and Figure 17 show the primary cause of injuries for each of the datasets. “Damage by Outside Forces” dominates the 1984 dataset. The bulk of these injuries were reported as third party damage. The 2004 dataset also shows 20+ injuries from “Excavation.” “Corrosion” was responsible for approximately 75 injuries related to steel piping. “Other” was also reported often in both datasets. Material, joints, and components attributed for a small number of injuries in any given material. Figure 18 demonstrates the total cost of the reported incidents per material. The cost of damages to steel was greater than damages to plastic materials for both datasets. Hurricane Katrina caused more than \$450M in damages. It was classified as “No data” for material type. The incident was reported for the entire city of New Orleans and likely included multiple material types.

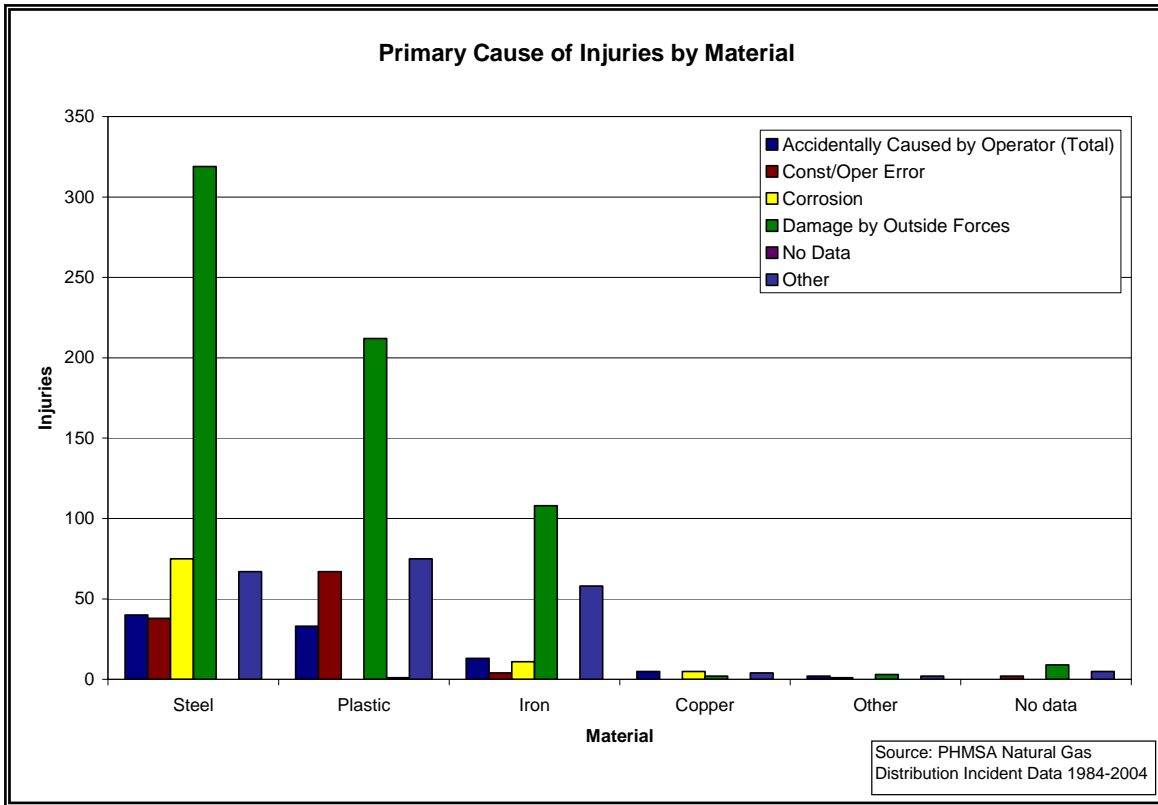


Figure 16. Injuries by Primary Cause As Reported From 1984 - March 2004

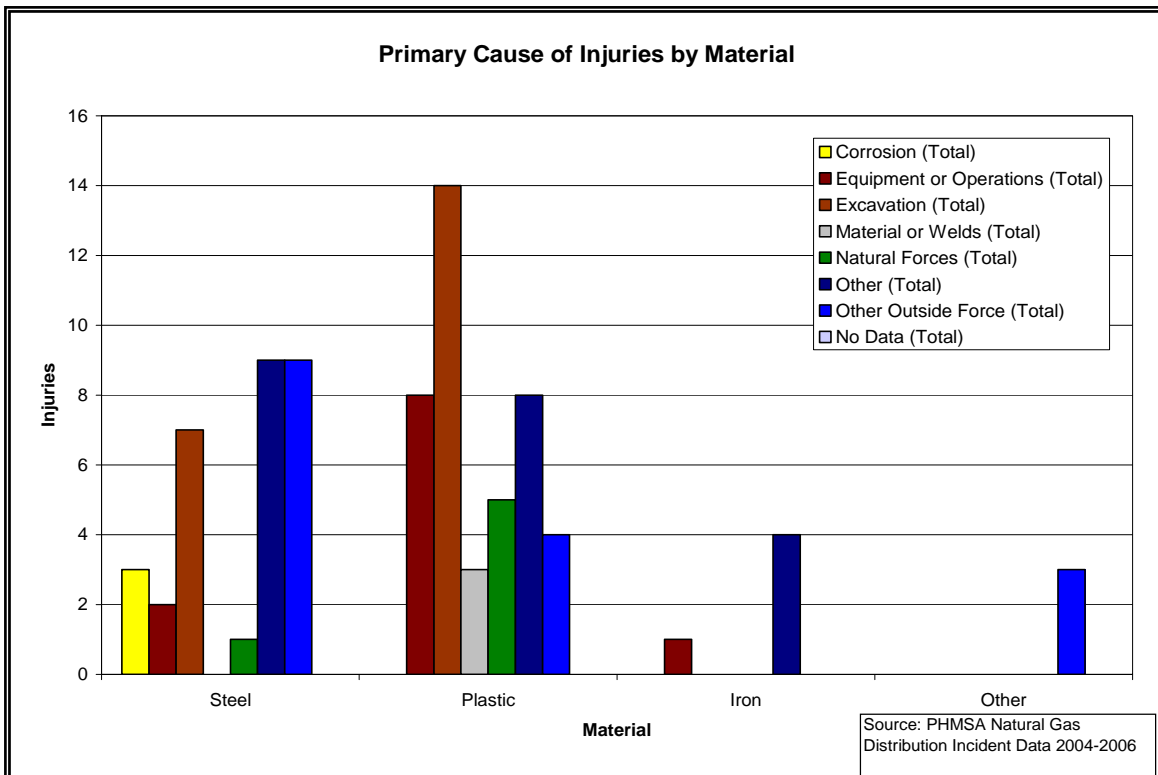


Figure 17. Injuries by Primary Cause As Reported From March 2004 - 2006

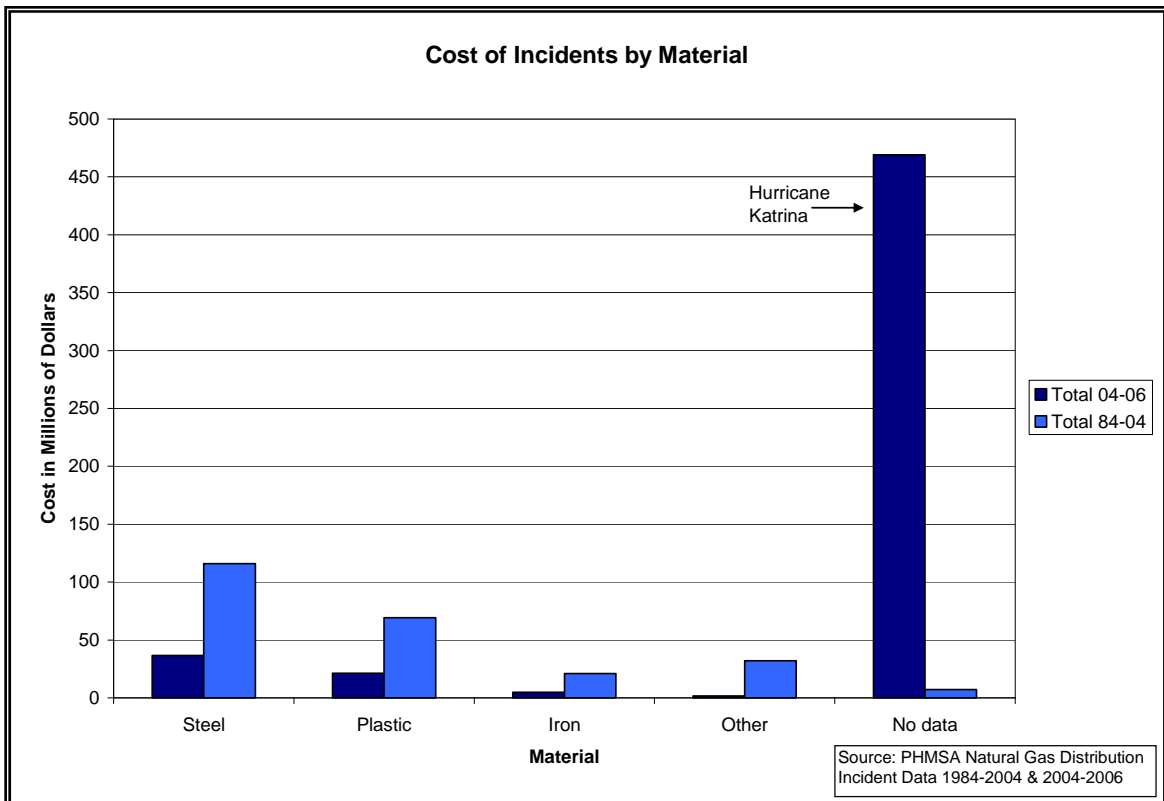


Figure 18. Total Cost of Reported Incidents for Each Data Period

Frequency of Failures

Looking at the statistical data from 1984 to 2006, the predominant cause of plastic and steel pipe failures was third party damage. Fire is the next significant cause of incidents in plastic piping. Reports on earth movement from the 1984 to 2004 dataset may be slightly high because they include items that were described as “object in backfill”, “settling”, and “tree roots”. Operator excavation and earth movement were about equally common and when combined cause roughly the same number of failures as fire. Beyond that, little can be said with any certainty based on the data other than without third party damage and fire; gas transport via plastic piping is incredibly safe. The frequencies of failures are categorized by primary cause and material in Figure 19 and Figure 20.

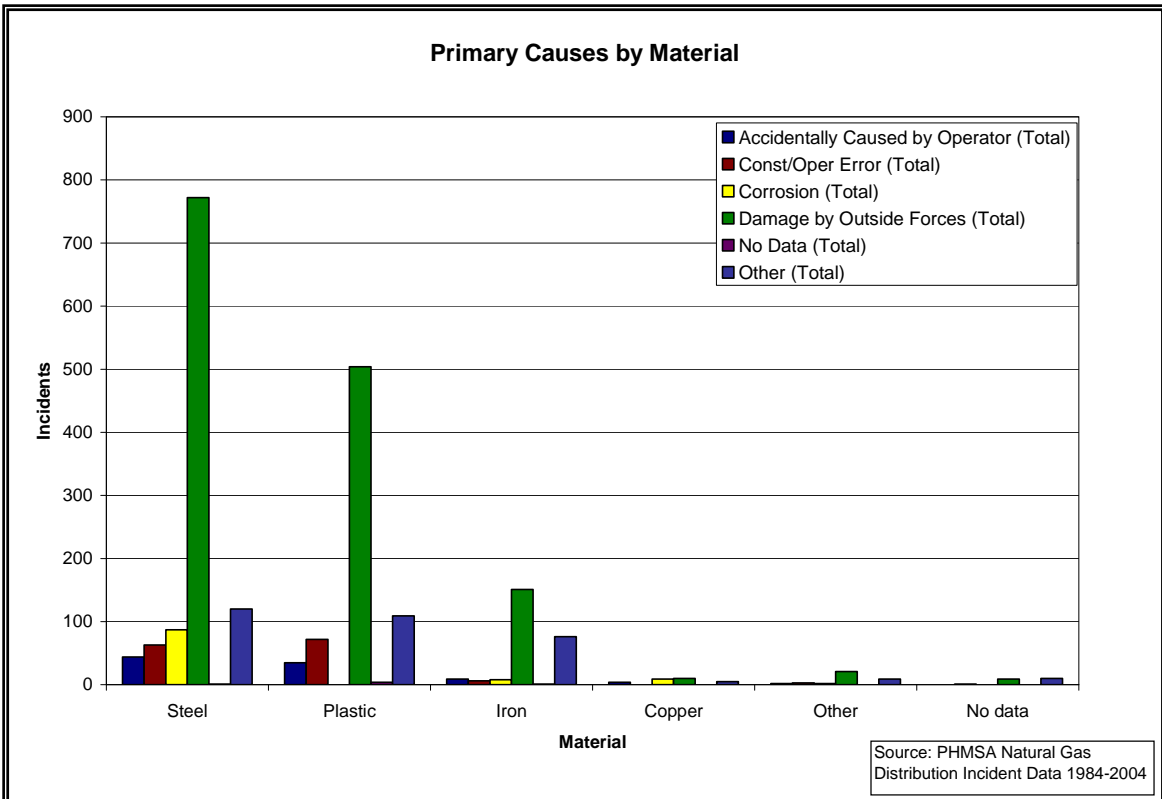


Figure 19. Frequency of Failures by Cause from 1984 - March 2004

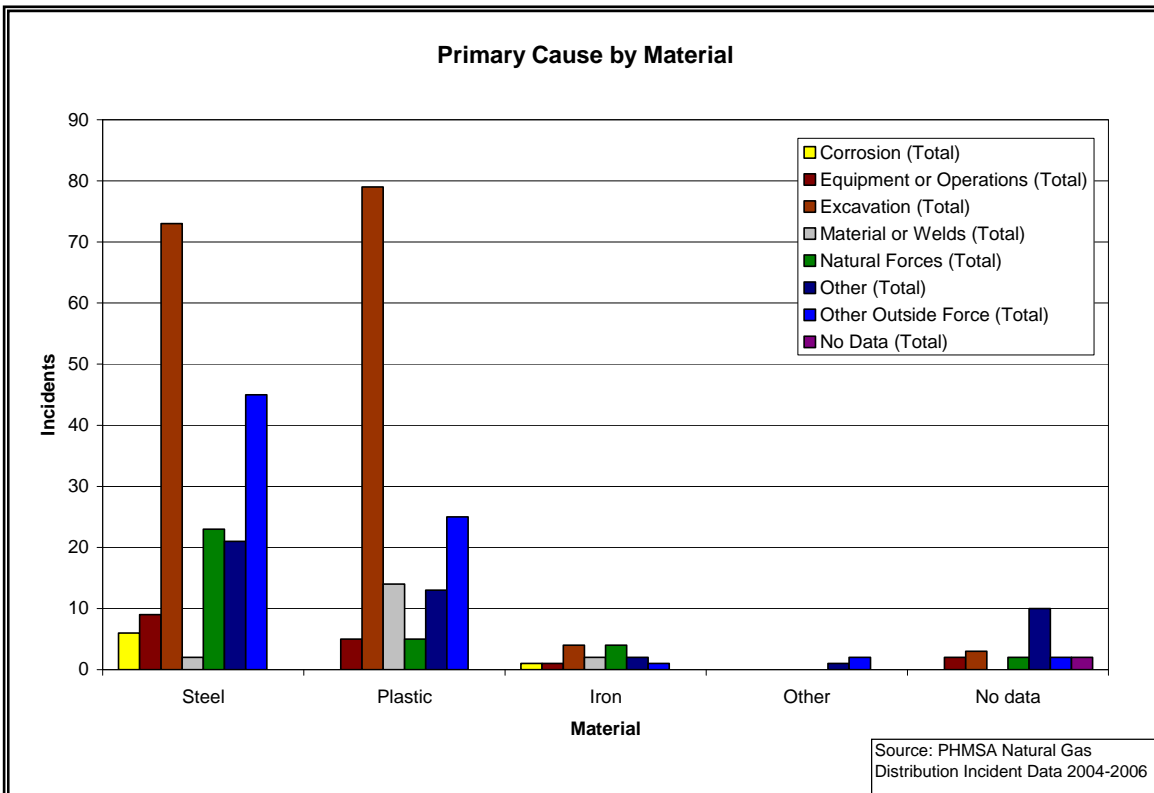


Figure 20. Frequency of Failures by Cause from March 2004 - 2006

Failure by PE type was also analyzed. Unfortunately, the material specification was not consistently reported. Roughly one-third of the 1984 to 2004 data was specified. The chart generated from this data is shown in Figure 21. The most common material specified was PE 2306 which may represent the amount of the material installed or the crew member's familiarity with the material making it recognizable, resulting in the ability to report this particular PE. PE 2406 was also highly reported. The failures by PE type are shown in Figure 21 and Figure 22 for 1984 to 2004 and 2004 to 2006 respectively. In the latter chart, only a small number of types were reported. PE 2406 and 3406 were reported more often than other material designations.

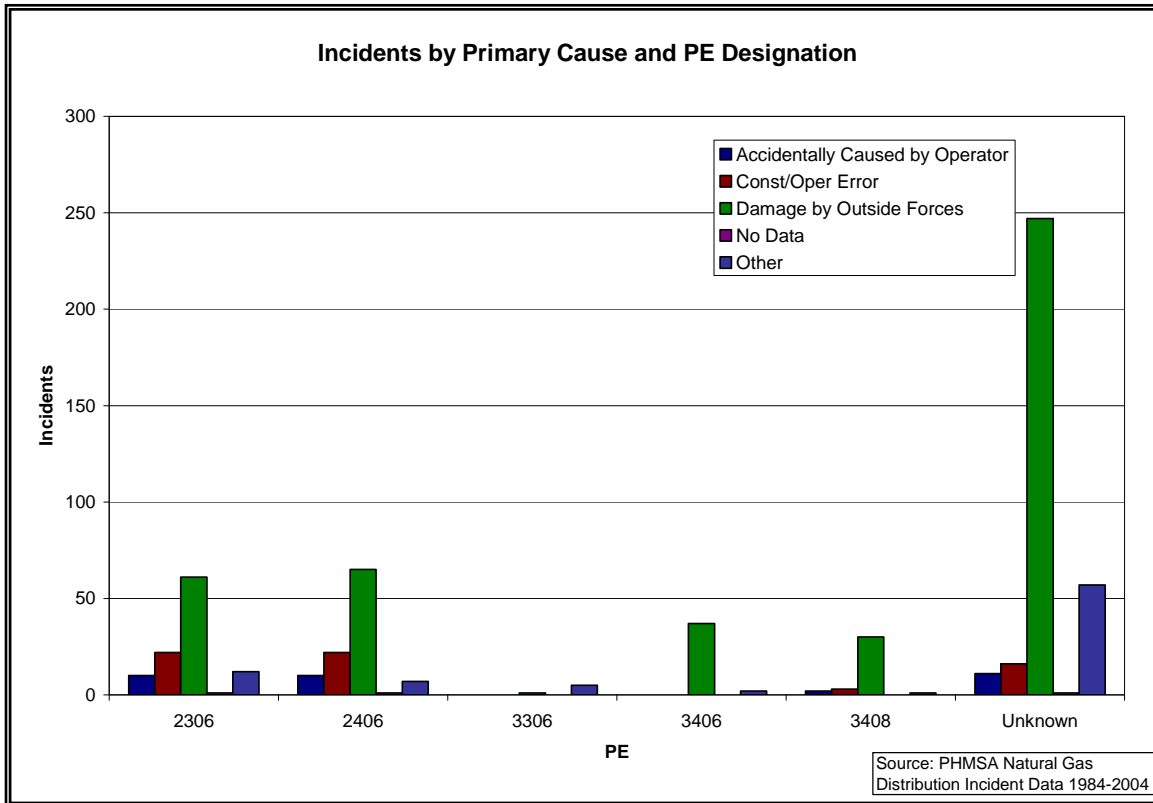


Figure 21. Frequency of Failures by Type of PE and Cause for 1984 - 2004

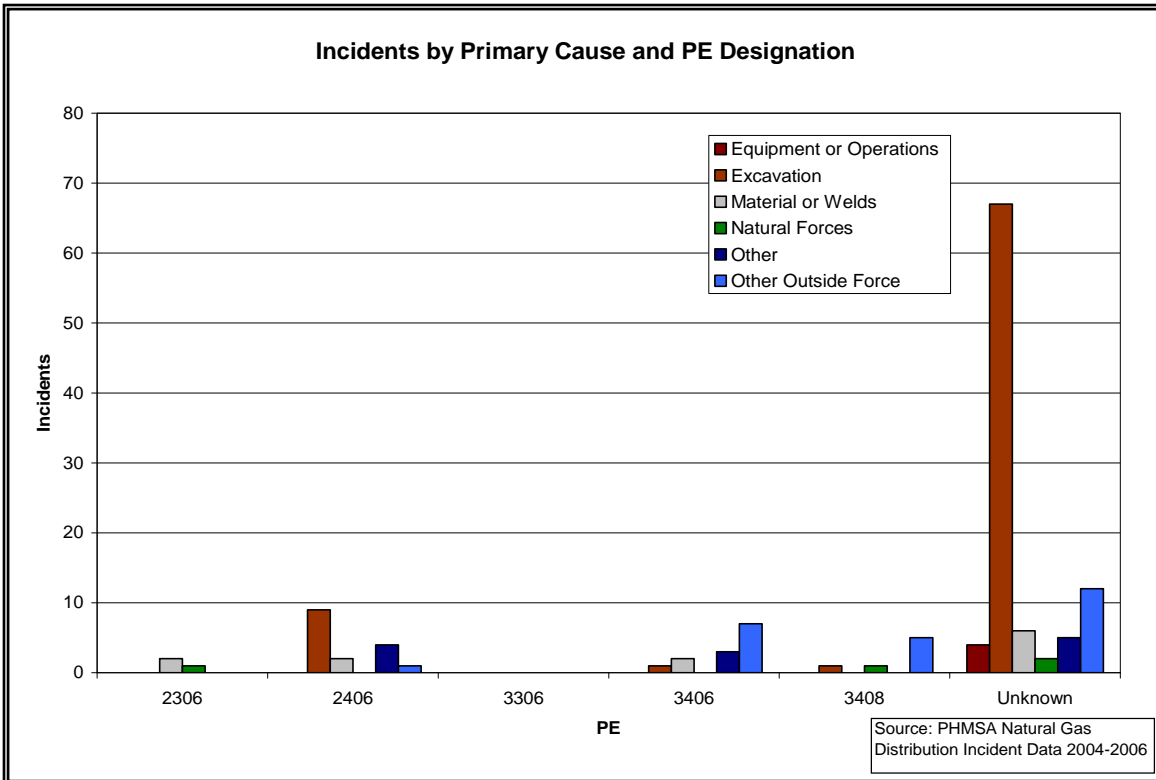


Figure 22. Frequency of Failures by Type of PE and Cause for 2004 - 2006

A chart was also created to look at the failures by manufacturer and cause for the 1984 dataset. Drisco Phillips, DuPont, and Plexco were the top three reported. This should correlate to the amount of these materials in the ground but cannot be concluded without knowing how much of these materials are still in operation. The chart is shown in Figure 23.

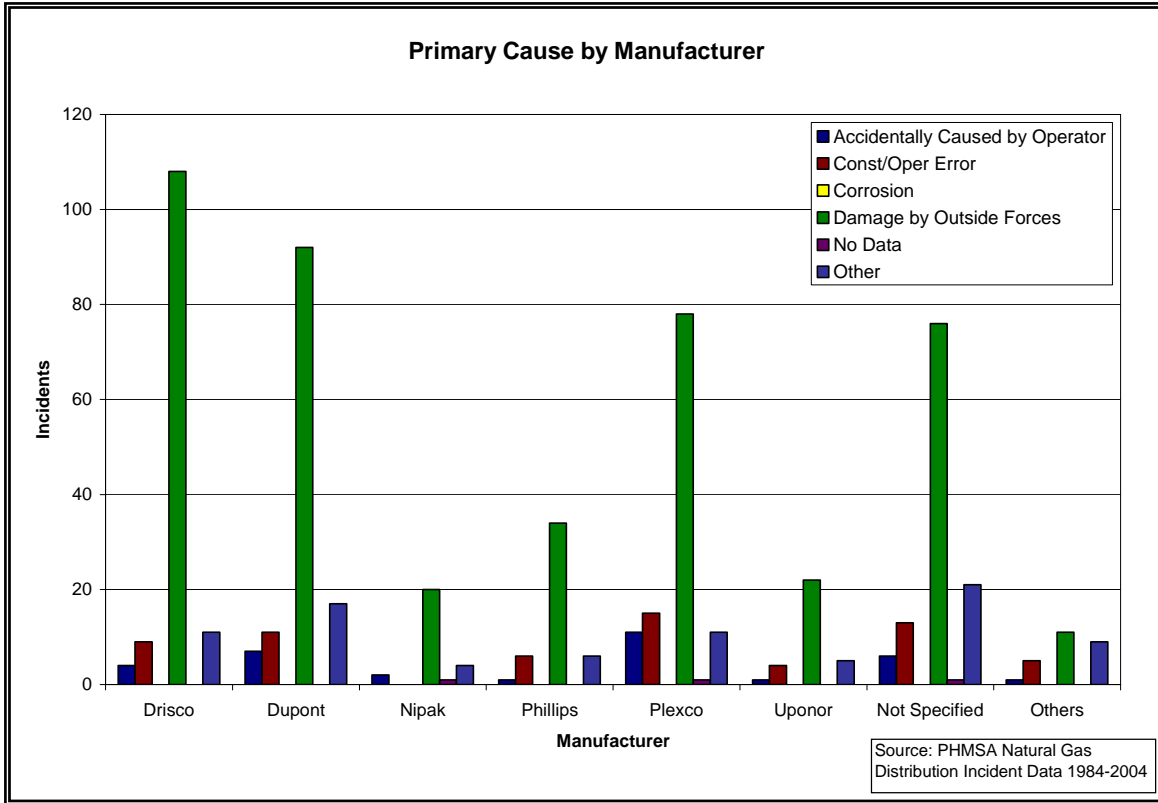


Figure 23. Frequency of Incidents by Manufacturer and Cause for 1984 - March 2004

A chart was also created for the failures by manufacturer and cause for the second dataset. It is shown in Figure 24. Again, Drisco and Plexco were among the top. Most of the plastic piping damaged by third party was not specified by manufacturer in either chart.

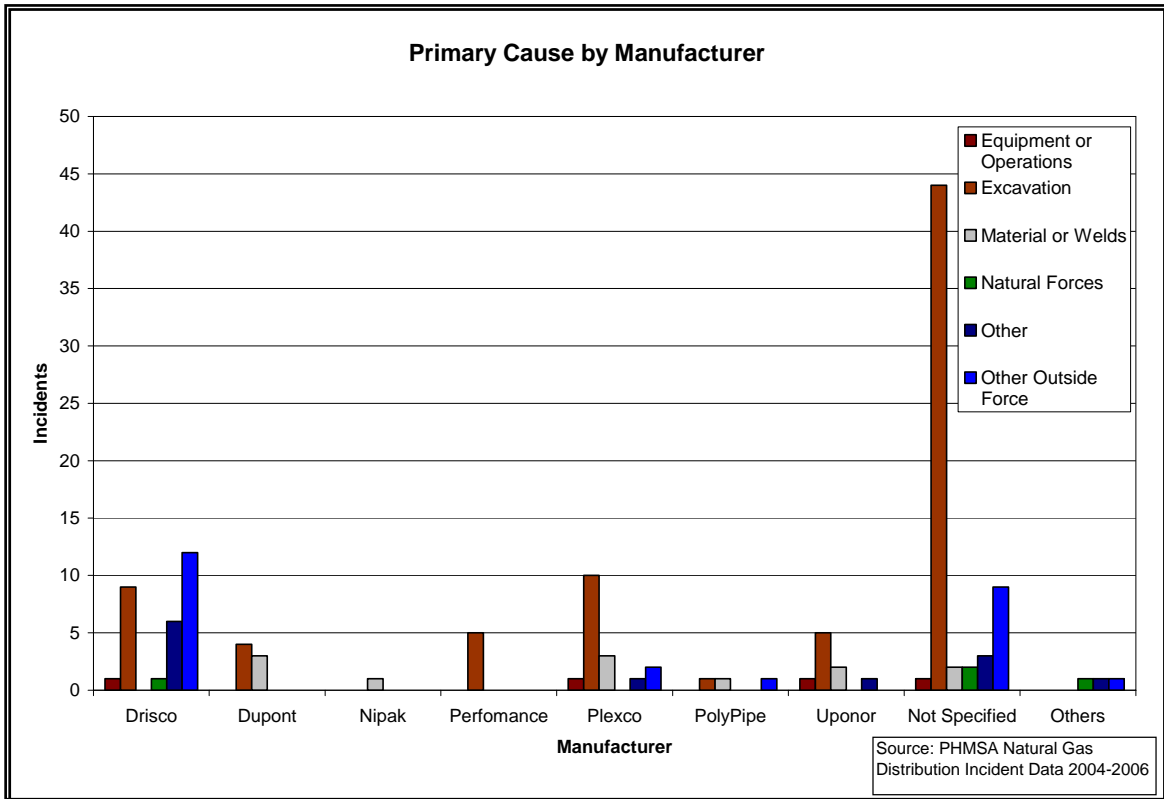


Figure 24. Frequency of Incidents by Manufacturer and Cause for March 2004 - 2006

Another analysis made was the failure types by time of day. The number of incidents peaked between 8 A.M. and 6 P.M. Most of these failures are reported as damage by outside forces and excavation. Third party damage as a secondary failure was included in the charts in Figure 25 and Figure 26. Fire and lightning and fire or explosion as secondary causes were also included and are more common in the hours after midnight and around lunchtime.

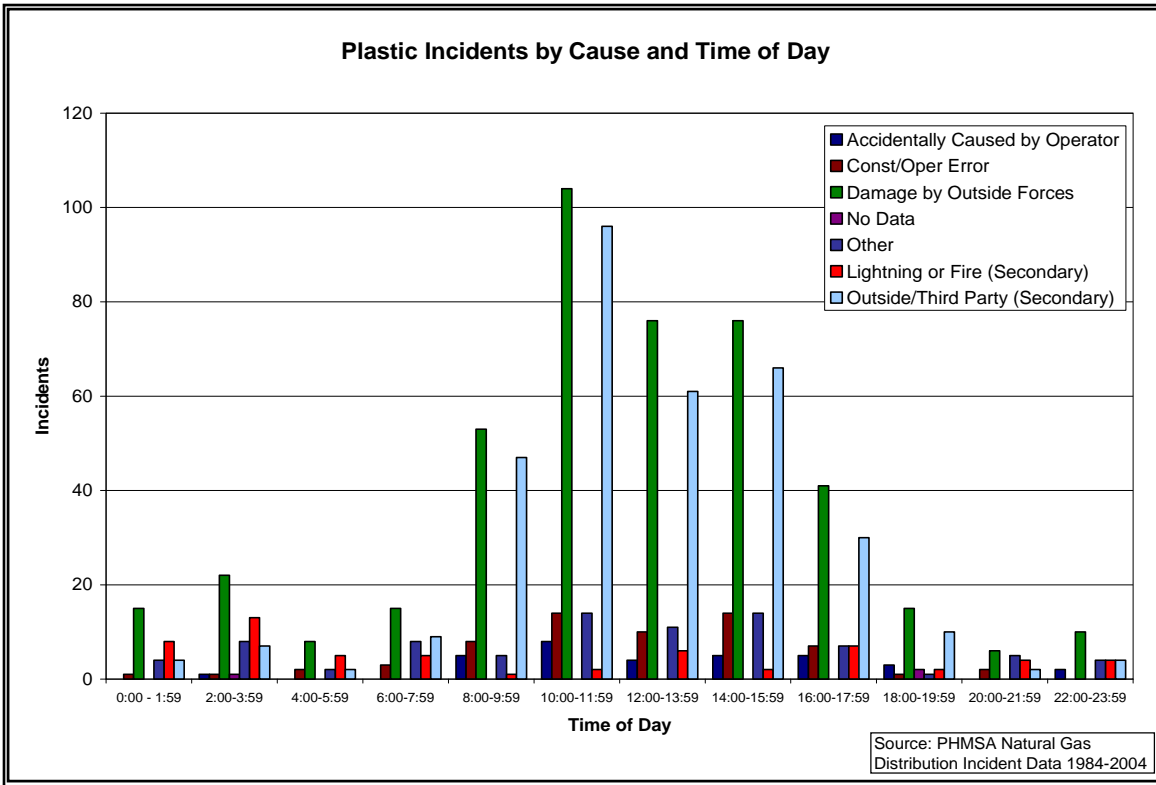


Figure 25. Frequency of Plastic Incidents by Time of Day from 1984 - March 2004

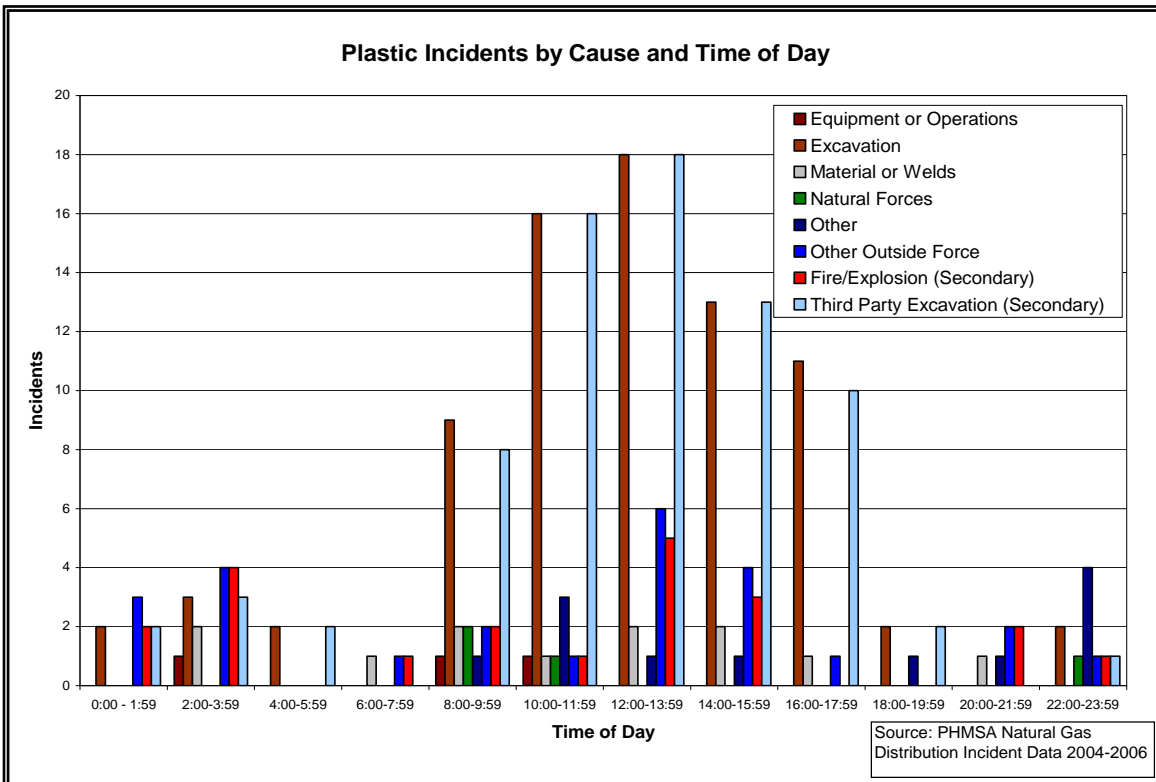


Figure 26. Frequency of Plastic Incidents by Time of Day from March 2004 – 2006

Susceptibility of PE to Slow Crack Growth Failures

Objective

The objectives of the slow crack growth task were to utilize GTI's database to determine the susceptibility of plastic gas pipe materials and fusion joints to slow crack growth and to predict their remaining life expectancies using engineering models.

Types of PE Gas Pipe Materials in GTI Database

The plastic pipe materials comprising GTI database were of different diameters and SDR's and were manufactured during the period extending from about 1965 to about 2003. A few of the pipe materials were manufactured during the same year but in different months and were installed by different gas companies. The PE gas pipes comprising the GTI database were installed in many different geographical regions throughout the U.S.

The GTI database includes many plastic PE gas pipes that were made from different PE resin materials and extruded into pipe form by several different pipe manufacturers. Many of these PE resin manufacturers and pipe extruders are no longer in business. The plastic gas pipe materials in the database were made from several different medium-density polyethylene (MDPE) and high-density polyethylene (HDPE) gas-grade resin materials.

The DuPont Company began manufacturing Aldyl-A MDPE pipe materials for gas distribution applications in the 1960's. DuPont continued to manufacture Aldyl-A pipe materials until about 1991. Uponor Company purchased the Aldyl-A pipe product line during the period 1991-1992. Uponor continued to manufacture and market Aldyl-A pipe product line until about 1999. Uponor began using their company name during the period 1992.

Aldyl-A pipe materials are medium-density polyethylene (MDPE) gas-grade pipe materials. From the 1960's to about 1986, Aldyl-A MDPE pipe materials were categorized/designated by ASTM as PE 2306 grade. In 1986, the Aldyl-A MDPE pipe materials were designated by ASTM as PE 2406 grade.

During the period 1965 to 1987, DuPont was one of the largest PE pipe manufacturers and had more than 40% of the market share. Many gas distribution companies installed Aldyl-A pipes in their system. Because of this, this report presents substantial information on Aldyl-A PE gas pipe materials.

Detailed List of PE Resin and Pipe Manufacturers

A detailed list of the names of many PE resin producers and pipe extruders that manufactured the largest percentage of the PE pipe materials comprising GTI database, is presented in GTI Report Number GRI-98/0355 entitled "Handbook of Hydrostatic Stress-Rupture Data for Plastic Pipe Materials Used for Gas Distribution".

Visual and Optical Examinations of Slow Crack Growth Failures

Figure 27 shows an Aldyl-A MDPE pipe sample that experienced a SCG axial slit failure/leak while in a standard long-term laboratory test under a constant internal pressure. Microscopic examinations showed that the failure initiated at a very small (less than 5-mills in depth) surface pin-size hole on the inner pipe surface. The examination also showed that the pin-

size hole grew in an SCG mode along the axial direction and through the pipe wall. The final failure was in the form of an axial slit visible on the pipe outer surface.



Figure 27. Pipe Exhibited Through Wall Axial Slit While Under Internal Pressure

The SCG fracture morphology depicted above in Figure 8 is typical of failures that occur in PE gas pipes subjected to internal pressure and/or internal pressure combined with a secondary stress such as those induced by an impinging rock, a squeeze-off, or an earth or soil load. However, under a combined load involving an internal pressure and a secondary stress, the location and orientation of the SCG axial slit are different than that shown in Figure 27.

SCG Failures Due to Rock Impingement Loads

Visual examinations show that rock impingement field failures exhibit a surface indentation on the outer pipe surface. Typically, the failure in a pipe specimen subjected to both internal pressure and a rock impingement load is visually observed to be a slit through the wall. The slit is oriented slightly off the pipe axis.

Figure 28 shows a slit on the outer surface of an Aldyl-A pipe sample that experienced failure as a result of internal pressure combined with a rock impingement indentation load. The failure initiated on the inner pipe surface underneath the impinging rock/indenter. The failure grew through the pipe wall and in a direction that was oriented at an angle of about 20-degree relative to the pipe longitudinal axis.



Figure 28. Rock Impingement Failure

Figure 29 shows that a slit failure induced by an impinging rock load, initiated on the inner pipe surface. Examinations of pipes that failed due to rock impingement loads clearly show that the failure morphology is SCG brittle slit processes similar to that observed in pipes subjected to internal pressure as shown in Figure 8.



Figure 29. Off-Axis Slit Failure that Initiated on the ID Due to an Impinging Rock

Figure 30 shows a PLEXCO PE 2306 MDPE gas pipe specimen that failed in field service due to an impinging rock. Visual and microscopic examinations showed that this rock-impingement field failure resulted in a slit that initiated on the inner pipe surface and grew

through the pipe wall to the outer surface. The orientation of the slit was slightly off the pipe longitudinal axis.



Figure 30. Rock Impingement Failure Induced in Field Service

The fracture surface was examined using optical microscopy. Figure 31 shows the fracture surface morphology under magnification. This figure shows the crack initiation point on the ID and the progressive SCG growth of the damage zone and the crack. This SCG failure process is manifested in the form of the striation marks corresponding to the progressive incubation, initiation and growth of the crazed material over several periods.

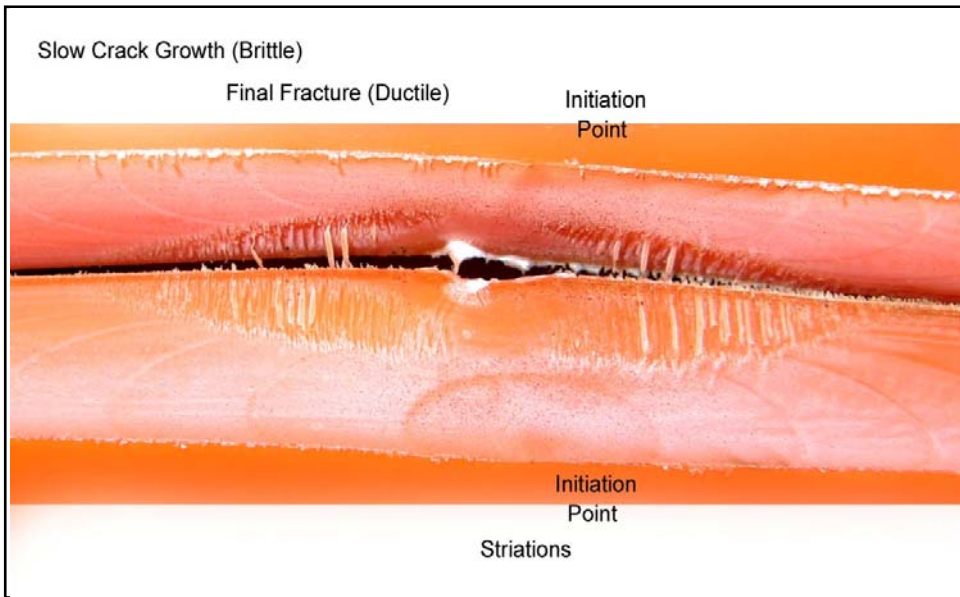


Figure 31. Micrograph of the SCG Fracture Surface of a Rock Impingement Failure

SCG Failures Due to Squeeze-Off Operations

When a pipe is subjected to a squeeze-off, for instance along the 6 o'clock-12 o'clock direction, the amount or percent of squeeze is measured from the point at which the two inner pipe surfaces first establish surface-to-surface contact. Laboratory examinations of some older MDPE gas pipe materials that failed due to a squeeze-off show that between about 15% and 25% squeeze, damage initiates on the inner pipe surface at the squeeze "ears" that are produced along the 3 o'clock-9 o'clock direction.

Figure 32 is a photograph of an Aldyl-A pipe sample that exhibited SCG failure/leak at the ears of the squeeze-off. Figure 33 shows the inner surface of the Aldyl-A pipe sample shown in Figure 32.

Figure 32 and Figure 33 demonstrate that the squeeze-off caused material crazing manifested in the form of material whitening, discoloration, and some surface roughening. The craze initiated first on the inner surface at the squeeze "ears". Then the damage grew through the wall and unto the outer surface. As the amount of squeeze, or pipe wall compression increased, more of the material experienced crazing/damage.



Figure 32. Failure of an Aldyl-A Pipe at Squeeze Ears



Figure 33. Inner Surface of an Aldyl-A Pipe Subjected to About 15% Squeeze

With excessive squeeze-off, large voids, whitening, and cracks develop at the squeeze ears on the inner pipe surface. At the ears, the pipe undergoes permanent localized large plastic deformations and wall thinning. Also, an axial slit can initiate on the inner pipe surface at the “ears” and grow axially through the pipe wall. Photographs of a MDPE 2306 pipe that failed in field service due to excessive squeeze-off are shown in Figure 34 to Figure 36.



Figure 34. MDPE Pipe that Failed in Field Service Due to a Squeeze-Off

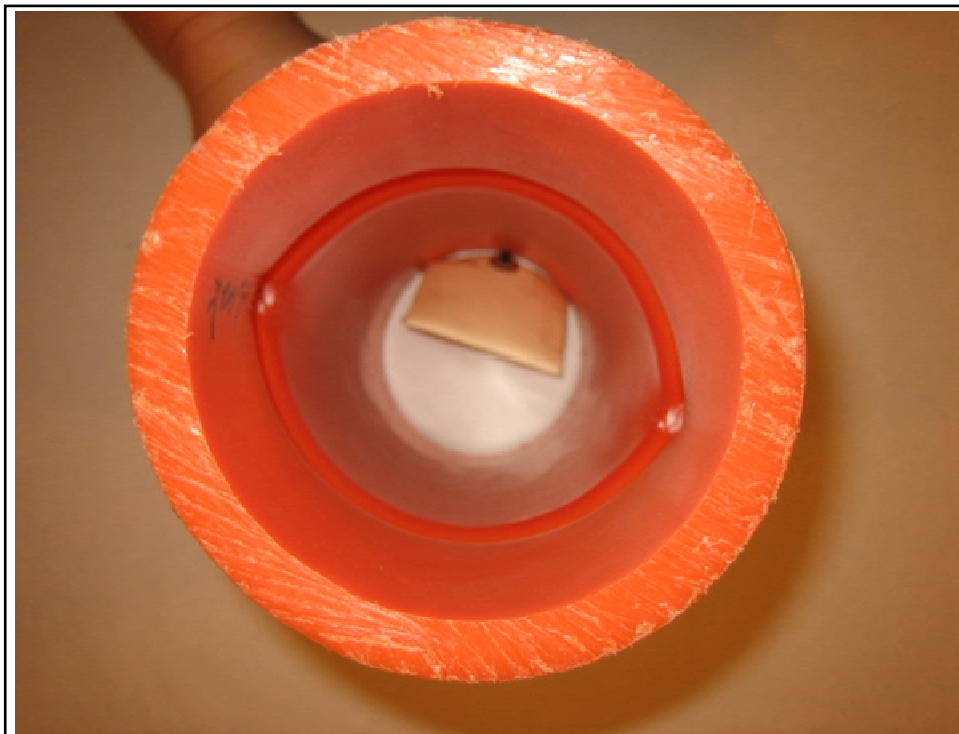


Figure 35. End View Depicting Large-Scale Deformations Due to a Squeeze-Off



Figure 36. Pipe ID with Axial Slit at the Ears of Pipe Shown in Figure 34

The observed SCG slit failure mode in the squeezed pipe specimen is similar to failures exhibited by specimens subjected to internal pressure or internal pressure combined with a rock impingement load. The SCG failure mode observed in squeeze-off involves the progressive striations indicative of incubation and growth of the crack-tip-opening displacement (CTOD) through the pipe wall.

Short-Term Laboratory Tests

A number of short-term tests have been performed on plastic pipe materials received from different gas companies and resin and pipe manufacturers. The short-term tests were performed to determine whether or not the material properties and/or the short-term mechanical strength properties of PE gas pipe materials have undergone any detrimental changes due to aging in field service. Melt Index, Tensile Strength, Quick Burst, PENT, and Bend-Back Tests were conducted to determine whether or not they can provide information on the relative susceptibility of PE pipe materials to SCG failures.

Melt Index

Table 2 presents the Melt Index data published by DuPont on Aldyl-A pipe materials manufactured during the period 1965 to 1992. However, other sources of information (unconfirmed by DuPont) reported that DuPont made several changes to the PE resin, the co-polymer, and/or polymerization catalyst used for manufacturing Aldyl-A gas pipe materials during the period 1965 to 1992. Table 3 presents data made available to GTI by other sources (unconfirmed by DuPont) on the various Aldyl-A pipe materials manufactured by DuPont. Table 2 lists the Aldyl-A material density, the name and type of resin, and the amount or the type of the co-polymer used for manufacturing Aldyl-A pipe materials during the period 1965 to 1992.

ALDYL-A Melt Index and Density Data (1965 – 1992)

Table 2. Aldyl-A Melt Index Data 1965 - 1992 (DuPont)

Manufacturing Period	Manufacturer Reported Melt Index (g/10 min)
1965 – 1970	1.9
1971 - 1983	1.2
1983 - 1987	1.1
1988 - 1991	1.1
1992	1.1

Table 3. Aldyl-A Density Data, 1965 -1992 (unconfirmed by DuPont)

Manufacturing Period of an Aldyl-A Pipe Group	Density (g/cm ³)	Resin Trade Name/Number	Co-Monomer Type
1965 to 1969	0.933	Alathon/5040	Butene
1970 to 1983	0.938	Alathon/5043	Butene
1984 to 1987	0.938	Alathon/5046	Octane
1988	0.938	Alathon/5046 C	Octane (increased amount)
1989	0.933	Alathon/5046 U	Octane (increased amount)
1990 to 1991	0.933	Alathon/5046 O	Octane (changed amount and type)
1992	0.933	UAC 2000 / TR-418	Hexene

The melt index and density are important material properties of the resin. Changes in these properties are indicative of changes in the resin, co-polymer, catalyst and crystallinity, molecular structure, aging, or potential degradation of the PE material.

Changes in the PE monomer resin, the co-polymer, and or the catalysts used during polymerization have direct effect on the Melt Index (MI), the density, and the molecular weight, number, and distributions. The MI is related to the PE material molecular weight and distribution. The MI is an important material property of a PE pipe material. Changes in the MI can have a direct and important effect on the amount of melted material and flow rates, bonding, and solidification rates during heat-fusion or electro-fusion joining of PE gas pipe materials.

Changes in the MI of a PE pipe material are indicative of changes in density and crystallinity. Tests have shown that as the density increases, the amount of crystallinity of PE materials increases and the melt flow index decreases.

GTI database includes laboratory test data on the melt flow index of a several Aldyl-A pipe lot materials. The melt index data were obtained per ASTM D 1238 Specifications.

GTI’s MI test data presented in Table 4 is the average of three replicate test specimens prepared from pipe samples removed from field service. The MI test data presented in Table 4 was measured by GTI for several Aldyl-A pipe materials made of 4-inch and 6-inch pipe sizes and manufactured during different periods including 1971, 1983, and 1988 (see Table 2). For comparative evaluations, Table 4 also gives the MI data generated by DuPont for similar unexposed (virgin) resins or pipe materials.

Table 4. Comparative of Melt Index Test Data

Test Sample #	Pipe Diameter (Inches)	Pipe Manufacturing Year	Manufacturing Period of the Resin Group	Melt Index-GTI Lab Data (g/10min)	Melt Index-DuPont Data (g/10min)
1a	4	1980	1971	1.28	1.2
2a	4	1984	1983	1.09	1.1
3a	4	1986	1983	1.08	1.1
4a	4	1988	1988	1.00	1.1
1b	6	1980	1971	1.12	1.2
2b	4	1981	1971	1.24	1.2
3b	6	1982	1971	1.18	1.2
1c	4	1983	1983	1.08	1.1
2c	6	1984	1983	0.93	1.1
3c	4	1985	1983	1.08	1.1
4c	6	1985	1983	1.02	1.1
1d	4	1986	1983	1.19	1.1
2d	6	1986	1983	0.91	1.1

Comparative evaluations show negligible difference between the average MI of the Aldyl-A pipes that were in underground gas service for about 25 years and the average MI data of the virgin unexposed pipe materials that were published by DuPont. The negligible differences in the MI measurements are most likely due to laboratory-to-laboratory variability.

Therefore, it may be concluded that aging in field service had negligible effects on the MI of the listed Aldyl-A materials even though DuPont used different resins and copolymers in processing these materials (see Table 3).

It may be concluded that Melt Index test data may not provide information on the relative susceptibility of PE gas pipe materials to SCG field failures.

Tensile Strength

GTI database includes data obtained from several short-term mechanical strength tests. One of these tests is the Tensile Test conducted in accordance with ASTM D638. Tensile tests were conducted on Aldyl-A pipe samples that were removed from gas service. Table 5 presents the average tensile strength data (of several replicate samples) obtained on the listed Aldyl-A MDPE pipe samples and on a newer shelf-aged “virgin” MDPE gas pipe material manufactured in 2001. It may be noted that these pipe material were manufactured during different years spanning the period 1970 to 1991 and were installed in different geographical regions throughout the U.S. Hence, some samples were in gas service for 30 years and others were in service for 12 years. One of the Aldyl-A pipe materials listed in Table 5 was in gas service for about 10 years.

Since any changes in the tensile strength properties may be indicative of aging in field service and consequently increased susceptibility to SCG failures, one may compare the tensile strength properties of the Aldyl-A MDPE gas pipe materials listed in Table 5.

Table 5. Comparative of Average Tensile Strength Test Data

Pipe Material /Year of Manufacture	Tensile Strength (psi)	% Elongation at Break	% Elongation at Yield	Modulus (psi)	Stress at Break (psi)
3" IPS SDR 11.5 DuPont Aldyl A /1970	2,775	635	15	121,000	1,947
3" IPS SDR 11.5 DuPont Aldyl A /1977	2,773	588	13	141,000	1,767
4" IPS SDR 11.5 DuPont Aldyl A	2,758	534	12	136,000	1,683
3" IPS SDR 11.5 DuPont Aldyl A /1983	2,862	605	14	139,00	1,885
4" IPS SDR 11.5 DuPont Aldyl A /1991	2,799	625	14	131,000	2,324
2" SDR 11 Aldyl-A Pipe /1973 (Removed from Service in 1983)	2,275			105,000	
Uponor UAC 2000 MDPE /2001	3,180	619	12	122,000	3,179

It should be noted that the newer Uponor MDPE pipe manufactured in the year 2001 was compounded using a totally different resin and processing methods. The Uponor material is listed to show the significantly increased tensile strength and the stress at break compared to the other older Aldyl-A materials.

On the basis of the comparative evaluations, it may be noted that there are negligible differences between materials in the tensile strength, percent elongation at break and at yield, and

tensile modulus. The stress at break of the 1991 pipe material is about 10-15% greater than the average of other samples.

Hence, aging in field service had negligible effects on the tensile strength properties even though DuPont used different resins and copolymers in processing these materials (see Table 3).

It may be concluded that short-term tensile strength properties may not provide information on the relative susceptibility of PE gas pipe materials to SCG field failures.

Quick Burst

Another short-term mechanical strength test performed is the Hydrostatic Quick Burst Test. It is performed in accordance with ASTM D1599 on pipe samples removed from gas service.

Table 6 presents the average Quick Burst (QB) pressure test data, as an average of several replicate specimens, determined for the listed pipe materials. Again, it should be noted that these pipe material were manufactured during different years spanning the period 1970 to 1991. Some of the pipe materials were in gas service for about 30 years and others were in service for about 12 years.

Table 6 also presents the average hoop stress corresponding to the measured QB pressure. The hoop stress is computed using a simple formula developed in books on mechanics of materials for thin-wall pipe. This formula is given as Equation 1 in a subsequent section.

Table 6. Comparative of Average Quick Burst Pressure Test Data

Pipe Material	Average Ductile Quick Burst Pressure, psig	Average Ductile Hoop Stress, psi
3" IPS SDR 11.5 DuPont Aldyl-A (1970)	627	3,145
4" IPS SDR 11.5 DuPont Aldyl-A (1980)	659	3,232
3" IPS SDR 11.5 DuPont Aldyl-A (1983)	667	3,294
4" IPS SDR 11.5 DuPont Aldyl-A (1988)	647	3109
2"SDR11 Aldyl-A Pipe (1973) Removed from Gas Service in 1983	668	3,340
Uponor UAC 2000 (2001)	592	2,866

Comparative evaluations of the QB pressure test data or the average hoop stress show negligible differences in the average QB pressure determined for the various pipes.

Therefore, it may be concluded that aging in field service had negligible effects on the quick burst pressure properties of the listed Aldyl-A materials even though DuPont used different resins and copolymers in processing these materials (see Table 3).

It may also be concluded that Quick Burst Pressure test data may not provide information on the relative susceptibility of PE gas pipe materials to SCG field failures.

PENT

The "PENT" test was developed to measure the resistance of PE gas pipe materials to SCG failure. It is performed in accordance with ASTM F 1473 Specification entitled "Notch Tensile Test to Measure the Resistance to SCG of polyethylene pipes and resins". It is conducted on

notched rectangular specimens cut from either a PE pipe or from a compression molded PE plaque material. Figure 37 shows a schematic illustration of the PENT test specimen. Figure 38 shows three notched PE PENT test samples.

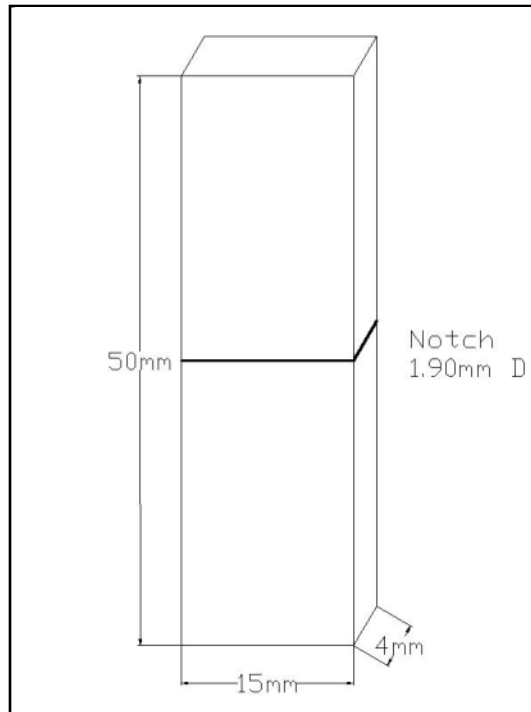


Figure 37. Schematic Illustration of the Rectangular PENT Test Specimen



Figure 38. Notched MDPE Test Specimens

The rectangular specimens are carefully notched and placed under a constant tensile load. The PENT test is conducted at a temperature of 80°C and under a tensile stress of 2.4 MPa. The time to failure of a specimen in the PENT test is a measure of the resistance of the PE material to SCG-failure. The greater the PENT failure time, the greater is the resistance to SCG failure. The

PENT test failure time is measured from the instant that the tensile load is applied and until the PENT test specimen experiences complete SCG fracture.

To simulate field failures, the PENT test specimens should exhibit brittle SCG failures. Thus, in PENT tests, the magnitude of the tensile test loads should be properly determine and applied in order to mitigate any bending. In the PENT test, the fracture initiates at the tip of the main notch and grows step-wise in a brittle SCG manner through the specimen thickness. The brittle SCG crack growth continues and finally the outermost (skin) layer of the PENT specimen experiences ductile cleavage/fracture.

Figure 39 and Figure 40 show the mating fractured surfaces, at low magnification, of two PENT test specimens, that experienced SCG brittle fracture in the PENT test. The two specimens were prepared from two different PE gas pipe materials. The brittle SCG failure mode in the PENT test specimen is evident from the observed discoloration, whitening and the crack-growth striations (rings) that are observed in the fractured surface.

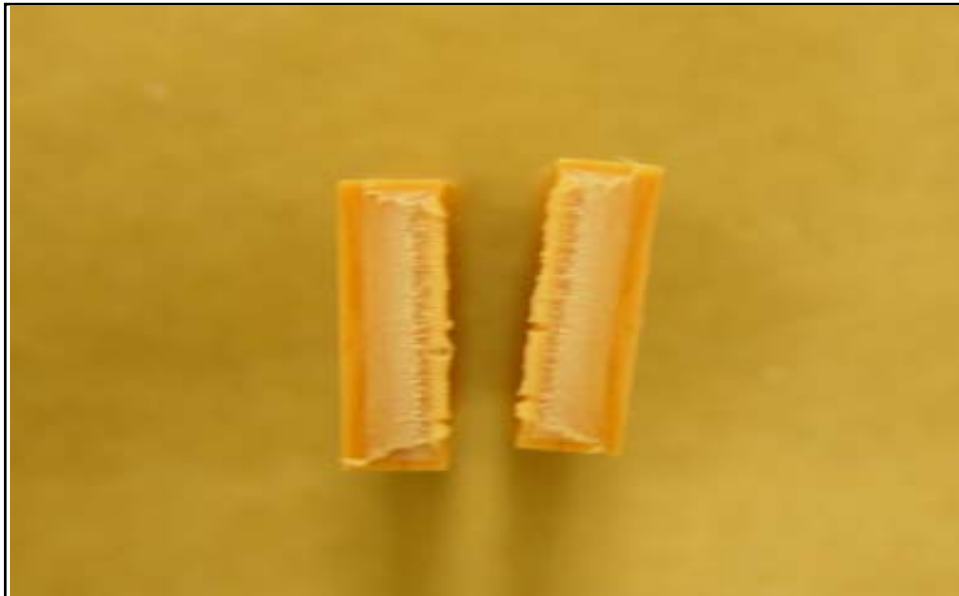


Figure 39. Brittle SCG Failure of a PLEXCO MDPE 2406 PENT Test Specimen

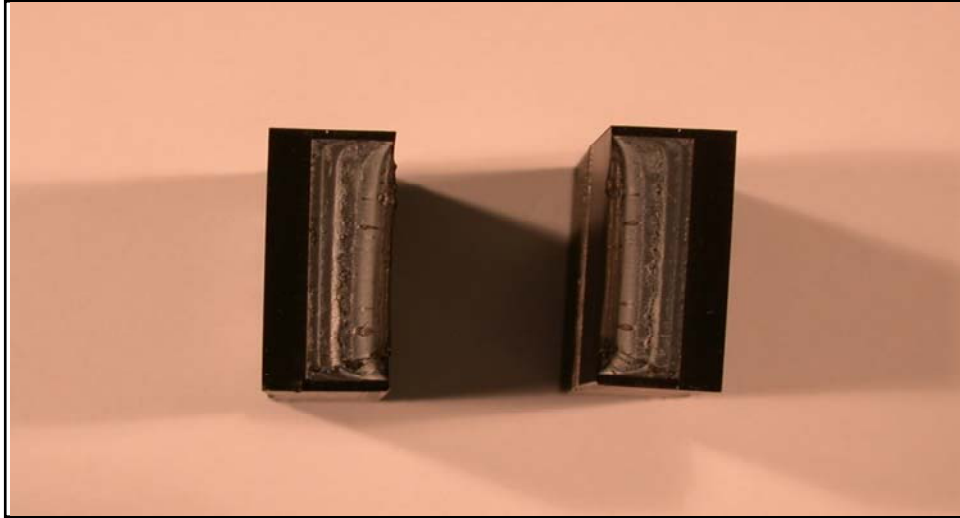


Figure 40. Brittle SCG Failure of HDPE Performance Pipe PENT Test Specimen

GTI database includes a large body of PENT test data on many different MDPE and HDPE gas pipe materials including Aldyl-A pipes. GTI performed PENT tests on many different Aldyl-A pipe materials. A few of these pipe materials were manufactured in the same year but were installed at different geographical regions through-out the U.S.

Table 7 through Table 10 present the PENT test data including the PENT failure times, at a test temperature of 80°C for 14 different Aldyl-A pipe materials. The Tables also give the specimen and notch dimensions. For each pipe material, the PENT test failure time is the average of a minimum of three replicate test specimens.

Table 7 presents the measured PENT test failure times of three different Aldyl-A pipe materials manufactured in 1973, 1974, and 1975, respectively.

Table 7. PENT Test Failure Time of Aldyl-A Pipe Lots (1973 - 1975)

Year of Pipe Production	Specimen	Failure Time (Hrs)	Length (mm)	Width (mm)	Thickness (mm)	Cross-Sect. Area (mm) ²	Notch Depth (mm)	Side Notch Depth (mm)	Weight Grams	Station Arm Ratio (In.)	Avg. Failure (Hrs)
1973	3A	1.4	49.97	14.89	5.95	88.60	2.49	0.50	4327	5.015	
1973	3B	1.4	49.94	14.92	5.90	88.03	2.48	0.50	4299	5.015	
1973	3C	1.4	49.92	14.94	5.91	88.30	2.48	0.50	4323	5.003	1.4
1973	4A	1.2	49.92	14.93	5.84	87.19	2.46	0.50	4259	5.015	
1973	4B	1.3	49.91	14.89	5.80	86.36	2.46	0.50	4225	5.007	
1973	4C	1.3	49.91	14.92	5.93	88.48	2.48	0.50	4321	5.015	1.3
1974	1A	0.8	50.03	15.04	5.88	88.44	2.47	0.50	4319	5.015	
1974	1B	1.6	50.01	14.96	5.80	86.77	2.46	0.50	4238	5.015	
1974	1C	1.4	49.98	14.87	5.77	85.80	2.45	0.50	4191	5.015	1.3
1974	5A	1.7	49.99	14.97	5.89	88.17	2.48	0.50	4307	5.015	
1974	5B	1.6	49.92	14.99	5.70	85.44	2.43	0.50	4173	5.015	
1974	5C	1.3	49.97	14.97	5.88	88.02	2.47	0.50	4299	5.015	1.5
1975	2A	1.2	49.97	14.98	5.88	88.08	2.47	0.50	4302	5.015	
1975	2B	1.3	49.99	14.96	5.90	88.26	2.48	0.50	4311	5.015	
1975	2C	1.1	49.99	15.08	5.77	87.01	2.45	0.50	4250	5.015	1.2
1975	6A	3.4	49.92	15.11	6.01	90.81	2.50	0.50	4435	5.015	
1975	6B	2.7	49.92	15.08	5.86	88.37	2.47	0.50	4316	5.015	
1975	6C	2.6	49.84	15.10	5.86	88.49	2.47	0.50	4322	5.015	
1975	6D	3.2	49.85	15.09	6.02	90.84	2.50	0.50	4437	5.015	3.0

Table 8 lists the measured PENT failure times for four different Aldyl-A pipe materials manufactured in 1976, 1977, 1978, and 1979.

Table 8. PENT Test Failure Time of Aldyl-A Pipe Lots (1976 – 1979)

Year of Pipe Production	Specimen	Failure Time (Hrs)	Length (mm)	Width (mm)	Thickness (mm)	Cross-Sect. Area (mm) ²	Notch Depth (mm)	Notch Depth (mm)	Weight Lbs.	Weight Grams	Station Arm Ratio (In.)	Avg. Failure (Hrs)
1976	A	1.3	49.94	15.01	5.76	86.46	2.45	0.50	9.31	4223	5.015	
1976	B	1.1	49.96	14.99	5.75	86.19	2.45	0.50	9.28	4210	5.015	
1976	C	1.1	49.94	15.04	5.74	86.33	2.44	0.50	9.32	4227	5.003	1.2
1977	A	0.5	49.89	15.11	5.73	86.58	2.44	0.50	9.32	4229	5.015	
1977	B	0.6	49.94	15.01	5.74	86.16	2.44	0.50	9.29	4215	5.007	
1977	C	0.6	49.89	15.09	5.76	86.92	2.45	0.50	9.36	4245	5.015	0.6
1978	A	2.9*	49.94	14.99	5.75	86.19	2.45	0.50	9.28	4210	5.015	*
1978	B	0.6	49.91	14.99	5.72	85.74	2.44	0.50	9.23	4188	5.015	
1978	C	0.8	49.91	15.06	5.72	86.14	2.44	0.50	9.28	4207	5.015	0.7
1979	A	1.2	49.86	24.92	8.28	206.34	3.00	0.50	22.22	10078	5.015	
1979	B	1.0	49.91	25.04	8.14	203.83	2.97	0.50	21.95	9955	5.015	
1979	C	1.1	49.89	24.87	3.00	74.61	1.84	0.50	8.03	3644	5.015	1.1

Table 9 lists the PENT test failure times for four Aldyl-A pipe materials manufactured in 1979, 1980, 1981, and 1982.

Table 9. PENT Test Failure Time of Aldyl-A Pipe Lots (1979 – 1982)

Year of Pipe Production	Specimen	Failure Time (Hrs)	Length (mm)	Width (mm)	Thickness (mm)	Cross-Sect. Area (mm) ²	Notch Depth (mm)	Side Notch Depth (mm)	Weight Lbs.	Weight Grams	Station Arm Ratio (In.)	Avg. Failure (Hrs)
1979	A	0.9	49.78	15.24	5.73	87.33	2.44	0.50	9.40	4265	5.015	
1979	B	0.9	49.91	15.06	5.74	86.44	2.44	0.50	9.31	4222	5.015	
1979	C	0.9	49.86	15.01	5.74	86.16	2.44	0.50	9.30	4218	5.003	0.9
1980	A	0.8	49.81	15.01	5.76	86.46	2.45	0.50	9.31	4223	5.015	
1980	B	0.9	49.86	15.09	5.73	86.47	2.44	0.50	9.33	4230	5.007	
1980	C	0.9	49.91	14.96	5.76	86.17	2.45	0.50	9.28	4209	5.015	0.9
1981	A	0.5	49.86	15.01	5.74	86.16	2.44	0.50	9.28	4208	5.015	
1981	B	0.7	49.86	15.01	5.76	86.46	2.45	0.50	9.31	4223	5.015	
1981	C	1.1	49.86	15.06	5.74	86.44	2.44	0.50	9.31	4222	5.015	0.8
1982	A	0.6	49.81	14.91	5.74	85.58	2.44	0.50	9.22	4180	5.015	
1982	B	0.7	49.83	14.94	5.74	85.76	2.44	0.50	9.23	4188	5.015	
1982	C	1.6	49.94	15.06	5.74	86.44	2.44	0.50	9.31	4222	5.015	1.0

Table 10 lists the PENT test failure times for three Aldyl-A pipe materials manufactured in 1983, 1984, and 1985.

Table 10. PENT Test Failure Time of Aldyl-A Pipe Lots (1983 – 1985)

Year of Pipe Production	Specimen	Failure Time (Hrs)	Length (mm)	Width (mm)	Thickness (mm)	Cross-Sect. Area (mm) ²	Notch Depth (mm)	Side Notch Depth (mm)	Weight Lbs.	Weight Grams	Station Arm Ratio (In.)	Avg. Failure (Hrs)
1983	A	0.9	49.86	15.06	5.75	86.60	2.45	0.50	9.32	4229	5.015	
1983	B	0.8	49.81	15.14	5.77	87.36	2.45	0.50	9.41	4267	5.015	
1983	C	1.0	49.89	14.91	5.76	85.88	2.45	0.50	9.27	4205	5.003	0.9
1984	A	6.5	49.89	15.06	5.72	86.14	2.44	0.50	9.28	4207	5.015	
1984	B	8.5	49.86	15.04	5.73	86.18	2.44	0.50	9.29	4216	5.007	
1984	C	6.9	49.99	14.96	5.74	85.87	2.44	0.50	9.25	4194	5.015	7.3
1985	A	22.6	49.83	14.86	5.73	85.15	2.44	0.50	9.17	4159	5.015	
1985	B	20.0	49.81	14.88	5.75	85.56	2.45	0.50	9.21	4179	5.015	
1985	C	21.7	49.76	15.11	5.75	86.88	2.45	0.50	9.36	4244	5.015	21.4

From Table 7 through Table 10, it may be noted that the PENT failure time for Aldyl –A pipe materials manufactured during the period 1973 to 1983 ranged between 0.6 hours and 3.0 hours. The PENT failure time for the Aldyl-A pipe materials manufactured in 1984 and 1985 increased to about 7.3 hours and 21.4 hours, respectively.

It should be noted that all the Aldyl-A pipe materials presented in Table 7 through Table 10 have a PENT failure time ranging between 0.6 hours and 21.4 hours. However these Aldyl-A pipe materials continue to remain in gas service. Some of these materials have been in gas service for more than 35 years.

Table 11 lists the PENT failure times for two newer “virgin” un-exposed PE gas pipe materials that were manufactured in 2001 and 2002, namely: Polypipe 4810 HDPE 3408 and Driscopipe 8100 HDPE 3408. Neither of these pipe materials was installed in gas service. The average PENT failure time of the Polypipe material was about 229.1 hours. The Driscopipe had an average PENT test time of 524 hours. The PENT failure times for both of these materials is significantly improved compared to the above listed Aldyl-A pipes.

Table 11. PENT Test Failure Times for Polypipe 4810 and Driscopipe 8100

Specimen	Failure Time (Hrs)	Length (mm)	Width (mm)	Thickness (mm)	Cross-Sect. Area (mm) ²	Notch Depth (mm)	Side Notch Depth (mm)	Weight Lbs.	Weight Grams	Station Arm Ratio (In.)
Print line: POLYPIPE 4810 GAS PE 3408 2" IPS SDR11 ASTM D2513 CDC API 15 LE X33 LO4 3GD 03APR02										
D4	220.9	50.00	15.00	6.02	90.30	2.50	0.50	9.72	4410.46	5.015
D5	250.8	50.02	15.08	6.03	90.93	2.51	0.50	9.79	4441.35	5.015
D6	215.7	50.06	15.04	6.01	90.39	2.50	0.50	9.73	4414.87	5.015
Print line: 2" IPS DR11 DRISCOPIPE 8100® GAS PE 3408 CEC ASTM D2513 WT11 12 DEC 01 A3 R (WITH YELLOW JACKET REMOVED)										
G4	528.1	50.07	15.02	6.03	90.57	2.51	0.50	9.75	4423.67	5.015
G5	503.1	50.00	15.02	6.03	90.57	2.51	0.50	9.75	4423.67	5.015
G6	540.9	50.00	15.04	6.03	90.69	2.51	0.50	9.81	4451.76	4.990

The applicability of the PENT test has been the subject of several investigations that were conducted by different organizations. The Plastics Pipe Institute (PPI) published its report number TN-21/2000 entitled “PPI PENT Test Investigation”. This report presented the test results of a “round-robin” study on the PENT test performed by several different laboratories. This report stated that the test data showed that there is no apparent correlation between the PENT results and those of the Accelerated LTHS Rupture Test per ASTM D 1598. The ASTM D 1598 test is used to determine the long-term strength and the corresponding Hydrostatic Design Basis (HDB) of PE pipe materials. The results of the PPI investigation have shown significant laboratory-to-laboratory variability in the PENT test data.

It should be noted that the PENT test is not considered a short-term test. PENT test failure times for some newer PE pipe materials may exceed 10,000 hours. However, for the Aldyl-A pipe materials presented above, the PENT Failure time was less than about 25 hours; this is why in this section the PENT test is considered a short-term test.

Correlations between the PENT failure time and the field failure time of PE gas pipe materials are currently inconclusive. Therefore, it may be concluded that the PENT failure time may provide some useful relative reference on the susceptibility of PE gas pipe materials to SCG field failures.

Bend Back

The purpose of the bend-back test is to visually determine whether or not a PE pipe material is a problematic low ductile inner wall (LDIW) pipe material. LDIW materials were the result of improper extrusion and/or cooling during manufacturing during the period 1971-1972. This improper processing caused a few Aldyl-A pipe lots to be manufactured with inferior material and poor physical properties. These inferior Aldyl-A pipe lot materials consisted of a coarse “granular-like” microstructure referred to as a spherulitic microstructure.

The LDIW type of PE material has low fracture resistance and is highly susceptible to premature brittle slow-crack-growth (SCG) failure. Several inferior LDIW pipe lot materials exhibited pre-mature brittle SCG failure in gas service. During the period 1972-1973, the pipe manufacturer (DuPont) identified this problematic pipe material and introduced corrective pipe processing and cooling methods.

To perform a bend-back test on a PE pipe material, 1-inch wide rings are cut from the pipe material. Each ring is then cut into two sectors. Each ring sector or strip is bent-back on itself (i.e. inside surface is bent outwards). Figure 41 shows a typical ring-sector before and after the bend-back test.

During the bend-back test, the bent test sector specimen is visually inspected to determine if any surface crazing or damage manifested in the form of whitening, discoloration, and/or surface roughening is visible on the inside surface of the sector-strip. The crazing consisting of whitening and surface roughening indicates material damage and is indicative of the presence of “LDIW” material and the high probability that the PE pipe material will experience pre-mature SCG field failure.



Figure 41. Ring Sector Specimen Before and After the Bend Back Test

Bend-Back Test Conducted on a LDIW Material from February 1971

For comparative purposes, the results of the bend-back test are presented to visually illustrate the presence of LDIW material. Sector specimens prepared from an Aldyl-A PE 2306 material manufactured in February 1971 were subjected to bend-back tests. Figure 42 shows the surface crazing consisting of discoloration, whitening, and surface roughening. The observed material crazing is typical of a LDIW pipe material and is indicative of an inferior spherulitic microstructure that is susceptible to pre-mature brittle SCG failure.

Figure 42 can be used as a reference to compare with other PE pipe materials.



Figure 42. Bend-Back Test Exhibiting LDIW Surface Features

Bend-Back Test Conducted on a LDIW Material from March 1971

The results of the Bend-Back test on this LDIW material are also presented for comparative evaluations. Figure 43 shows a sector specimen made from the Aldyl-A PE 2306 pipe material manufactured in March 1971. Figure 43 shows the surface crazing consisting of discoloration, whitening, and surface roughening. The observed crazing is indicative of an inferior LDIW Aldyl-A pipe material due to a spherulitic microstructure that is susceptible to pre-mature brittle SCG failure.

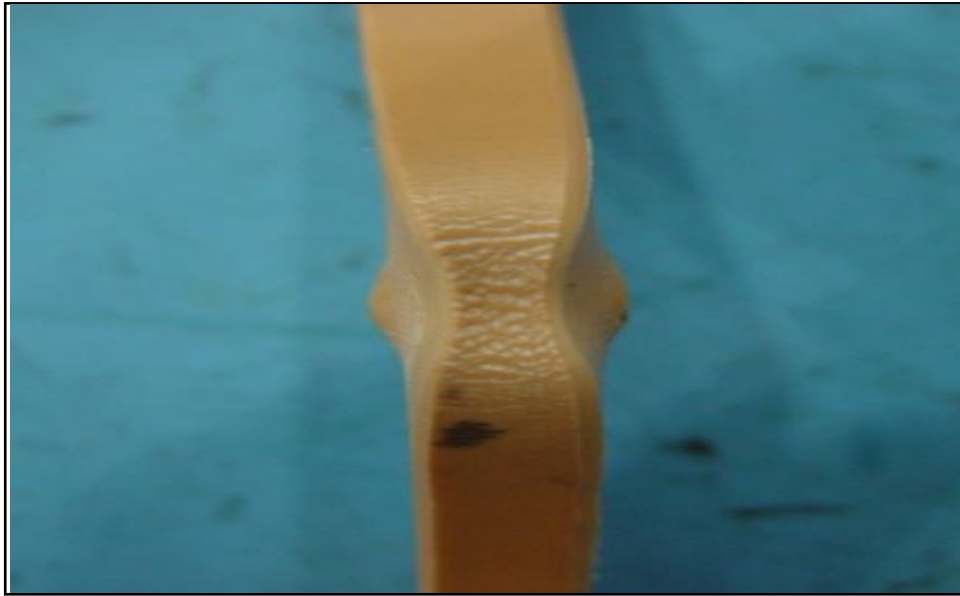


Figure 43. Bend-Back Test Exhibiting LDIW Surface Features

Bend-Back Tests Conducted on Non-LDIW Materials (1970, 1972-1993)

Bend-back tests were performed on many other Aldyl-A pipe materials that were manufactured in 1970 and during the period 1972 to 1993. Figure 44 through Figure 51 show photographs of bend-back tests performed on ring-sector specimens prepared from pipe materials manufactured in 1970, 1972, 1973, 1974, 1976, 1986, 1991, and 1993, respectively. Tests results showed that none of these pipe materials exhibited any surface discoloration, whitening, or surface roughening suggesting that none of these test samples have the LDIW material.



Figure 44. Bend Back Test of a 1970 Aldyl-A Material

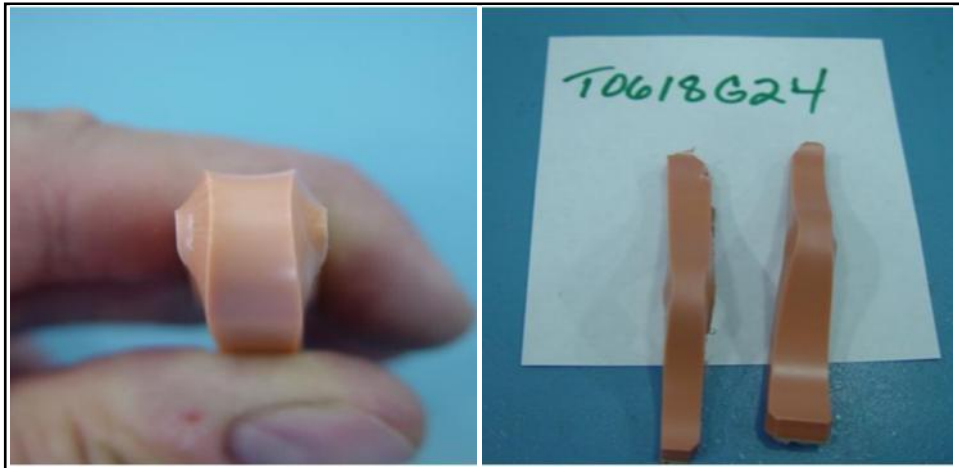


Figure 45. Bend Back Test of a 1972 Aldyl-A Material (During and After)

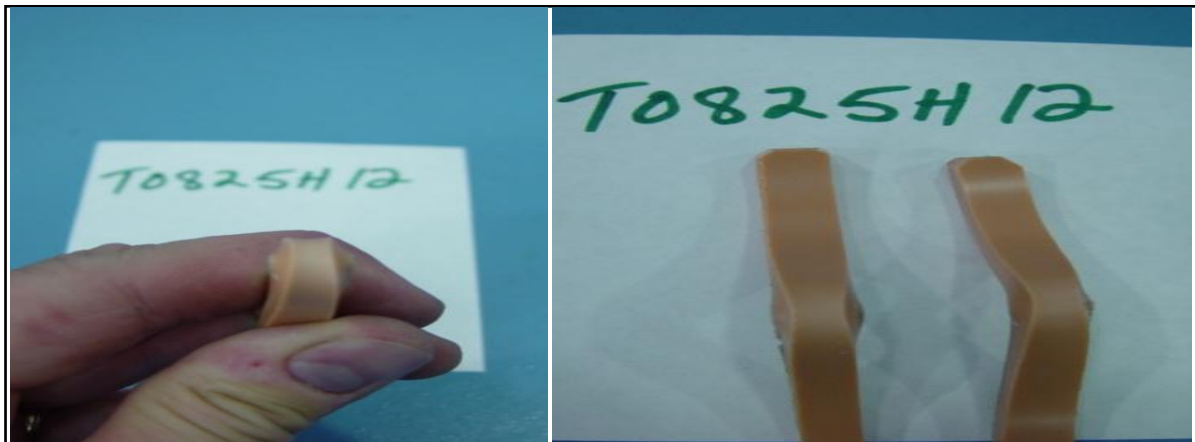


Figure 46. Bend Back Test of a 1973 Aldyl-A Material (During and After)



Figure 47. Bend Back Test of a 1974 Aldyl-A Material

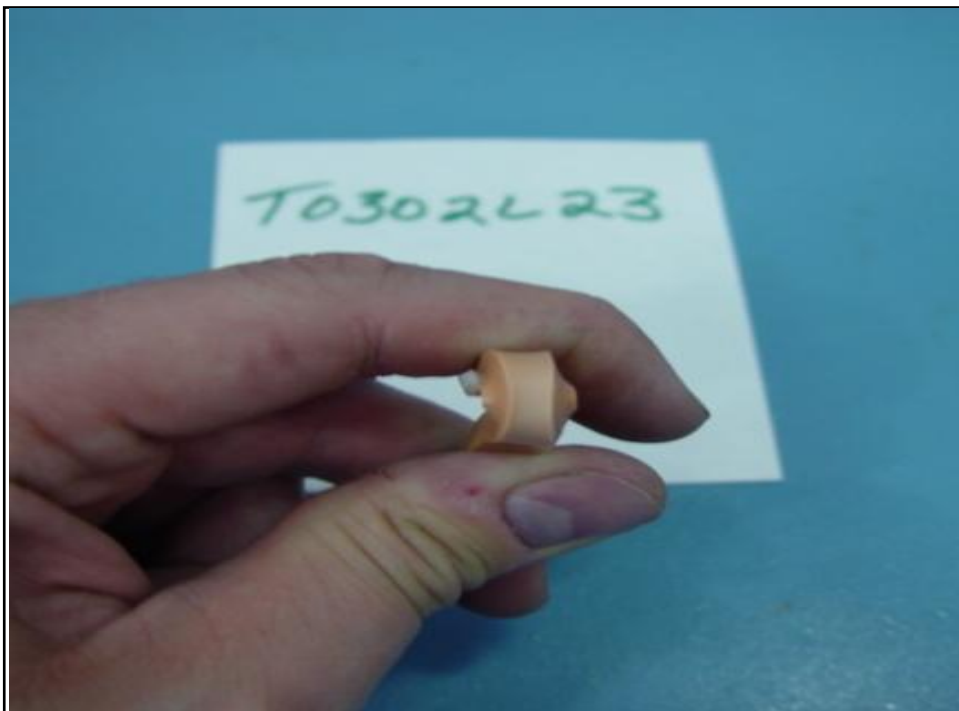


Figure 48. Bend Back Test of a 1976 Aldyl-A Material



Figure 49. Bend Back Test of a 1986 Aldyl-A Material



Figure 50. Bend Back Test of a 1991 Aldyl-A Material



Figure 51. Bend Back Test of a 1993 Aldyl-A Material

Comparative evaluations of Figure 41 through Figure 51 show that Aldyl-A pipe materials manufactured in 1970, 1972, 1973, 1974, 1976, 1986, 1991, and 1993 do not exhibit any of the surface characteristics typical of materials having the LDIW inferior microstructure.

The test data and information presented above show that the Bend-Back test may be used to visually observe and identify qualitatively PE gas pipe materials that have the inferior LDIW material and hence a high probability that these materials will experience brittle SCG field failure.

Accelerated Long Term Hydrostatic Stress-Rupture (LTHS) Tests

Extensive accelerated LTHS test data have been generated by GTI and others on PE gas pipe materials removed from service. The LTHS tests are conducted in accordance with ASTM D1598 Specification entitled: Standard Test Method for Time-to-Failure of Plastic Pipe under Constant Internal Pressure. Time-to-failure is measured for test specimens held at a constant internal pressure in a controlled environment. LTHS test data is used to determine hydrostatic design basis (HDB) by establishing a relationship between hoop stress and failure time.

GTI database includes accelerated LTHS test data generated at several elevated test temperatures including 80°C and 90°C and at several internal test pressures.

Accelerated LTHS Tests with Secondary Stresses

In addition to internal pressure, field operations and service conditions cause pipes to be subjected to secondary stresses or external loads. The secondary stresses include those due to impinging rocks, squeeze-offs, soil loads and subsidence, or pipe bending.

GTI database includes accelerated LTHS test data generated at several elevated test temperatures including 80°C and 90°C and several test pressures combined with a secondary stress simulating a rock impingement load, a squeeze-off, a pipe bending moment, or a transverse earth or soil load.

Squeeze-Off

To subject PE pipe test specimens to squeeze-off, GTI used commercially available double-bar squeeze-off tools. Figure 52 shows one of the commercial tools used to squeeze-off PE pipes. The commercial squeeze-off tool was used to squeeze the pipe test specimens to the stops built into the tool, along the 12 o'clock-six o'clock direction. The pipe specimen was maintained in the maximum squeezed-off position for a period of about four hours. Then, the squeeze-off bar was released and the squeezed specimen was subjected to accelerated LTHS tests. Pipe squeeze-offs were performed on each of the pipe test specimens in accordance with ASTM F 1041 - Standard Guide for Squeeze-Off of Polyolefin Gas Pressure Pipe and Tubing.



Figure 52. Double Bar Squeeze-Off Tool

Rock Impingement

The laboratory fixture shown in Figure 53 was utilized in LTHS tests to subject PE pipes to a surface load that simulated a rock impingement load. The PE pipe test sample was inserted between the two parallel steel plates. A threaded bolt was installed in the center hole of the top plate. A ball bearing was inserted between the pipe outer surface and the tip of the center threaded bolt as shown in Figure 54. The center threaded bolt was turned until the ball bearing was just tight enough to prevent it from slipping. Four outer bolts were then tightened just enough so as not to increase the indentation depth. Then, by turning the center threaded bolt a few additional pre-specified number of turns, an indentation with the required depth was induced in the pipe wall.

Using the rock impingement fixture, several laboratory experiments have been performed to determine the indentation depth that is required to induce the necessary rock impingement load for different pipe sizes and PE pipe materials. GTI has also conducted several analytical evaluations and field experiments to determine the range of magnitude of the rock impingement field loads.



Figure 53. Rock Impingement Loading Fixture

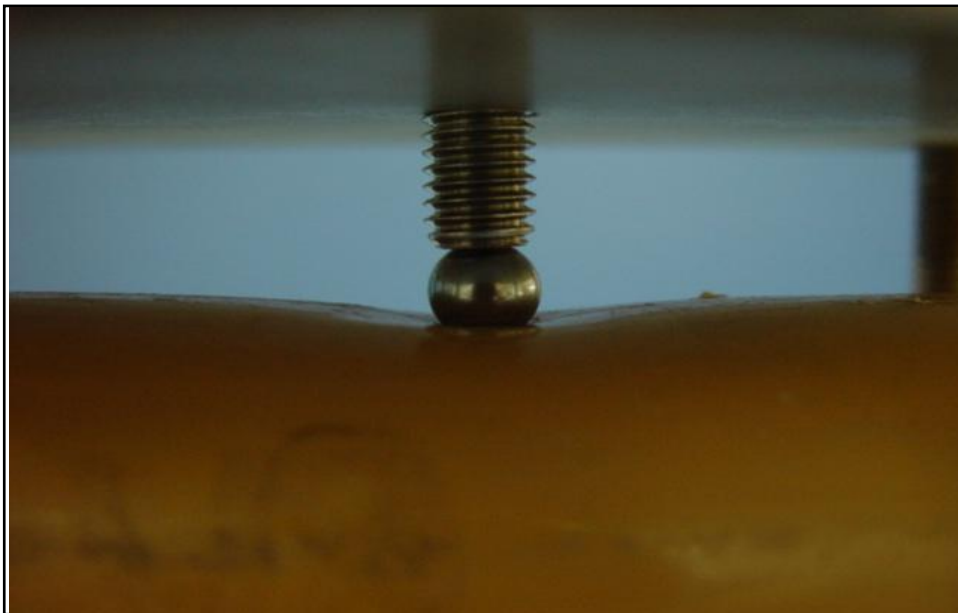


Figure 54. Indentation onto the Pipe Using Ball Bearing

Bending

Figure 55 shows the four-point pipe bending fixture that GTI used to subject PE pipe samples to bending stresses in LTHS tests. The pipe bending fixture consists of two inner adjustable support brackets and two outer adjustable loading brackets. In this laboratory fixture, the pipe test specimen is simply supported by the two inner brackets. The two outer brackets are used to apply a pre-specified bending moment or load on the test specimen.

For testing, the PE pipe test specimens were subjected to a bending radius of about 20 times the pipe outer diameter. While in the fixture under bending, the pipe specimen was pressurized and subjected to accelerated LTHS tests.



Figure 55. Pipe Bending Fixture

Transverse Deflections or Soil Loads

The laboratory fixtures shown in Figure 56 were used to subject PE pipe specimens to transverse deflections secondary stresses. The fixtures consist of two parallel steel plates held together with six threaded bolts. The pipe test specimen was inserted between the two plates, centered and aligned. The six threaded bolts were turned equally until the top plate was slightly pressing against the pipe test specimen. Then, each of the bolts was turned a few additional turns to induce a transverse pipe deflection/deformation of about 5% of the pipe (OD).¹

The end-capped pipe test specimens were maintained in the soil loading fixture when subjected to accelerated LTHS tests.

¹ Pipe manufacturers recommend that in field installations, the pipe transverse vertical deflection due to earth loads should not exceed 5% of the pipe outside diameter OD.



Figure 56. PE Pipe Test Specimens Installed in Earth Load Fixtures

GTI Database on Accelerated LTHS Tests

Utilizing the above described test fixtures and protocols, GTI developed a large database on accelerated LTHS tests on PE pipe test specimens subjected to:

- Internal pressure only;
- Internal pressure combined with a simulated rock impingement load;
- Internal pressure combined with a simulated soil deflection/load;
- Internal pressure combined with a simulated pipe bending load/moment; or
- Internal pressure combined with a secondary stress induced by a pipe squeeze-off.

In accelerated LTHS tests, PE pipe specimens were subjected to the above-described loads until they exhibited a failure manifested in the form of a leak. To accelerate the failure process, the largest percentage of the accelerated LTHS tests was performed at a test temperature of 80°C or 90°C. The time to failure in the LTHS tests was monitored and automatically recorded.

An examination was undertaken to determine the failure mode of all the test specimens that failed/leaked in LTHS tests at elevated temperatures and under internal pressure combined with a secondary stress. The examinations showed that all the pipe specimens in the LTHS tests exhibited a SCG failure process.

Stresses that Drive Crack Initiation and Growth through Pipe Walls

Because of the pipe cooling process, residual circumferential (hoop) and axial stresses develop in the pipe wall. These stresses develop due to the differences in thermal strains resulting from the contractions and expansions experienced by the various material layers making-up the pipe wall. Several experimental investigations were conducted by GTI and other researchers to measure the magnitudes and distribution of residual stresses created in the pipe wall during manufacturing.

Experimental evaluations have shown that the residual circumferential stress component has its maximum tensile magnitude at the pipe inner diameter (ID) surface. This residual hoop stress component decreases continuously with increasing wall thickness and attains a minimum compressive magnitude at the pipe outer diameter (OD) surface.

For Aldyl-A pipe materials, laboratory measurements showed that the magnitude of the residual tensile hoop stress component on the ID is in the range of 200psi to 450psi and the compressive hoop stress on the OD is in the range -850psi to -1000psi. Similarly, laboratory measurements showed that the longitudinal residual axial stress component in Aldyl-A pipes has a maximum tensile magnitude of about 350psi.

Figure 57 shows a plot of the experimentally measured magnitude and distribution of the circumferential residual stress component as a function of distance or wall depth measured from the ID of the pipe for a 2-inch SDR11 Aldyl-A pipe manufactured during 1973. The solid line represents actual lab measurements and the dotted line represents theoretical predictions. The presented data show that the circumferential residual stress component has a maximum tensile magnitude of about 200psi at the pipe ID. This residual stress decreases and attains a zero magnitude at a depth of about 0.7 of the wall thickness. This residual stress component decreases continuously and attains a minimum compressive value of about -950psi at the pipe outer surface.

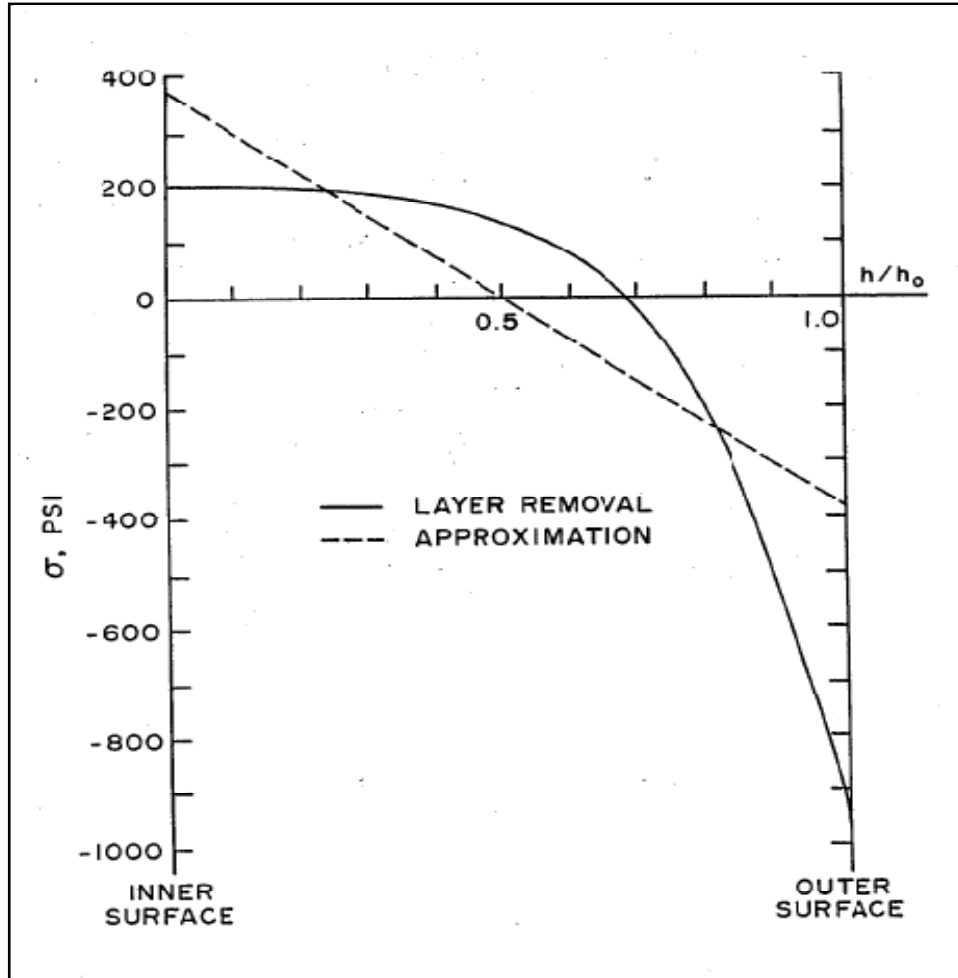


Figure 57. Circumferential Residual Stress Component as a Function of the Wall Depth

The residual circumferential stress component acts in combination with the hoop stress induced by the internal pressure. The hoop stress induced by the internal pressure is defined by the following equation.

$$S = \frac{P(DR - 1)}{2} \quad (1)$$

Where:

S = hoop stress

P = internal pressure

DR = dimension ratio

Applying the equation to the 2-inch SDR 11 pipe from above at an internal pressure of about 60 psig; the circumferential tensile hoop stress component at the pipe ID that is equal to 300psi.² From Figure 57, the tensile circumferential residual stress component at the pipe ID is equal to about 200psi. Adding these two stress components gives a resultant circumferential tensile hoop stress equal to +500psi acting on the inner pipe wall.

At the pipe OD, the resultant circumferential hoop stress is compressive equal to - 650psi (+300psi due to internal pressure - 950psi due to the compressive residual hoop stress).

Therefore, the residual circumferential tensile stress component is significantly effective in increasing the resultant stress that drives the initiation and growth of defects and cracks on the inner pipe surface into axial slits through the pipe wall. On the outer pipe surface, the residual compressive circumferential (hoop) stress component is very effective in reducing the resultant stress and consequently retarding and inhibiting the growth of defects, notches and cracks on the pipe OD.

Effects of Elevated Test Temperatures

The effects of elevated temperatures on the residual stresses were measured for several Aldyl-A pipes. For the 2-inch SDR 11 Aldyl-A pipe that was installed in gas service in 1973 and removed during 1983, Figure 57 shows a plot of the measured residual circumferential tensile stress component as a function of different test temperatures (including 80 °C and 90 °C) and several test periods (including 1, 10, and 100 hours). Figure 58 shows that after a test period of about 100 hours at 80°C or higher test temperatures, the residual circumferential stress acting on the pipe ID decreased by more than 50%.

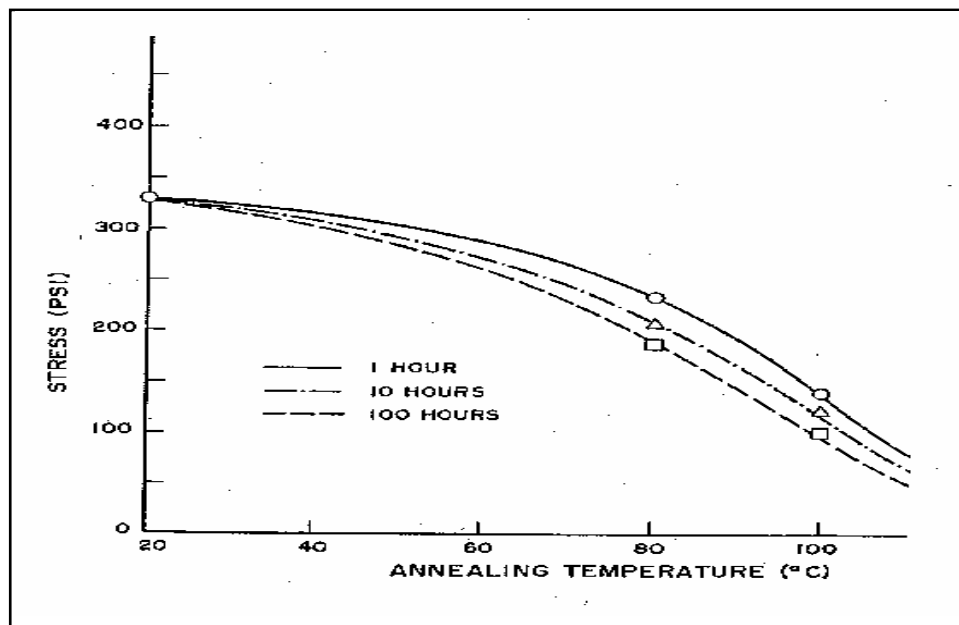


Figure 58. Effect of Test Temperature and Time on Residual Hoop Stress Component

² The internal pressure also causes a tensile axial stress of about 150psi to act on the pipe wall.

Specimens of this pipe material were also subjected to long-term hydrostatic stress rupture tests at 80°C and a test pressure of about 117psig; this pressure induced a tensile hoop stress of about 580psi. The laboratory LTHS test results generated for this Aldyl-A pipe material that was in field service for 10 years are reported in Table 12.

Table 12. Test Data for a 2 Inch Aldyl-A Pipe Manufactured In 1973 and Removed From Gas Service in 1983.

	Tensile Yield Strength, psi	Quick Burst Pressure, psig	Long-Term Hydrostatic Stress Rupture Test		Tensile Residual Hoop Stress on Inner Surface, psi	Compressive Residual Hoop Stress on Outer surface, psi	Density	Crystallinity
			Hoop Stress, psi	Failure Time, hours				
As-Received Pipe	2275	668	580	399	338	-831	0.9526	0.7138
Lab. Annealed at 80°C for 100 hours	2490				98	-246	0,9548	0.7277
Lab. Annealed at 80°C for 1 hour		684	580	663				

The data in Table 12 show that the tensile circumferential residual stress at the inner pipe surface of the “As-Received” pipe was equal to about 338psi. The resultant tensile hoop stress on the pipe ID was about 918psi (580psi due to pressure plus 338psi due to the residual hoop stress component). For this as-received pipe, LTHS tests were performed at a temperature of about 40°C; at this temperature, the test failure time was about 399 hours.

After 100 hours at 80°C test temperature, the residual hoop stress component decreased to 98psi (a 70% decrease).

Another pipe sample of this lot was annealed at 80°C for only one hour prior to the LTHS test; then, it was subjected to LTHS testing at 117psig pressure; the induced pipe hoop stress was 580psi. For the annealed pipe sample, the resultant tensile hoop stress was about 678psi (580psi due to pressure + 98psi due to the residual hoop stress component). The annealed sample failed in LTHS testing after about 663 hours; an increase in failure time of about 66% compared to the LTHS failure time obtained at a test temperature of about 40°C.

The above test results show that long-term hydrostatic stress-rupture (LTHS) tests at elevated temperatures of 80°C or 90°C, cause the resultant hoop stress acting on the inner pipe

surface to be about 50% less than that acting on pipes at room or field service temperatures. This lower circumferential resultant tensile stress results in greater LTHS test failure times.

Several additional experimental investigations at 80°C or higher temperatures have demonstrated that the decrease in residual stresses leads to an increase in the LTHS test failure time of PE pipes by more than 50%.

Even though elevated temperature testing accelerates the failure process in PE pipes it also has the un-intended and undesirable effect of eliminating the contribution of the residual stresses in driving the initiation and growth of defects, notches, and cracks.

At temperatures higher than about 50°C (120°F), elevated LTHS test temperatures have substantial effects in reducing the residual stresses and the resultant hoop stress that drives crack growth on the pipe ID by about 50%; this has the effect of increasing the LTHS failure times by about 50%.

At temperatures lower than about 120°F, the effects of elevated LTHS temperatures on the residual stresses and the resultant hoop stress are minimal; thus, at lower LTHS test temperatures, the effect on the LTHS failure time may be neglected.

Engineering Methods to Predict Life Expectancy

The results presented in the previous sections show that the majority of the short-term laboratory tests that are typically implemented provide, at best, qualitative information on the relative susceptibility of PE gas pipe materials to SCG field failures. Based on extensive investigations it is concluded that the predicted remaining life expectancy is a key measure that can be used to rank the susceptibility of PE gas pipe materials to SCG field failures.

Researchers have predicted PE pipe life expectancy using methods and analytical models developed in principles of engineering fracture mechanics. To apply these models, measurements of SCG or Crack Tip Opening Displacement (CTOD) rates are obtained for PE pipe materials using accurate monitoring devices under well-controlled laboratory conditions.³ In some cases, the SCG rates were determined experimentally by measuring the rate of the CTOD in a notched “PENT” specimen.

In other cases, the SCG rates for PE pipe materials were determined through careful experimental measurements of the CTOD in a notched PE pipe sector specimen subjected to a three-point bending load. These rates were developed for PE LIFESPAN FORECASTING software which was used to predict the life expectancy of PE gas pipe materials. The LIFESPAN software implements methods of linear fracture mechanics combined with measurements of SCG rates. Several investigations have shown excellent correlations between the life predictions made using the LIFESPAN software and actual field failure times of PE gas pipes.

There are significant costs associated with measuring SCG or CTOD rates using either the notched “PENT” test specimen or the notched pipe sector specimen. As a result, SCG or CTOD rates are not available for many different PE gas pipe materials. Also, it is substantially less costly and significantly quicker to apply materials science and engineering models to LTHS tests data to predict the life expectancy of PE gas pipe materials.

One of two materials science models is typically implemented. The two materials science/engineering models are the Bi-Directional Shift Functions (BDSF) and the three-coefficient Rate Process Method (RPM). Both of these models are based on a fundamental law of physics involving the “Second Law of Thermodynamics”. Both of these models have been used and validated for PE gas pipes by several researchers. To apply these models, the failure times are first obtained using the LTHS test performed in accordance ASTM D1598. The LTHS test is conducted on PE pipe test specimens prepared from the “As-received” pipe material. Then, the pipe life expectancy is predicted by applying either the BDSF or the RPM. Numerous investigations have shown excellent correlations between the life predictions made using LTHS test data combined with the BDSF or the RPM method and the actual field failure times of PE gas pipes

Because of the above and the extensive LTHS database, it was decided that the predicted remaining life expectancy made using the LTHS test data combined with either the BDSF or the

³ GTI published several reports that presented fracture mechanics models used to predict the SCG failure time. These reports include the following publications: GRI-91/0360, GRI-92/0479, GRI-92/0480, GRI-92/0481, GRI-93/0105, and GRI-93/0106.

RPM model may be used to rank the relative susceptibility of different PE gas pipes to SCG field failures.

Original Bi-Directional Shift Functions Model

The BDSF, denoted as F_1 and F_2 , allow projections using laboratory test failure time ($Time_t$) generated at a laboratory test pressure (P_t) and at a specific test temperature (T_t) to predict the specific pressure (P_s) and the specific failure time ($Time_s$) corresponding to any specific temperature (T_s).

$$F_1 = e^{0.109(T_t - T_s)} \quad (2)$$

$$F_2 = e^{0.0116(T_s - T_t)} \quad (3)$$

$$Time_s = Time_t F_1 \quad (4)$$

$$P_s = \frac{P_t}{F_2} \quad (5)$$

Where:

P_t = laboratory test pressure

T_t = laboratory test temperature

$Time_t$ = laboratory test failure time

T_s = specific temperature including field service temperature

P_s = predicted pressure (psig) corresponding to T_s

$Time_s$ = predicted failure time corresponding to T_s

To implement the BDSF, the laboratory tests may be conducted at only one set of test conditions. This condition involves testing pipe specimens at a test temperature and a test pressure to be specified properly so that it can be projected to give the pressure (psig) P_s corresponding to the specified temperature T_s .

Modified Bi-Directional Shift Functions Equations

The original BDSF is appropriate for projecting to temperatures $>50^\circ\text{C}$. However, when projecting to temperatures $<50^\circ\text{C}$, these functions should be modified to compensate for the effect of elevated LTHS test temperatures in reducing the stress driving crack initiation and growth. This can be accomplished by introducing the Temperature Factor (TF) as follows:

$$P_s = \frac{P_t}{F_2(TF)} \quad (6)$$

Where:

P_t = laboratory test pressure

Ps = predicted pressure (psig) corresponding to Ts

TF = 2, for Ts <50°C; and

TF = 1, for Ts >50°C

Original Three-Coefficient Rate Process Method

The three-coefficient RPM is based on the Arrhenius equation describing thermally activated processes; it may be expressed in terms of the following equation:

$$\text{Log}_{10}\text{Time} = A + \frac{B}{T} + \frac{C\text{Log}_{10}P}{T} \quad (7)$$

Where:

T = absolute temperature in Kelvin (°K=°C+273)

P = pressure

Time = average failure time corresponding to T and P

The three coefficients **A**, **B**, and **C** are unknown constants that are, in general, functions of the material properties, temperature, stresses or applied loads, and geometrical variables.

To apply the RPM, first it is necessary to determine the values of the three unknown coefficients for the PE material when subjected to internal pressure and/or a specific secondary stress. Hence, three sets of LTHS tests should be conducted on replicate sets of test specimens at three distinct test conditions. The three distinct test conditions may involve the use of two different test temperatures and two different test pressures.

The RPM allows one to predict the life expectancy for a broader range of pressures and many different field temperatures. However, the BDSF allow one to make a life prediction corresponding to only one specific field temperature.

In cases involving laboratory tests performed at less than three distinct test conditions, the BDSF may be implemented to make predictions.

Modified Three-Coefficient Rate Process Method

The original RPM is appropriate for projecting to temperatures >50°C. However, when projecting to temperatures <50°C, these functions should be modified to compensate for the effect of elevated LTHS test temperatures in reducing the stress driving crack initiation and growth. This can be accomplished by introducing the Temperature Factor (TF) as follows:

$$\text{Log}_{10}\text{Time} = A + \frac{B}{T} + \frac{C\text{Log}_{10}P(TF)}{T} \quad (8)$$

Where:

T = absolute temperature in Kelvin (°K=°C+273)

P = pressure

Time = average failure time corresponding to T and P

TF = 2, for $T_s < 50^\circ\text{C}$; and

TF = 1, for $T_s > 50^\circ\text{C}$

Note: The researchers who developed the original BDSF and the RPM models may not have intended the use of the models for predictions at temperatures lower than LTHS test temperatures by more than 30°C or 40°C .

Sample Set on the Predicted Remaining Life Expectancy

GTI database includes information on many different PE gas pipe materials and sizes that were manufactured from several PE resins and pipe extruders. These pipe materials were installed in many different geographical regions throughout the U.S. These pipe materials were subjected to different underground day-to-day and seasonal temperatures. Also, these pipes materials were installed in different soils with varying topographies and under several different installation conditions.

Because of the above, for any predictions made on the remaining life expectancy and the pipe pressures to be applicable and accurate for a specific pipeline they should be made based on the temperature, soil topography, field installation conditions and operations that correspond to those specific to where the pipe is installed.

Again it should be emphasized, that the predictions on the remaining life expectancy of PE pipes presented in this section represent only one sample set of predictions for an assumed specific average annual underground temperature. Also, the presented sample set of life predictions presented in this section assume a specific set of external loads due to the field secondary stresses induced by impinging rock loads, squeeze-offs, pipe bending, or earth/soil loads.

Therefore the remaining life expectancy predictions presented in this section do not necessarily apply to any geographic region or any pipeline operator system. Thus, the presented predictions should NOT be considered a reference but only as a sample for an arbitrarily selected set of assumed service conditions. The assumed set of conditions used is one from an exceedingly large group of possible service conditions and geographic locations.

Table 13 presents predictions of the remaining life expectancy and pressure for several PE gas pipe materials for an assumed average annual underground field temperature of 60°F . The predictions are made for pipes subjected to internal pressure or internal pressure combined with a secondary stress induced by an impinging rock load, a squeeze-off, a pipe bending moment, or a soil/earth load. The selected magnitudes of the secondary stresses are based on a maximum limiting value determined to be typical for that installation period.

The predictions are made using accelerated LTHS laboratory test data determined at test temperatures of 80°C and 90°C . The RPM model and/or the BDSF model were implemented in making the predictions presented in Table 13. The predictions are presented only for purposes of discussion.

Table 13. Predicted remaining life expectancy for PE gas pipe

Material	Year Manufacture	Pipe Diameter/SDR	Predicted Remaining Life Expectancy, Years					
			Pipe Pressure, psig	Pipe Pressure Only	Pipe Pressure and Rock Impingement.	Pipe Pressure and Squeeze-off	Pipe Pressure and Pipe Bend. Rad 20 x OD	Pipe Pressure and Pipe Deflection-5% x OD
Aldyl-A MD	1970	3"/11	60 psig	158 yr	42 yr	28 yr	79 yr	50 yr
Aldyl-A MD	1971	2"/11	60 psig		33 yr			
Aldyl-A MD	1971	4"/11	60 psig	21 yr		15 yr		
Aldyl-A MD	1972	2"/11	60 psig	28 yr	19 yr	16 yr	22 yr	24 yr
Aldyl-A MD	1973	2"/11	60 psig	58 yr	38 yr	47 yr	50 yr	55 yr
Aldyl-A MD	1974	2"/11	60 psig	49 yr	24 yr	32 yr	35 yr	43 yr
Aldyl-A MD	1974	2"/11	60 psig	51 yr	26 yr	19 yr		27 yr
Aldyl-A MD	1976	2"/11	60 psig	62 yr	18 yr	23 yr	42 yr	57 yr
Aldyl-A MD	1977	3"/11.5	60 psig	129 yr				
Aldyl-A MD	1980	4"/11.5	60 psig	174 yr				
Aldyl-A MD	1983	3"/11.5	60 psig	71 yr	31yr	36 yr	42 yr	57 yr
Aldyl-A MD	1984	4"/11.5	60 psig	353 yr				
Aldyl-A MD	1984	3"/11.5	60 psig	249 yr				
Aldyl-A MD	1985	3"/11.5	60 psig	>500 yr				
Aldyl-A MD	1986	2"/11	60 psig	76 yr	35 yr	28 yr	39 yr	52 yr
Aldyl-A MD	1986	3"/11.5	60 psig	>500 yr				
Aldyl-A MD	1986	4"/11.5	60 psig	>500 yr				
Aldyl-A MD	1988	4"/11.5	60 psig	220 yr				
Aldyl-A MD ¹	1989	6"/11.5	53psig	>300 yr				
Aldyl-A MD ²	1989	6"/11.5	53psig	>300 yr				
Aldyl-A MD ³	1989	6"/11.5	53psig	>300 yr				
Aldyl-A MD	1990	2"/11	60 psig	>500 yr	>500 yr	>500 yr	>500 yr	>500 yr
Aldyl-A MD	1990	4"/11.5	60 psig	>500 yr				
Aldyl-A MD ⁴	1990	6"/11.5	53psig	>300 yr				
Aldyl-A MD	1991	4"/11.5	60 psig	>500 yr	>500	>500 yr	>500 yr	>500 yr

					yr			
Aldyl-A MD	1991	3"/11.5	60 psig	>500 yr				
Aldyl-A MD	1993	2"/11	60 psig	>500 yr				
Aldyl-A MD	1993	3"/11.5	60 psig	>500 yr				
Plexco Yel. MD ⁵	1994	6"/11.5	53psig	131 yr (cap fracture)				
Plexco Yel. MD ⁶	1994	6"/11.5	53psig	>300 yr				
Plexco Yel. MD ⁵	1999	6"/11.5	50psig	176 yr (cap fracture)				
Plexco Yel. MD ¹	1999	6"/11.5	53psig	>300 yr				
Driscoplex6500 MD ⁶	2002	6"/11.5	53psig	>300 yr				
Driscoplex6500 MD ⁶	2002	6"/11.5	53psig	>300 yr				

Note Superscript

1. Heat fusion saddle tee
2. Heat fusion saddle tee and butt fusion
3. Heat fusion saddle tee and electro-fusion socket couplings
4. Electro-fusion saddle tee
5. Heat-fusion saddle tee and socket coupling– Top of Cap fractured at thread
6. Electro-fusion saddle tee and socket coupling.

Table 13 lists a few PE pipe sections containing heat-fusion saddle tees and laterals. For two of these, the top of the cap on the saddle tee fractured at the thread. The life expectancy for these cases is reported.

Secondary Stress Effects

For a few PE pipe materials, Table 13 presents the forecasted pipe remaining life expectancy for pipes subjected to an internal pressure combined with a secondary stress induced by a rock impingement, a squeeze-off, a bending moment, or a soil load. It was found that for certain PE pipe materials, rock impingement loads cause the greatest stress and hence lead to the shortest predicted life expectancy. For other PE pipe materials, a squeeze-off causes the greatest stress and hence may lead to the shortest life expectancy.

For an assumed annual average underground field temperature of 60°F, Figure 59 presents graphical plots giving the predicted remaining life expectancy for an older Aldyl-A pipe

subjected to internal pressure or internal pressure combined with either a rock impingement load, a squeeze-off, a bending moment or a soil load. Figure 59 shows that impinging rocks and /or pipe squeeze-offs may induce the greatest stress that drives crack initiation and growth and hence a shorter life expectancy. In general, rock impingements and/or pipe squeeze-offs have more severe effect on PE pipes than pipe bending or an excessive soil load due to compaction.

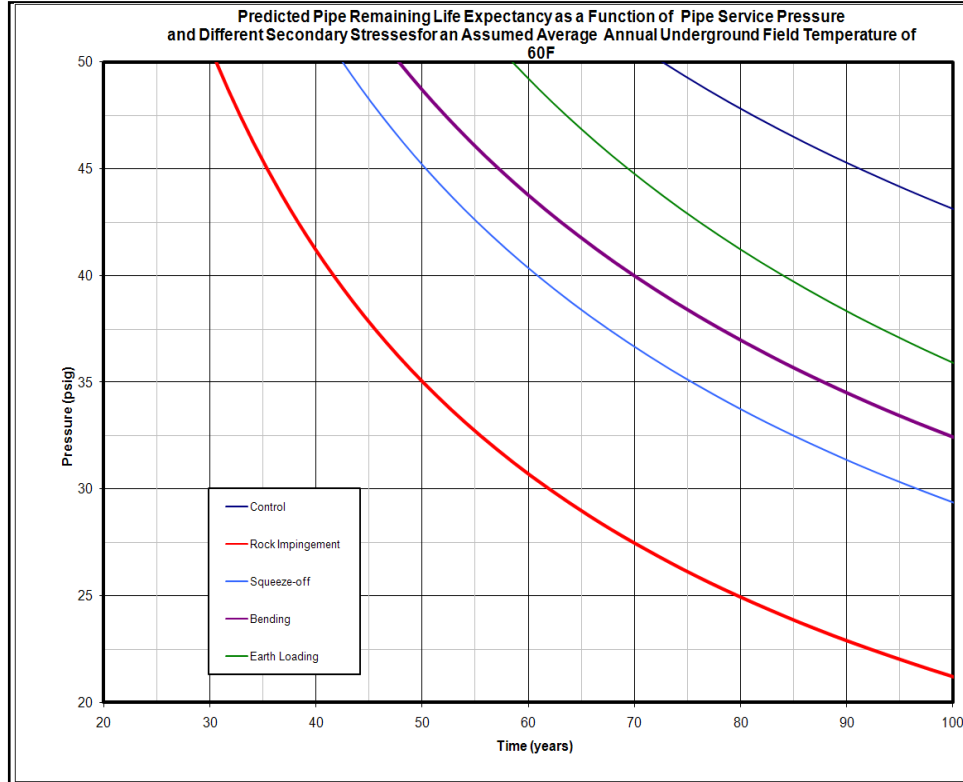


Figure 59. Predicted Remaining Life Expectancy of an Older Aldyl-A Pipe

Field Temperature Effects

It should be noted that the BDSFs and the RPM models are both based on exponential relationships. These models and the generated laboratory test data show that the PE pipe failure time or alternatively the remaining life expectancy, increase exponentially with decreasing temperatures and decreasing pressures. Therefore, the lower is the underground field temperature; the greater is the remaining pipe life expectancy.

Figure 60 presents graphical plots for the predicted life expectancy as a function of the average annual underground field temperature for an older Aldyl-A pipe material subjected to pressures of 40psig, 50psig, or 60psig. This figure clearly shows that the life expectancy of the PE pipe increases exponentially with decreasing field temperature.

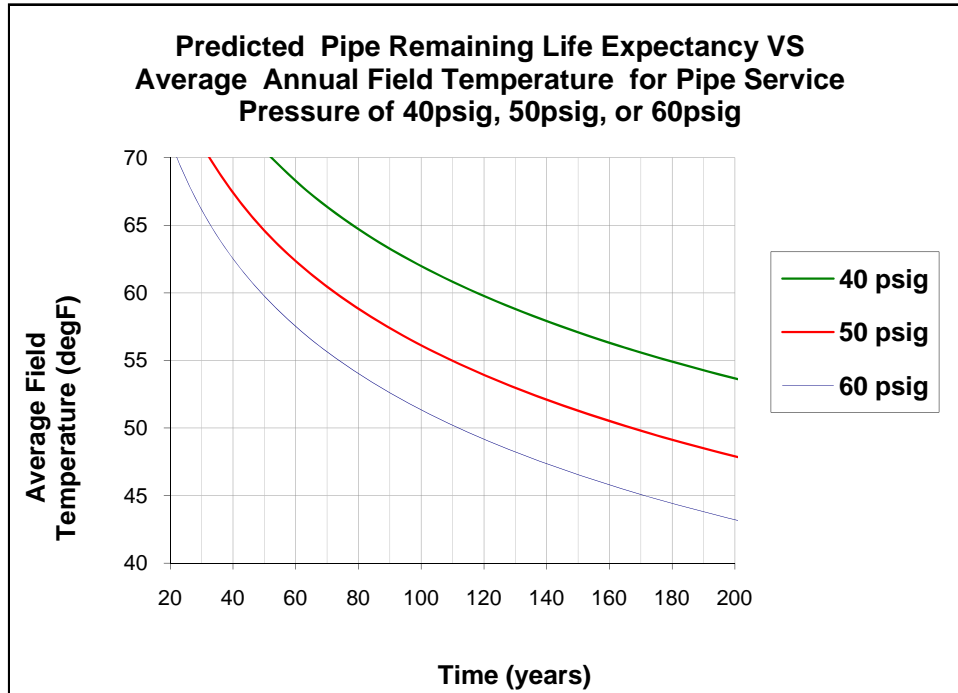


Figure 60. Predicted Remaining Life Expectancy as a Function of Temperature

The predictions are presented to show that the pipe life expectancy is a key measure of the susceptibility of PE gas pipe materials to SCG field failures and that these predictions are applicable and accurate only when they consider the specific conditions for a specific PE pipeline.

Slow Crack Growth Conclusion

The objective of the work task was to identify the susceptibility of plastic gas pipe materials to brittle SCG field failures. To accomplish the objectives of this task, a thorough review of the literature including GTI database on PE gas pipe materials was conducted.

Other than failures caused by excavation, the review indicated that the majority of the PE gas pipe materials that fail under typical field conditions exhibit SCG fracture morphology. Using optical and SEM- microscopic examinations, the SCG fracture process exhibited by several different PE pipe samples was investigated and described.

Several laboratory tests and methods were evaluated to determine whether or not they can be used to provide information on the susceptibility of PE gas pipe materials to SCG field failure. These tests included the Tensile, Quick Burst Pressure, Melt Index, Density, Bend-Back, and PENT.

The review showed that the short-term mechanical strength tests may not provide qualitative or quantitative information on the relative susceptibility of PE gas pipe materials to SCG field failures. The review indicated that the Density or Melt Index (or Melt Flow) may provide qualitative information on the relative susceptibility of PE gas pipe materials to SCG field failures.

Qualitative information on the susceptibility of different PE pipe materials to SCG field failures may be obtained using optical and SEM microscopy.

The Bend-Back test can provide accurate qualitative information on the susceptibility of PE gas pipe materials to early pre-mature brittle SCG failures. Visual examinations of specimens subjected to the Bend-Back test identified several Aldyl-A MDPE pipes that have inferior Low-Ductile Inner Wall (LDIW) materials which are highly susceptible to pre-mature early brittle SCG field failures. It was found that several Aldyl-A MDPE pipe lots manufactured in 1971 have LDIW materials and are highly susceptible to pre-mature SCG field failure.

Data obtained using the notched PENT test were evaluated. For many Aldyl-A MDPE pipe materials manufactured during the period 1970 to 1985, the PENT test failure times ranged between 0.6 hours and 21.4 hours. However these Aldyl-A pipe materials continue to provide good field service. Some of these materials have been in gas service for more than 35 years.

Correlations between the PENT failure times of older PE pipe materials and the field failure times are currently inconclusive. However, PENT test data on newer materials suggest that the PENT test may provide a useful quantitative relative reference on the susceptibility of PE gas pipe materials to SCG field failures.

Extensive evaluations of various tests showed that the predicted remaining life expectancy is a key quantitative measure that can be used to rank the susceptibility of PE gas pipe materials to SCG field failures. To predict the life expectancy of a PE gas pipe material, researchers utilized long-term laboratory test data combined with either of two materials science models, the BDSF or the three-coefficient RPM.

Review of GTI database showed that numerous PE gas pipe materials were subjected to LTHS tests. Accelerated LTHS test data were generated at several elevated test temperatures including 80°C and 90°C and using several test pressures. Many LTHS tests were conducted on PE pipes subjected to internal pressure or internal pressure combined with a secondary stress

simulating a rock impingement load, a squeeze-off, a pipe bending moment, or a transverse earth or soil load.

Annealing and LTHS laboratory tests showed that at temperatures higher than about 50°C (120°F), the stress that drives crack initiation and growth on the pipe ID is reduced by about 50%; this has the effect of increasing the LTHS test failure times by about 50%. At temperatures lower than about 50°C (120°F), the effects of elevated LTHS temperatures on the stress that drives crack initiation and growth are negligible.

Hence, if the pipe life expectancy is predicted for temperatures less than about 50°C (120°F), then one should compensate for the effects of elevated LTHS-test temperatures. This compensation may be implemented through the use of a **Temperature Factor, denoted as TF**.

Laboratory test data showed that the Temperature Factor, TF, is equal to about two (2).

Therefore, to compensate for the effects of elevated LTHS-test temperatures in reducing the stress driving the crack initiation and growth, the BDSF and the RPM models should be modified through the implementation of a temperature factor TF. The modified BDSF and the RPM models that incorporate a Temperature Factor are presented above.

For the modified BDSF and the RPM models, it is important to emphasize that:

TF = 1, for predictions made at temperatures > 50°C (about 120°F): and

TF = 2, for predictions made at temperatures < 50°C (about 120°F).

The remaining life expectancy is predicted for several PE gas pipe materials assuming a sample set of field and operational conditions. The presented predictions on the pipe remaining life expectancy assume a specific set of secondary stresses induced by impinging rock loads, squeeze-offs, pipe bending, or earth/soil loads. The assumed set of conditions is one from an exceedingly large group of possible service conditions and geographic locations. The predictions are made using accelerated LTHS laboratory test data determined at test temperatures of 80°C and 90°C combined with the modified RPM model and/or the modified BDSF model

The test results and the predictions show that rock impingements and/or squeeze-offs, in general, induce the greatest stress in PE pipes thus causing the greatest damage and resulting in the shortest remaining life expectancy.

The models, laboratory test data, and predictions show that the remaining life expectancy of PE pipe materials increases exponentially with decreasing field temperatures and decreasing pressures. Therefore, the lower is the underground field temperature the greater is the remaining pipe life expectancy.

The predicted life expectancy of a PE gas pipe provides one of the most reliable and accurate quantitative measure of the relative susceptibility of the PE pipe material to SCG field failure. However, for these predictions to be applicable, accurate, and reliable, it is critically important to take into account the actual field temperatures, soil topography, and installation conditions that are specific to that pipeline and its geographic location.

Root Cause Analysis of Field Failures

GTI received and documented 55 plastic pipe samples that were removed from service due to leaks/failures. Eight samples underwent extensive laboratory testing to determine the root cause of the leak failure. The remainder were photographed and visually examined. All have been categorized on the basis of the most probable cause of failure: material, procedural, quality control, or miscellaneous. The information obtained for the samples has been incorporated with an additional database to provide insight to where defects occur and how they lead to in-service failures. Of the samples received, failures occurred in:

- Elbows
- Fusion Joints
 - Butt
 - Socket
 - Saddle
- Mechanical Fittings
- Pipe walls due to impingement, loading, and squeeze-offs
- Service Tee Threads
- Tapping Tee Caps
- Transition Fittings.

Failure Categories

Failures were divided into four categories: Material, Procedural, Quality Control, and Miscellaneous. On some occasions, the failure category could not be determined due to a lack of information. These have been placed in split categories after the four primary classifications.

Material Failures are those which can be attributed to the imposition of a mechanical load that the polyethylene gas pipe or fitting is unable to sustain. This category includes slow crack growth and rapid crack propagation failures. Slow crack growth failures in pipe have occurred because of rock impingement, squeeze-off, insert renewal, bending, and earth settlement. Slow crack growth at joints and in fittings have occurred in butt joints, socket joints and fittings, saddle joints, and tapping tee caps, and because of internal pressure.

Procedural Failures are those failures that occurred as a result of improper field operations. This category includes separation of joints because of improper heat-fusion joining conditions in butt joints, socket joints and fittings, and saddle joints and tapping tees.

Quality Control Problems are attributable to defects in the extruded plastic pipe or fitting or to resin-related problems which adversely affect the expected performance of the material. Often these problems are detected prior to installation. They illustrate problems with pipe quality that can occur during production. Quality control problems can be detected as improper dimensional tolerances, visible or microscopically visible defects, or as melt irregularities.

Miscellaneous Problems are those that do not fall clearly into one of the foregoing categories. (GRI-98/0202)

Laboratory Field Failure Analysis Procedure

The laboratory analysis procedure used for this project is described for sample number #602533. This specimen is identified as a 4" IPS SDR 11.5 DuPont Aldyl-A PE 2306 manufactured in 1984. It was removed from service in 2008 and submitted to GTI for analysis. Upon receipt, the specimen was photographed and examined. The as received sample is shown in Figure 61. Background and service information are summarized in Table 14.

Impingement – #602533

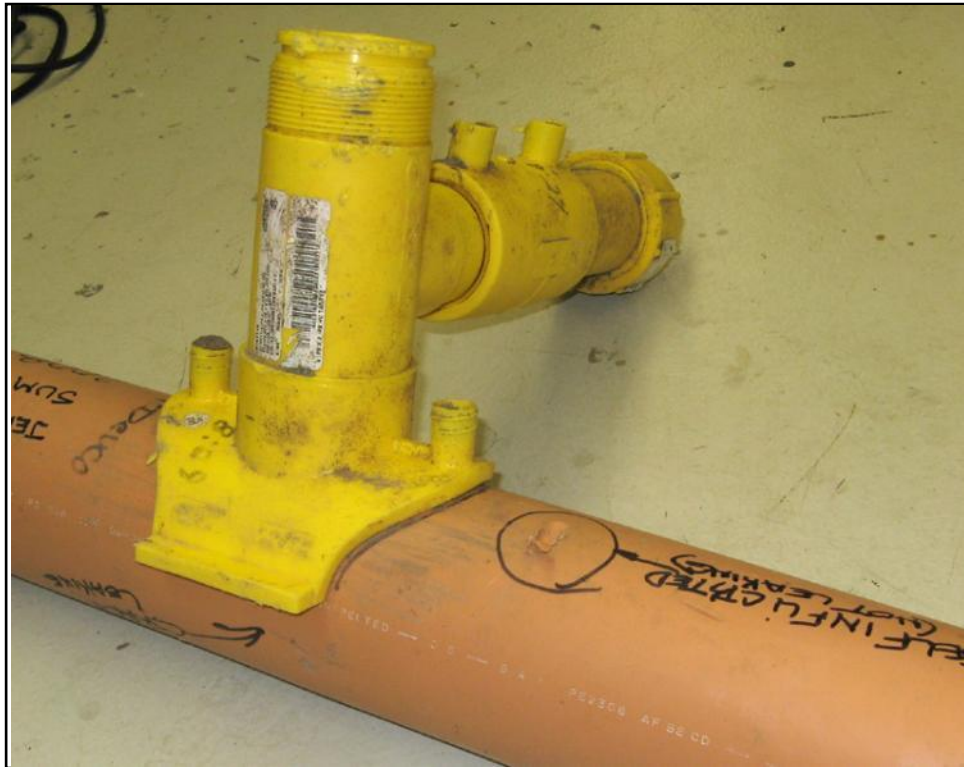


Figure 61. As Received Sample with Attached 4" X 2" Electrofusion Tapping Tee

Table 14. Impingement Background

Pipe Information	602533
Diameter	4"
SDR	11.5
Resin	PE 2306
Manufacturer	DuPont
Design Pressure	60psig
Service Information	
Operating Pressure	60 psig at 65°F / 45 psig at 0°F
Service Temperature	60°F
Comments	NA
Timeline	
Placed in Service	August 1984
Installation Method	Direct Lay
Removed from Service	January 2008
Comments	Tee was installed in 2004
Environmental	
Soil Type	Rocky, sandy and silty
Evidence of 3rd Party Damage	Possibly

Visual Examination

The sample revealed an off-axis slit failure which grew in two directions from an indentation in the outer wall. The specimen was cut in half to reveal an approximately 3" slit on the inner wall. The outer and inner wall of the pipe can be seen in Figure 62 and Figure 63 respectively. The specimen was cut from each end to within about ¼" of the crack. It was then force fractured using liquid nitrogen to reveal the fracture face as seen in Figure 64 and Figure 65.



Figure 62. Slit Failure Growing Away From Impingement Point



Figure 63. View of the Slit from the Inner Wall



Figure 64. Pipe Was Force Fractured to Reveal the Fracture Faces



Figure 65. Close Up View of the Fracture Faces

Using high powered optical microscopy, the fracture faces were examined. The photographs taken with the stereo optical microscope were stitched together and are shown in Figure 66. The initiation point is noted on the photograph and was found to be on the inner wall directly opposite of the indentation on the outer wall. The crack left visible striations as it grew step-wise from the initiation point on the inner wall to the outer wall. Two ductile rupture zones are also visible.

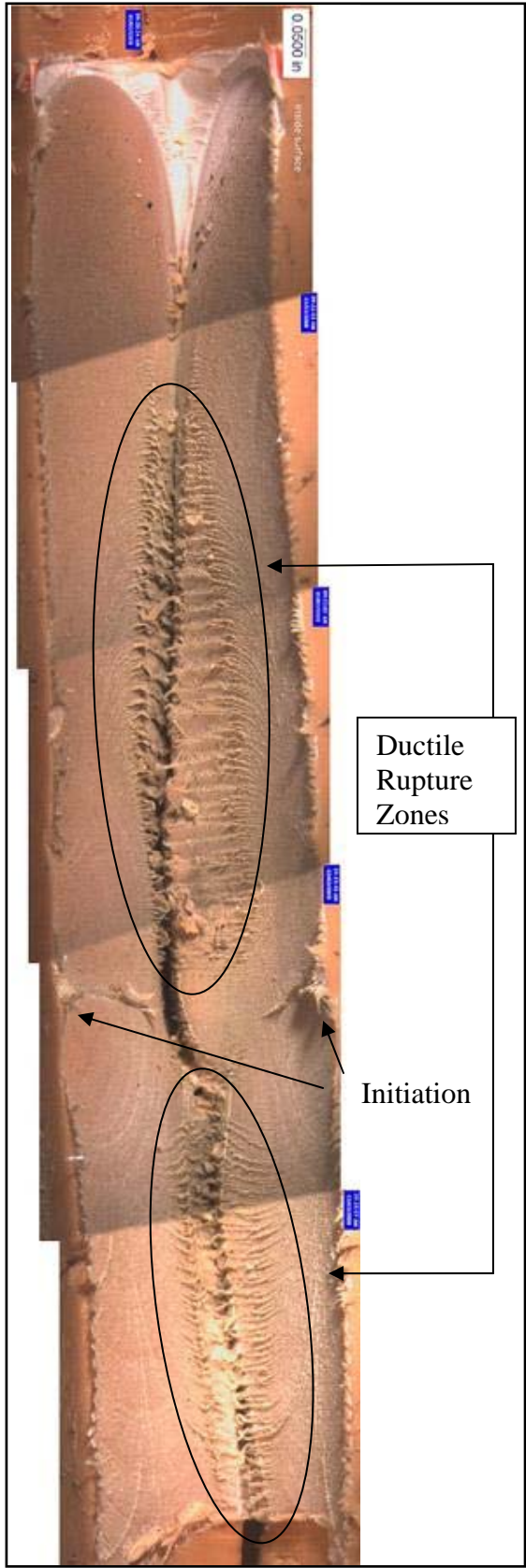


Figure 66. Microscopy

In addition to visual inspections, the tests outlined in Table 15 were also performed. Density and melt flow tests were used to determine if the material was within manufacturer specification when it was extruded. Oxidation Induction Time (OIT) and Differential Scanning Calorimetry (DSC) were used to determine the oxidation and the melting point/ heat of fusion of the pipe material. Fourier Transform Infrared Spectroscopy (FT-IR) tests were run to check for material degradation and contamination.

Table 15: Test Methods Used in Root-Cause Evaluation

Test Method	Revision	Title
Leak Test*		GTI Internal Method
Density*		GTI Internal Method for Density by Helium Pycnometer
ASTM D1238	04	Standard Test Method for Melt Flow Rates of Thermoplastics by Extrusion Plastometer
ASTM D3895	07	Standard Test Method for Oxidative-Induction Time by Differential Scanning Calorimetry
ASTM D3418	03	Standard Test Method for Transition Temperatures of Polymers By Differential Scanning Calorimetry
FT-IR*		GTI Internal Method for Infrared Analysis
* GTI's laboratory maintains A2LA accreditation to ISO/IEC 17025 for specific tests listed in A2LA Certificate 2139-01 and meets the relevant quality system requirements of ISO 9000:2000. Test/calibration/inspection method(s) and results are not covered by our current A2LA accreditation.		

Density

The skeletal density of the pipe was determined to be 0.942g/cc using the helium pycnometer. This is consistent with medium density polyethylene gas pipe material from the time period sample #602533 was manufactured.

Melt Flow

Portions of the pipe sections were prepared and subjected to ASTM D1238 melt flow testing.

Table 16: Melt Flow Measurements

Sample ID	Trial #	Rate (g/10min)
602533-001	1	1.458
602533-001	2	1.158
602533-001	3	1.151
Average		1.256±0.1752

These results were consistent with medium density polyethylene gas pipe material.

Thermal Analysis

Specimens were prepared from the pipe section and subjected to ASTM D3418 differential scanning calorimetry. The resulting thermograms (Figure 67) indicated a heat of fusion of 157J/g and no additional melting or exotherms were detected which would have suggested the presence of contamination. In addition, ASTM D3895 was performed on the prepared specimen and indicated an oxidative-induction time of 49.6 minutes as seen in Figure 68. This was consistent with the age of the PE considering it has absorbed organic materials from the gas supply over time. These organic compounds are relatively easily oxidized when compared to PE.

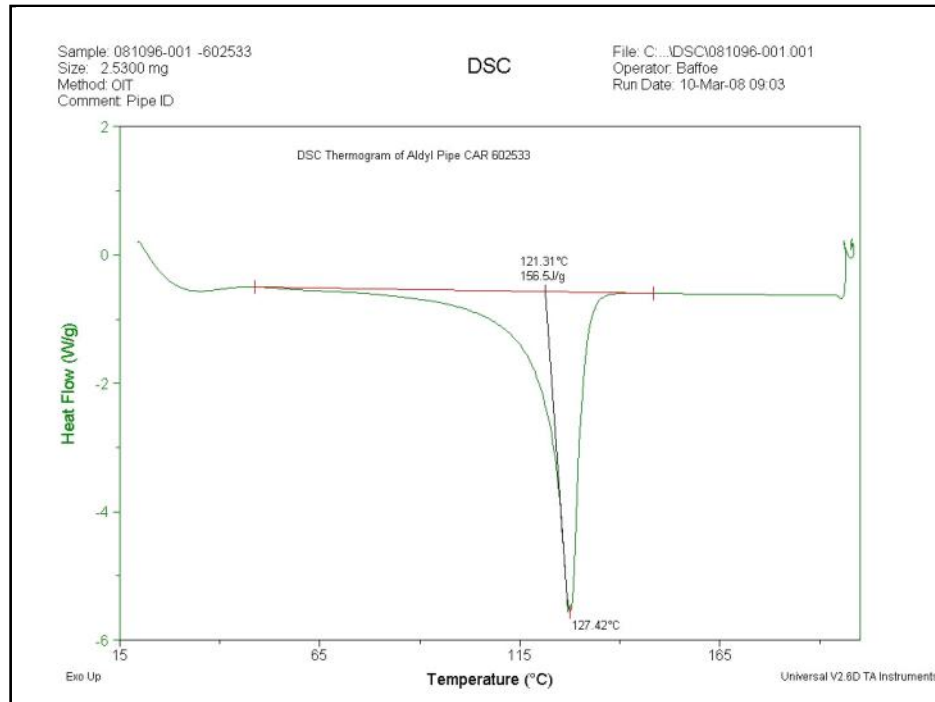


Figure 67. Differential Scanning Calorimetry

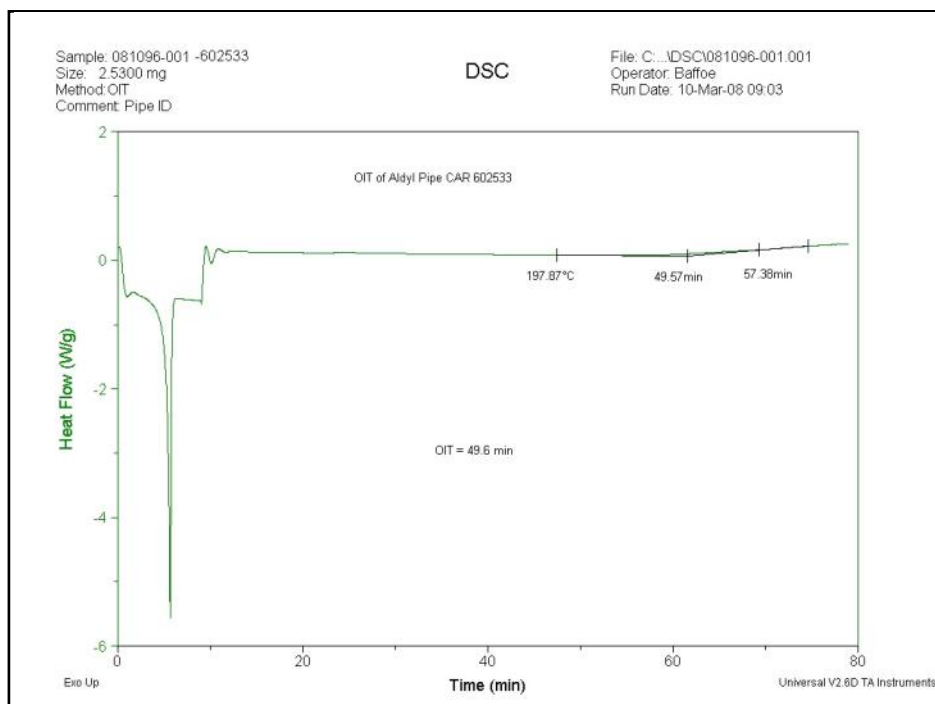


Figure 68. Oxidative Induction Time

Infrared Analysis

A comprehensive analysis was performed to determine the condition of the pipe and to detect the presence of any organic materials not associated with the pipe material using Fourier-Transform - Infrared Spectroscopy. The results did not indicate the presence of foreign organic materials in the outer (Figure 69), middle (Figure 70), or inner (Figure 71) pipe wall within the detectability of the instrument. The 1650cm^{-1} to 1750cm^{-1} region of the resulting spectra was also examined. Absorbencies in this region are associated with polyethylene oxidative products though none were detected for this sample. This suggested that the pipe was manufactured and stored acceptably prior to installation.

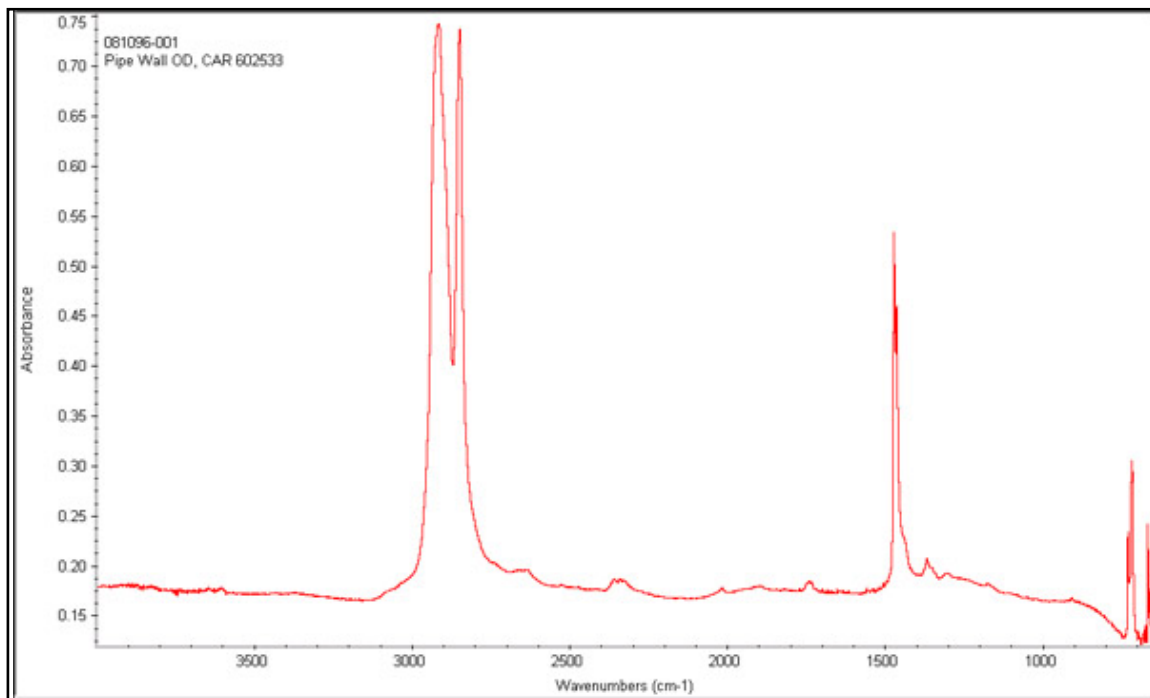


Figure 69. FT-IR Outer Wall

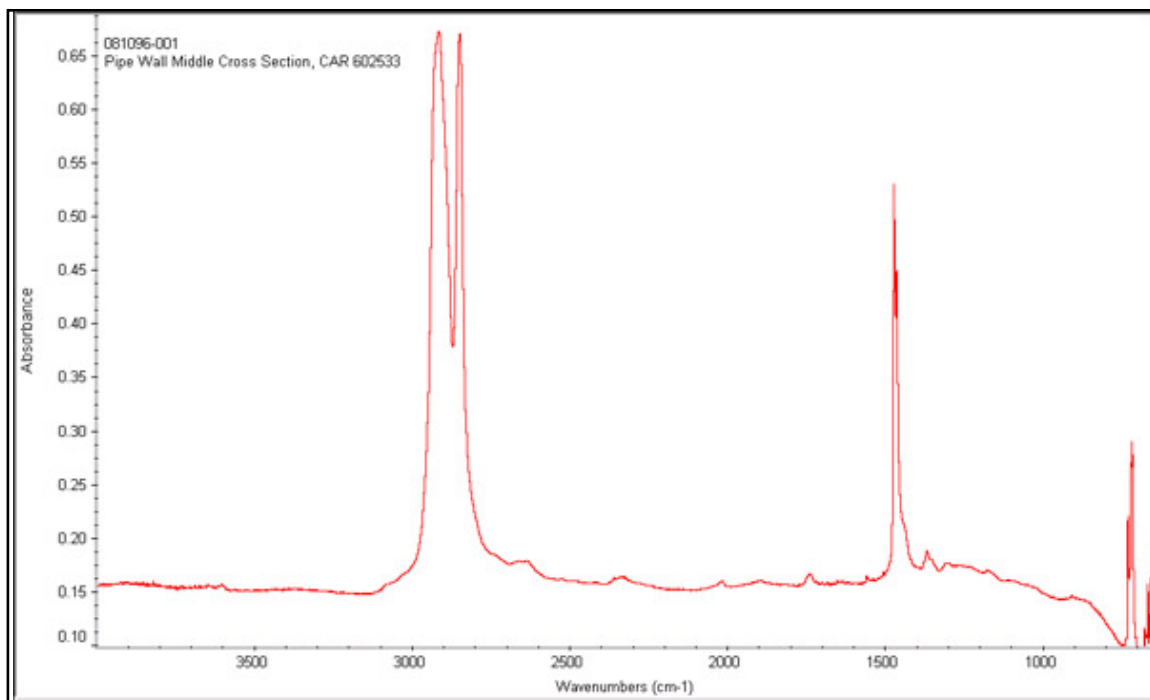


Figure 70. FT-IR Middle Wall

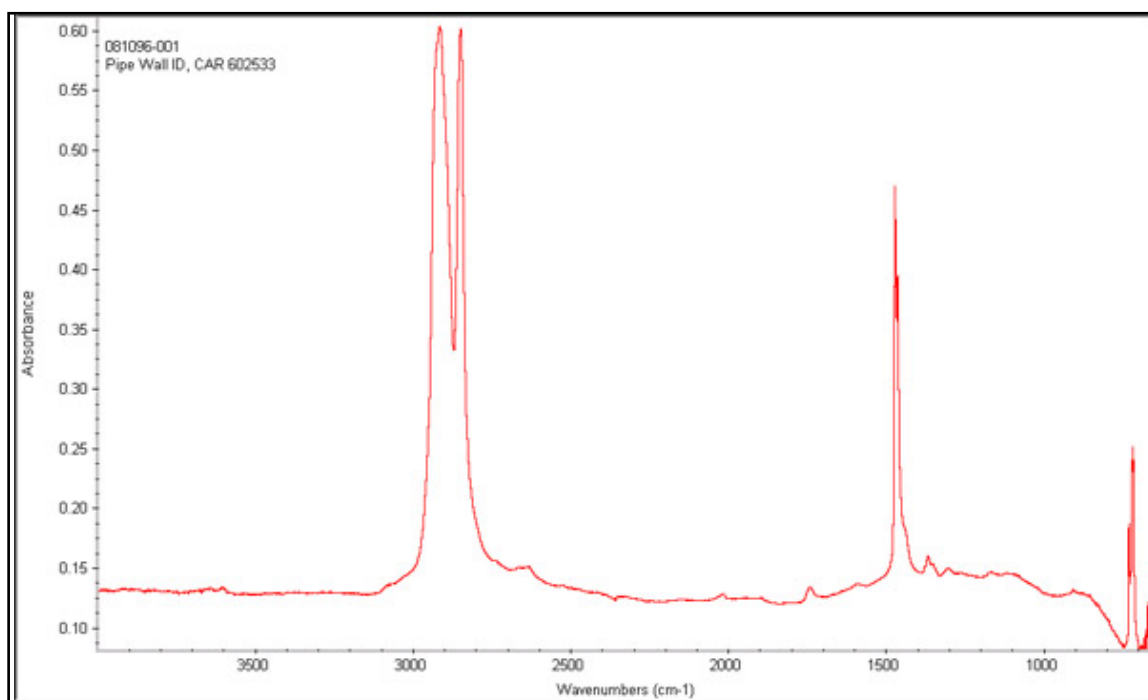


Figure 71. FT-IR Inner Wall

Conclusions

Because the battery of tests suggests nothing was out of the ordinary with the pipe material, it is quite unlikely that the pipe extrusion process contributed to the slow crack growth failure. It was concluded that the highly localized stresses induced on the pipe wall by a foreign body, most likely a rock, led to the initiation of a slit failure on the inner pipe wall. The crack grew stepwise in two directions away from the initiation point with the final through wall fracture occurring in a ductile manner. This sample is classified as a material SCG failure due to rock impingement.

Research Approach

Eight samples were evaluated using the procedure described above and have been placed at the beginning of their respective section. Roughly 50 additional pipe samples were received from field service for failure evaluation. As the budget could not support full analysis of this many samples, only visual examinations were performed on the remainder. Photographs, background data, and visual examination results are provided.

Material Failures

Tap Tee – #678156



Figure 72. As Received Sample with Two Tees. Leak Occurred At Untapped Tee, Left



Figure 73. Untapped Tee with Circumferential Slit

Table 17. Tap Tee Background

Pipe Information	678156
Diameter	2"
SDR	11
Resin	PE 2306
Manufacturer	DuPont
Design Pressure	60psig
Service Information	
Operating Pressure	60 psig at 65°F / 30 psig at 0°F
Service Temperature	60°F
Comments	NA
Timeline	
Placed in Service	August 1980
Installation Method	Direct Lay
Removed from Service	November 2007
Comments	Leak at untapped tee
Environmental	
Soil Type	Rocky, sandy and silty
Evidence of 3rd Party Damage	No

Visual Examination

The submitted pipe section was subjected to initial examination. The examination indicated the presence of a slit immediately adjacent to one side of the tee with minimal bead and rollback as shown in Figure 73. The section was leak tested to verify the leak location at the observed slit as shown in Figure 74. The section was cut longitudinally to expose the inner surface (Figure 75) then further cut to expose both fracture surfaces (Figure 76). The fracture surfaces contained debris on the surface consistent with soil. A spherical particle was observed and initially thought to be imbedded in the pipe wall on the tee side of the fracture but closer inspection revealed the absence of a companion dimple on the pipe side of the fracture. It was concluded that this particle had deposited itself post fracture. The particle can be seen in Figure 79.



Figure 74. Underwater Leak Test Revealing Leak Location

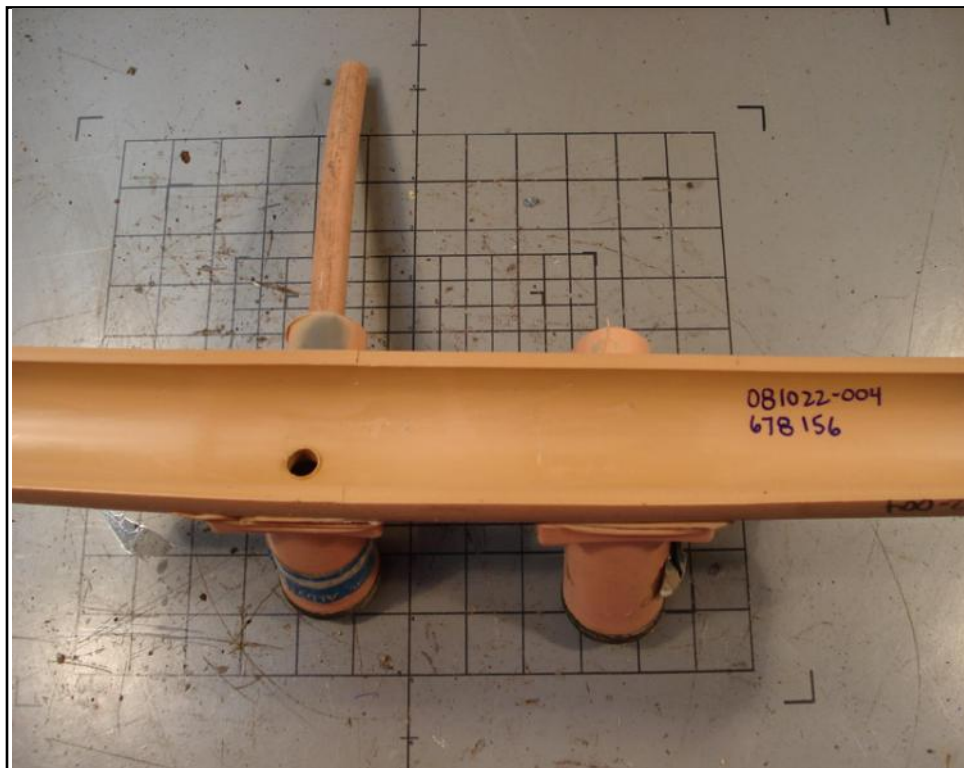


Figure 75. Sample Was Cut to Show Inner Pipe Wall



Figure 76. Close Up of the Circumferential Slit on the Inner Wall



Figure 77. Length of Fracture Faces Identified with Red Marker



Figure 78. Close up of the Fracture Face Away from the Tee



Figure 79. Close up of the Fracture Face towards the Tee with Area of Interest Identified

The surfaces were examined with a stereo optical microscope and revealed that the SCG fracture originated from the inner wall of the pipe and proceeded outward as shown in Figure 80. Another area exhibited a secondary SCG fracture origin originating near the outer surface of the pipe then proceeding inward, suggesting a change or compound loading of the area. The secondary origin is identified in Figure 81.



Figure 80. Microscopy of the Fracture Face Away From the Tee

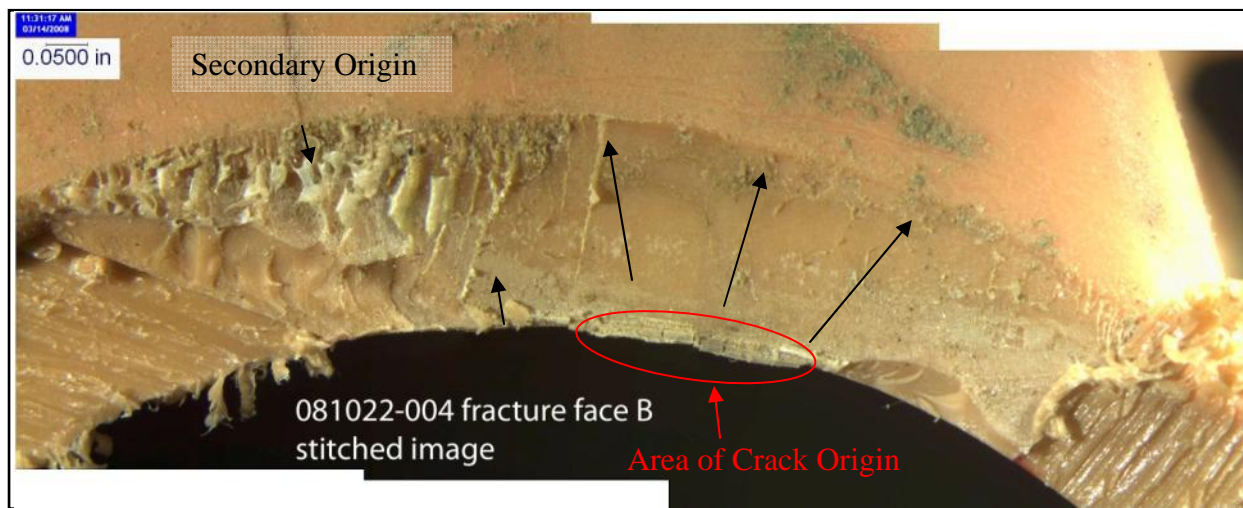


Figure 81. Microscopy of the Fracture Face towards the Tee

Density

The skeletal density of the pipe was determined to be 0.939g/cc using the helium pycnometer. This is consistent with medium density polyethylene gas pipe material from the time period sample #678156 was manufactured.

Melt Flow

Sections of the pipe were prepared and subjected to ASTM D1238 melt flow testing.

Table 18: Melt Flow Measurements - Pipe

Sample ID	Trial #	Rate (g/10min)
678156-001	1	0.9200
678156-001	2	1.4360
678156-001	3	1.4060
Average		1.2540±0.2896

These results were consistent with medium density polyethylene gas pipe material.

Thermal Analysis

Specimens were prepared from the pipe section and subjected to ASTM D3418 differential scanning calorimetry. The resulting thermograms indicated a heat of fusion of 182.8J/g and no additional melting or exotherms were detected which would have suggested the presence of contamination. The results are shown in Figure 82. In addition, ASTM D3895 was performed on the prepared specimen to determine OIT. The test ran for 85 minutes but the material never oxidized as shown in Figure 83. This was consistent with the age of the PE considering it has absorbed organic materials from the gas supply over time. These organic compounds are relatively easily oxidized when compared to PE.

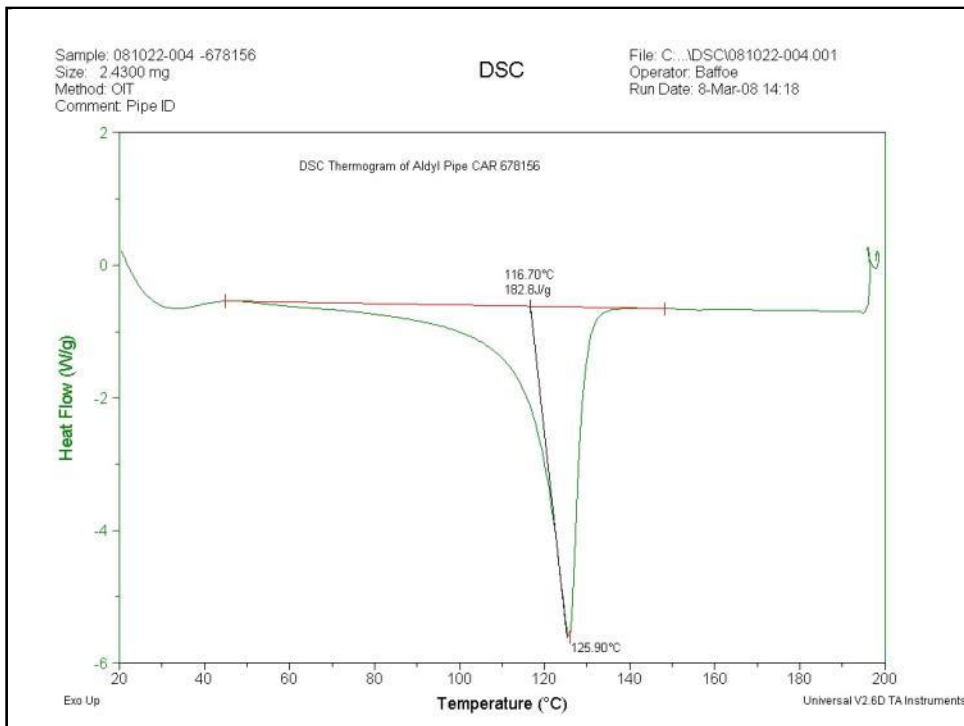


Figure 82. Differential Scanning Calorimetry

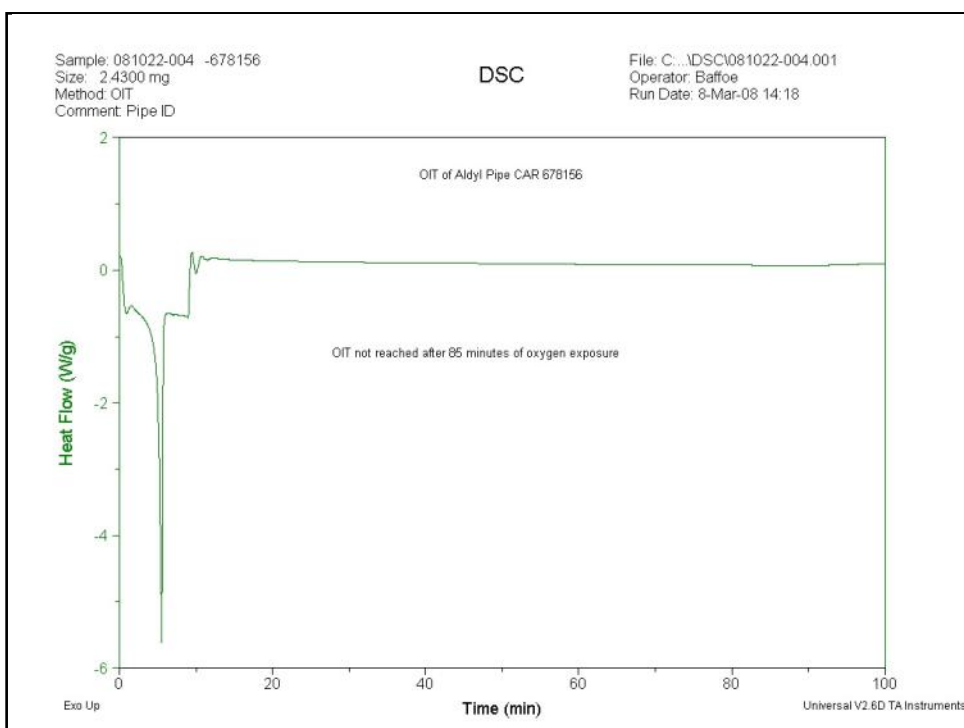


Figure 83. Oxidative Induction Time

Infrared Analysis

A comprehensive analysis was performed to determine the condition of the pipe and to detect the presence of any organic materials not associated with the pipe material using Fourier-Transform - Infrared Spectroscopy. The results did not indicate the presence of foreign organic materials in the outer (Figure 84), middle (Figure 85), or inner (Figure 86) pipe wall within the detectability of the instrument. The 1650cm^{-1} to 1750cm^{-1} region of the resulting spectra was also examined. Absorbencies in this region are associated with polyethylene oxidative products. Weak absorbencies were observed in this region that indicated minimal oxidation had occurred. This suggested that the pipe was manufactured and stored acceptably prior to installation.

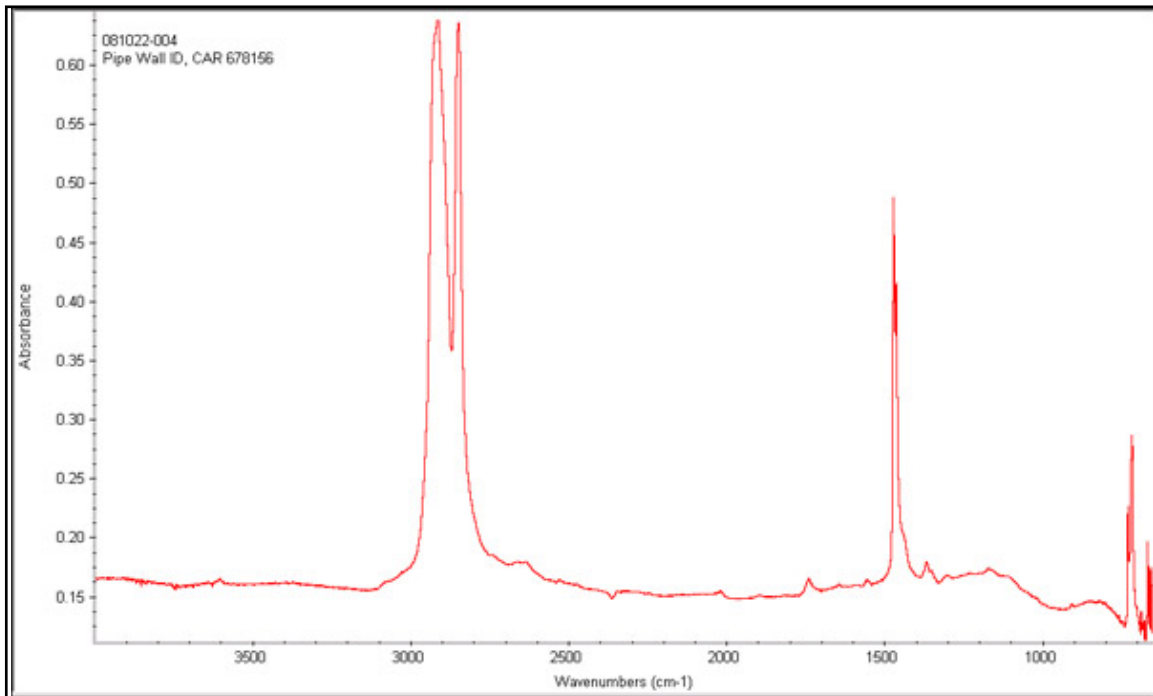


Figure 84. FT-IR Outer Wall

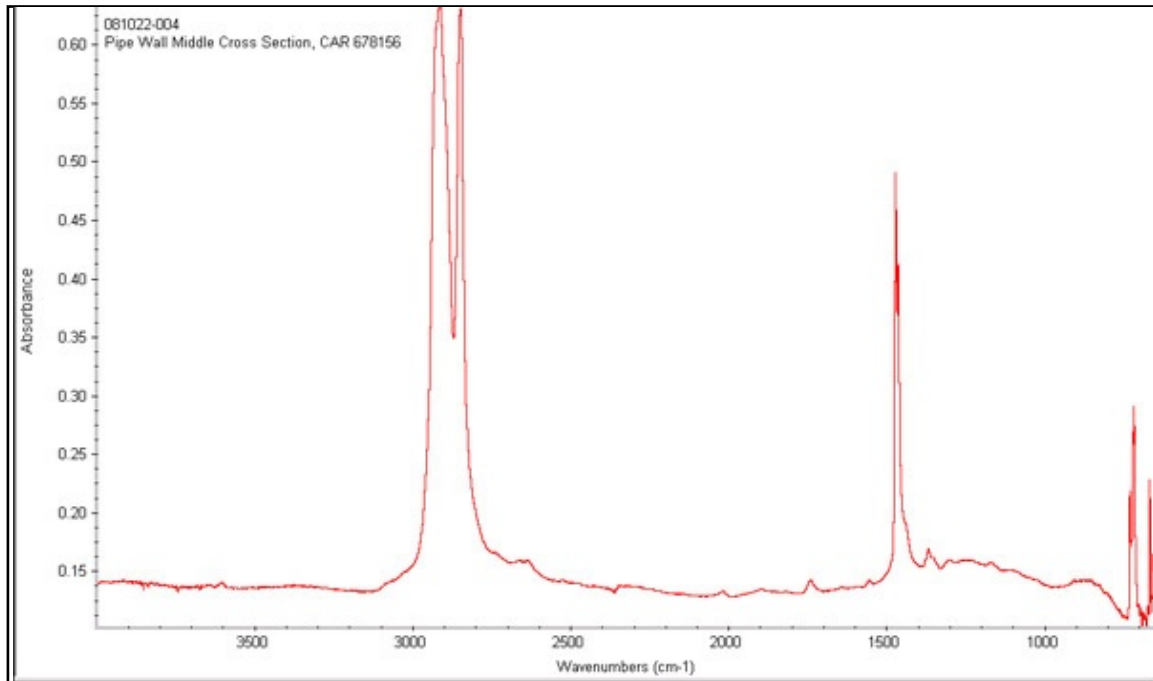


Figure 85. FT-IR Middle Wall

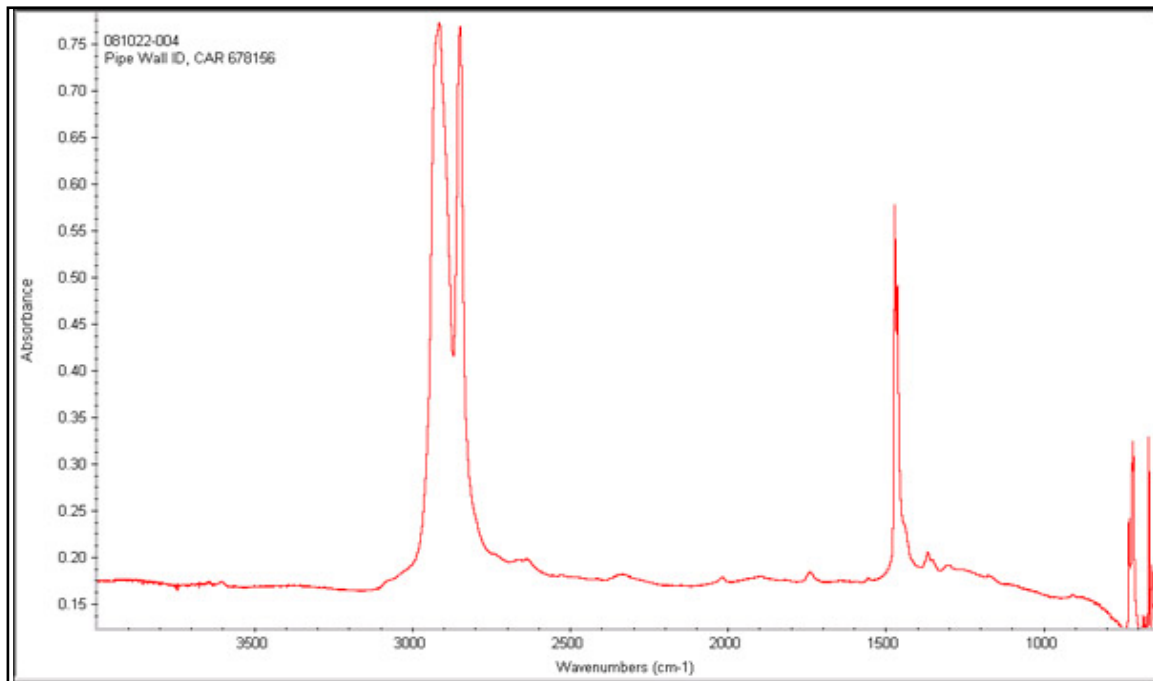


Figure 86. FT-IR Inner Wall

Conclusions

Based on the tests performed, it was concluded that the submitted section failed due to the stress concentration at the edge of the fusion tee. Typical loads associated with pipe burial/settling and the relatively low resistance to crack propagation of older generation PE material combined with the stress concentrator to lead to the observed SCG failure.

Impingement - #00590



Figure 87. As Received Condition

Table 19. Impingement Background

Pipe Information	00590
Color	Orange
Diameter	4"
SDR	11.5
Resin	PE 2306
Manufacturer	Driscopipe
Design Pressure	-
Service Information	
Operating Pressure	-
Service Temperature	55°F
Comments	-
Timeline	
Placed in Service	-
Installation Method	-
Removed from Service	September 2007
Comments	-
Environmental	
Soil Type	-
Evidence of 3rd Party Damage	No

Visual Examination

The sample contained a crack approximately 6.25" in length in the outer wall of the pipe (Figure 88) and a dimple in the exterior surface of the pipe located approximately midway in the crack length (Figure 89). Examination of the inner pipe wall confirmed that the crack had traversed through the pipe wall as shown in Figure 90.



Figure 88. Crack on Outer Wall



Figure 89. Close Up, Dimple and Crack



Figure 90. Crack As Seen On Inner Wall

The pipe was the carefully cut so as to expose the fracture surface while minimizing opposing fracture surface contact and associated smearing of the surface morphology during the cutting operation. Once the fracture surfaces were exposed they were visually examined at magnifications up to 160X. The origin of the fracture, visible in Figure 91 and Figure 92, was found in the inner wall; located almost directly beneath the dimple in the outer wall. There was no evidence of defects or foreign material in the pipe wall.

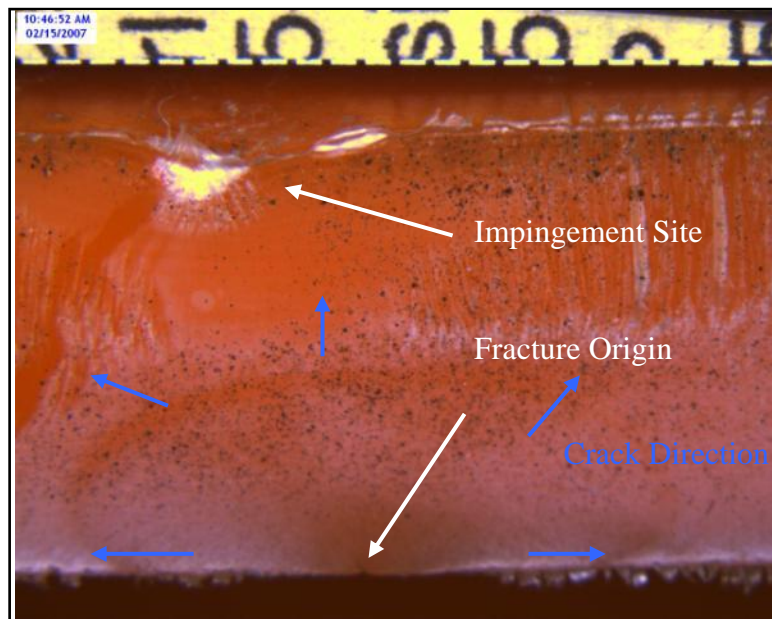


Figure 91. Fracture Origin

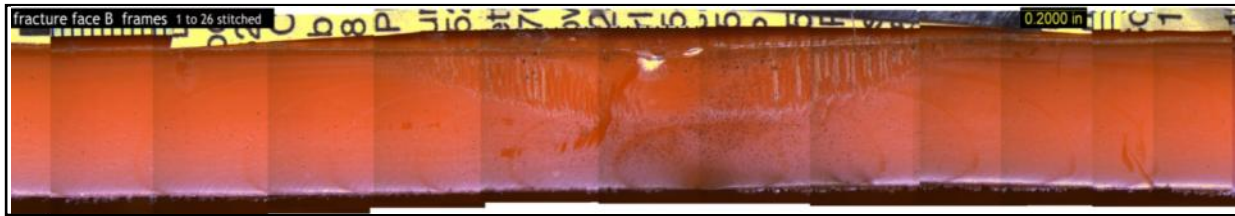


Figure 92. Composite Photo, Fracture Surface - Outer Wall at Top

Density and Melt Flow

A portion of the pipe material was removed and subjected to melt flow analysis in accordance with ASTM D1238. The results of this testing indicated that the pipe material had a MFR of 0.16g/10min. Density testing was also performed using a helium pycnometer. This test indicated that the material had a density of 0.942g/cc.

Conclusions

Based on the tests performed it was concluded that:

- 1) The fracture in the submitted pipe section resulted from rock impingement with the crack propagating by SCG process,
- 2) There were no observed pre-existing defects in the pipe; and
- 3) The pipe was consistent with properly extruded PE 2306 material.

Impingement - #04020731



Figure 93. Bottom Side of as Received Sample

Table 20. Slit Failure Background

Pipe Information	04020731
Color	Tan
Diameter	2"
SDR	-
Resin	PE 2306
Manufacturer	DuPont Aldyl A
Design Pressure	-
Service Information	
Operating Pressure	1-60 psig
Service Temperature	60°F
Comments	Pressure tested at 100 psig
Timeline	
Placed in Service	February 1971
Installation Method	Direct Burial; Bored
Removed from Service	September 2007
Comments	40" depth of cover; Pipe laying on rock in ditch
Environmental	
Soil Type	Sand; Rock
Evidence of 3rd Party Damage	No

Visual Examination

The failure report and background documentation provided with this sample indicated the presence of a rock in the ditch at the failure location. The impingement point is expressed by a green circle in Figure 94 below. Figure 95 shows the slit as seen on the inner wall. The location of the slit on the inner wall corresponds to the outer wall location. The impingement of the rock resulted in localized pipe loading/deformation leading to an axial slit wise crack. Most likely, it initiated on the ID (under tensile load) and grew through the wall to the OD.



Figure 94. Axial Slit on Outer Wall



Figure 95. Axial Slit on Inner Pipe Wall

External Loading - #26020806



Figure 96. As Received Sample

Table 21. External Loading Background

Pipe Information	26020806
Color	Orange
Diameter	4"
SDR	-
Resin	PE 2306
Manufacturer	-
Design Pressure	-
Service Information	
Operating Pressure	1-60 psig
Service Temperature	60°F
Comments	Pressure tested at 100 psig for 150 minutes; Pipe was resting on a 4" steel main
Timeline	
Placed in Service	August 1976
Installation Method	Direct Burial; Bored
Removed from Service	January 2008
Comments	30" depth of cover
Environmental	
Soil Type	Sand
Evidence of 3rd Party Damage	No

Visual Examination

According to background information provided by the submitting company, the pipe was found resting on a 4-inch steel main. This resulted in a localized shell bending load and deformation of the plastic pipe. An axial slit-wise crack was observed centered on the inner wall at the load point. The slit on the inner wall was measured at approximately 4" long. The crack exhibited full wall penetration resulting in a 1" slit on the outer wall.

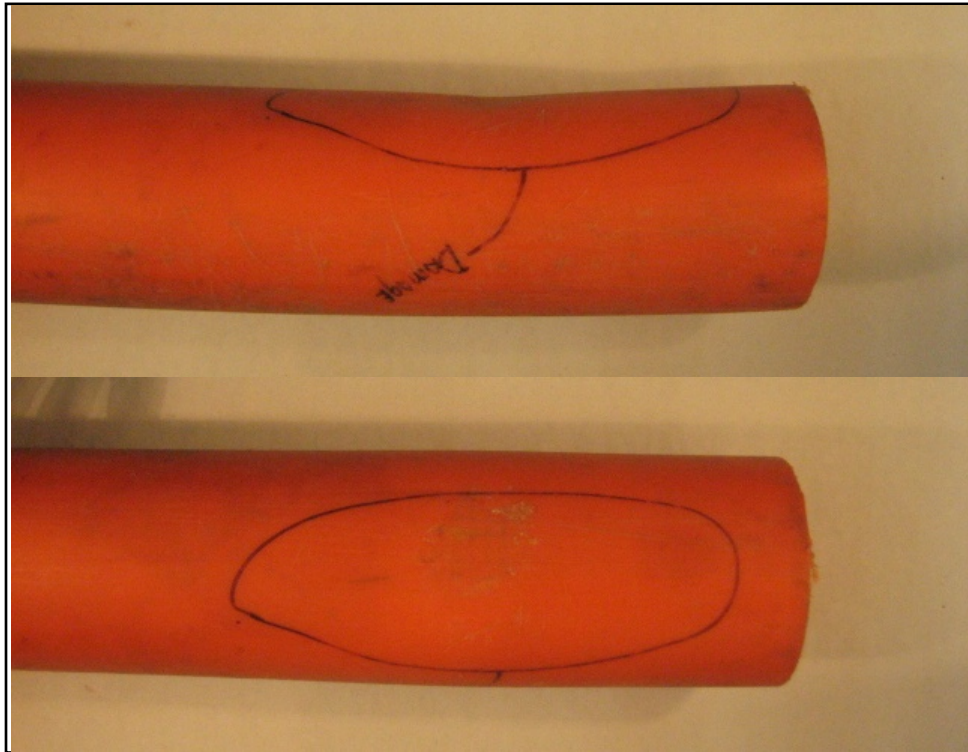


Figure 97. Side and Bottom View of Sample



Figure 98. Slit on Outer Wall

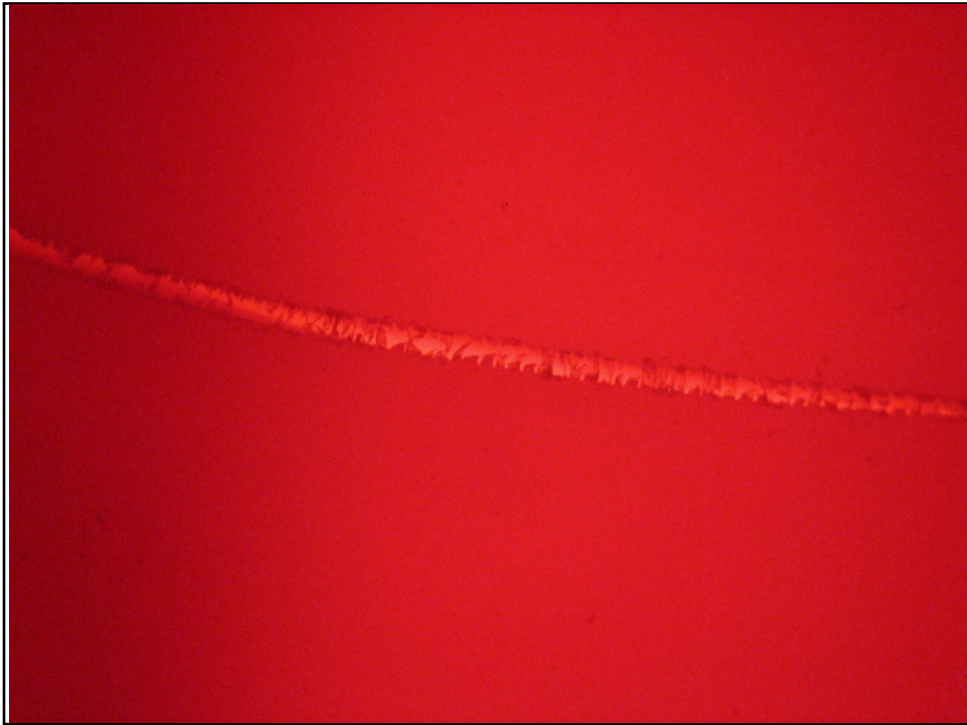


Figure 99. Slit on Inner Wall

Tee Caps

Cap #50020726



Figure 100. As Received Cap

Background data was not available for this sample.

Visual Examination

The cap was transversely split in two. The topside of the cap contained an o-ring for sealing the cap to the tee. This o-ring was free of nicks, had no embedded material and was also free of cracking. The actual cap material adjacent to the o-ring was free of scratches and gouges suggesting that the cap was tightened down without the top of the tee coming in contact with the cap which would have suggested potential over-tightening of the cap during installation. Both the top side (Figure 101) and bottom side (Figure 102) fracture surfaces were lightly covered with dirt from the installation site with more dust on the open-side fracture surface. The cap threads were free from distortion and damage as shown in Figure 103.

The top-side fracture surface was further examined using the stereo optical microscope with magnification capabilities to 320X. The results of this examination failed to indicate a single fracture origin. Instead it was determined that the fracture originated at the root of the last thread (nearest the top of the cap) and radiated outward tangent to this thread root. The fracture surface exhibited no indication of a torsional force component. White streaks were observed in the fracture surface as seen in Figure 104.



Figure 101. Topside Fracture Surface



Figure 102. Bottom Side Fracture Surface



Figure 103. Cap Threads

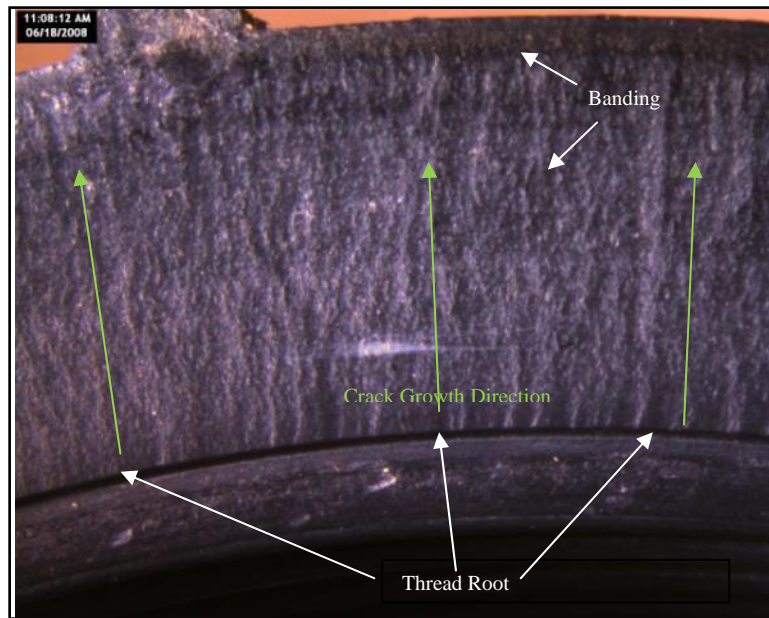


Figure 104. Topside Fracture Surface

Infrared Analysis

A specimen was prepared from the cap and subjected to infrared analysis. The resulting spectrum, shown in Figure 105, contained absorbencies consistent with a nylon (polyamide) thermoplastic.

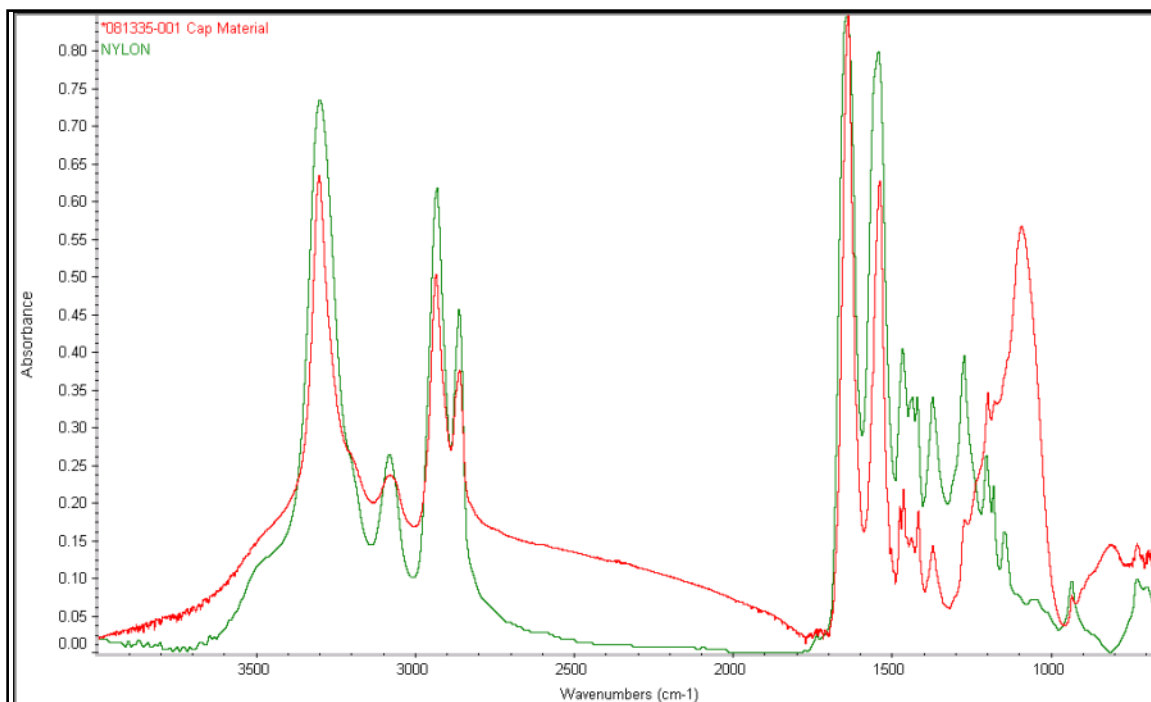


Figure 105. FT-IR Spectrum of the Cap Material

Differential Scanning Calorimetry

Since infrared analysis cannot conclusively determine the type of nylon, another specimen was prepared and analyzed for melting temperature by DSC. The resulting thermogram, seen in Figure 106, indicated a peak melt at 252°C. This was consistent with nylon 6,6 thermoplastic. No other melts were present that would have indicated the presence of a contaminant material.

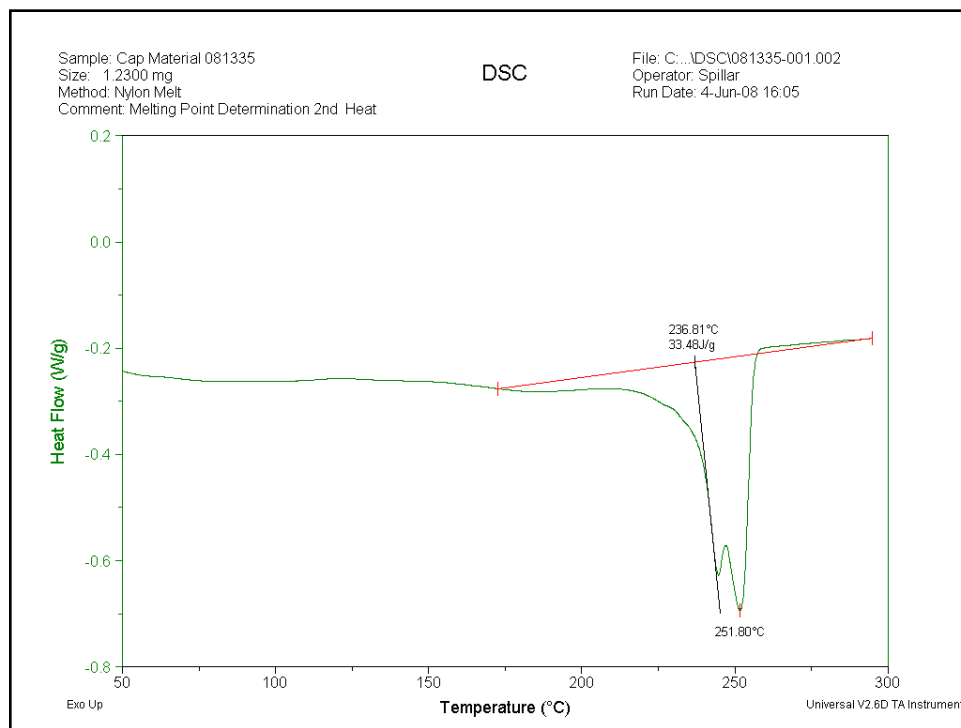


Figure 106. DSC Thermogram of the Cap Material

Thermogravimetric Analysis and Energy Dispersive X-ray

To further identify the cap material, a final specimen was prepared and analyzed using Thermogravimetric Analysis (TGA) to determine the ash content. The resulting TGA plot (Figure 107) indicated that the material had an ash content of 40%. Subsequent analysis by Energy Dispersive X-ray (EDX) indicated that the ash contained significant amounts of silicon (Si), aluminum (Al), oxygen (O). This suggested the presence of kaolin, a common filler material. Titanium (Ti) was also present to a lesser extent and suggested the presence of titanium dioxide, a common filler, pigment, and flattening agent used in plastics and coatings. The EDX spectrum can be seen in Figure 108.

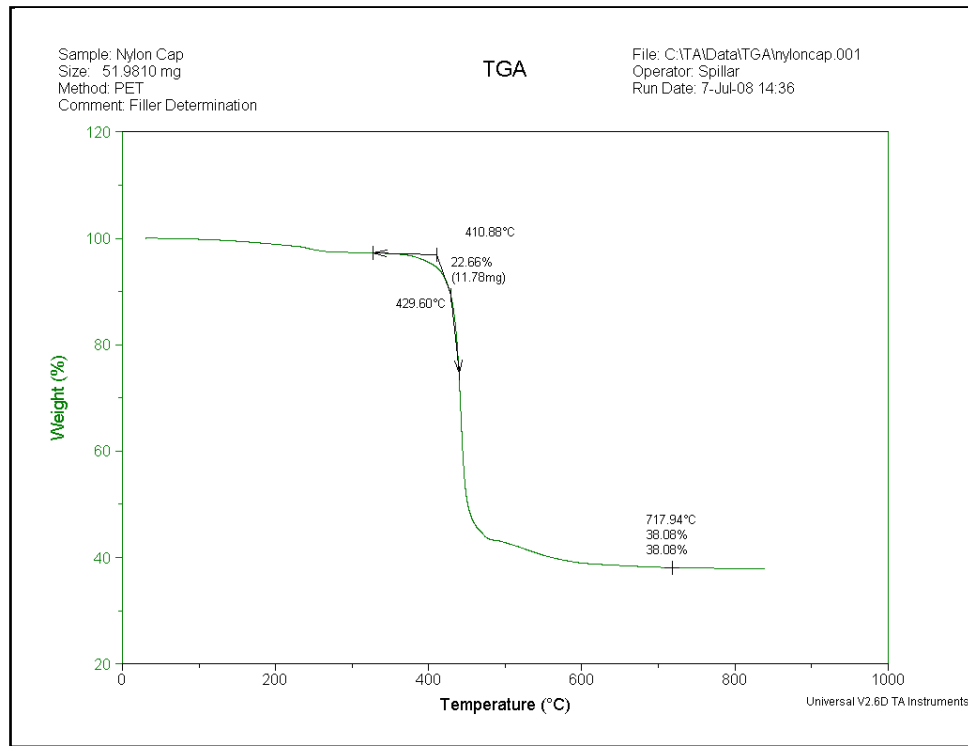


Figure 107. TGA Plot

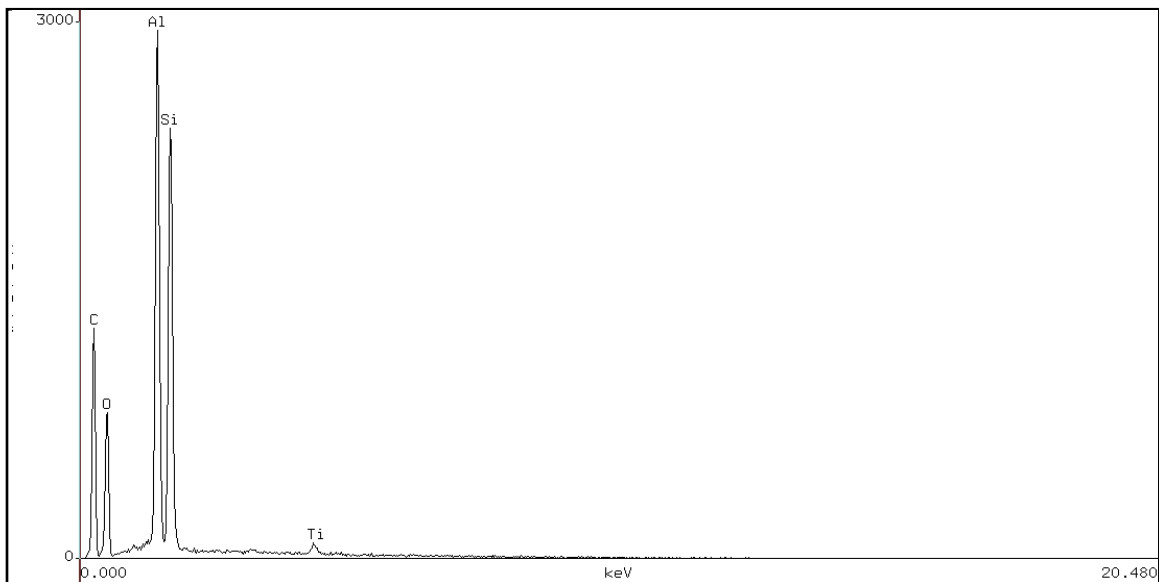


Figure 108. EDX Spectrum of the Cap Material Ash

Conclusions

Based on the tests performed it was concluded that:

- 1) Nylon materials are known to be to generally tough materials. The subject cap was manufactured from nylon, a 40% Kaolin filled (polyamide) 6,6. Nylon 6,6 the most commonly used of this material family.
- 2) The cap failure initiated in the root of the thread nearest the top off the cap. This area served to concentrate the tensile stress resulting from the mating of the cap to the companion tee.
- 3) There were no indications of over tightening or improper processing of the cap.
- 4) The banding observed in the fracture surfaces was the result of a differential cooling rate across the thickness of the part. This is common and was not a major contributor to the cap failure.
- 5) The white material found on the fracture surfaces was later determined to be unpigmented nylon 6,6 and was not a major contributor, if at all, to the cap failure.

Cap - #20020447



Figure 109. As Received Cap

Table 22. Cap Background

Pipe Information	20020447
Color	Black
Diameter	2" x 3/4" Service Tee
SDR	-
Resin	-
Manufacturer	Wayne
Design Pressure	-
Service Information	
Operating Pressure	1-60 psig
Service Temperature	60°F
Comments	Pressure tested at 90 psig for 120 minutes
Timeline	
Placed in Service	November 1993
Installation Method	-
Removed from Service	April 2004
Comments	12" depth of cover
Environmental	
Soil Type	Loam
Evidence of 3rd Party Damage	No

Visual Examination

This cap, manufactured by Wayne, exhibited a crack which extended approximately 230° around the circumference. The crack appeared to have originated in the first thread. Gouges indicative of the use of a wrench were apparent as seen to the left in Figure 109 though it is not possible to determine whether these marks were created during installation, service, or removal.



Figure 110. Crack Seen Inside the Cap.

Cap - #21020739



Figure 111. As Received Cap

Table 23. Cap Background

Pipe Information	21020739
Color	Black
Diameter	-
SDR	-
Resin	
Manufacturer	Wayne
Design Pressure	-
Service Information	
Operating Pressure	1-60 psig
Service Temperature	60°F
Comments	Pressure tested at 90 psig for 15 minutes
Timeline	
Placed in Service	December 1993
Installation Method	-
Removed from Service	November 2007
Comments	36" depth of cover
Environmental	
Soil Type	Clay
Evidence of 3rd Party Damage	No

Visual Examination

This cap exhibited a crack which ran about 200° around the circumference. The crack on this cap appears to have started at the first thread and also exhibited signs of wrench use.

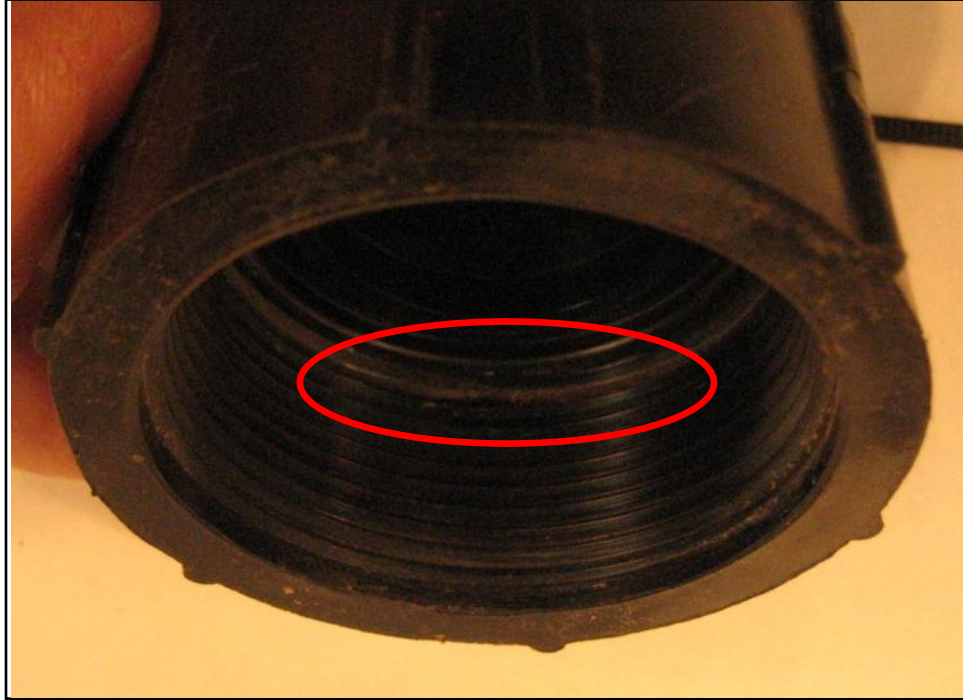


Figure 112. Soil on Interior Surface

Cap - #22020733



Figure 113. As Received Cap

Table 24. Cap Background

Pipe Information	22020733
Color	Black
Diameter	-
SDR	-
Resin	
Manufacturer	Wayne
Design Pressure	-
Service Information	
Operating Pressure	1-60 psig
Service Temperature	60°F
Comments	Pressure tested at 30 psig for 15 minutes
Timeline	
Placed in Service	January 1978
Installation Method	-
Removed from Service	October 2007
Comments	24" depth of cover
Environmental	
Soil Type	Gravel
Evidence of 3rd Party Damage	No

Visual Examination

This cap exhibited a crack which extended approximately 215° around the circumference. The crack appears to have originated in the first thread as indicated by the soil visible on the interior of the cap shown in Figure 114.



Figure 114. Dirty Interior Surface

Cap - #23020464



Figure 115. As Received Cap

Table 25. Cap Background

Pipe Information	23020464
Color	Black
Diameter	-
SDR	-
Resin	-
Manufacturer	-
Design Pressure	-
Service Information	
Operating Pressure	1-60 psig
Service Temperature	60°F
Comments	-
Timeline	
Placed in Service	1980
Installation Method	-
Removed from Service	June 2004
Comments	40" depth of cover
Environmental	
Soil Type	Clay
Evidence of 3rd Party Damage	No

Visual Examination

This cap from an unknown manufacturer exhibited a crack which was visible around the entire circumference. The crack appeared to have originated in the first thread. Gouges indicative of the use of a wrench were apparent as seen in Figure 116.



Figure 116. Cracked Cap with Wrench Marks

Cap - #24020499



Figure 117. As Received Cap

Table 26. Cap Background

Pipe Information	24020499
Color	Black
Diameter	-
SDR	-
Resin	-
Manufacturer	Wayne (cap)
Design Pressure	-
Service Information	
Operating Pressure	1-60 psig
Service Temperature	60°F
Comments	-
Timeline	
Placed in Service	November 1993
Installation Method	-
Removed from Service	December 2004
Comments	24" depth of cover
Environmental	
Soil Type	Clay
Evidence of 3rd Party Damage	No

Visual Examination

This cap exhibited a crack which extended approximately 240° around the circumference. The crack appeared to have originated in the same place as the previous caps. Gouges indicative of the use of a wrench can be seen in Figure 118.



Figure 118. Yellow Tee Visible Through the Crack

Caps - #25020718 and #49020718



Figure 119. As Received Service Tee with Broken Cap

Table 27. Cap Background

Pipe Information	25020718
Diameter	2"
SDR	-
Resin	-
Manufacturer	Wayne
Design Pressure	-
Service Information	
Operating Pressure	1-60 psig
Service Temperature	60°F
Comments	-
Timeline	
Placed in Service	1992 (main)
Installation Method	-
Removed from Service	2007
Comments	24" depth of cover
Environmental	
Soil Type	Loam
Evidence of 3rd Party Damage	No

Visual Examination

The received sample contained two service tees. The caps on each tee were completely severed. As seen in Figure 121, the cracks originated at the first thread on one of the caps.



Figure 120. Fracture Surfaces of Cap



Figure 121. Fracture Surface of the Top of the Cap

Cap - #31020649



Figure 122. As Received Cap

Table 28. Cap Background

Pipe Information	31020649
Color	Tan
Diameter	2" (main) 1 – ¼" (service)
SDR	-
Resin	PE 2306
Manufacturer	DuPont Aldyl A(pipe and tee)
Design Pressure	-
Service Information	
Operating Pressure	1-60 psig
Service Temperature	60°F
Comments	Pressure tested at 100 psig
Timeline	
Placed in Service	November 1970
Installation Method	-
Removed from Service	December 2006
Comments	36" depth of cover
Environmental	
Soil Type	Clay
Evidence of 3rd Party Damage	No

Visual Examination

The cap was extensively damaged yet all of the external threads appeared to have remained intact. The corresponding internal threads in the saddle tee were intact as well. The cap exhibited multiple fracture planes with associated multiple fracture origins. Fifty 50% of the upper portion of the cap was missing along with the o-ring. The general orientation of the major fracture planes suggested that the cap may have been subjected to significant loading from above.

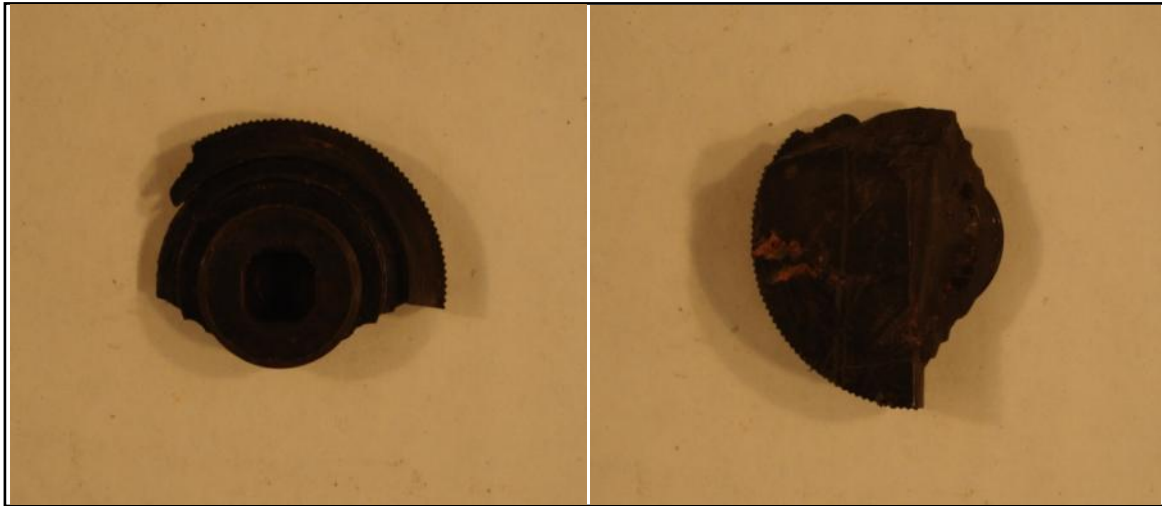


Figure 123. Cap, Underside Left and Topside Right



Figure 124. Internal Threads of the Saddle Tee

Thread Inserts

Service Tee Threads - #15020650



Figure 125. As Received Tee

Visual Examination

The sample was missing background data and companion cap upon submission. GTI was unable to obtain either. The failure initiated at root of the second thread. The thread root acted as a stress concentrator to the tensile forces produced by tightening the cap.

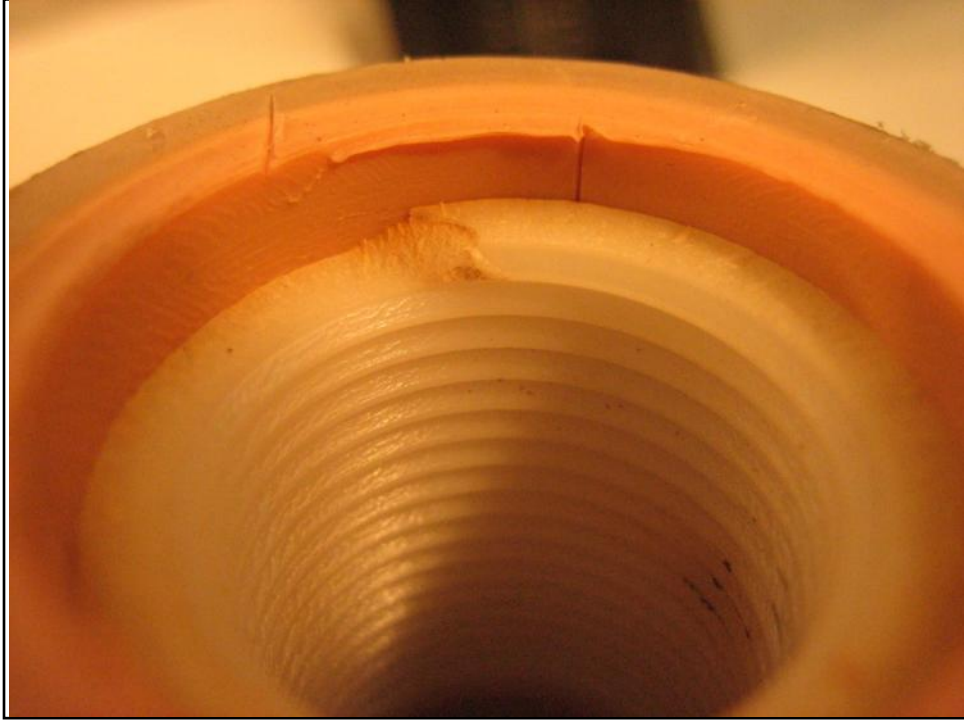


Figure 126. Close-up View of Thread Insert

Service Tee Threads - #29020510

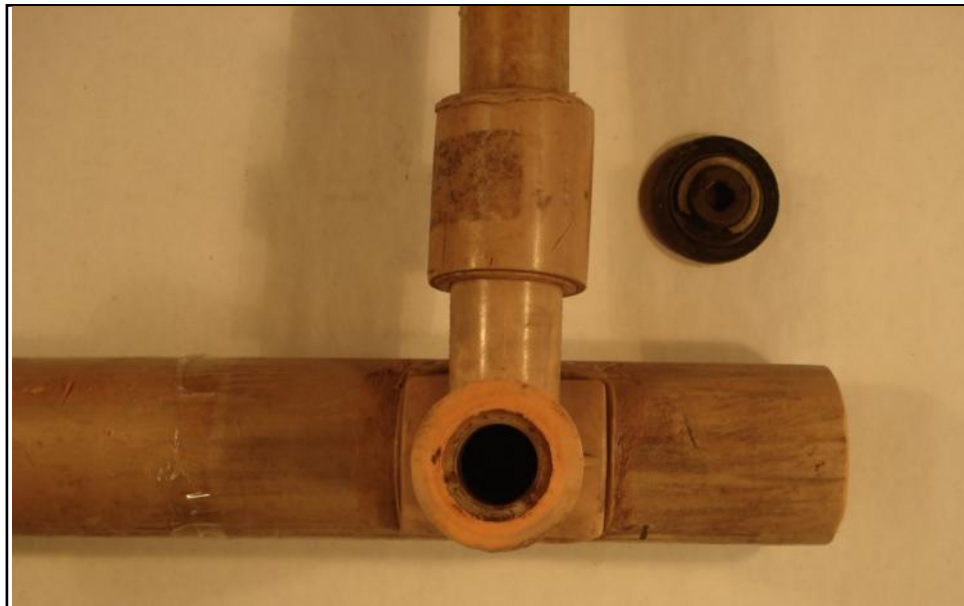


Figure 127. As Received Tee

Table 29. Service Tee Threads Background

Pipe Information	29020510
Color	Tan
Diameter	2"
SDR	-
Resin	PE 2306
Manufacturer	Aldyl-A
Design Pressure	-
Service Information	
Operating Pressure	1-60 psig
Service Temperature	60°F
Comments	Pressure tested at 100 psig
Timeline	
Placed in Service	May 1970
Installation Method	Direct Burial
Removed from Service	January 2005
Comments	36" depth of cover
Environmental	
Soil Type	Clay
Evidence of 3rd Party Damage	No

Visual Examination

The threaded insert fractured about 300° at the second thread which remained attached to the cap. The thread root acted as a stress concentrator to the tensile forces produced by tightening the cap. The cap contained deposits consistent with an aged lubricant that was most likely applied to the o-ring on a previous occasion. Lubricants can embrittle certain types of plastic but without identifying this particular insert material it cannot be stated with certainty.



Figure 128. Close up of Severed Insert



Figure 129. Cap with Insert Attached

Socket Couplings

Socket Coupling - #30020542



Figure 130. As Received

Table 30. Coupling Background

Pipe Information	30020542
Color	Black
Diameter	2"
SDR	-
Resin	-
Manufacturer	-
Design Pressure	-
Service Information	
Operating Pressure	1-60 psig
Service Temperature	60°F
Comments	Pressure tested at 100 psig for 360 minutes
Timeline	
Placed in Service	January 1972
Installation Method	Direct Burial
Removed from Service	May 2005
Comments	60" depth of cover
Environmental	
Soil Type	Sand
Evidence of 3rd Party Damage	No

Visual Examination

The coupling exhibited complete separation in plane with the end of the orange pipe. Preliminary examination of the fracture surface indicated the presence of torsional loading of the coupling and adjacent pipe. Approximately 50% of the face of the failure exhibited features similar to SCG. The crack appears to have initiated on the ID then grew towards the OD with final ductile rupture at the OD surface. In Figure 132, the whitened area below the yellow line shows the SCG features. The ductile rupture area is above the yellow line.

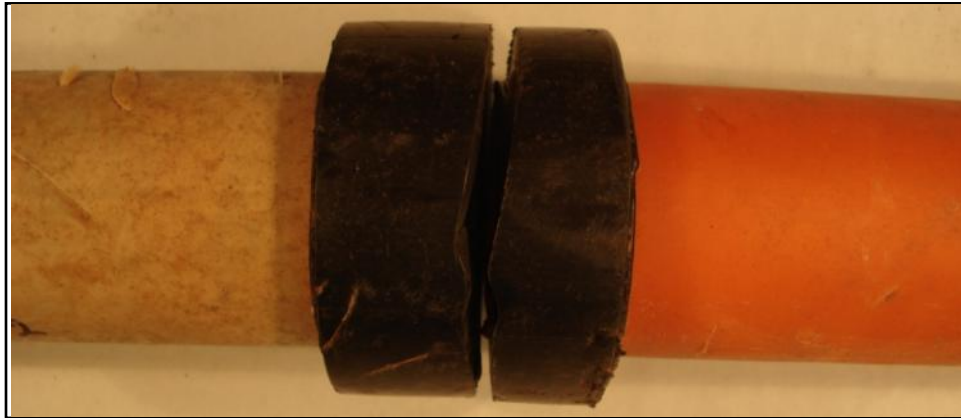


Figure 131. Severed Coupling

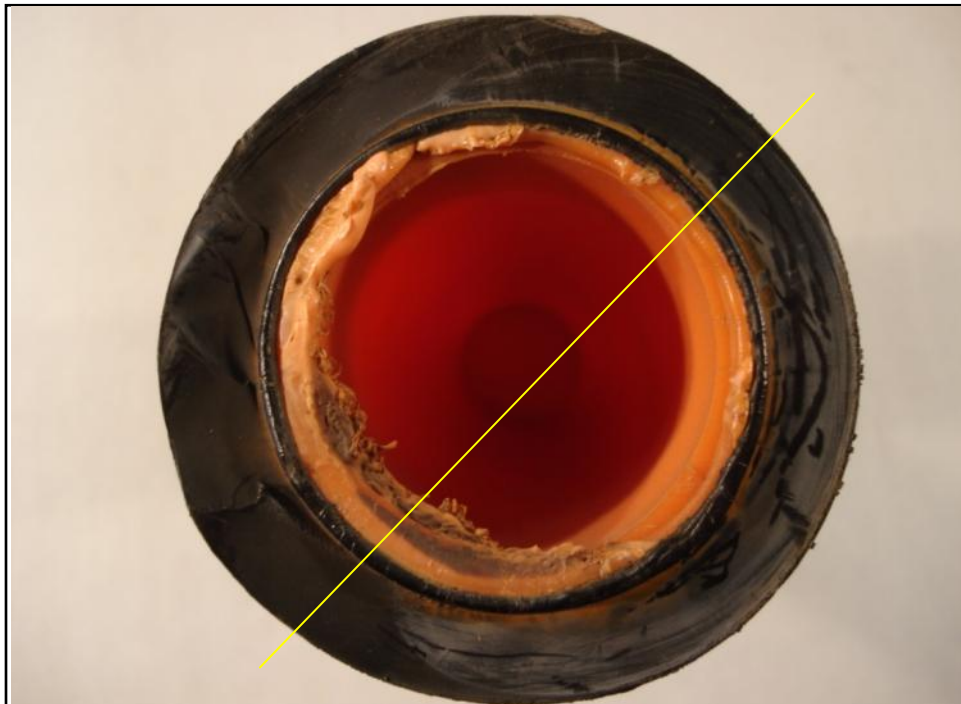


Figure 132. Fracture Face

Socket Coupling - #35020485



Figure 133. As Received Service Tee with Socket Coupling

Table 31. Socket Coupling Background

Pipe Information	35020485
Color	Orange
Diameter	1"
SDR	-
Resin	-
Manufacturer	-
Design Pressure	-
Service Information	
Operating Pressure	1-60 psig
Service Temperature	60°F
Comments	Pressure tested at 100 psig for 15 minutes
Timeline	
Placed in Service	October 1971
Installation Method	-
Removed from Service	October 2004
Comments	36" depth of cover
Environmental	
Soil Type	
Evidence of 3rd Party Damage	No

Visual Examination

The socket coupling showed signs of overheating to the point of deformation. A 1 – ¾” circumferential slit was observed on the underside of the socket. The slit appears to line up with end of the service line pipe. The side view of the specimen in Figure 134 shows the service line in parallel misalignment. The direction of the misalignment relative to the location of the crack indicates that an excessive bending stress was applied.



Figure 134. Side View



Figure 135. Bottom View

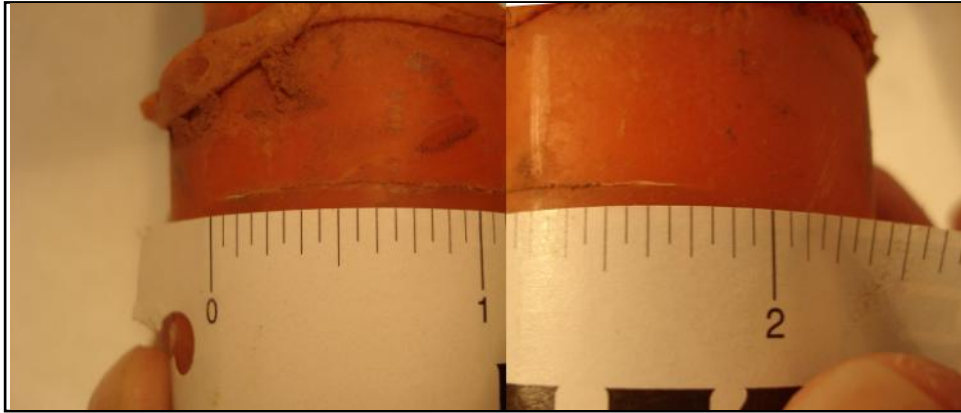


Figure 136. 1 - $\frac{3}{4}$ " Circumferential Slit on Underside of Coupling

Socket Coupling - #39020605

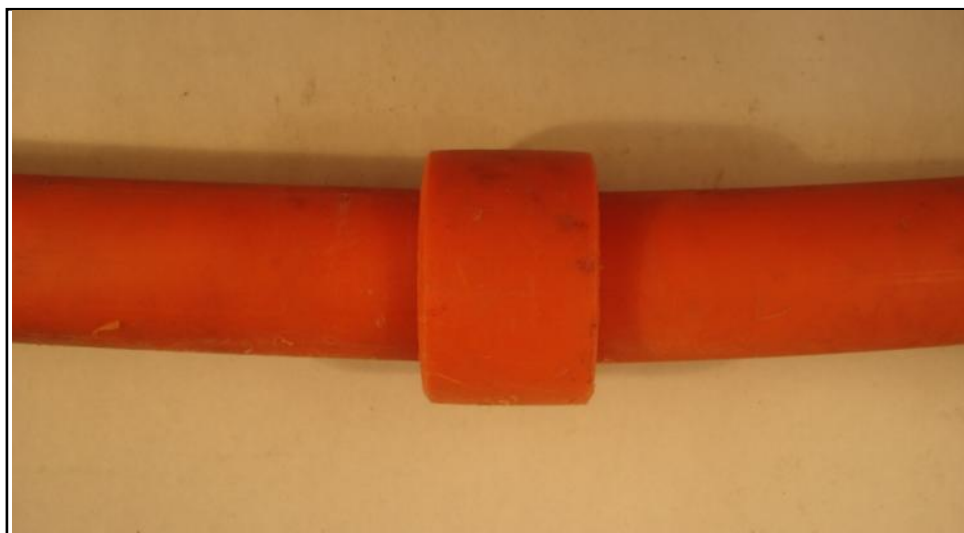


Figure 137. As Received Coupling

Table 32. Socket Coupling Background

Pipe Information	39020603
Color	Orange
Diameter	2"
SDR	11
Resin	PE 2306
Manufacturer	Driscopipe 6500 (pipe) Unknown (coupling)
Design Pressure	-
Service Information	
Operating Pressure	1-60 psig
Service Temperature	60°F
Comments	Pressure tested at 100 psig for 4 hours
Timeline	
Placed in Service	1982
Installation Method	-
Removed from Service	January 2006
Comments	40" depth of cover
Environmental	
Soil Type	Clay
Evidence of 3rd Party Damage	Loading from excavation in area

Visual Examination

As seen in Figure 137, the pipe was under a bending moment from installation conditions. Because the bending made it impossible to observe the entire inside of the pipe, one end was cut off. A slit failure in the circumferential direction was observed on the pipe wall as seen in Figure 138. The crack lined up with the edge of the coupling which is also where external leak location was identified during pressure testing as identified by an arrow in Figure 139. The direction of the misalignment relative to the location of the crack indicates that an excessive bending stress was applied.



Figure 138. Crack in Pipe Wall on ID

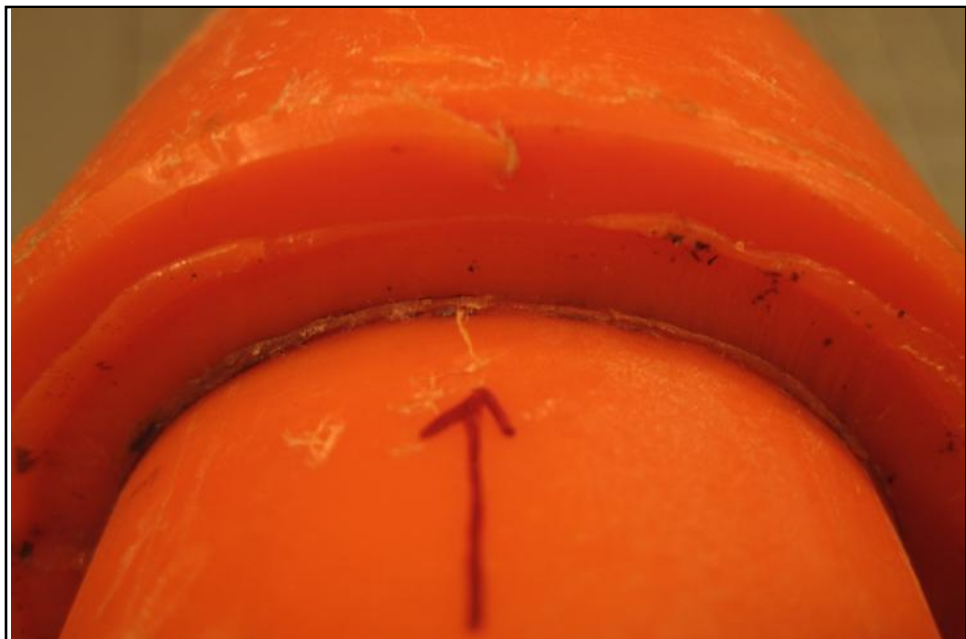


Figure 139. Side View of Socket Fusion

Socket Tees

Socket Tee - #19020414



Figure 140. As Received Socket Tee

Table 33. Socket Tee Background

Pipe Information	19020414
Color	Orange
Diameter	4"
SDR	-
Resin	-
Manufacturer	Unknown (pipe) Unknown (tee)
Design Pressure	-
Service Information	
Operating Pressure	1-60 psig
Service Temperature	60°F
Comments	Pressure tested at 100 psig for 120 minutes
Timeline	
Placed in Service	1978
Installation Method	-
Removed from Service	March 2004
Comments	48" depth of cover
Environmental	
Soil Type	Rock
Evidence of 3rd Party Damage	No

Visual Examination

A thru wall circumferential slit on the socket was observed. The 4" slit appeared to line up with the end of the pipe. Also of note, the socket displayed some radial distortion. Interference between the pipe and the socket could be responsible for elevating stresses at the pipe edge/socket interface.



Figure 141. Circumferential Slit in Fitting

Socket Tee - #33020602



Figure 142. As Received Socket Tee

Table 34. Socket Tee Background

Pipe Information	33020602
Color	Orange
Diameter	3 Way Tee 2" in all directions
SDR	11.5
Resin	PE 2306
Manufacturer	Unknown (pipe) unknown (tee)
Design Pressure	-
Service Information	
Operating Pressure	1-60 psig
Service Temperature	60°F
Comments	Pressure tested at 90 psig for 60 minutes ; Interference fit slit
Timeline	
Placed in Service	September 1972
Installation Method	Direct Burial
Removed from Service	January 2006
Comments	30" depth of cover
Environmental	
Soil Type	Clay
Evidence of 3rd Party Damage	No

Visual Examination

A 2” circumferential slit crack in the socket that grew completely through the socket wall was observed. The slit was approximately lined up with the end of the pipe where stress was most likely concentrated due to radial distortion also noted on this sample.

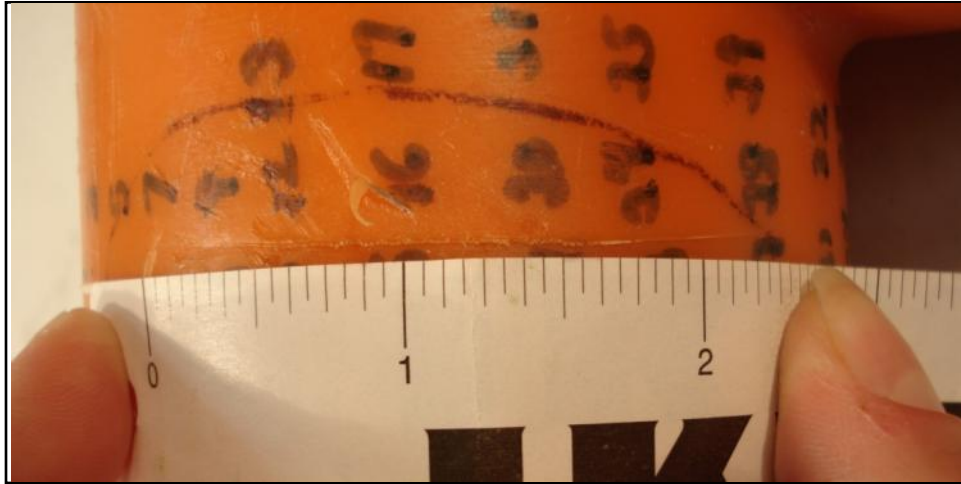


Figure 143. Circumferential Slit in Socket

Supplemental Inspection

This sample was shared with another PHMSA sponsored project “Nonmetallic Joint Quality Assessment” (Project #217 Contract Number: DTPH56-07-T-000001). The objective of this project is to develop non-destructive inspection techniques for heat fusion joints. Ultrasonic measurements were used on this and other samples and provided information on flaws in the interior of the pipe and fitting. The numbers visible on the sample mark locations where measurements were made and recorded using ultrasonic sensor. The measurements showed the crack direction from the OD to the ID angles into the body of the socket tee.

Socket Tee - #34020623

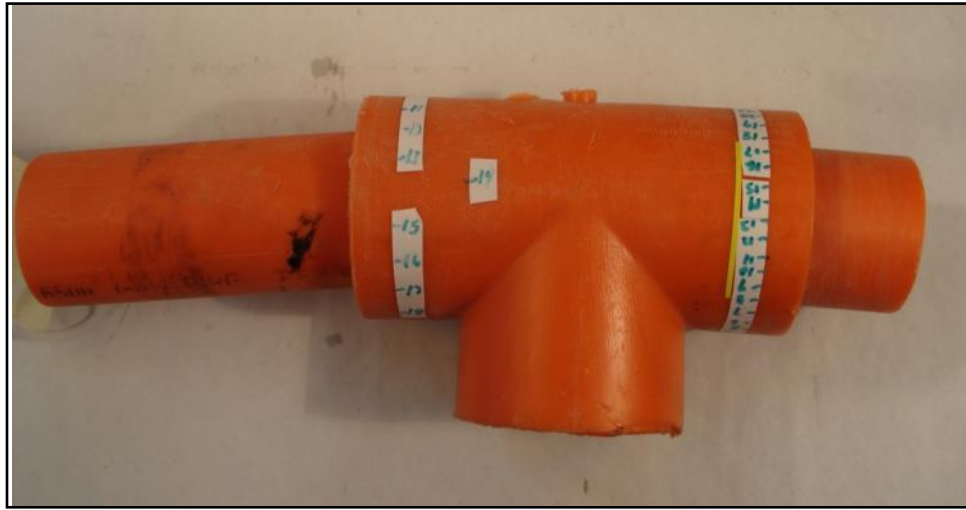


Figure 144. As Received Socket Tee

Table 35. Socket Tee Background

Pipe Information	34020623
Color	Orange
Diameter	2"
SDR	-
Resin	PE 3206
Manufacturer	Driscopipe 6500 (pipe) Unknown (tee)
Design Pressure	-
Service Information	
Operating Pressure	1-60 psig
Service Temperature	60°F
Comments	Pressure tested at 90 psig for 4 hours
Timeline	
Placed in Service	August 1983
Installation Method	Direct Burial; Bored
Removed from Service	March 2006
Comments	48" depth of cover
Environmental	
Soil Type	Sand
Evidence of 3rd Party Damage	No

Visual Examination

A crack was observed on the face of socket tee as seen in Figure 145. Looking into the fitting, a ledge was observed, suggesting this is a molded part rather than an extruded pipe. A circumferential crack extending 60° around the circumference and discoloring were also observed. These three features are identified by arrows in Figure 146.



Figure 145. Crack on Socket Surface

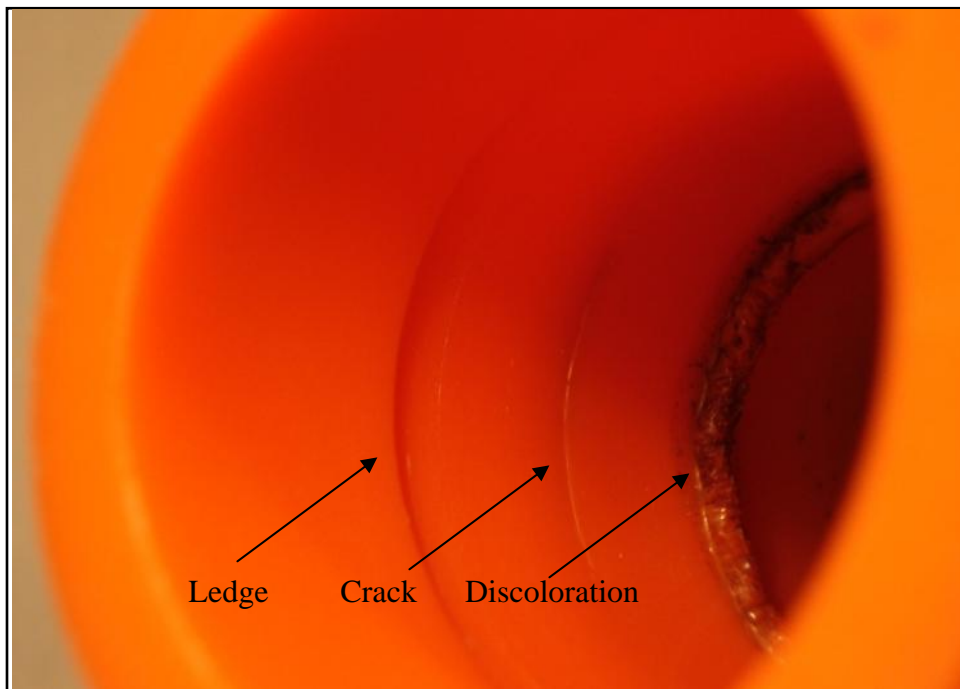


Figure 146. Features on ID

Supplemental Inspection

This sample was also shared with PHMSA sponsored project “Nonmetallic Joint Quality Assessment” (Project #217 Contract Number: DTPH56-07-T-000001). Black dots seen in Figure 147 show ultrasonic measurement locations. The measurements showed poor fusion quality at the pipe/coupling interface for a distance of 0.3” in from the edge of the socket tee. This area is marked by green arcs in Figure 147. Beyond this area, fusion quality improved dramatically going towards the body of the tee. The location of the crack on the molded part/pipe was 0.3” from the edge of the socket tee. The information suggests gas escaped out of the crack and through the un-bonded area between the pipe and coupling.



Figure 147: Photograph of Tee Showing Location of Leak

Procedural Failures

High Volume Tapping Tee - #00632



Figure 148. Close-up of Pipe Section with Tee as Seen in the Field.

Table 36. 4" x 2" HVTT Background

Pipe Information	00632
Diameter	4"
SDR	11.5
Resin	PE 2406
Manufacturer	Plexco
Design Pressure	60 psig
Service Information	
Operating Pressure	20-35 psig
Service Temperature	55°F
Comments	Pressure tested to 100 psig
Timeline	
Placed in Service	January 23, 1997
Installation Method	Direct bury with stiffener sleeve
Removed from Service	September 12, 2007
Comments	Sleeve was installed prior to tee
Environmental	
Soil Type	In situ and sand shading
Evidence of 3rd Party Damage	No

Visual Examination

Areas of uneven rollback or no rollback were discovered at the tee-pipe interface as shown in the photos in Figure 149. A gap was noted on the inside of the tee between the tee and the pipe outer wall as seen in Figure 150. This gap suggested an area of discontinuous fusion.

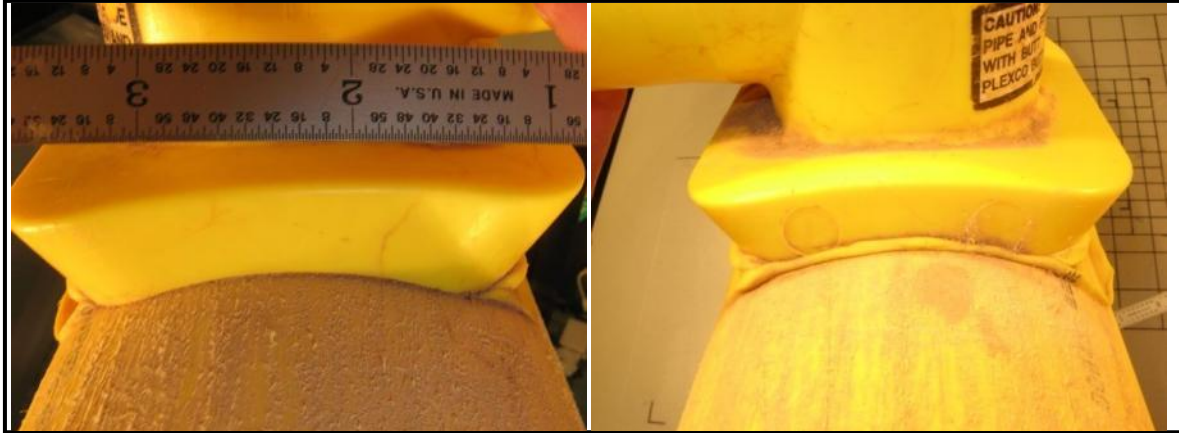


Figure 149. Left Side with No Bead Rollback and Right Side with Uneven Bead Rollback

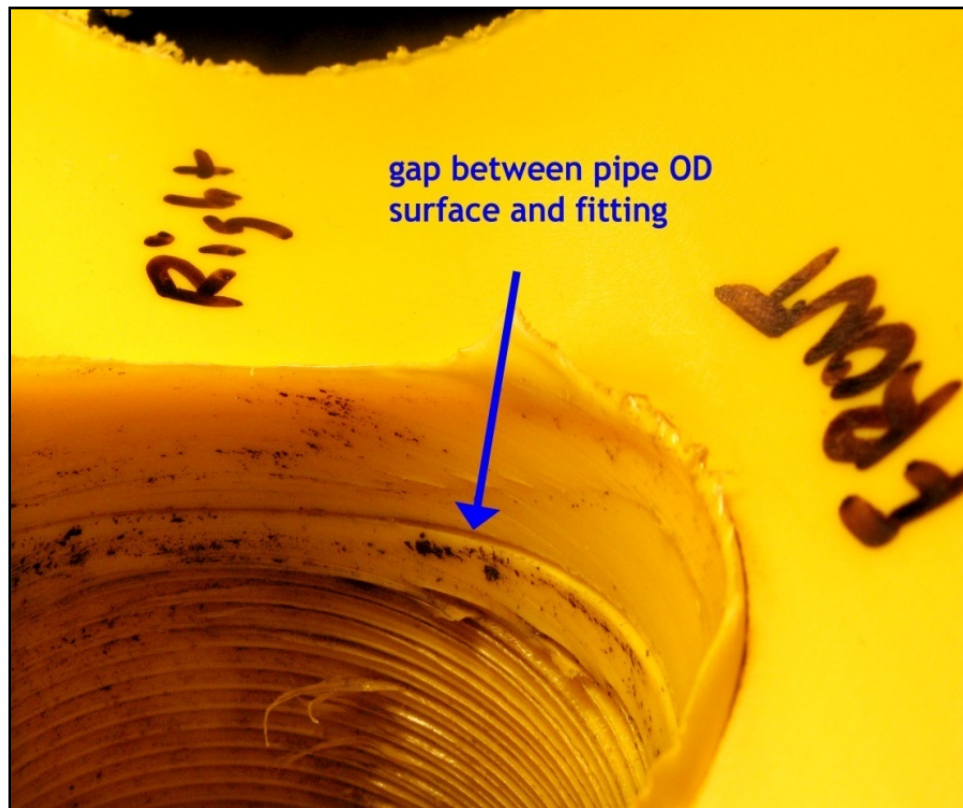


Figure 150. Close-up of Gap between Pipe Surface and Fitting

The specimen was capped, immersed in water, and pressurized to 15 psi to verify the location of the leak. As seen in Figure 151, the leak was found on the backside of the tee at the fusion interface.



Figure 151. Pressure Test to Identify Leak Location

After the initial leak test, the tee and companion pipe segment were sectioned and force fractured with liquid nitrogen in order to expose the area of the detected leak. Once the tee was separated from the pipe, a shifting of the print line was observed as seen in Figure 152.

Line drawings were overlaid on the photograph to illustrate the complexity of the surface condition. The damage encircled by purple was caused by GTI scraping to obtain sample material for differential scanning calorimetry. The area lined by red was observed as being shiny and smooth as well as depressed relative to the surrounding areas. Coloring in the red area matched the coloring of the scraped areas around the tee though more yellow. This suggested heating in this area was minimal and a corresponding minimal fusion, if any, had occurred. The area lined by grey indicated rough, raised areas. The surface was somewhat grey in color and exhibited signs of some adhesion. The blue area was also depressed and matched the shape of the edge of the tee's saddle. The red, grey, and blue areas had matching surfaces on the underside of the tee. The opposing face to the red area was smooth and the opposing face to the grey area was relatively rough. The blue area's mating face showed transfer of the print line. This transfer can be seen in Figure 153. A close up examination of this area revealed the presence of fibers imbedded in the surface. The fibers likely transferred from a material used in the pre-fusion cleaning process.

Scraped by GTI
Shiny, smooth, depressed area
Rough, grey colored area
Depressed area



Figure 152. Pipe Segment Surface from Under the Tee on the Side Containing the Leak



Figure 153. Mating Surfaces of the Tee and Pipe

Density

The densities of the pipe and tee material were determined to be 0.9421g/cc and 0.9404g/cc respectively. This was consistent with medium density polyethylene gas pipe material.

Melt Flow

Portions of the pipe and tee sections were prepared and subjected to ASTM D1238 melt flow testing.

Table 37: Melt Flow Measurements - Pipe

Sample ID	Trial #	Rate (g/10min)
632-001a	1	0.1709
632-001a	2	0.1732
632-001a	3	0.1748
Average		0.173±0.002

Table 38: Melt Flow Measurements - Tee

Sample ID	Trial #	Rate (g/10min)
632-001b	1	0.1683
632-001b	2	0.1690
632-001b	3	0.1692
Average		0.1688±0.0005

These results were consistent with medium density polyethylene gas pipe material.

Thermal Analysis

Specimens were prepared from the pipe section by removing material from the pipe fusion surface, middle of the pipe wall, and the inner pipe wall surface. These specimens were subjected to ASTM D3418 differential scanning calorimetry. The resulting thermograms indicated consistent levels of crystallinity for each of the specimens. No additional melting or exotherms were detected which would have suggested the presence of contamination. In addition, ASTM D3895 oxidative-induction time was performed on another set of prepared specimens. The scraped surface prepared for the fusion exhibited a slightly lower induction time than the middle and inner layers of the pipe. This was consistent with pipe that has been in the field. The OIT and DSC thermograms are shown in Figure 154, Figure 155, and Figure 156.

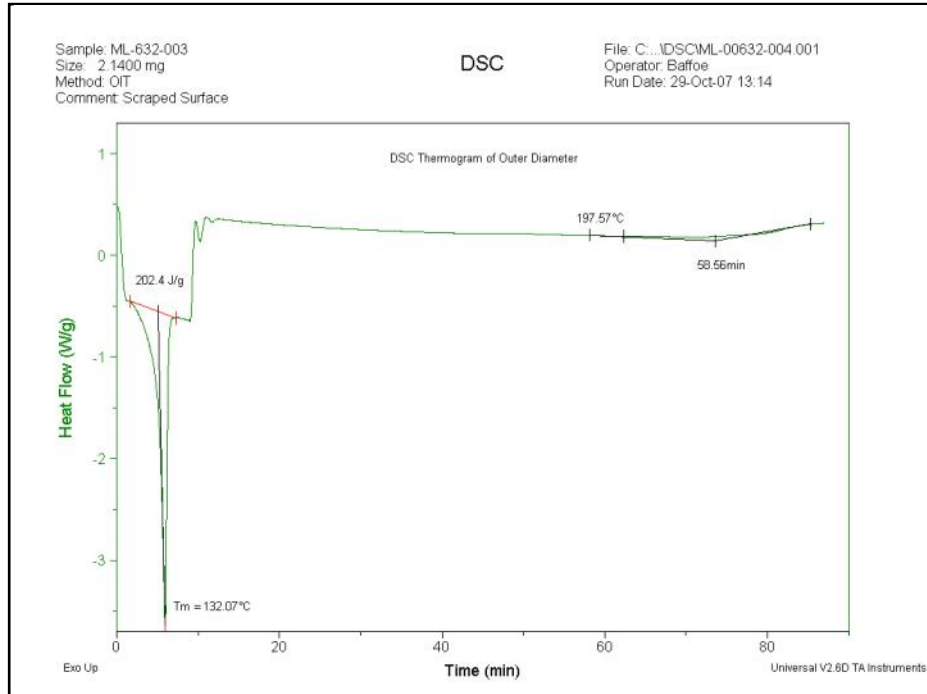


Figure 154. OIT and DSC – Outer Wall – Pipe

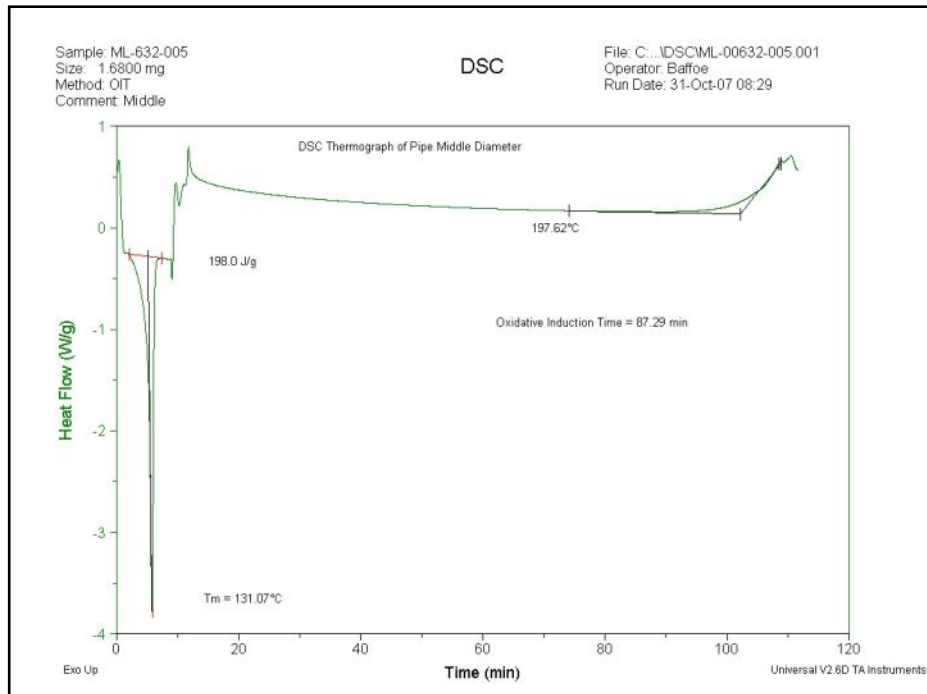


Figure 155. OIT and DSC – Middle Wall – Pipe

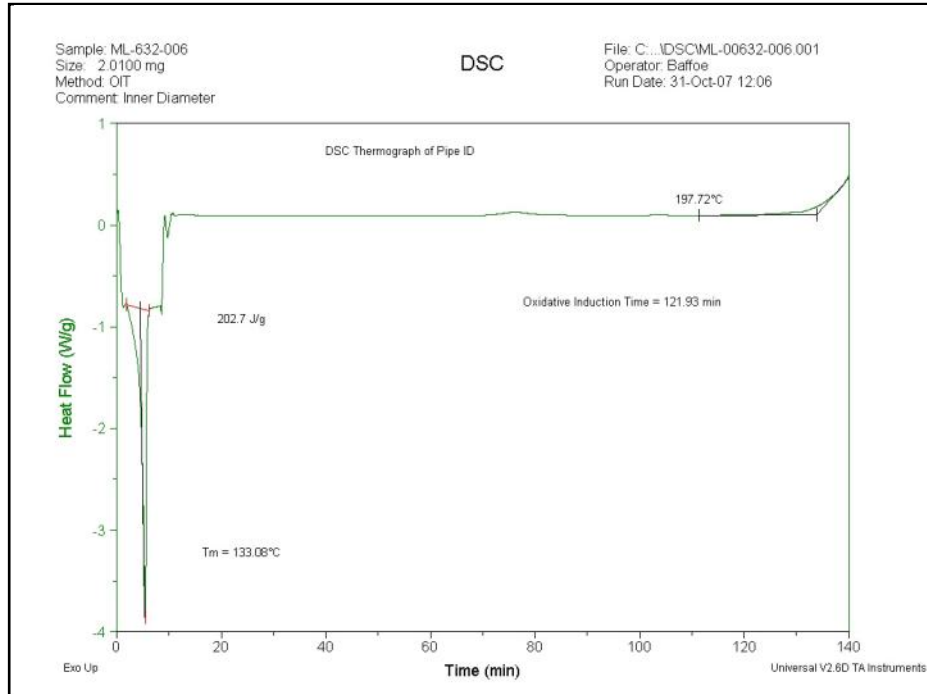


Figure 156. OIT and DSC – Inner Wall – Pipe

Infrared Analysis

A comprehensive analysis was performed to determine the condition of the pipe and tee sections as well as detect the presence of any organic materials not associated with the pipe material. The resulting spectra were analyzed and indicated no any foreign organic materials in the outer diameter fusion area, middle, and inner diameter surfaces. The 1650cm-1 to 1750cm-1 region of the resulting spectra were closely examined. Absorbencies in this region are associated with PE oxidative products. No absorbencies were detected in this region. This suggested that the pipe was manufactured and stored acceptably prior to installation. The FT-IR charts for the outer, middle, and inner walls can be seen in Figure 157, Figure 158, and Figure 159, respectively.

Acetone extractions of the good (adjacent to proper rollback on fusion bead) and poor (adjacent to area with no fusion bead) fusion areas of the tee were performed to see if any organic materials not associated with the tee material could be detected. No abnormal absorbencies were detected in the resulting spectra shown in Figure 160 and Figure 161.

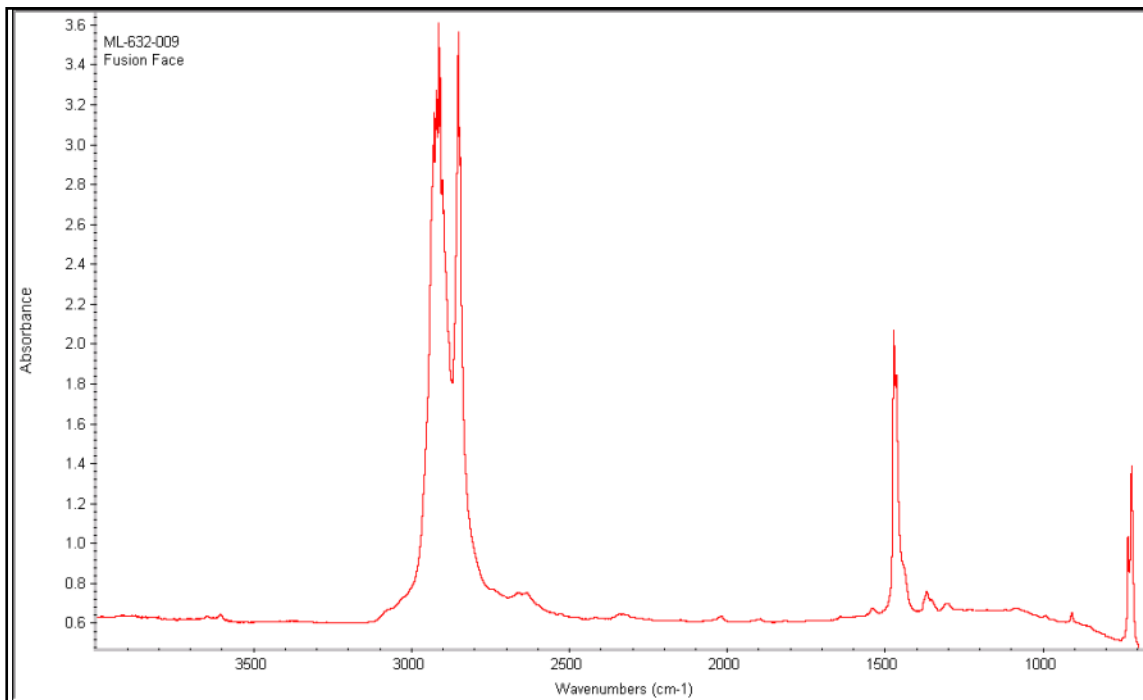


Figure 157. FT-IR - Outer Wall – Pipe

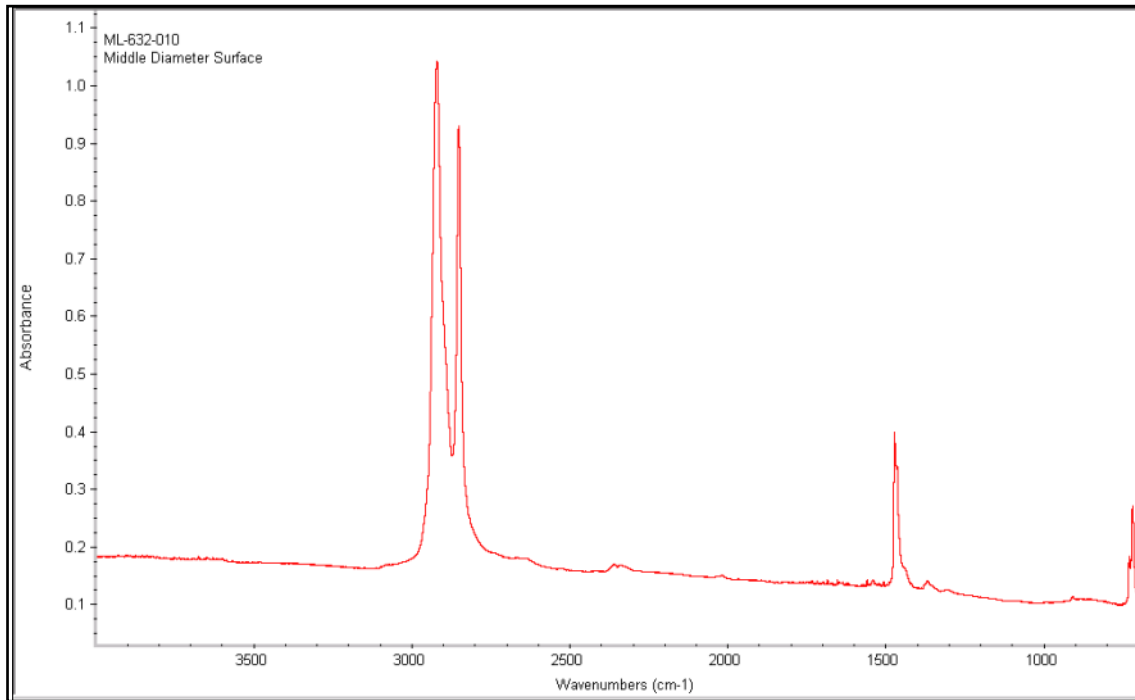


Figure 158. FT-IR - Middle Wall – Pipe

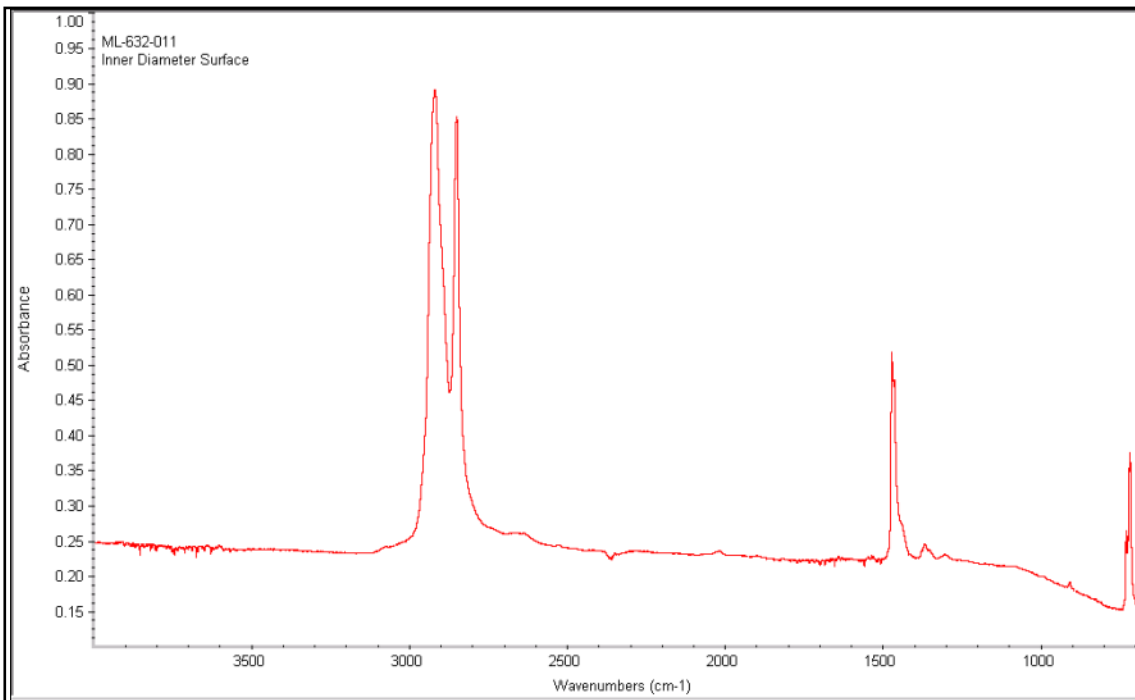


Figure 159. FT-IR - Inner Wall – Pipe

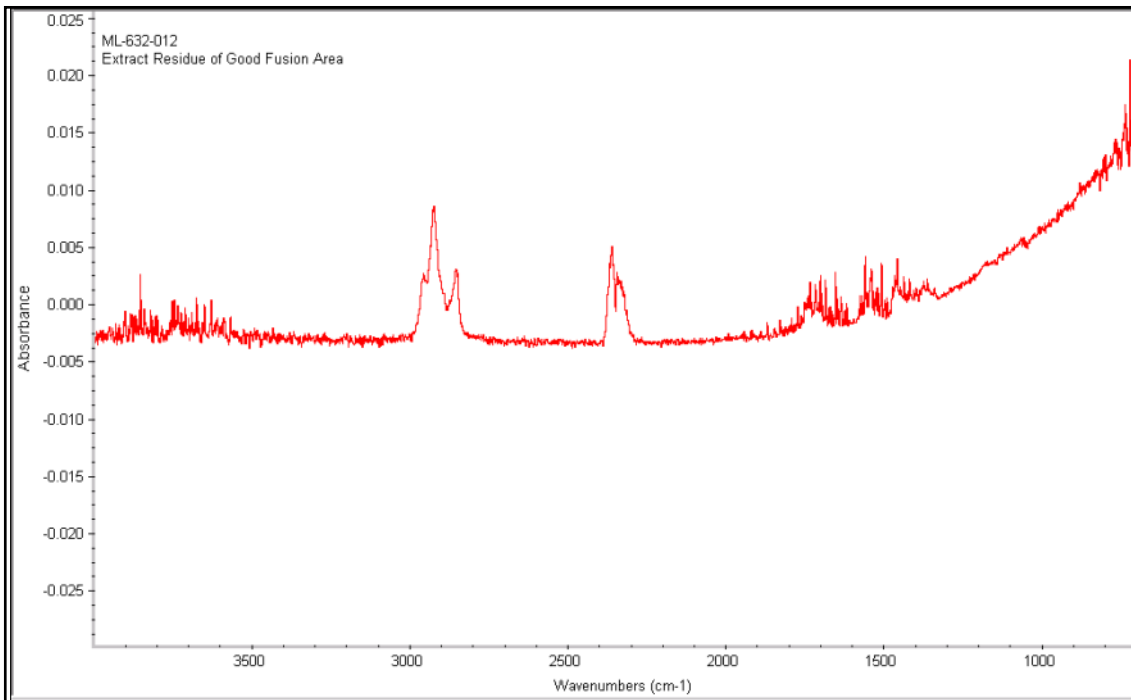


Figure 160. FT-IR – Good Fusion Area

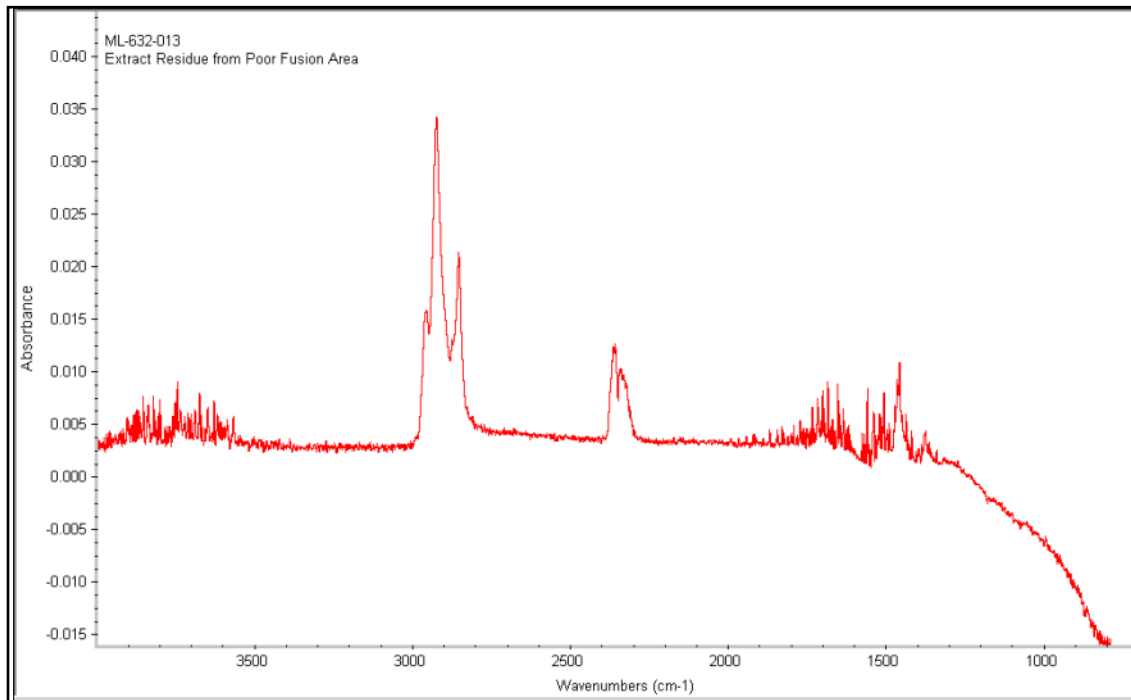


Figure 161. FT-IR - Poor Fusion Area

Conclusions

Based on the tests performed and the information provided it was concluded that:

- 1) The 4" pipe had a preexisting deflection when the fusion procedure was performed preventing the entire face of the tee from fusing to the pipe wall. The pipe surface was concave at the fusion interface which caused unequal application force across the face where more force was realized on the left and right side of the tee than in the midsection. The surfaces of the two parts indicated that the fusion was more complete on the sides of the tee than in the center.
- 2) The large degree of movement of the pipe print line underneath indicated that the tee had moved significantly during the fusion most likely due to insufficient clamping and/or improper positioning. This was consistent with the observed poor, non-existent rollback and the significantly large areas of little or no fusion that were observed. Based on background information, difficult spatial circumstances may have prevented the operator from properly using aligning equipment.
- 3) The offset position of the sleeve relative to the nose of the tee indicated that the fill had settled. This offset applied downward stress to the nose thereby transferring additional stress to the fusion. This additional stress contributed to the failure.
- 4) The material properties of the pipe material were consistent with normal medium density PE material that was properly stored prior to installation and free of contaminants. It was determined that the pipe material did not contribute to the failure.

Butt Fusions

Butt Fusion - #060204100



Figure 162. As Received Butt Fusion

Table 39. 2" Butt Fusion Background

Pipe Information	060204100
Color	Orange
Diameter	2"
SDR	11
Resin	PE 2306
Manufacturer	Driscopipe
Design Pressure	-
Service Information	
Operating Pressure	1-60 psig
Service Temperature	60°F
Comments	-
Timeline	
Placed in Service	1979
Installation Method	-
Removed from Service	December 2004
Comments	32" depth of cover
Environmental	
Soil Type	Loam
Evidence of 3 rd Party Damage	No

Visual Examination

The internal and external beads were symmetric and displayed a proper amount of rollover. Examination of the fracture surfaces showed no indication of cold fusion or slow crack growth. Instead, the surfaces were indicative of a dynamic brittle fracture over the majority of the face with the final fracture location exhibiting ductile fibrils/tearing. These features are typical of an overload failure.

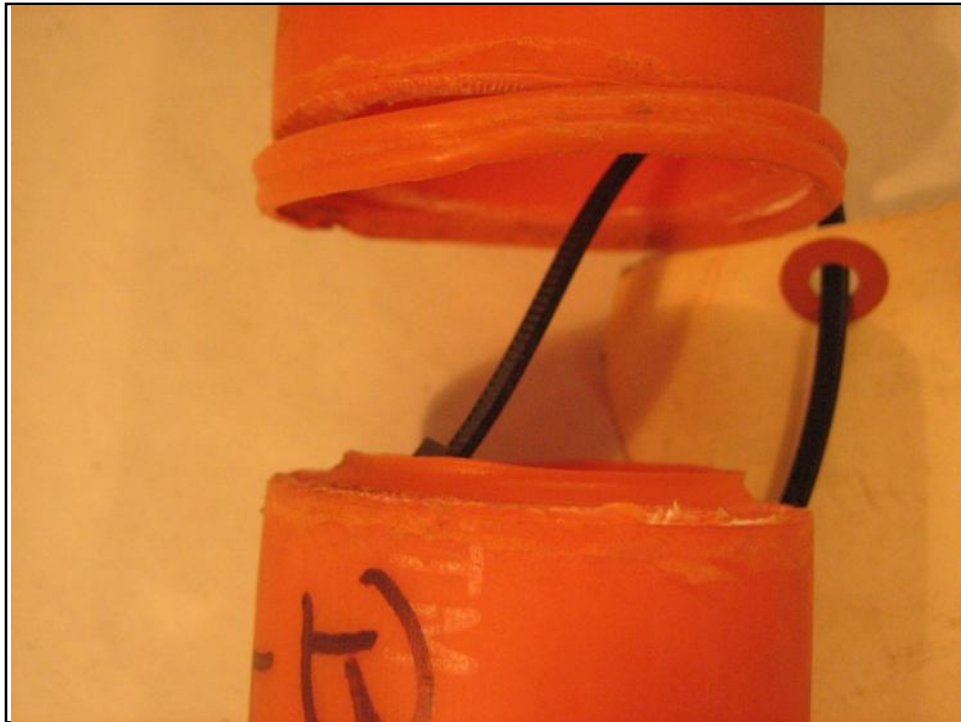


Figure 163. Side View of Butt Fusion



Figure 164. Fusion Faces



Figure 165. Inside Bead on One Side of Fusion

Butt Fusion - #07020714



Figure 166. As Received Butt Fusion

Table 40. 4" Butt Fusion Background

Pipe Information	07020714
Color	Orange
Diameter	4"
SDR	11.5
Resin	PE 2306
Manufacturer	Driscopipe 6500 20 May 83
Design Pressure	-
Service Information	
Operating Pressure	1-60 psig
Service Temperature	60°F
Comments	Pressure tested at 90 psig for 2 hours
Timeline	
Placed in Service	1983
Installation Method	Direct Burial; Bored
Removed from Service	March 2007
Comments	4' depth of cover
Environmental	
Soil Type	Clay
Evidence of 3rd Party Damage	No

Visual Examination

As can be seen in Figure 166, the sample exhibited an axial misalignment resulting in the appearance of mitered faces. The internal and external fusion beads did not exhibit complete rollover, as seen in Figure 167.



Figure 167. Incomplete Bead Rollover

Butt Fusion - #08020601



Figure 168. As Received Butt Fusion

Table 41. 3" Butt Fusion Background

Pipe Information	08020601
Color	Orange
Diameter	3"
SDR	11.5
Resin	PE
Manufacturer	-
Design Pressure	-
Service Information	
Operating Pressure	1-60 psig
Service Temperature	60°F
Comments	-
Timeline	
Placed in Service	May 1975
Installation Method	-
Removed from Service	January 2006
Comments	34" depth of cover
Environmental	
Soil Type	Clay
Evidence of 3rd Party Damage	No

Visual Examination

A 360° cold bond was observed on the mid-wall of both faces of the butt fusion. This depressed area is outlined with arrows in Figure 169. The weak to non-existent interface bond between the mid-walls was a result of improper heat/pressure/time variables in the joining procedure. Fusion occurred only in the melt bead and resulted in approximately 30 years of service before final separation.

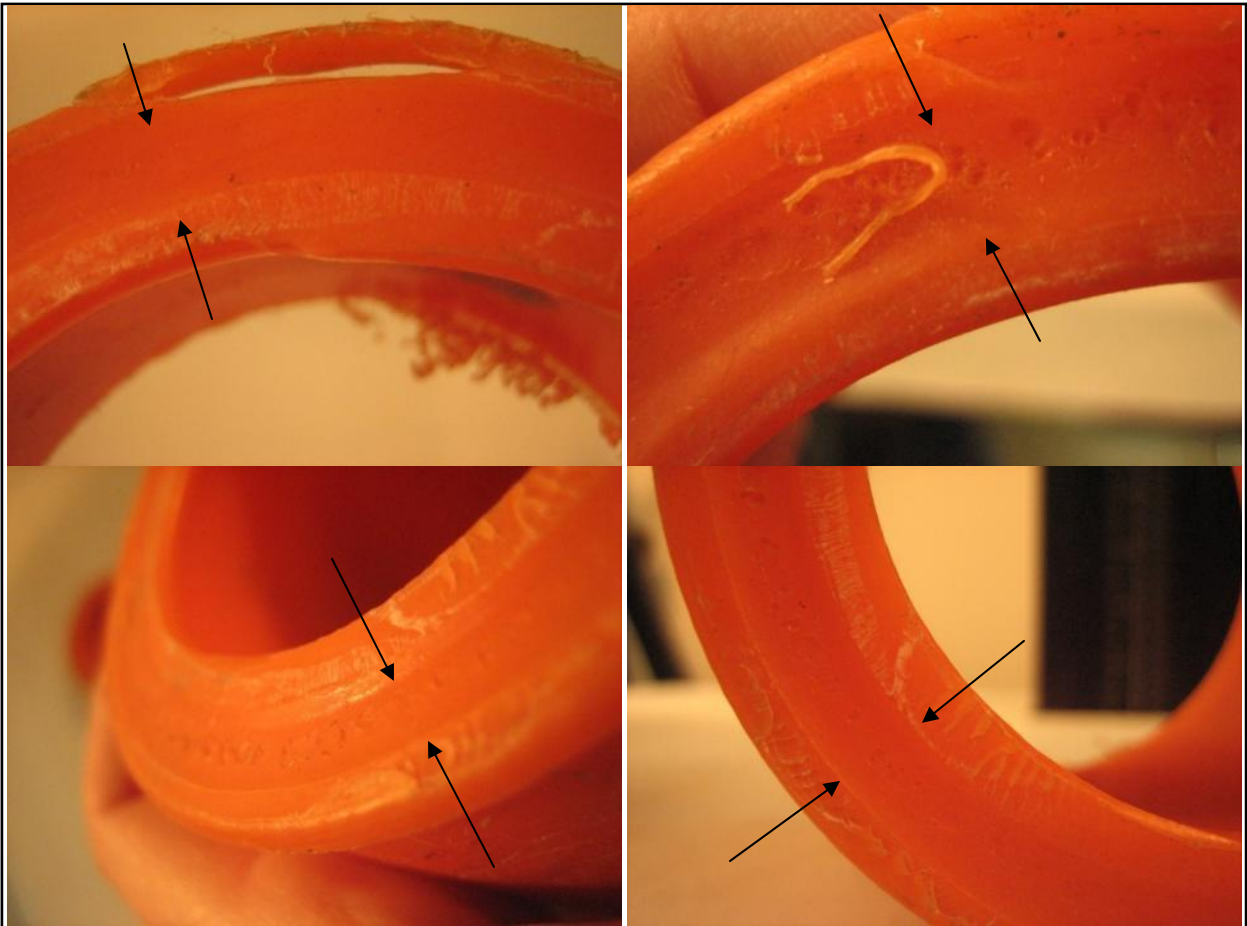


Figure 169. Fusion Faces Showing Cold Fusion Area

Butt Fusion - #09020552



Figure 170. As Received Butt Fusion

Table 42. 2" Butt Fusion Background

Pipe Information	09020552
Color	Orange
Diameter	2"
SDR	-
Resin	PE 2306
Manufacturer	Conind
Design Pressure	-
Service Information	
Operating Pressure	1-60 psig
Service Temperature	60°F
Comments	Pressure tested at 90 psig for 120 minutes
Timeline	
Placed in Service	1975
Installation Method	-
Removed from Service	September 2005
Comments	-
Environmental	
Soil Type	Clay
Evidence of 3rd Party Damage	No

Visual Examination

The overall workmanship of this fusion was poor. Relative to each other, the pipes displayed parallel misalignment (Figure 170) as well as asymmetric beads (Figure 171). Individual beads were not easily discernable. One was barely visible and neither showed proper rollover suggesting inadequate heat/time/pressure during the fusion procedure.

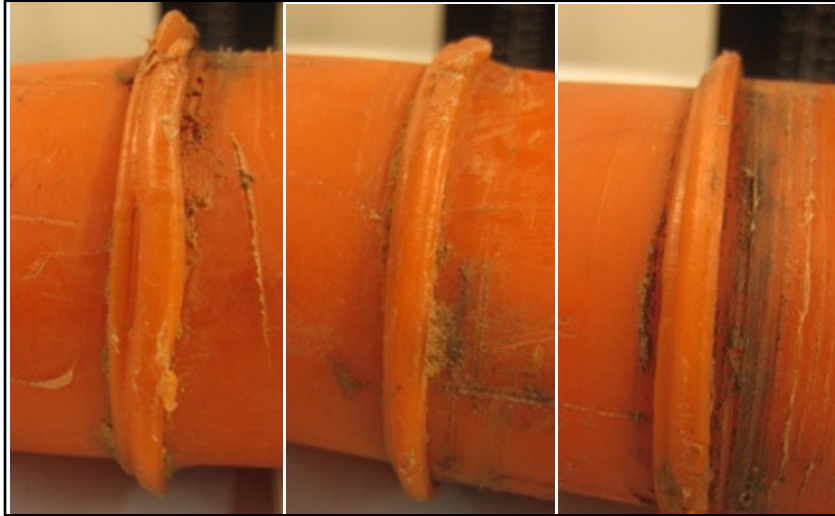


Figure 171. Uneven Rollback

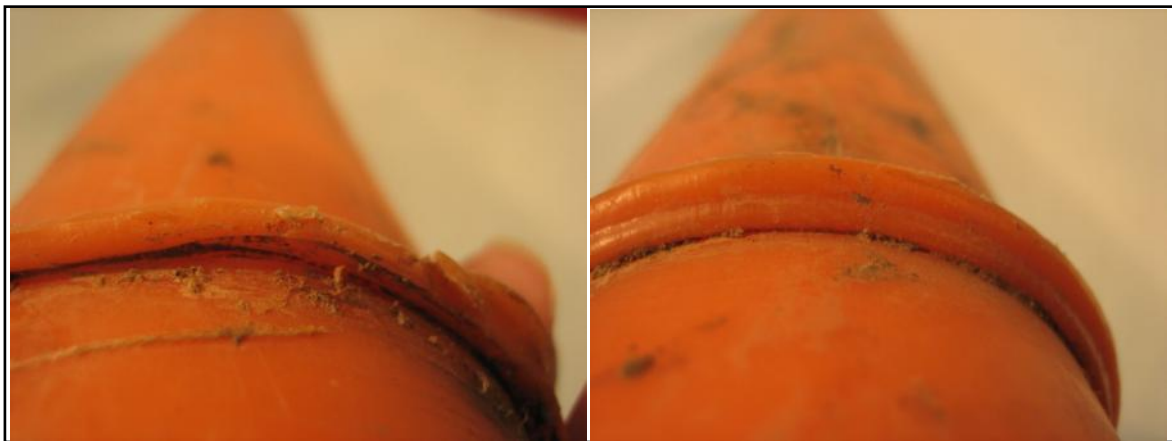


Figure 172. Side of Bead

Butt Fusion - #10020477



Figure 173. As Received

Table 43. 4” Butt Fusion Background

Pipe Information	10020477
Color	Orange
Diameter	4”
SDR	11.5
Resin	-
Manufacturer	Driscopipe 6500
Design Pressure	-
Service Information	
Operating Pressure	1-60 psig
Service Temperature	60°F
Comments	-
Timeline	
Placed in Service	1985
Installation Method	-
Removed from Service	August 2004
Comments	36” depth of cover
Environmental	
Soil Type	Sand
Evidence of 3rd Party Damage	No; Other excavation occurred

Visual Examination

The external bead rolover appeared adequate based on the visual exam. The internal bead did not appear to rolover completely. As seen in Figure 174, the mid-wall displayed a lack of bond penetration of approximately 20-30% cold fusion around the entire circumference.

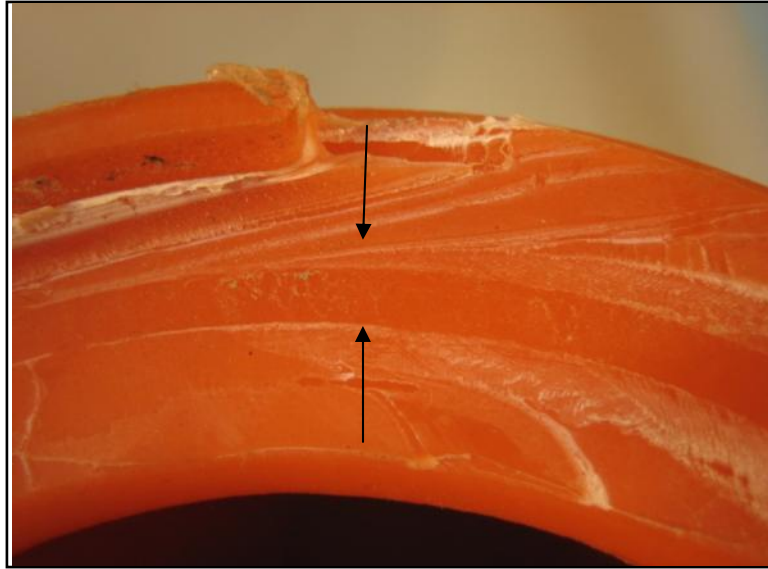


Figure 174. Area of Cold Fusion



Figure 175. Fusion Faces

Butt Fusion - #11020511



Figure 176. As Received Butt Fusion

Table 44. 4” Butt Fusion Background

Pipe Information	11020541
Color	Yellow
Diameter	4”
SDR	11.5
Resin	PE 2406
Manufacturer	Plexco
Design Pressure	-
Service Information	
Operating Pressure	1-60 psig
Service Temperature	60°F
Comments	Pressure tested at 100 psig for 18 hours
Timeline	
Placed in Service	February 1994
Installation Method	Direct Burial; Bored
Removed from Service	May 2005
Comments	48” depth of cover
Environmental	
Soil Type	Clay
Evidence of 3rd Party Damage	No

Visual Examination

Visually, this joint exemplified adequate bead size and rollover. A void was noticeable at the leak location, as identified by the arrow in Figure 177. Looking down the interior of the pipe revealed the presence of foreign matter (Figure 178). The foreign object, which resembled a plant (Figure 179), was embedded in the fusion at the location of the leak location identified on the external wall.



Figure 177. Leak Location at the Bead Weld



Figure 178. View down the Inside of the Pipe Section



Figure 179. Close-up of the Inner Weld Bead

Butt Fusion - #12020550

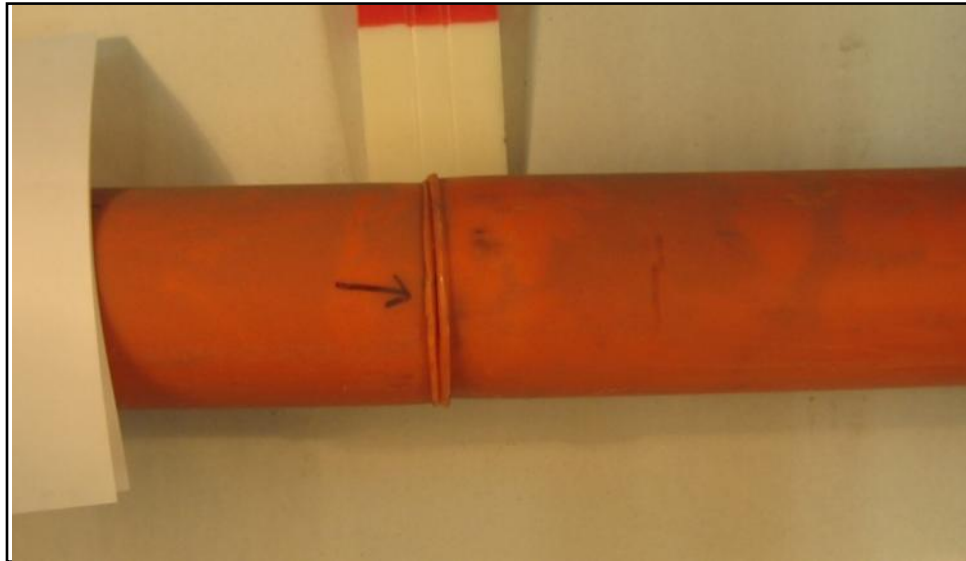


Figure 180. As Received

Table 45. 4" Butt Fusion Background

Pipe Information	12020550
Color	Orange
Diameter	4"
SDR	-
Resin	PE 2306
Manufacturer	_____TURE
Design Pressure	-
Service Information	
Operating Pressure	1-60 psig
Service Temperature	60°F
Comments	-
Timeline	
Placed in Service	-
Installation Method	-
Removed from Service	August 2005
Comments	48" depth of cover
Environmental	
Soil Type	Clay
Evidence of 3rd Party Damage	No

Visual Examination

This fusion joint displayed axial misalignment of the pipe ends (Figure 180) and a visible separation within the joint (Figure 181). Bead rolover was also inadequate and nonsymmetrical as seen in Figure 182.

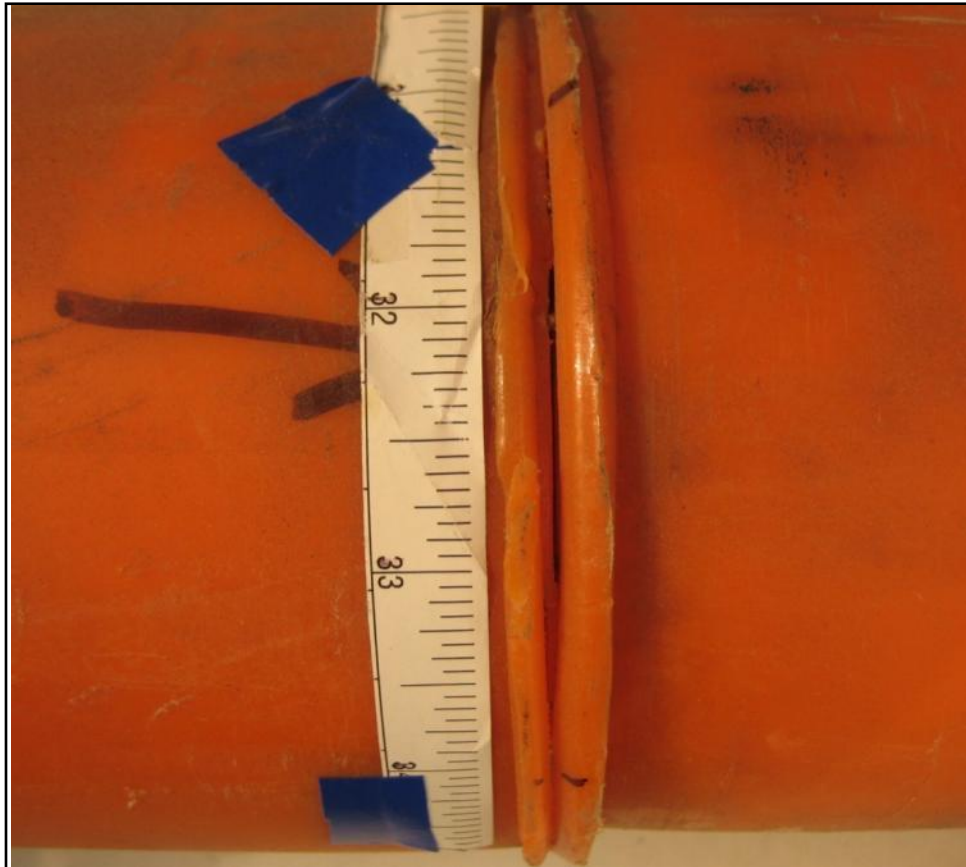


Figure 181. Weld Separation along ~3" Arc Length



Figure 182. Uneven Beads

Butt Fusion - #13020706



Figure 183. As Received

Table 46. 4" Butt Fusion Background

Pipe Information	13020706
Color	Orange / Yellow
Diameter	4"
SDR	-
Resin	PE
Manufacturer	Plexco
Design Pressure	60psig
Service Information	
Operating Pressure	1-60 psig
Service Temperature	60°F
Comments	Pressure tested at 95 psig for 2 hours
Timeline	
Placed in Service	December 1989
Installation Method	Bored
Removed from Service	February 2007
Comments	44" depth of cover
Environmental	
Soil Type	Clay
Evidence of 3rd Party Damage	No

Visual Examination

Cold fusion occurred over at least 50% of the fusion surface resulting in an inadequate bond. The bead shows inconsistent rollover. Using Figure 184 as a reference, the beads within the green box exhibited proper bead rollover. The beads within the black boxes did not roll over completely. The discrepancy of the beads indicates a problem with heat/time/pressure during the fusion process.

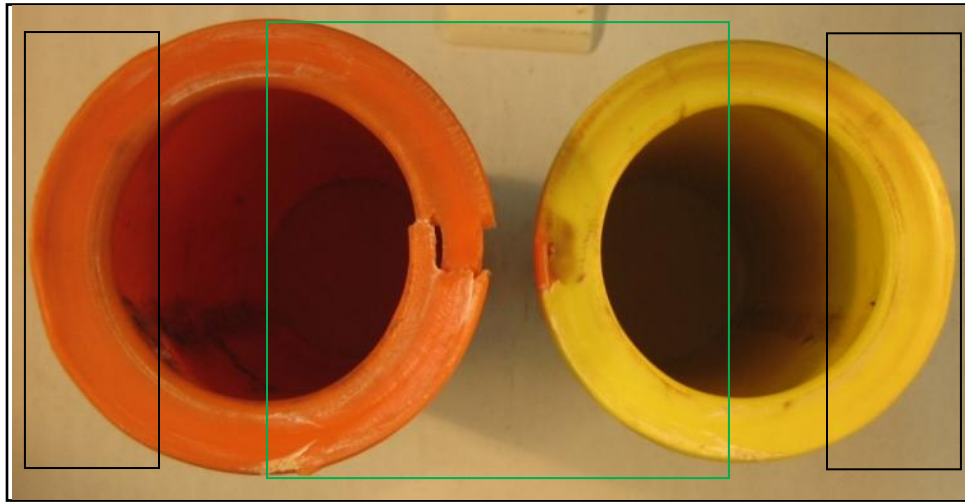


Figure 184. Fusion Faces

Butt Fusion - #45020551



Figure 185. As Received 6” Butt Fusion

Table 47. Poly Valve Butt Fusion Background

Pipe Information	45020551
Color	Yellow
Diameter	6”
SDR	11.5 (pipe); 11 (valve)
Resin	PE 2406 (pipe and valve)
Manufacturer	Uponor (pipe) ; Nordstrom (valve)
Design Pressure	-
Service Information	
Operating Pressure	1-60 psig
Service Temperature	60°F
Comments	-
Timeline	
Placed in Service	2000
Installation Method	-
Removed from Service	August 2005
Comments	60” depth of cover; Was exposed in 14’ hole when dirt bank caved
Environmental	
Soil Type	Clay
Evidence of 3rd Party Damage	No

Visual Examination

There does not appear to be any misalignment of the faces. Rollback looks even internally and externally. The fusion faces appeared to have about 80% cold fusion, shown in red in Figure 186. The fused portion occurred about 180° around the ID and on about 120° (6-10 o'clock) of the OD as seen on the valve side. The pipe surface has been grit blasted by gas flow.



Figure 186. Fusion Face, Valve

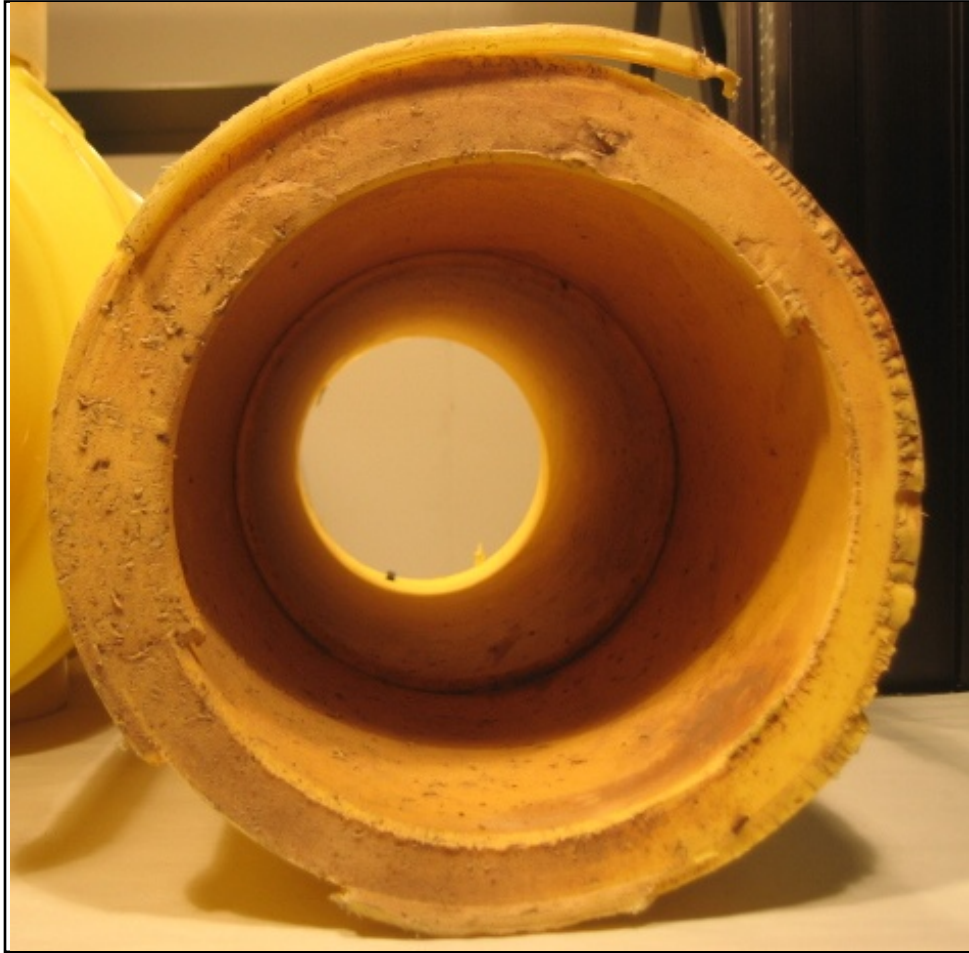


Figure 187. Fusion Face, Pipe

Multiple Fusion Joints - #40020413



Figure 188. As Received

Table 48. Multiple Fusion Joints Background

Pipe Information	40020413
Color	Orange
Diameter	3" and 1 - ½"
SDR	-
Resin	-
Manufacturer	-
Design Pressure	-
Service Information	
Operating Pressure	1-60 psig
Service Temperature	60°F
Comments	-
Timeline	
Placed in Service	-
Installation Method	-
Removed from Service	February 2004
Comments	8" depth of cover; System acquired from apartment property
Environmental	
Soil Type	Clay
Evidence of 3rd Party Damage	No

Visual Examination

This sample would require pressure testing to determine the leak location and sectioning to determine the cause. The entire sample consisted of sloppy workmanship. Poor bead rollover, parallel misalignment, and burn marks were all visible on the specimen.



Figure 189. Close Up View of Specimen



Figure 190. Misalignment and Poor Bead Rollover at the Reducing Coupling



Figure 191. Back to Back Couplings

Socket Couplings

Socket Coupling - #16020611



Figure 192. As Received

Table 49. Socket Fusion Coupling Background

Pipe Information	16020611
Color	Orange
Diameter	1"
SDR	11
Resin	PE 2306
Manufacturer	Conind Mark II (pipe) Unknown (coupling)
Design Pressure	-
Service Information	
Operating Pressure	1-60 psig
Service Temperature	60°F
Comments	-
Timeline	
Placed in Service	-
Installation Method	-
Removed from Service	February 2006
Comments	36" depth of cover
Environmental	
Soil Type	Loam
Evidence of 3rd Party Damage	No

Visual Examination

The leak location was marked by the field crew during removal of the section. The marking was approximately 1" around the circumference of the pipe as seen in Figure 193. The coupling and pipe were in parallel misalignment to each other. Due to the nature of this sample, the root cause cannot be determined without sectioning.



Figure 193. Leak Location

Socket Coupling - #31020649

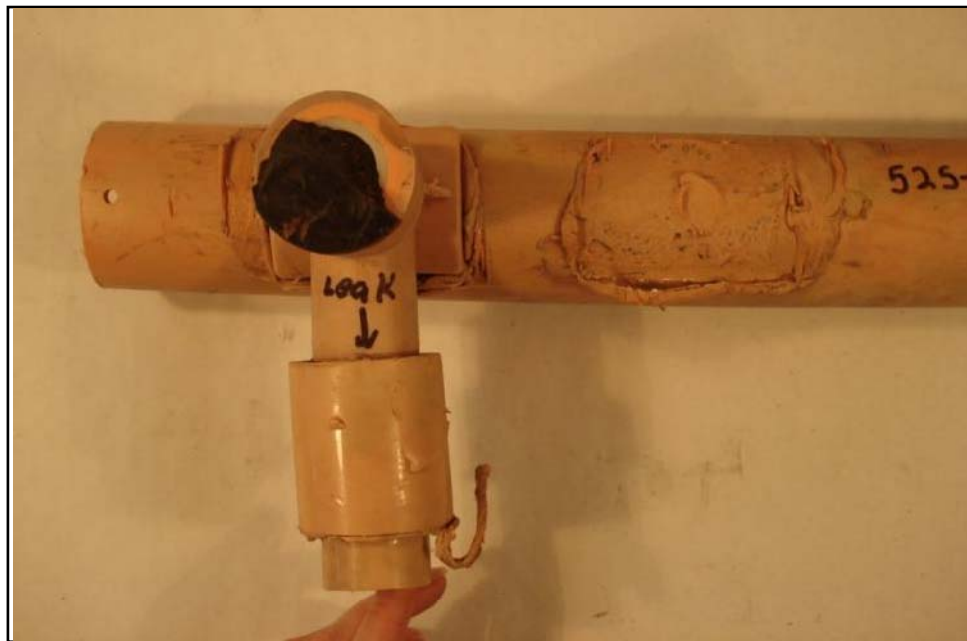


Figure 194. As Received

Table 50. Coupling Background

Pipe Information	31020649
Color	Tan
Diameter	2" (main) 1 – ¼" (service)
SDR	-
Resin	PE 2306
Manufacturer	DuPont Aldyl A(pipe and tee)
Design Pressure	-
Service Information	
Operating Pressure	1-60 psig
Service Temperature	60°F
Comments	Pressure tested at 100 psig
Timeline	
Placed in Service	November 1970
Installation Method	-
Removed from Service	December 2006
Comments	36" depth of cover
Environmental	
Soil Type	Clay
Evidence of 3rd Party Damage	No

Visual Examination

The sample exhibited poor workmanship though no obvious sign exists for the coupling leak. Ruler approximation of the “nose” of the tee relative to the edge of the coupling suggested inappropriate stab depth of the coupling onto the tee. This interior surface showed minimal to no rollback. The external surface where the leak location was noted showed little and inconsistent rollback of the companion materials. Further examination by destructive methods could provide better information.

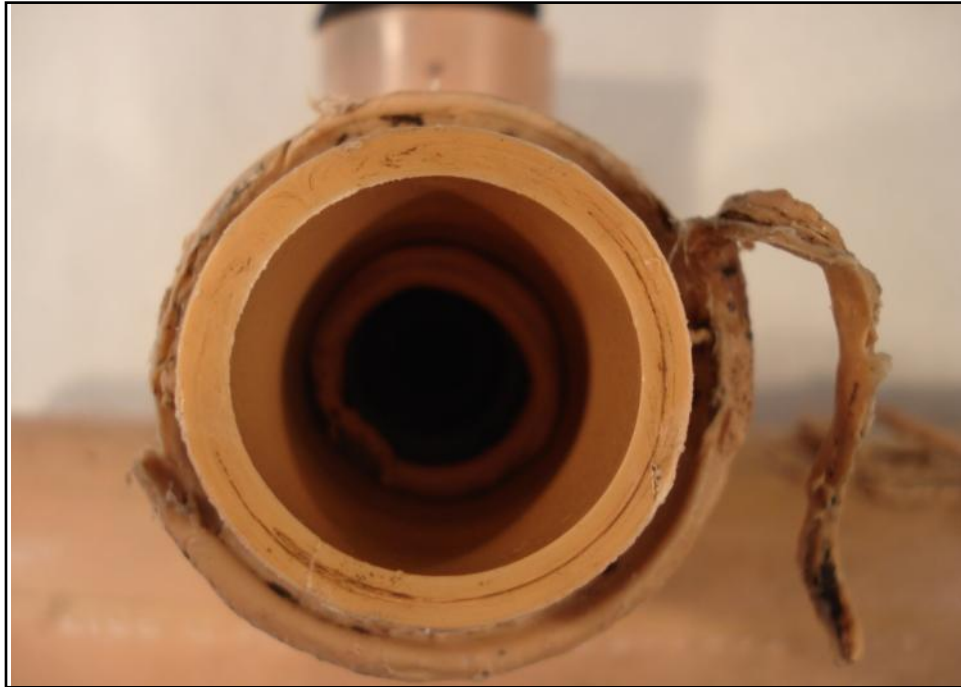


Figure 195. End View of Pipe



Figure 196. Leak Location as Identified by Utility

Socket Tees

Socket Tee - #36020713



Figure 197. As Received

Table 51. Socket Tee Background

Pipe Information	36020713
Color	Orange
Diameter	1 – ¼" all ways
SDR	-
Resin	-
Manufacturer	RAHN (Canada)
Design Pressure	
Service Information	
Operating Pressure	1-60 psig
Service Temperature	60°F
Comments	-
Timeline	
Placed in Service	-
Installation Method	-
Removed from Service	2007
Comments	-
Environmental	
Soil Type	-
Evidence of 3rd Party Damage	-

Visual Examination

Visually, the melting was improper but in order to determine the leak path and the root cause, the sample would need to be sectioned.

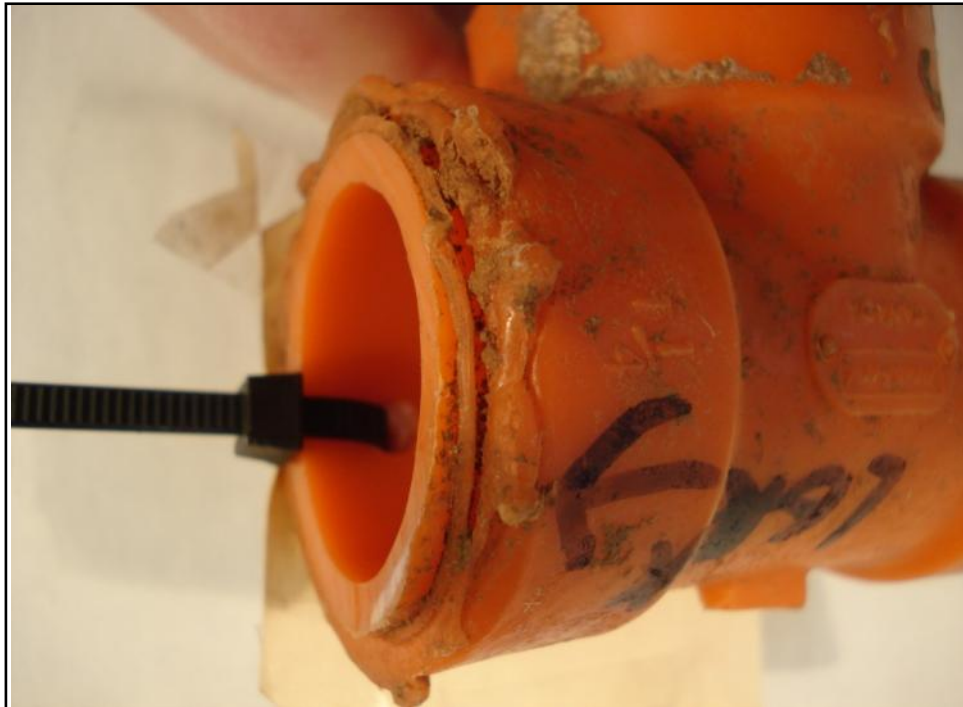


Figure 198. Leak Location as Identified by Utility

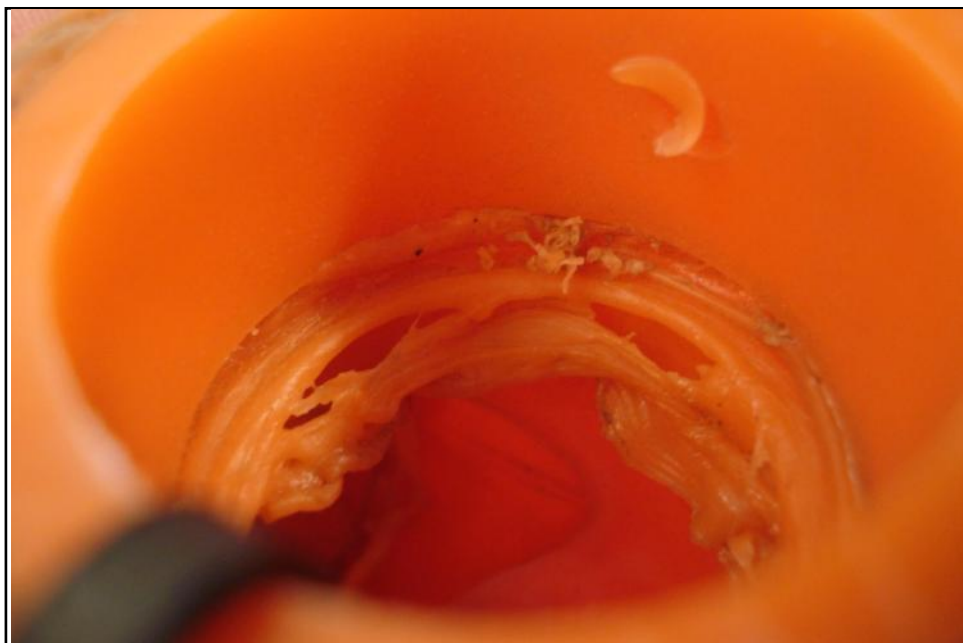


Figure 199. End View on Leak Side

Socket Tee - #47020565



Figure 200. As Received Socket Tee

Table 52. Socket Tee Background

Pipe Information	47020565
Color	Orange
Diameter	4"
SDR	11.5 (pipe)
Resin	PE 2306 TR 418 (pipe)
Manufacturer	Extron (tee); Plexco (pipe)
Design Pressure	-
Service Information	
Operating Pressure	1-60 psig
Service Temperature	60°F
Comments	Pressure tested at 100 psig for 240 minutes
Timeline	
Placed in Service	May 1973
Installation Method	Direct Burial; Bored
Removed from Service	December 2005
Comments	48" depth of cover
Environmental	
Soil Type	Clay
Evidence of 3 rd Party Damage	No

Visual Examination

Radial distortion as seen in Figure 201 was observed in the sockets. Misalignment of the pipes into the sockets was also apparent. This sample was submitted without any indication of the leak location. A pressure test was performed and determined that gas leaked out of the joint at the pipe/socket interface. As shown in Figure 202, the leak occurred over 3” of the circumference in the fusion joint. A close up of this area is shown in Figure 203.



Figure 201. Radial Distortion



Figure 202. Leak at Pipe/Socket Interface



Figure 203. Close up of Pipe/Socket Interface

Squeeze-offs

Squeeze-Off - #02020717

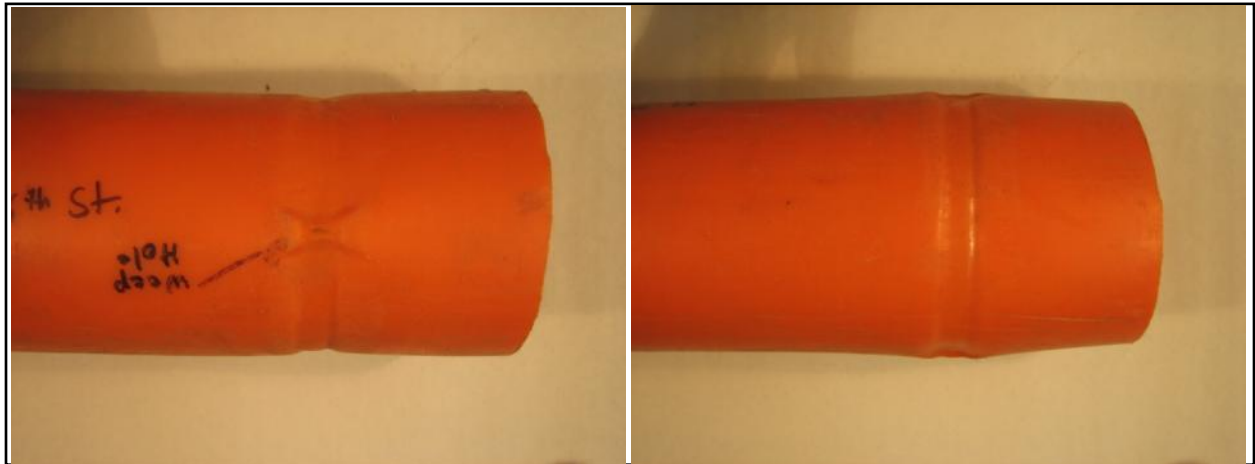


Figure 204. Top and Side View of as Received Squeeze-off

Table 53. 4" Single Bar Squeeze-off Background

Pipe Information	02020717
Color	Orange
Diameter	4"
SDR	11.5
Resin	PE 2306
Manufacturer	Conind Mark II 1-12-78 (Grating visible under UV)
Design Pressure	-
Service Information	
Operating Pressure	1-60 psig
Service Temperature	60°F
Comments	Pressure tested at 90 psig for 4 hours
Timeline	
Placed in Service	1978
Installation Method	-
Removed from Service	March 2007
Comments	5' depth of cover
Environmental	
Soil Type	Clay
Evidence of 3rd Party Damage	No

Visual Examination

The pipe was squeezed with a single bar squeeze off tool. Visual observations indicated the pipe was significantly over squeezed above recommended values. The excessive squeeze resulted in significant amounts of permanent deformation at the squeeze ears and apparent wall thinning. Large voids, whitening, and cracks were present at the squeeze ears on the inner surface of the pipe. These can be seen in Figure 205 and Figure 206. An axial slit at one ear was apparent at the outer surface, as seen in Figure 204, indicating the crack initiated on the inner surface and grew through the wall to the outer surface.

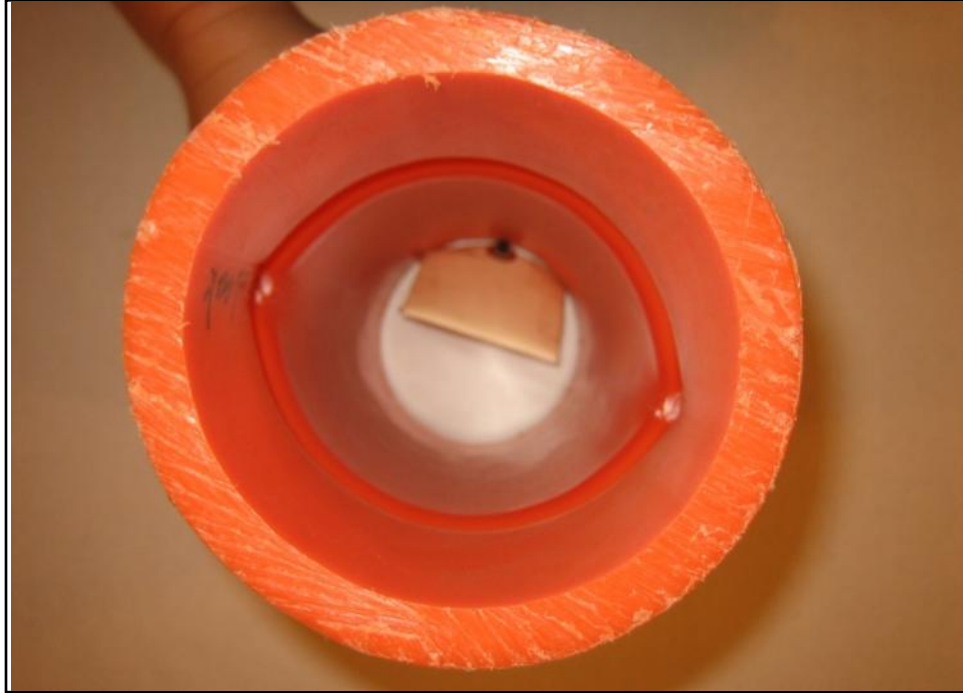


Figure 205. End View Showing Deformation

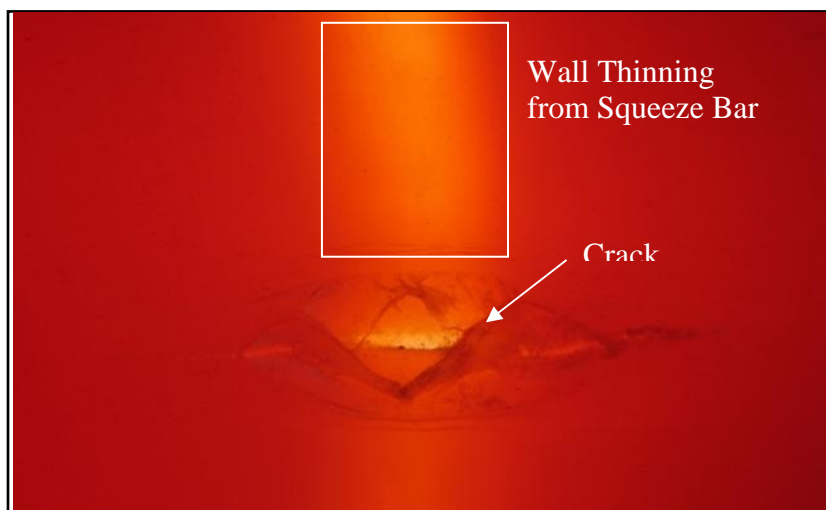


Figure 206. Slit as Viewed from Inner Wall

Squeeze-off - #03020647



Figure 207. Top and Side View of as Received Sample

Table 54. 2” Squeeze-off Background

Pipe Information	03020647
Color	Orange
Diameter	2”
SDR	-
Resin	PE 2306
Manufacturer	Driscopipe 6500
Design Pressure	-
Service Information	
Operating Pressure	1-60 psig
Service Temperature	60°F
Comments	Pressure tested at 100 psig for 170 minutes
Timeline	
Placed in Service	January 1979
Installation Method	Direct Burial
Removed from Service	November 2006
Comments	48” depth of cover
Environmental	
Soil Type	Clay
Evidence of 3rd Party Damage	No

Visual Examination

The sample appears to have been squeezed three times within an 8" length of pipe using a single bar squeeze tool. The deformations were about 3" and 4.5" center to center separation. It is possible that the squeeze tool was not equipped with stops resulting in excessive plastic deformation and yielding. Wall thinning, buckling, and dimpling were apparent on the outer wall as seen in Figure 208. On the inner wall, a yielded region was observed in the axial direction extending from one squeeze location to another.



Figure 208. Dimpling and Buckling

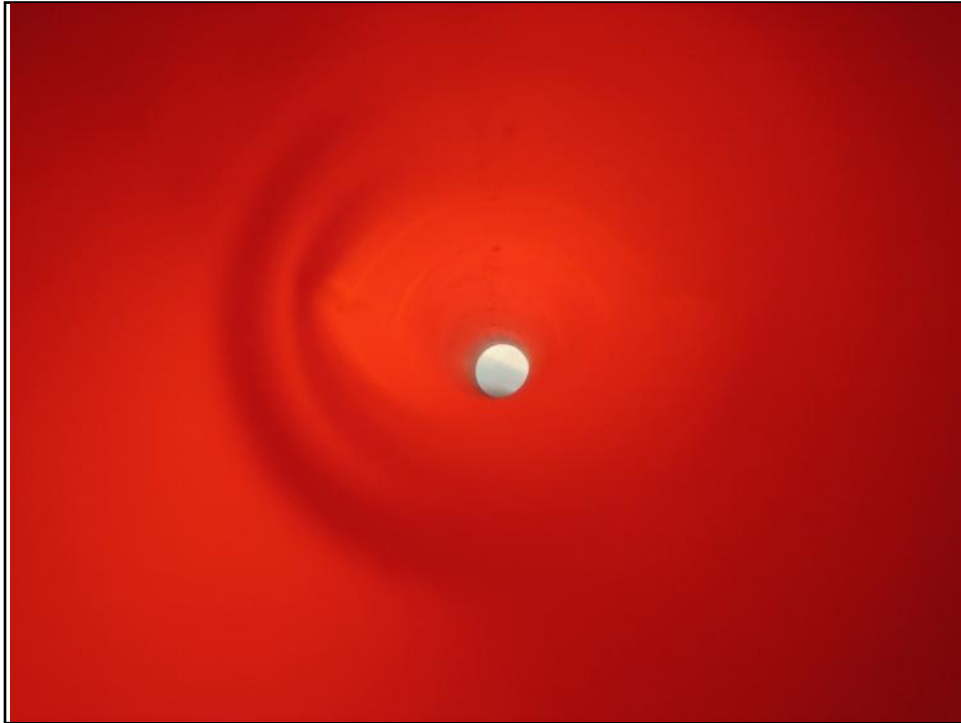


Figure 209. Two of Three Squeeze Points Visible on the Inner Wall

Squeeze-off - #05020548



Figure 210. As Received Squeeze-off Sample

Table 55. Squeeze-off Background

Pipe Information	05020548
Color	Orange
Diameter	2"
SDR	11
Resin	-
Manufacturer	Driscopipe
Design Pressure	-
Service Information	
Operating Pressure	1-60 psig
Service Temperature	60°F
Comments	Pressure tested at 100 psig for 120 minutes
Timeline	
Placed in Service	June 1982
Installation Method	Direct Burial
Removed from Service	August 2005
Comments	32" depth of cover
Environmental	
Soil Type	Clay
Evidence of 3rd Party Damage	No

Visual Examination

As with other samples, this pipe exhibited markings of a single bar squeeze off machine. In the ear region, a square shaped deformation (Figure 211) implied the pipe was not centered in the squeeze off machine. Observations of the inner wall show a large cavity (Figure 212) and an axial slit under the square shaped deformation.



Figure 211. Top and Sides of Squeeze Location

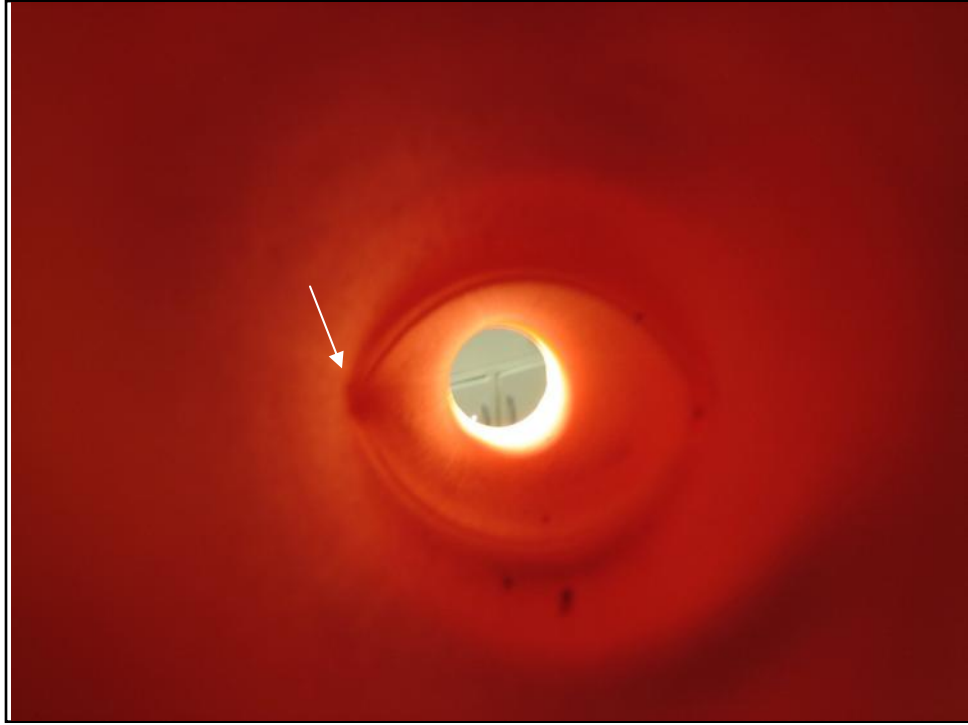


Figure 212. Cavity and Deformation on Inner Wall

Tap Tees

Tap Tee - #28020502



Figure 213. As Received Tap Tee

Table 56. 1 – ¼” x 1” Tap Tee Background

Pipe Information	28020502
Color	Orange
Diameter	1 – ¼” x 1”
SDR	-
Resin	-
Manufacturer	-
Design Pressure	-
Service Information	
Operating Pressure	1-60 psig
Service Temperature	60°F
Comments	Pressure tested at 50 psig for 15 minutes
Timeline	
Placed in Service	1975
Installation Method	-
Removed from Service	January 2005
Comments	39” depth of cover
Environmental	
Soil Type	Sand
Evidence of 3rd Party Damage	No

Visual Examination

This fusion exhibited a very asymmetric and poorly formed bead. The marked location of the leak was at a location with a high stress concentration between the pad and the pipe. During the visual examination no crack or void was seen so a leak test would need to be performed to verify the leak path. The likely cause for failure is poor workmanship.



Figure 214. Underside of the Pipe and Saddle

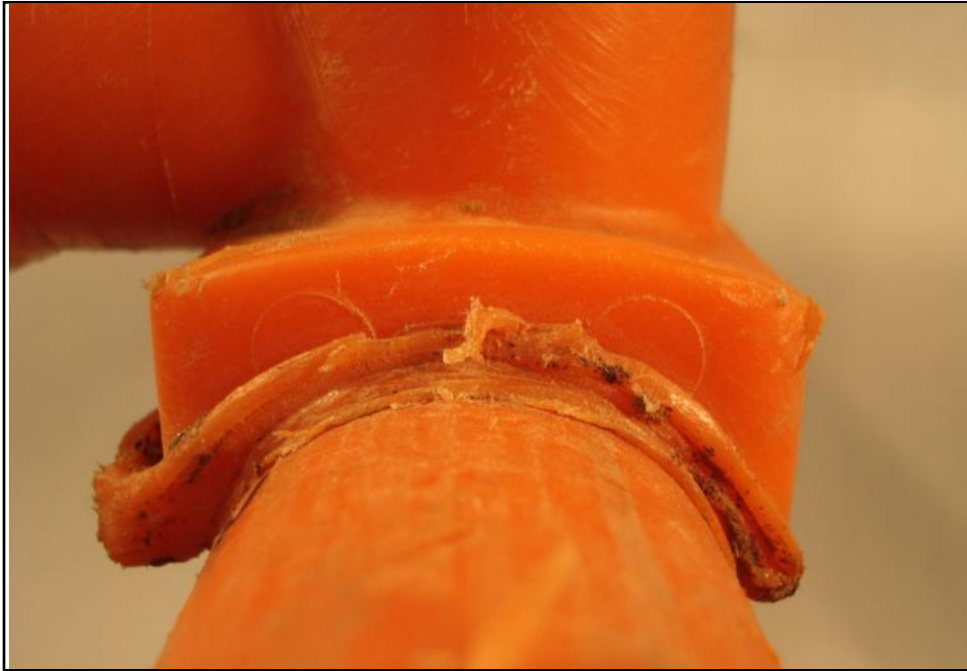


Figure 215. Side View of the Saddle



Figure 216. Leak Location

Tap Tee - #42020711

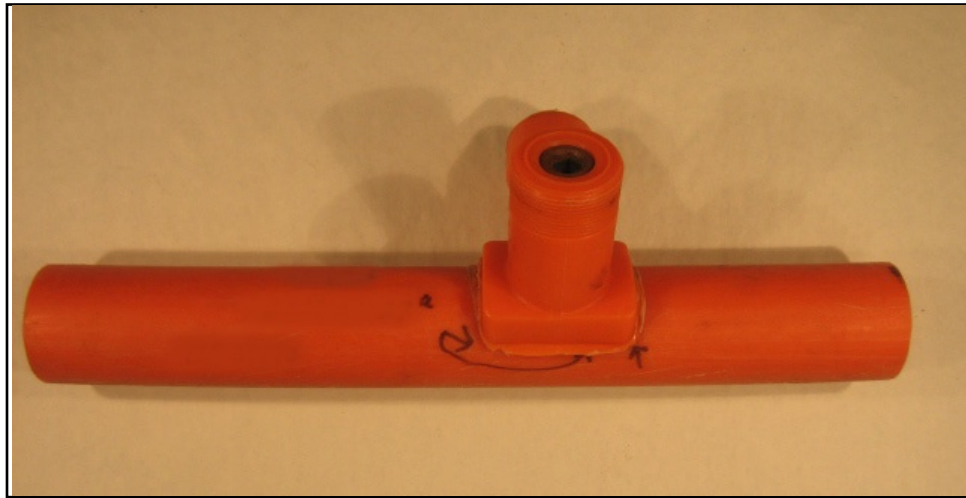


Figure 217. As Received Tap Tee

Table 57. 2" x 3/4" Tap Tee Background

Pipe Information	42020711
Color	Orange
Diameter	2"
SDR	11
Resin	PE 2306
Manufacturer	-
Design Pressure	-
Service Information	
Operating Pressure	1-60 psig
Service Temperature	60°F
Comments	-
Timeline	
Placed in Service	March 1976 (tee)
Installation Method	-
Removed from Service	April 2007
Comments	-
Environmental	
Soil Type	Clay
Evidence of 3rd Party Damage	No

Visual Examination

The sample had inadequate melt and roll over on the backside of the saddle tee where the leak locations are marked. This sample would require sectioning for further comment.



Figure 218. Backside of Saddle Tee



Figure 219. Close-up of Backside of Tee



Figure 220. Side of Tee

Tap Tee - #43020555



Figure 221. As Received Tap Tee

Table 58. 2" x 3/4" Tap Tee Background

Pipe Information	43020555
Color	Orange
Diameter	2" x 3/4" IPS
SDR	-
Resin	PE 2306 (pipe)
Manufacturer	Plexco (tee); Driscoplex (pipe)
Design Pressure	-
Service Information	
Operating Pressure	1-60 psig
Service Temperature	60°F
Comments	-
Timeline	
Placed in Service	1988
Installation Method	-
Removed from Service	October 2005
Comments	42" depth of cover
Environmental	
Soil Type	Loam
Evidence of 3rd Party Damage	No

Visual Examination

Examination showed cold fusion over about 90% of the fusion area. The fusion face on the pipe still had visible superficial scratches. These scratches would have been created during fusion preparation, which points to a lack of heat and fusion during the joining process.

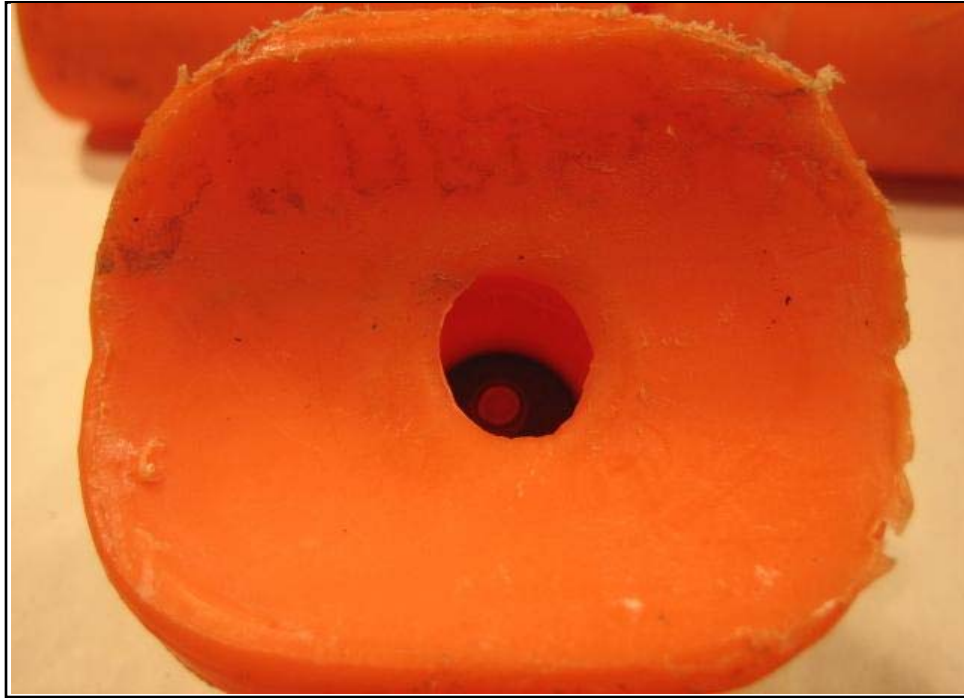


Figure 222. Saddle Face



Figure 223. Pipe Surface

Tap Tee - #44020539



Figure 224. As Received Tap Tee

Table 59. 1 – ¼” x 1” Tap Tee Background

Pipe Information	44020539
Color	Orange
Diameter	1 – ¼” x 1” (tee) 1 - ¼” (pipe)
SDR	10 (pipe)
Resin	PE 2306 (tee) TR 418 (pipe)
Manufacturer	Plexco (tee) Conind (pipe)
Design Pressure	-
Service Information	
Operating Pressure	1-60 psig
Service Temperature	60°F
Comments	Pressure tested at 10 psig for 10 minutes
Timeline	
Placed in Service	November 1978
Installation Method	-
Removed from Service	April 2005
Comments	36” depth of cover
Environmental	
Soil Type	Loam
Evidence of 3rd Party Damage	No

Visual Examination

Because no bead was present, inadequate melting due to poor workmanship is suspected as the primary reason for leaking.



Figure 225. Backside of Tee

Tap Tee – Socket Fusion - #32020543



Figure 226. As Received Tap Tee

Table 60. 2" x ½" Tap Tee - Socket Fusion Background

Pipe Information	32020543
Color	Orange
Diameter	2" IPS x ½" CTS
SDR	-
Resin	PE 2306
Manufacturer	Plexco
Design Pressure	-
Service Information	
Operating Pressure	1-60 psig
Service Temperature	60°F
Comments	-
Timeline	
Placed in Service	June 1982
Installation Method	-
Removed from Service	July 2005
Comments	30" depth of cover; Tee on angle
Environmental	
Soil Type	Loam
Evidence of 3rd Party Damage	No

Visual Examination

Background information provided with the sample included field notes indicating the tee was on an angle. This likely caused undue stresses on the service pipe which lead to an unrecoverable bending moment. Signs of ductile overload (Figure 228) and necking of the pipe wall thickness were present.

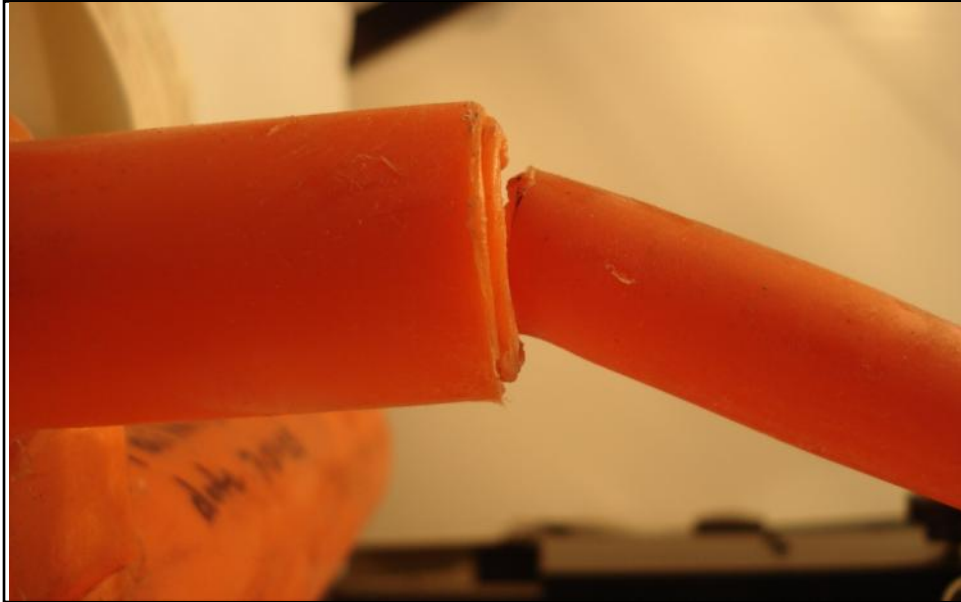


Figure 227. Socket of Tee, Side View



Figure 228. Ductile Tearing

Transition Fitting

Transition Fitting - #18020538



Figure 229. As Received

Table 61. Transition Fitting Background

Pipe Information	18020538
Color	Green Coated Steel to Orange PE
Diameter	1 – ¼”
SDR	10
Resin	TR 418
Manufacturer	--
Design Pressure	-
Service Information	
Operating Pressure	1-60 psig
Service Temperature	60°F
Comments	Pressure tested at 100 psig
Timeline	
Placed in Service	1988
Installation Method	-
Removed from Service	April 2005
Comments	38” depth of cover; Improper padding
Environmental	
Soil Type	Clay
Evidence of 3rd Party Damage	No

Visual Examination

The sample suffered excessive bending between the pipe and the stab fitting likely due to improper support on the underside of the pipe based on the field report.

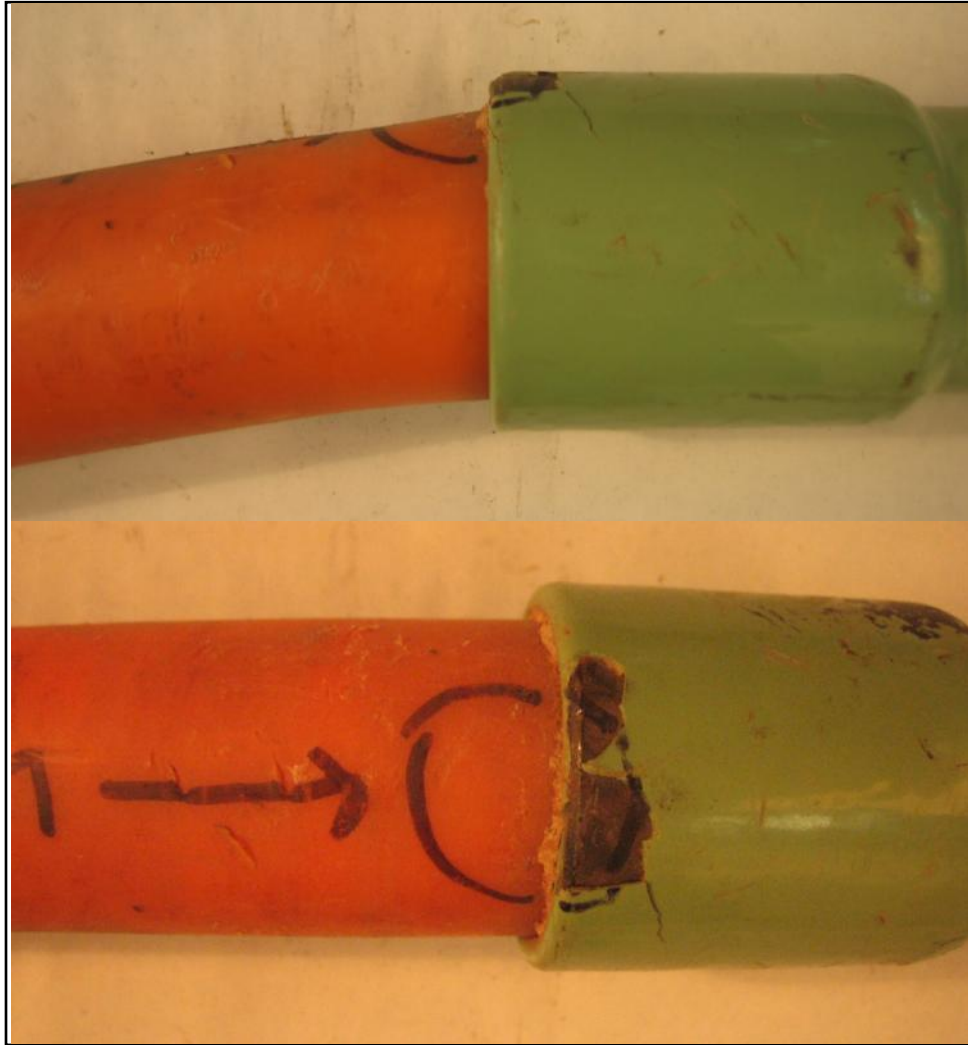


Figure 230. Side and Bottom View of Transition

Quality Control Problems

3" Elbow - #675540



Figure 231. As Received Sample - 3" Elbow

Table 62. 3" Elbow Background

Pipe Information	675540
Diameter	3"
SDR	11.5
Resin	PE 2306
Manufacturer	DuPont
Design Pressure	60psig
Service Information	
Operating Pressure	35 psig at 60°F / 10psig at 0°F
Service Temperature	60°F
Comments	NA
Timeline	
Placed in Service	1970
Installation Method	Direct Lay
Removed from Service	December 2007
Comments	NA
Environmental	
Soil Type	Rocky, sandy and silty
Evidence of 3rd Party Damage	No

Visual Examination

The submitted section was subjected to visual examination. The results of this examination indicated the presence of a circumferential slit in the injection molded elbow. The section was capped, pressurized, and subjected to leak testing using soap solution. Leaking occurred at the slit as seen in Figure 232. Next, the section was cut longitudinally (Figure 233) to examine the exposed inner surface. Radial distortion of the elbow and pipe were noted. A gap was detected in the socket fusion area at the pipe/elbow interface as identified in Figure 234 and Figure 235. The area was moderately flexed by hand and movement of the joint was observed and photographed.

The section containing the leak path was cooled with liquid nitrogen and force fractured to expose the associated surfaces as seen in Figure 237 through Figure 242. Examination of the surface confirmed the earlier observed area of significantly poor fusion. At higher magnification areas of banding (Figure 239) and ductile failure regions were observed as well as debris deposited by the gas leak. Closer scrutiny indicated the presence of dark spots imbedded in the fracture surfaces as seen in Figure 243 and Figure 244.

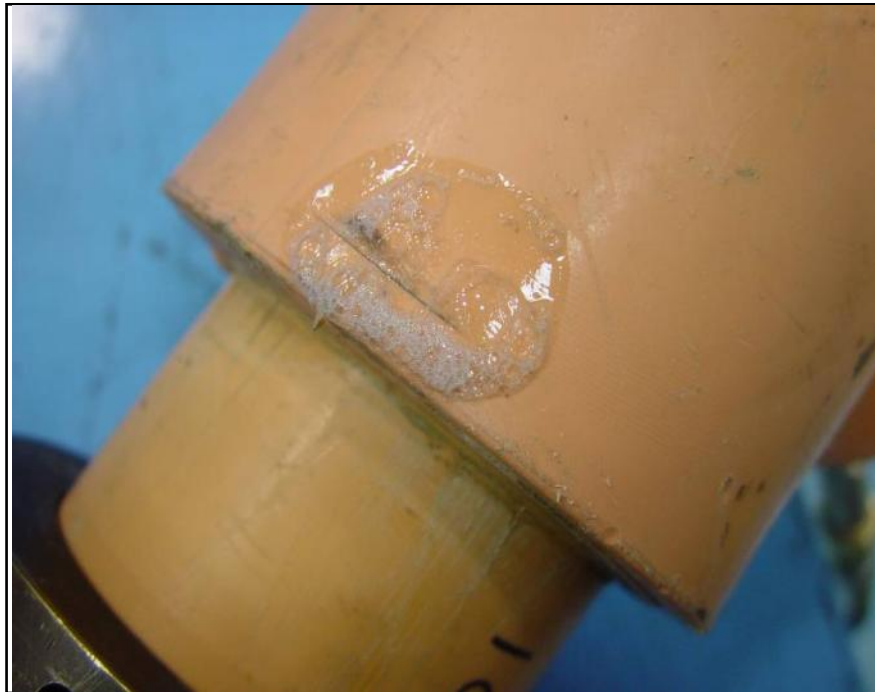


Figure 232. Leak Location As Identified By a Soap Solution

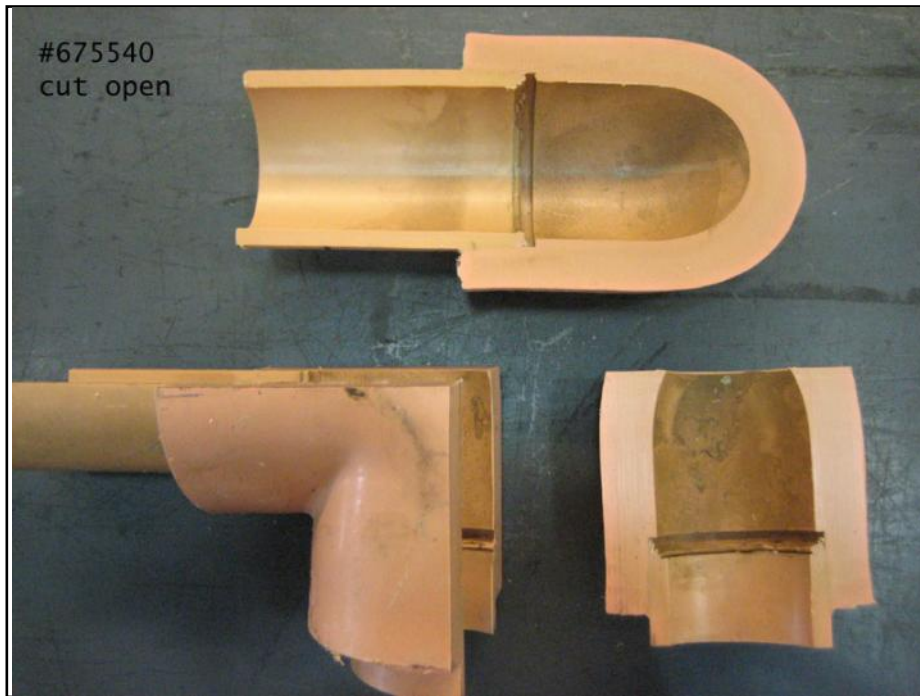


Figure 233. Cut Sample to Expose Inner Wall

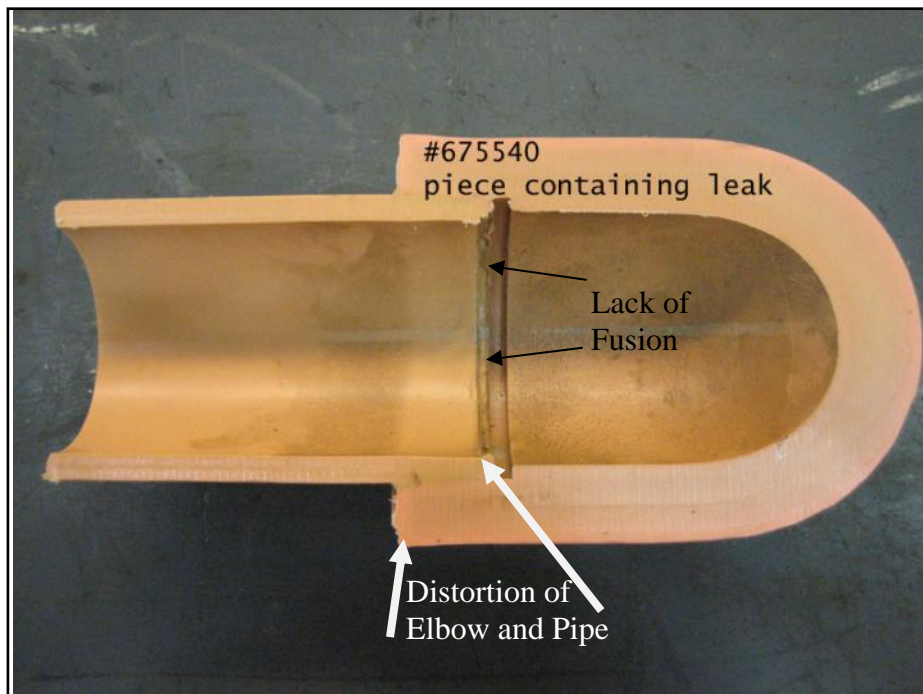


Figure 234. Portion of Elbow Containing Leak

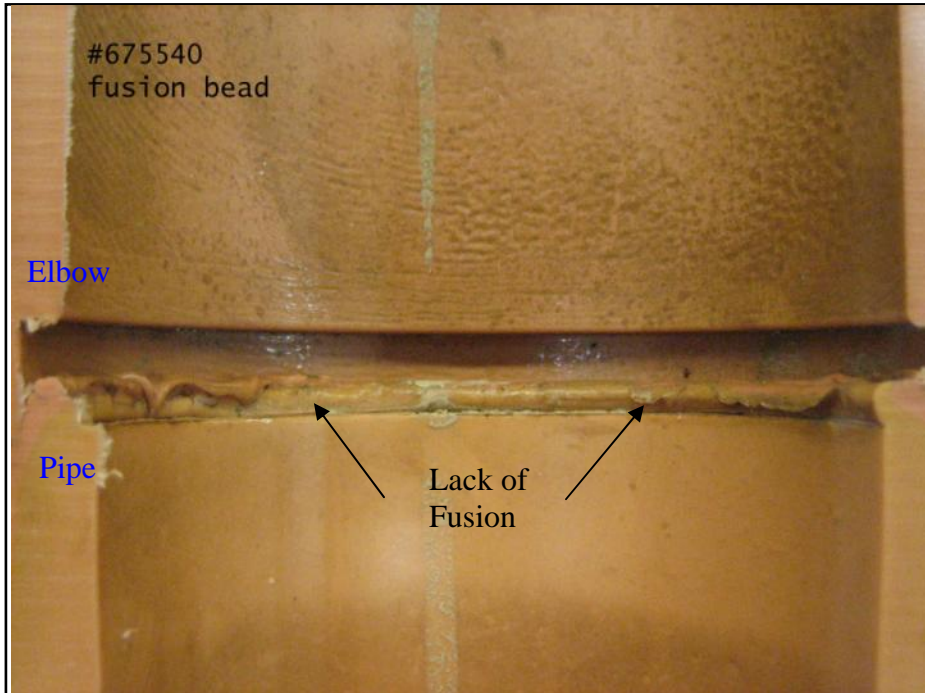


Figure 235. Inner Fusion Interface with Area of Observed Lack of Fusion

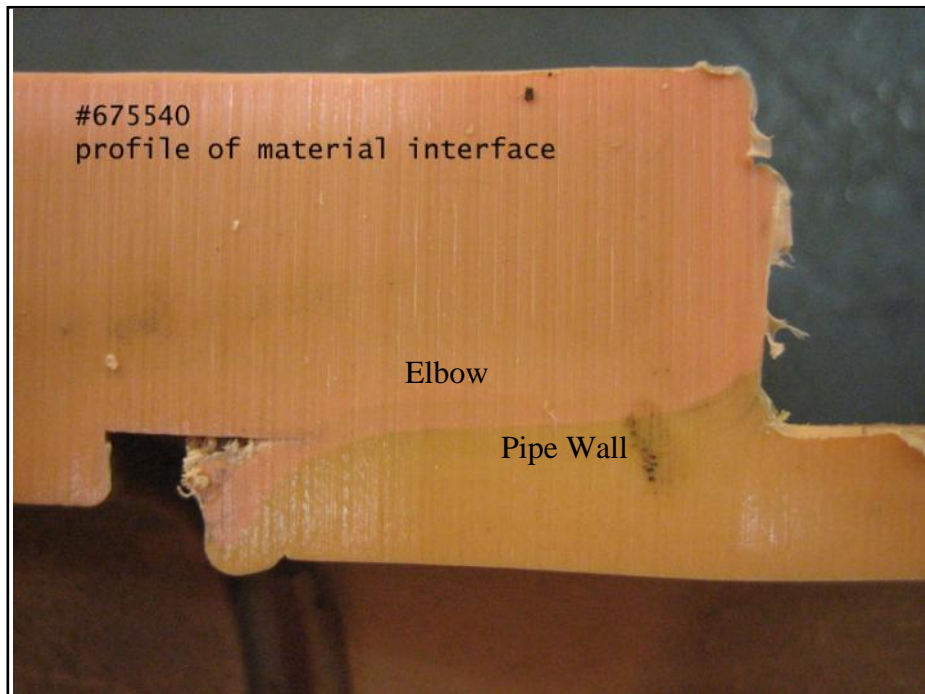


Figure 236. Fusion Interface

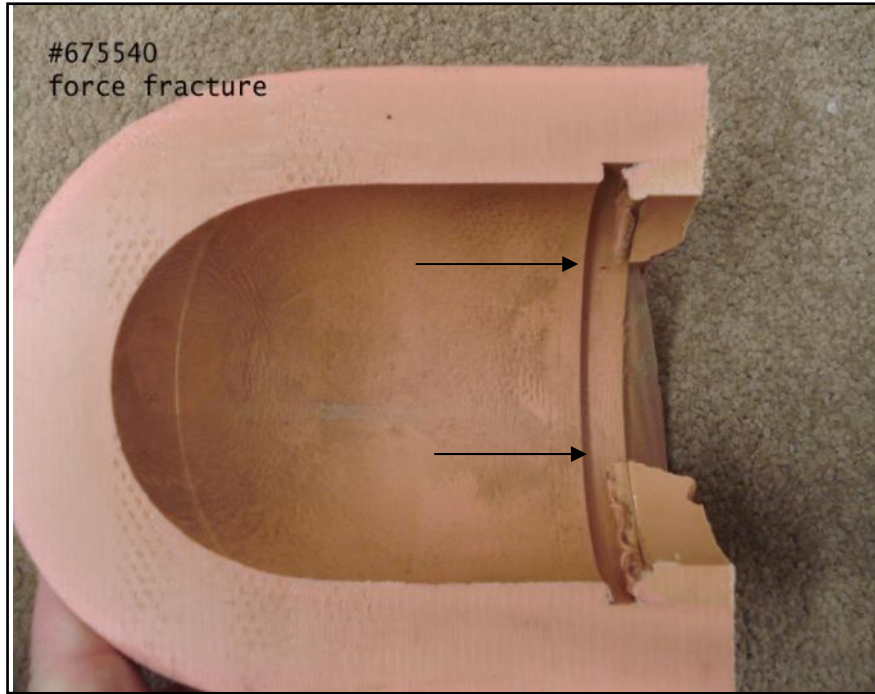


Figure 237. Force Fracture of the Sample, Showing Area of Observed Lack of Fusion

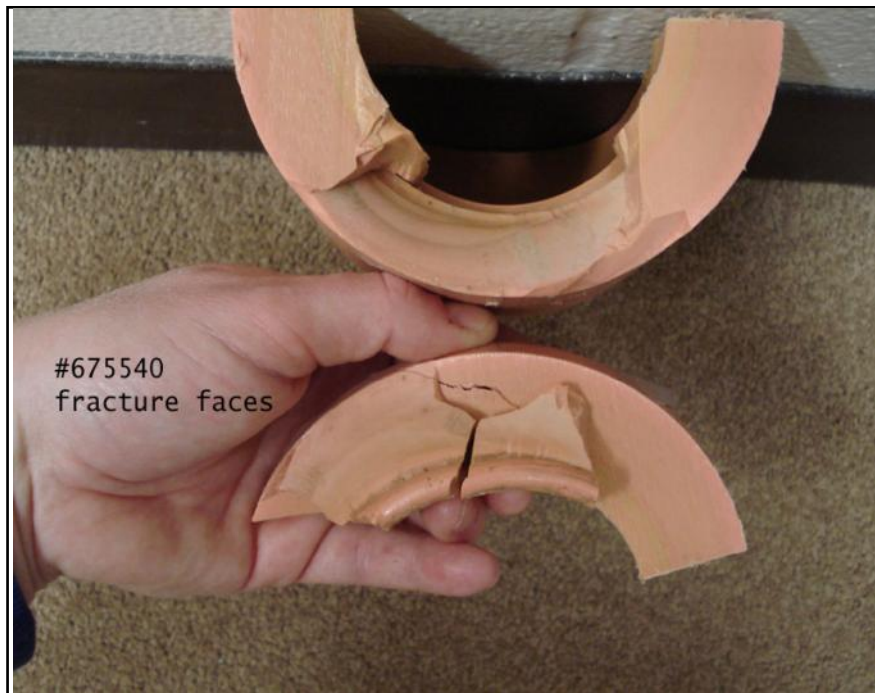


Figure 238. Fractured Sample with the Elbow Side, Top, and Pipe Side, Bottom.

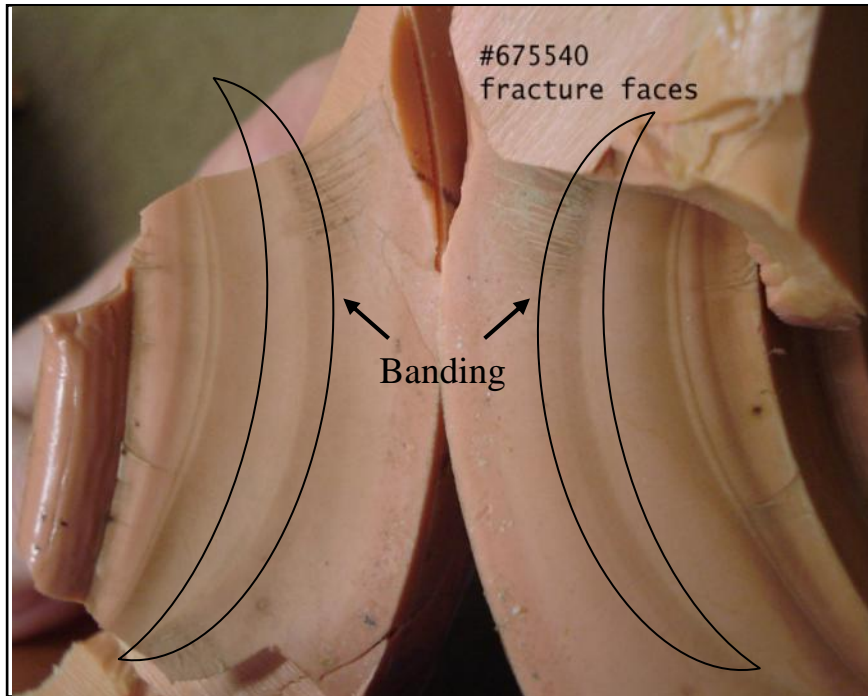


Figure 239. Close up of the Fracture Faces with the Elbow Side on the Right

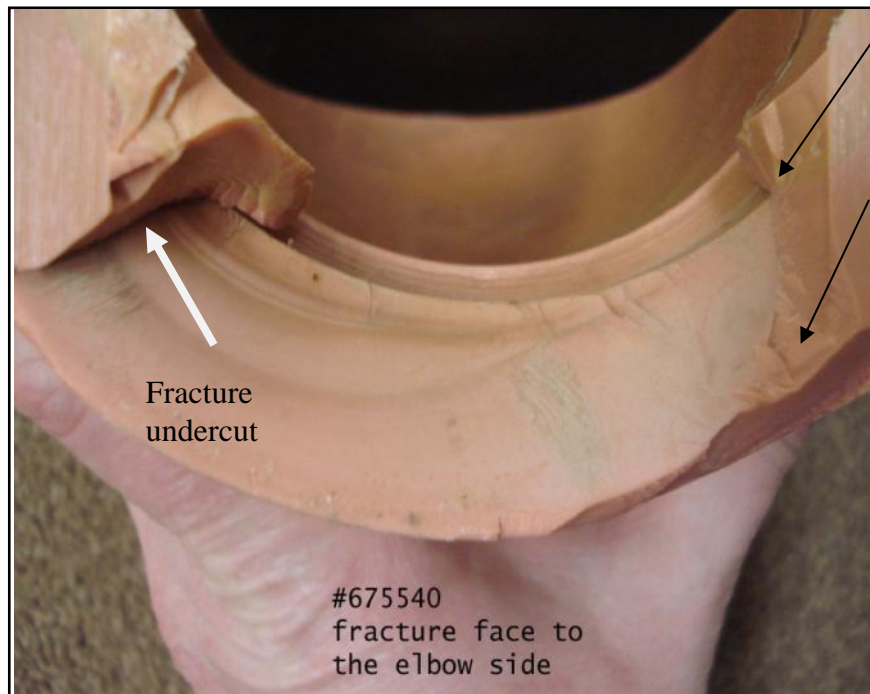


Figure 240. Fracture Face on the Elbow Side. Ductile Failure Region

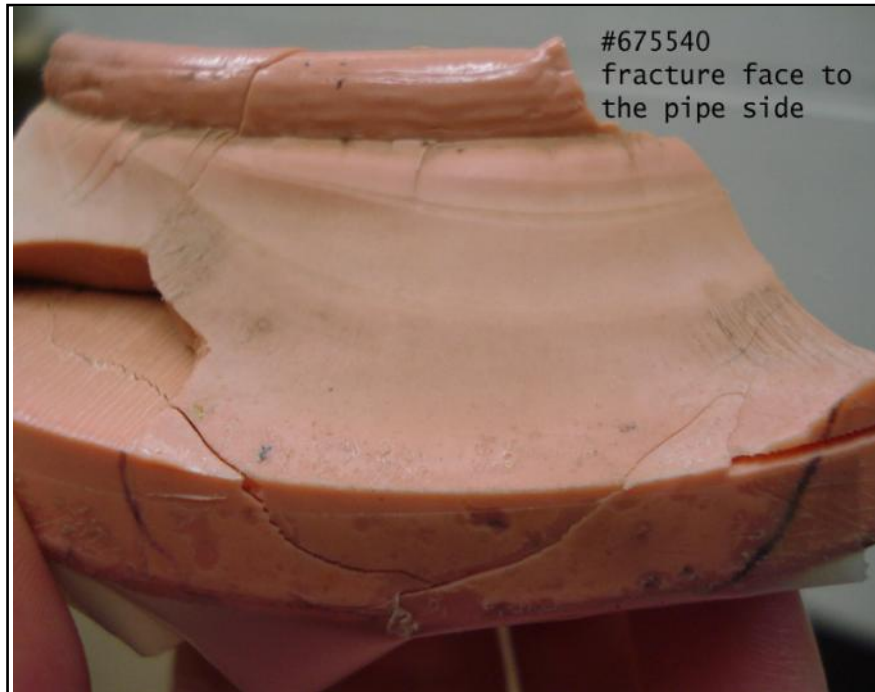


Figure 241. Close up of the Fracture Face on the Pipe Side

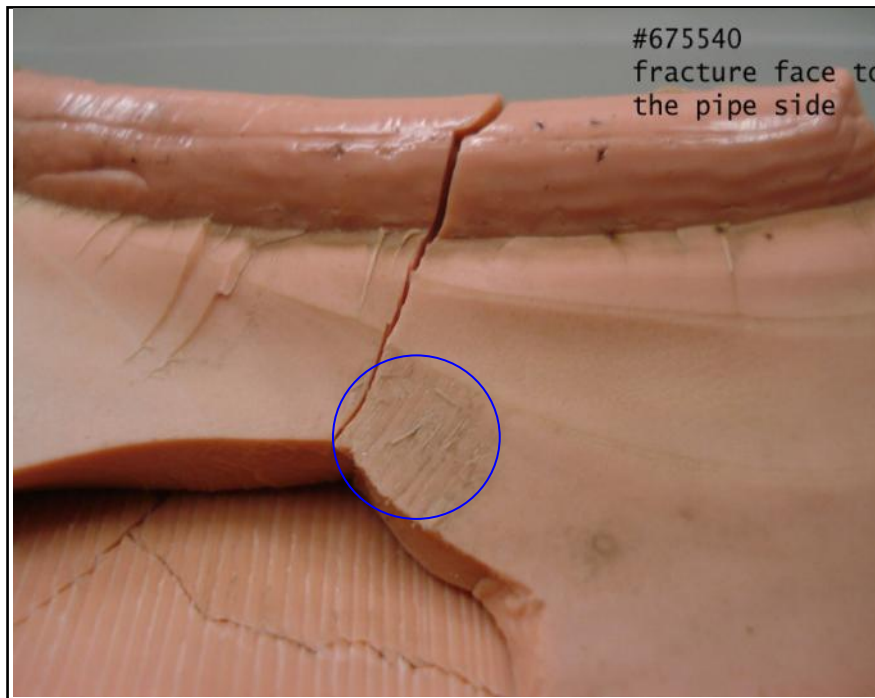


Figure 242. Fracture Face on the Pipe Side with an Area of Interest Identified



Figure 243. Microscopy - Fracture Face of Elbow – Toward the Elbow Side

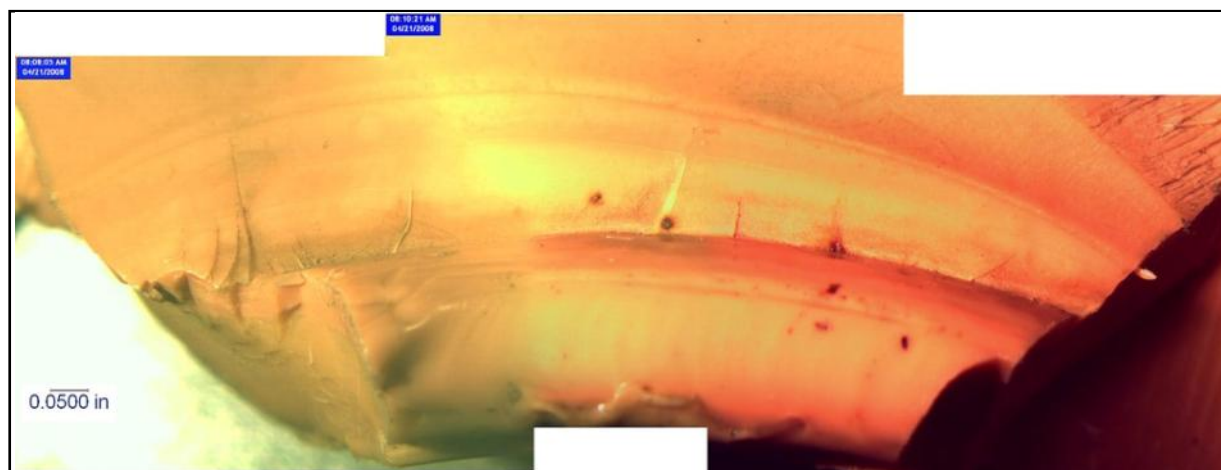


Figure 244. Microscopy – Fracture Face of Elbow – Toward the Pipe Side

Density

The skeletal density of the pipe was determined to be 0.940g/cc using the helium pycnometer. This was consistent with medium density polyethylene gas pipe material from the time period sample #675540 was manufactured.

The skeletal density of the elbow was determined to be 0.948g/cc using the helium pycnometer. The density was a little higher than the pipe which is an attribute of the manufacturing process as the part was molded rather than extruded. This was consistent with medium density polyethylene material.

Melt Flow

Portions of the pipe and elbow sections were prepared and subjected to ASTM D1238 melt flow testing.

Table 63: Melt Flow Measurements - Pipe

Sample ID	Trial #	Rate (g/10min)
675540-001a	1	1.0722
675540-001a	2	0.9900
675540-001a	3	1.1172
Average		1.0598±0.0645

Table 64: Melt Flow Measurements - Elbow

Sample ID	Trial #	Rate (g/10min)
675540-001b	1	1.2980
675540-001b	2	1.1580
675540-001b	3	1.1600
Average		0.2053±0.0803

These results were consistent with medium density polyethylene gas pipe material.

Thermal Analysis- Pipe Wall

Specimens were prepared from the pipe section and subjected to ASTM D3418 differential scanning calorimetry. The resulting thermograms indicated a heat of fusion of 160J/g as shown in Figure 245. No additional melting or exotherms were detected which would have suggested the presence of contamination. In addition, ASTM D3895 was performed on the prepared specimen and indicated an oxidative-induction time of 42.8 minutes as seen in Figure 246. This was consistent with the age of the PE considering it has absorbed organic materials from the gas supply over time. Many of these organic compounds are relatively easily oxidized when compared to PE.

Thermal Analysis - Elbow

Specimens were prepared from the elbow and subjected to ASTM D3418 differential scanning calorimetry. The resulting thermograms indicated a heat of fusion of 190.5J/g as shown in Figure 247. No additional melting or exotherms were detected which would have suggested the presence of contamination. In addition, ASTM D3895 was performed on the prepared specimen and indicated an oxidative-induction time of 40.37 minutes as shown in Figure 248. This was consistent with the age of the PE considering it has absorbed organic materials from the gas supply over time. Many of these organic compounds are relatively easily oxidized when compared to PE.

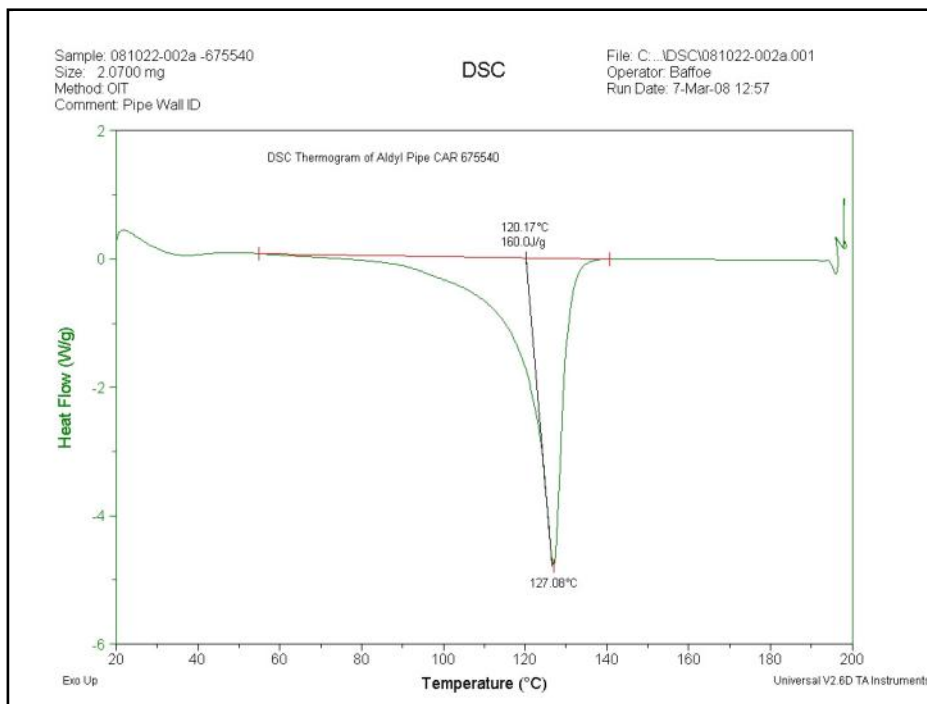


Figure 245. Differential Scanning Calorimetry – Pipe

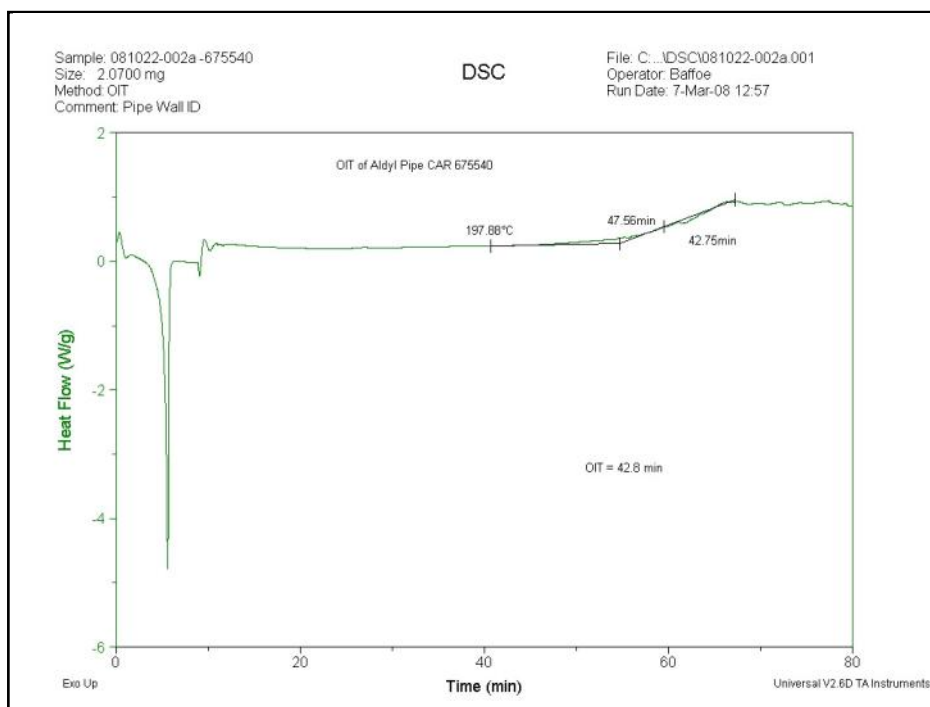


Figure 246. Oxidative Induction Time – Pipe

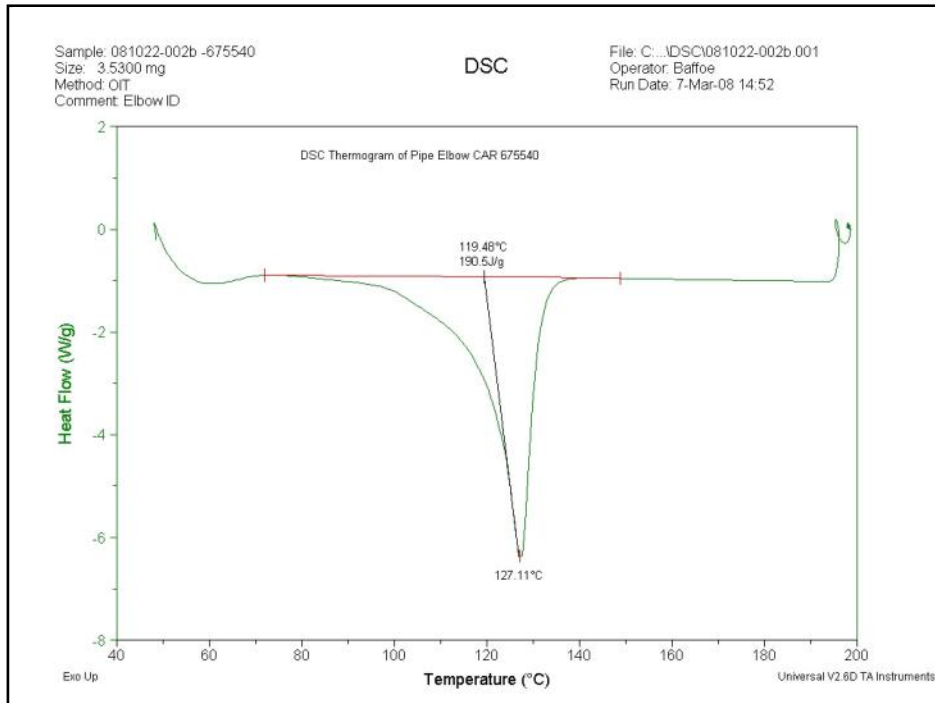


Figure 247. Differential Scanning Calorimetry - Elbow

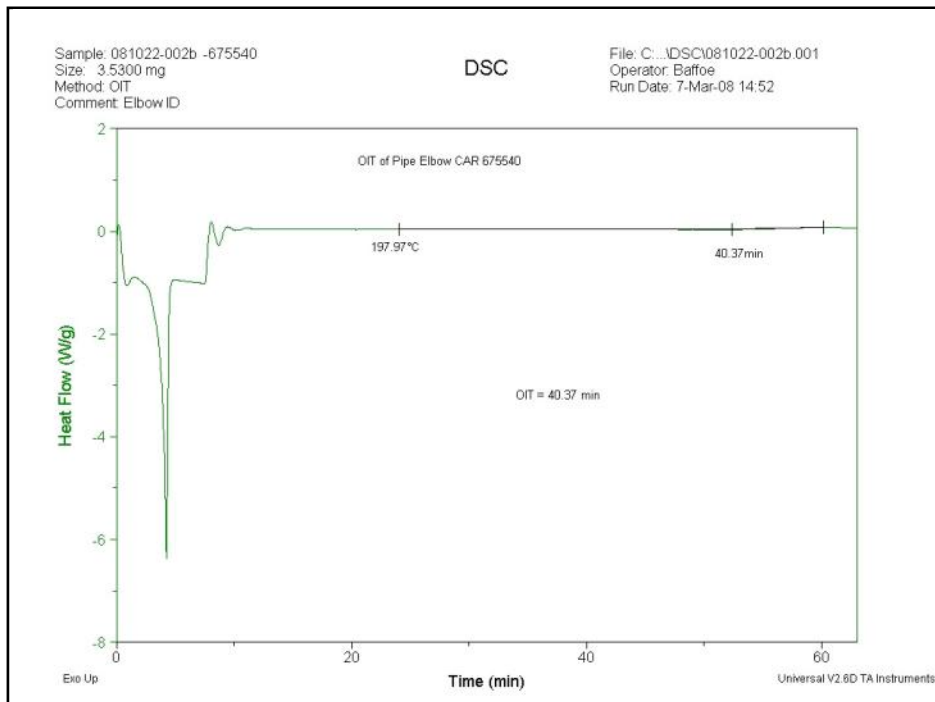


Figure 248. Oxidative Induction Time - Elbow

Infrared Analysis

A comprehensive infrared analysis was performed to determine the condition of the pipe and elbow and to detect the presence of any organic materials not associated with the respective material. The resulting spectra failed to indicate the presence of foreign organic materials in the pipe wall or elbow within the detectability of the instrument. The 1650cm^{-1} to 1750cm^{-1} region of the resulting spectra was also examined. Absorbencies in this region are associated with polyethylene oxidative products. Weak absorbencies were observed in this region that indicated minimal oxidation had occurred and suggested that the pipe was manufactured and stored acceptably prior to installation.

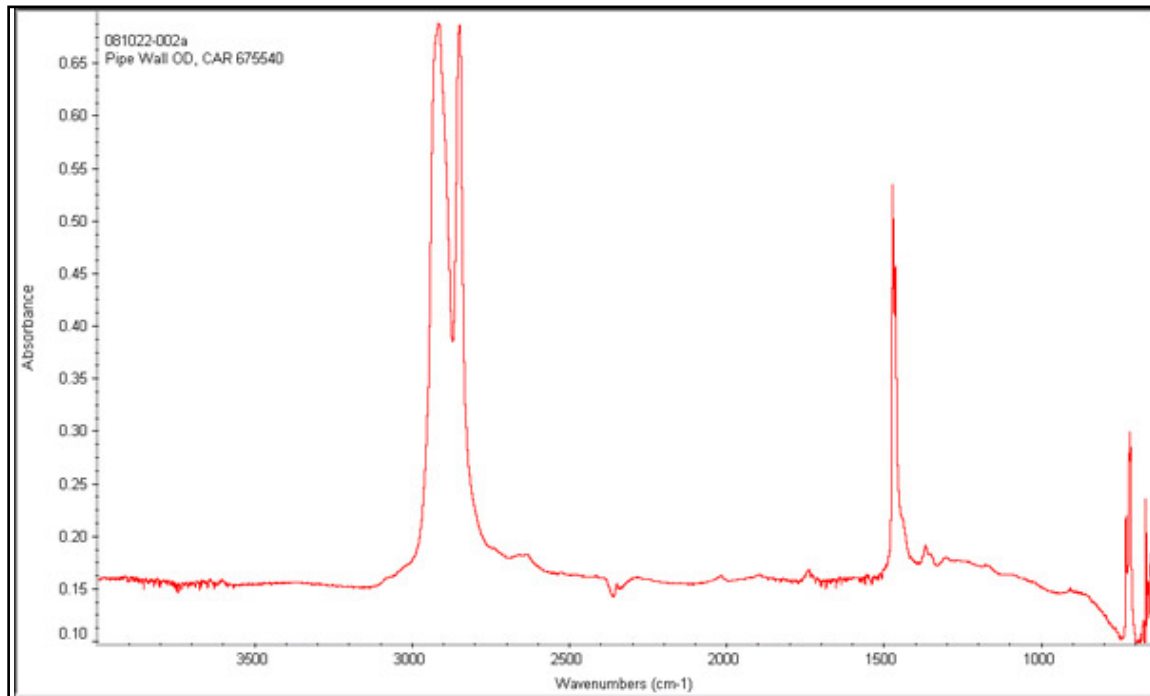


Figure 249. FT-IR Outer Wall – Pipe

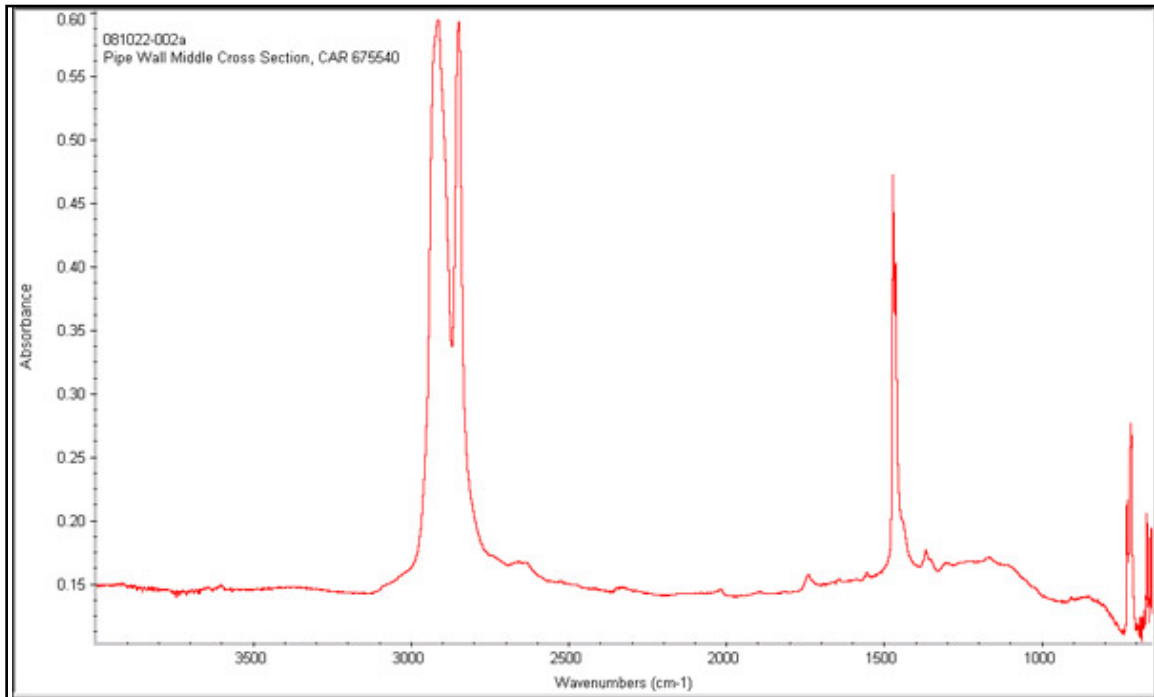


Figure 250. FT-IR Middle Wall – Pipe

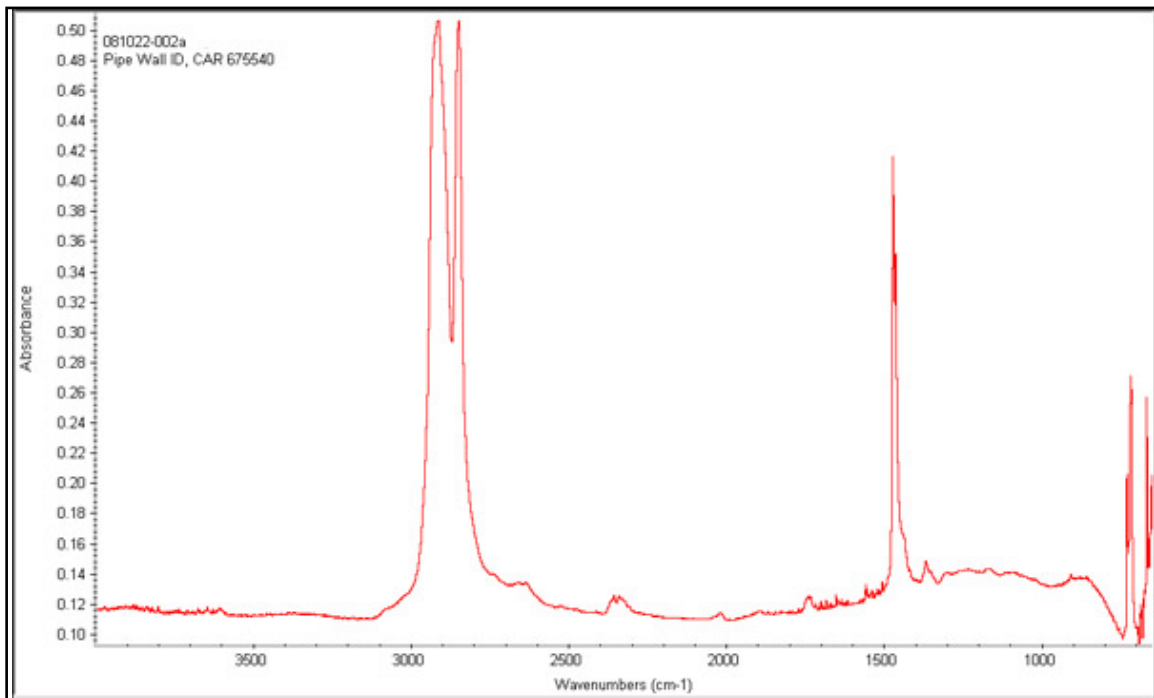


Figure 251. FT-IR Inner Wall – Pipe

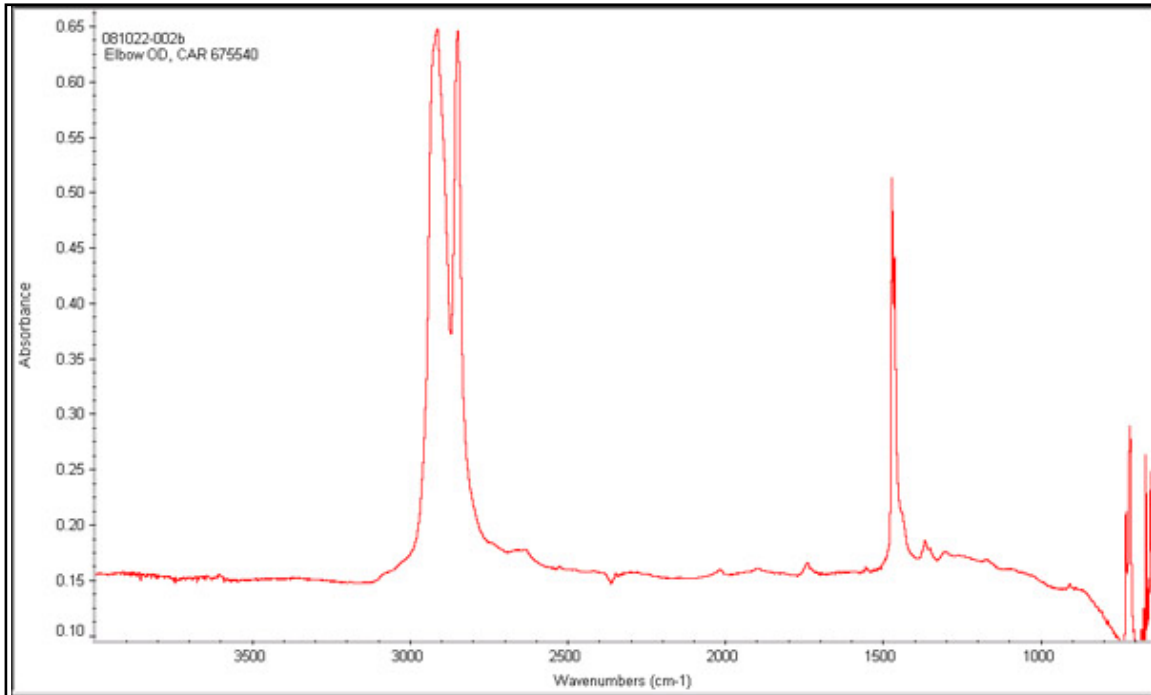


Figure 252. FT-IR - Outer Wall - Elbow

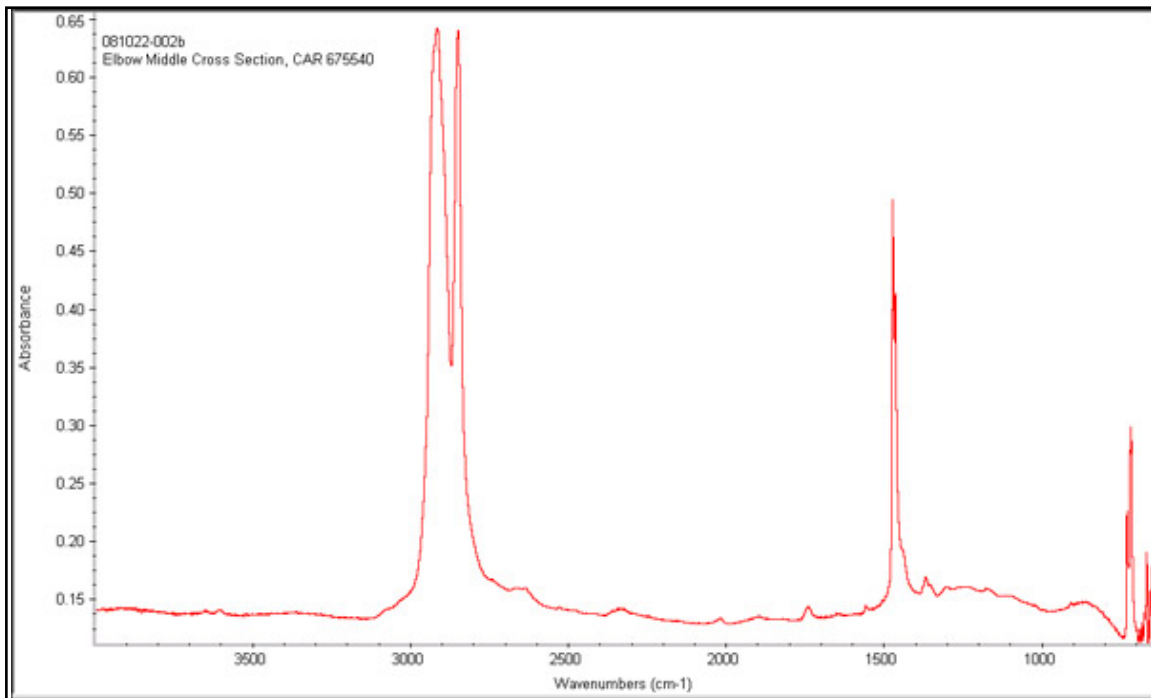


Figure 253. FT-IR - Middle Wall - Elbow

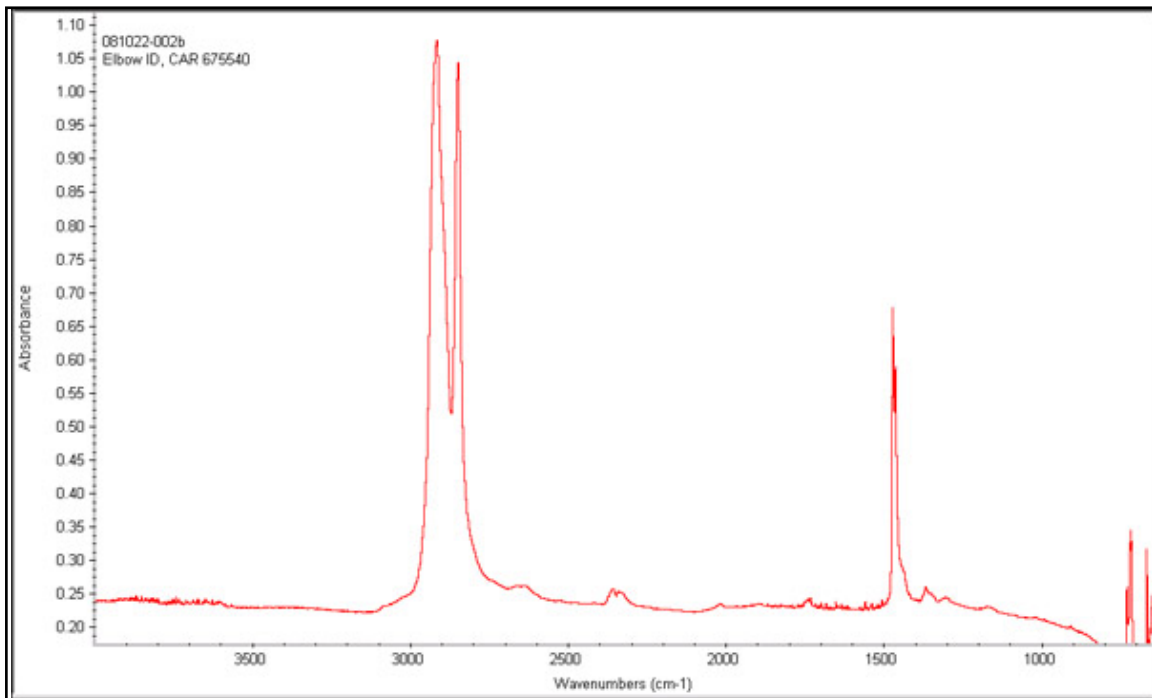


Figure 254. FT-IR - Inner Wall - Elbow

Conclusions

Based on the tests performed it was concluded that:

- 1) There was a significant area of poor fusion that contributed to the failure.
- 2) There were particles imbedded in the fracture surface of the elbow indicating that this material entered during the molding of the part that contributed to the failure.
- 3) The elbow and companion pipe exhibited radial distortion which indicated significant radial stress was present. This stress resulted from the interference fit between the elbow and pipe causing expansion of the elbow and resulted in peak stress concentration at the pipe edge/elbow interface. This elevated stress state aided the formation and propagation of the fracture.

3/4" Valve – #642535



Figure 255. As Received Sample Shown Leaking from Under the Cap

Table 65. 3/4" Valve Background

Pipe Information	642535
Diameter	3/4"
SDR	11
Resin	PE 2306
Manufacturer	DuPont (05-80)
Design Pressure	60psig
Service Information	
Operating Pressure	60 psig at 65°F / 45 psig at 0°F
Service Temperature	60°F
Comments	NA
Timeline	
Placed in Service	September 1980
Installation Method	Direct Lay
Removed from Service	October 2007
Comments	NA
Environmental	
Soil Type	Rocky, sandy and silty
Evidence of 3rd Party Damage	No

Visual Examination

Soap solution testing showed the leak originating from the underside of the valve as seen in Figure 255 and Figure 256. The entire valve was transversely sectioned and examined. The results of this examination did not detect any damage to the core, seal, or housing. As shown in Figure 257 and Figure 258. The examination focus was on the lower half of the valve. The position of the valve core was indexed relative to the housing using a series of markings shown in Figure 259. The valve was placed into a fixture and using appropriately sized tools, the core was carefully displaced from the valve body as shown in Figure 260. There were two o-rings on the core section. There was a noticeable loss of material observed on the bottom o-ring and a piece of rubber was observed wedged between the upper o-ring and its companion groove. These damaged areas can be seen in Figure 261, Figure 262, and, Figure 263. Upon removal the piece of rubber was found to match well with the damaged area of the bottom o-ring as demonstrated in Figure 264 and Figure 265. Lubricant was observed on all surfaces which is consistent with the fact that the o-rings are typically lubricated prior to assembly.



Figure 256. Valve with Leak Pinpointed

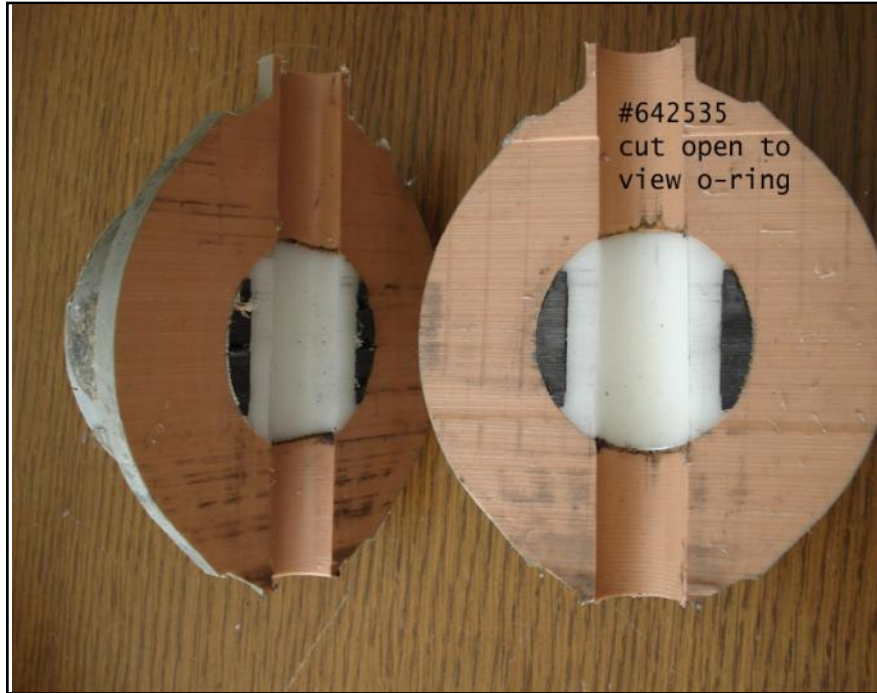


Figure 257. Valve Was Halved to Help Expose O-Ring

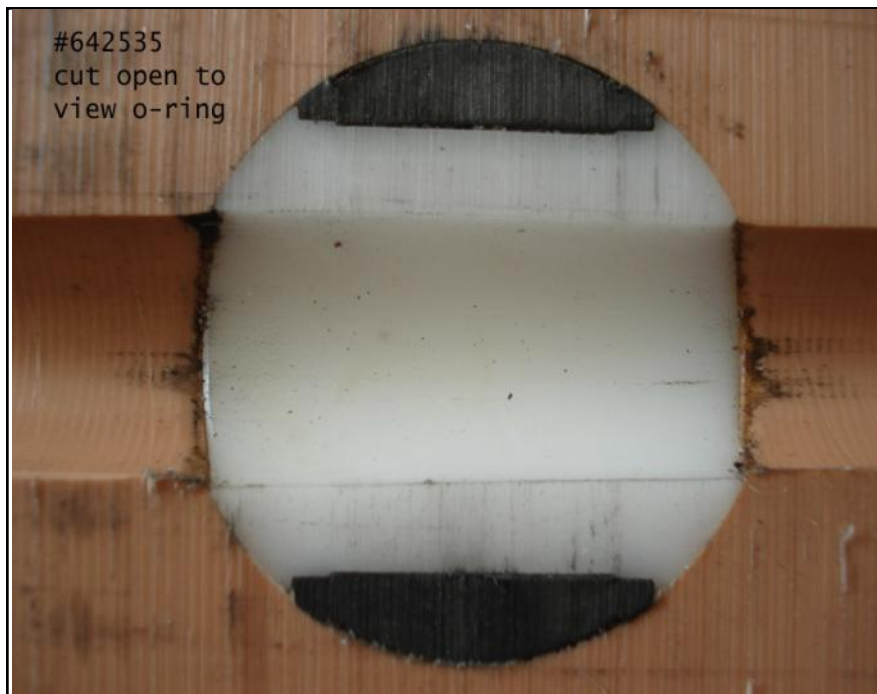


Figure 258. Close up of the Core and Seal



Figure 259. Valve Core with Indexing Marks



Figure 260. Valve Core Removed from Housing



Figure 261. Valve Core. Lower O-Ring Bottom

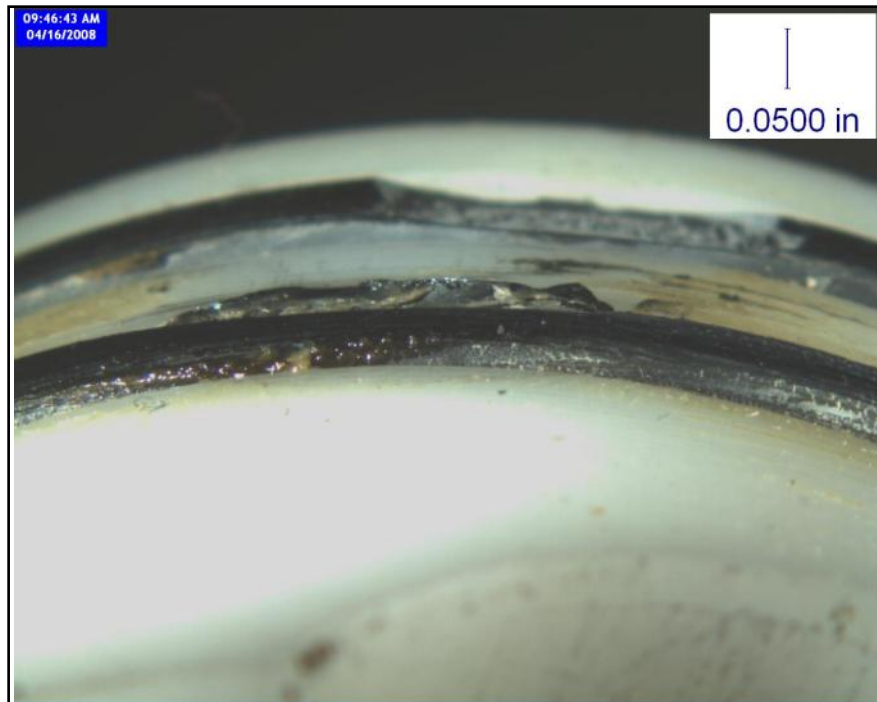


Figure 262. O-Ring Damage. Upper O-Ring, Foreground. Lower O-Ring, Background.

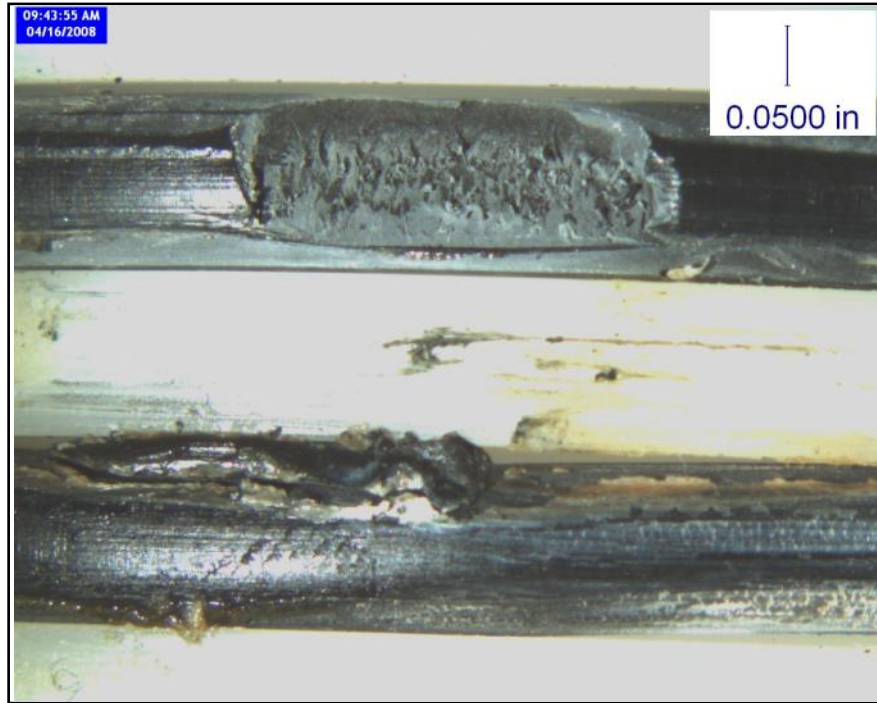


Figure 263. Imbedded Fragment Between Upper O-Ring and Core Land.

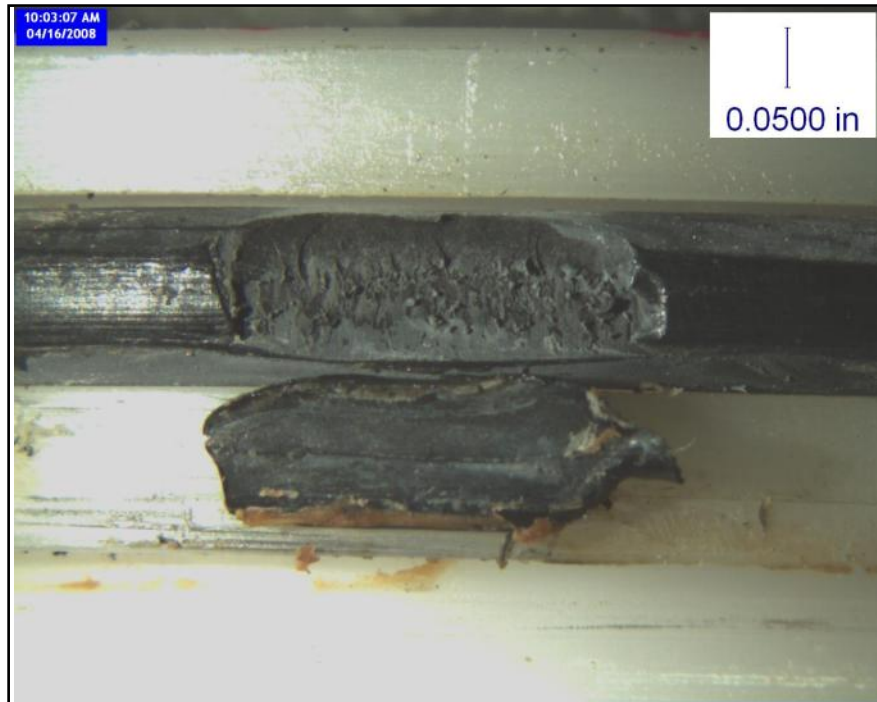


Figure 264. O-Ring Fragment Removed from the Upper O-ring Land Area.

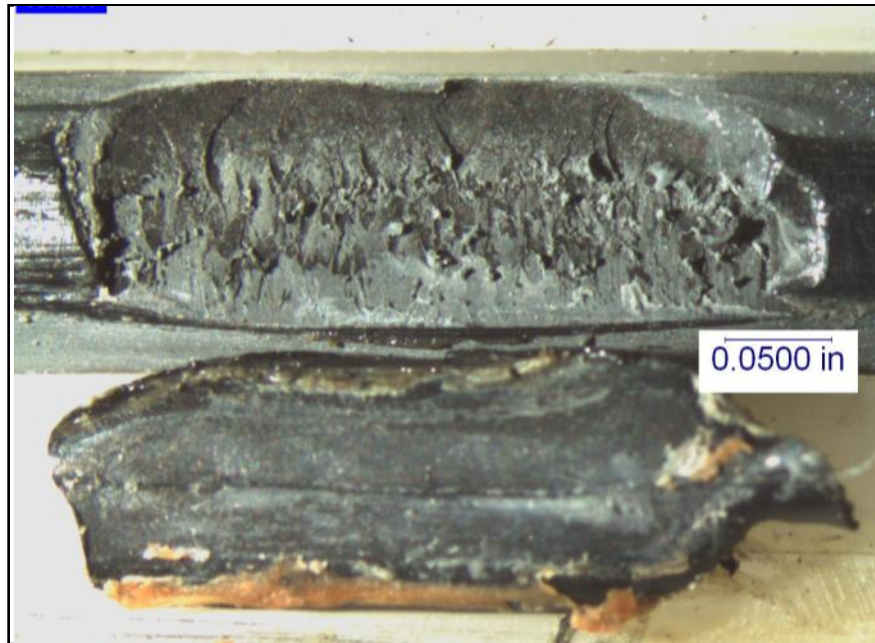


Figure 265. Higher Magnification of Figure 264

Infrared Analysis and Hardness Testing

Portions of the upper and lower o-ring rings were removed, cleaned, and subjected to infrared analysis. Both of the resulting spectra correlated well with absorbencies indicative of nitrile rubber. See Figure 266 and Figure 267. Subsequent hardness testing indicated that the material was 71-74 Shore A.

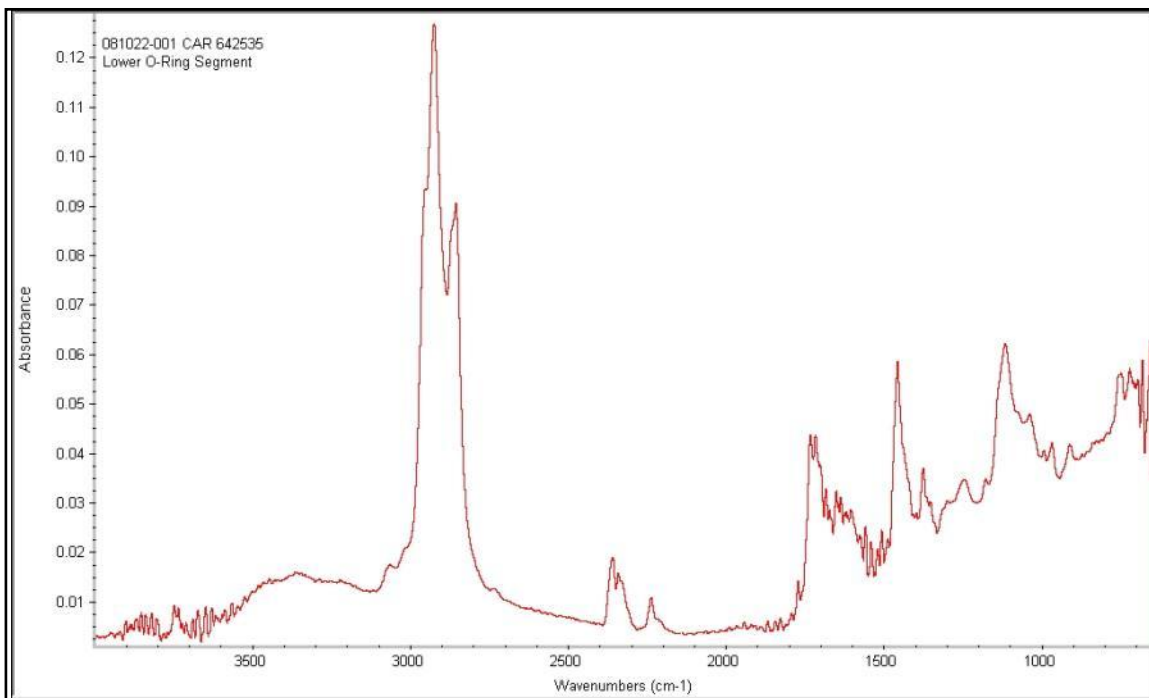


Figure 266. FT-IR - Lower O-Ring Nitrile Rubber

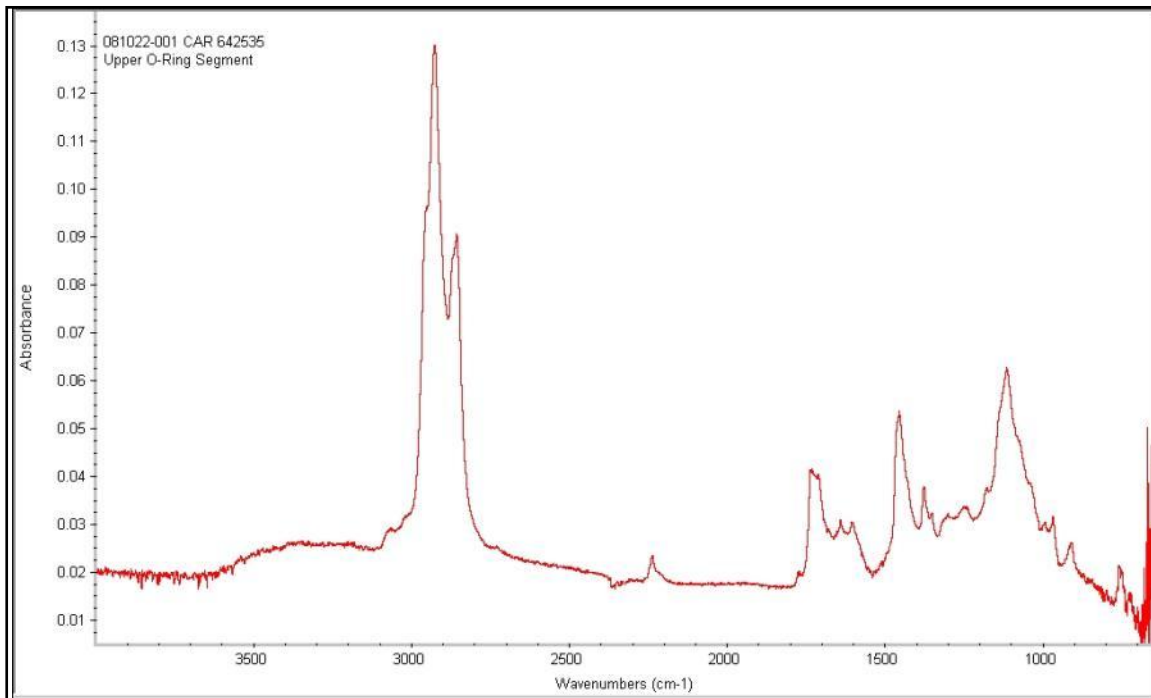


Figure 267. FT-IR - Upper O-Ring Nitrile Rubber

Conclusions

Based on the tests performed it was concluded that:

- 1) The cause of the leak was damage to the lower o-ring during assembly, which resulted in a section of rubber breaking off from the o-ring. In time, this rubber section migrated to and wedged itself between the upper o-ring and its groove. Both conditions reduced the sealing effectiveness of the o-rings.
- 2) Both o-rings were manufactured from nitrile rubber. Nitrile rubber is commonly used in natural gas systems. Hardness testing indicated Shore hardness of up to 74A. Typically as these materials age they become harder and their sealing effectiveness decreases. When the o-rings were new, they were still able to seal despite the observed damage. As the o-rings aged, they were no longer effective in maintaining a good seal.

Miscellaneous Problems

Charred Pipe – #01020436



Figure 268. As Received

Table 66. Charred ¾" Pipe Background

Pipe Information	010204336
Color	Yellow
Diameter	¾"
SDR	11
Resin	PE 2406
Manufacturer	Driscoplex 6500
Design Pressure	-
Service Information	
Operating Pressure	1-60 psig
Service Temperature	60°F
Comments	-
Timeline	
Placed in Service	2004
Installation Method	Bored
Removed from Service	February 2004
Comments	48" depth of cover
Environmental	
Soil Type	Loam
Evidence of 3rd Party Damage	No; In close proximity to electric cables

Visual Examination

This pipe section was exposed to excessive heating from a shorted electric cable. The pipe was installed by boring and may have caused the damage to the electric cable insulation.



Figure 269. Up Close View of Damaged Pipe Section

Tap Tee – #642909



Figure 270. As Received Sample of a Leaking Tee



Figure 271. Circumferential Slit on the Backside of the Tee

Table 67.1 - Tap Tee Background

Pipe Information	642909
Diameter	1 – ¼”
SDR	10
Resin	PE 2306
Manufacturer	DuPont (1-82)
Design Pressure	60psig
Service Information	
Operating Pressure	60 psig at 65°F / 50 psig at 0°F
Service Temperature	60°F
Comments	NA
Timeline	
Placed in Service	Main in 1982; Service in 1983
Installation Method	Direct Lay
Removed from Service	December 2007
Comments	NA
Environmental	
Soil Type	Rocky, sandy and silty
Evidence of 3rd Party Damage	Yes

Visual Examination

The results of this examination indicated that the pipe segment section was permanently deformed 90 degrees from the saddle fused service tee. On the back side of the tee, away from the service outlet, a fracture in the pipe was observed as seen in Figure 271. Also in this area immediately adjacent to the fracture, the saddle fusion appeared to have minimal roll back on this side of the tee. The opposite side of the tee exhibited a double bead and significantly more material roll back than the side immediately adjacent to the observed fracture.

The pipe segment was cut longitudinally approximately 180 degrees from the service tee. The area of interest was then carefully cut further aiding exposure of the fracture surfaces of the observed crack as shown in Figure 272 through Figure 274. After opening the fracture, the saddle fused service tee exhibited a large area of poor adhesion to the pipe as seen in Figure 275. Visual examination (Figure 276 and Figure 277) and higher magnification examination (Figure 278 and Figure 279) using a stereo optical microscope indicated that the fracture surfaces were white and exhibited characteristics consistent with ductile failure of the pipe wall.



Figure 272. Pipe Was Cut Away to Reveal the Inner Pipe Wall



Figure 273. Damage on the Inner Wall

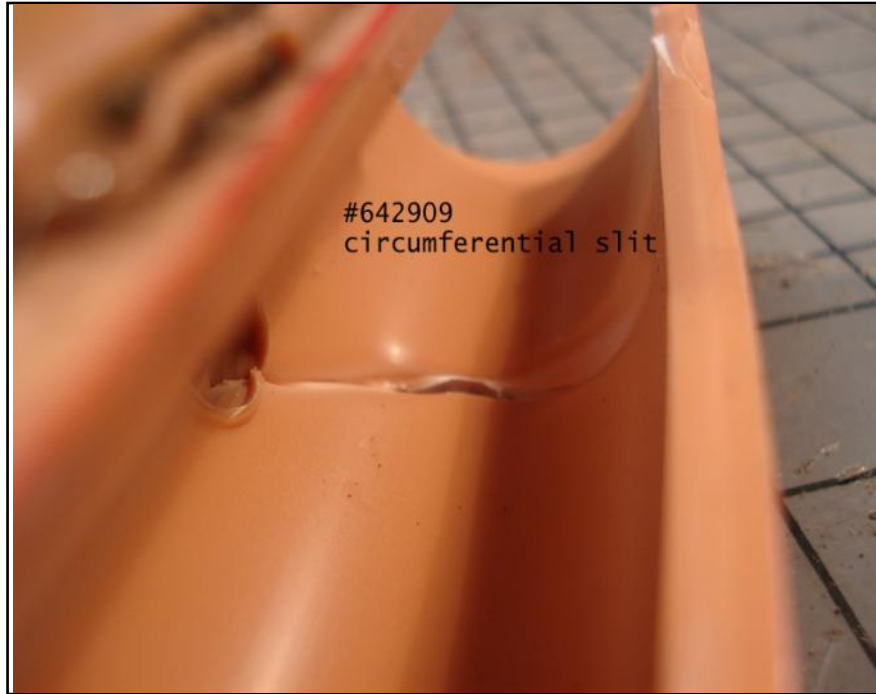


Figure 274. Damage on the Inner Wall



Figure 275. Tee Separated from Pipe during Force Fracture

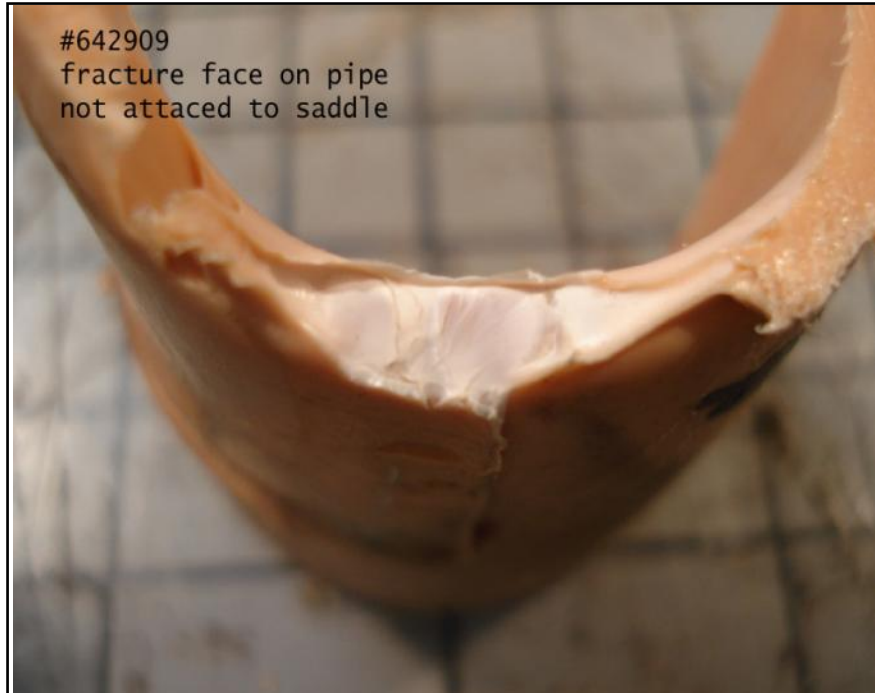


Figure 276. Fracture Face on the Pipe No Longer Attached to the Tee



Figure 277. Opposing Fracture Face

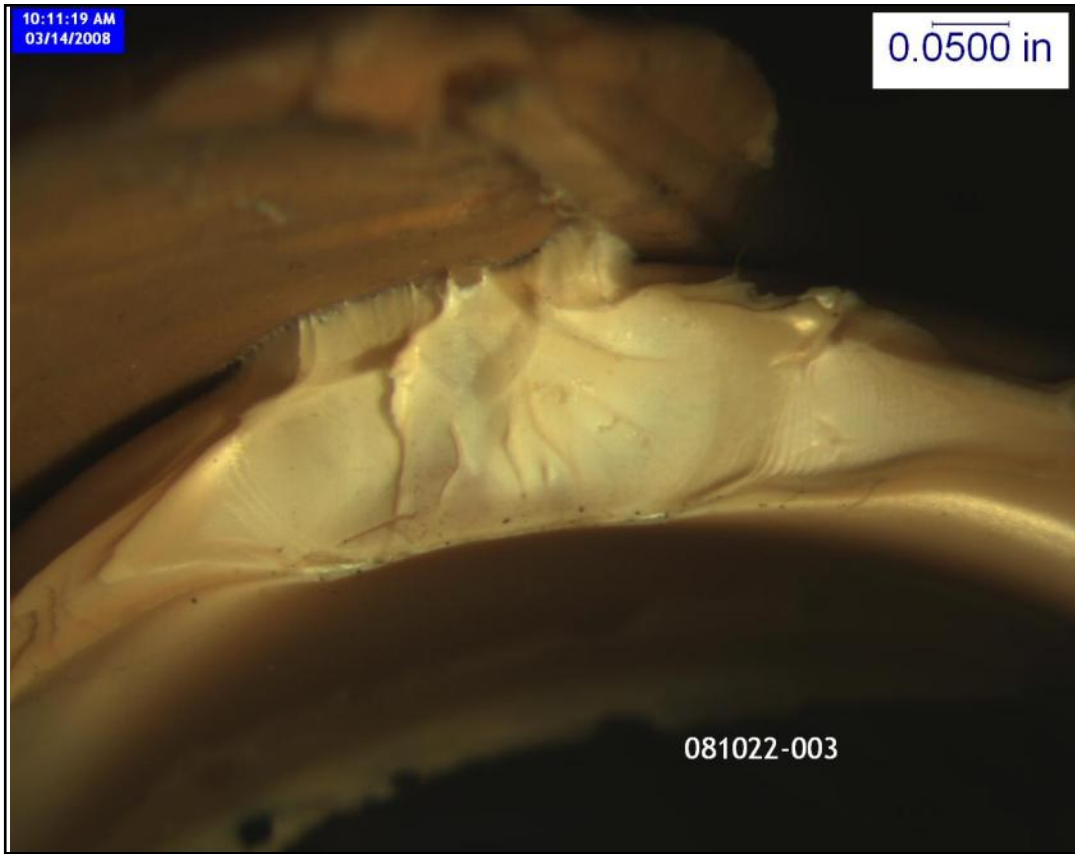


Figure 278. Fracture Face Microscopy on the Pipe No Longer Attached to the Tee

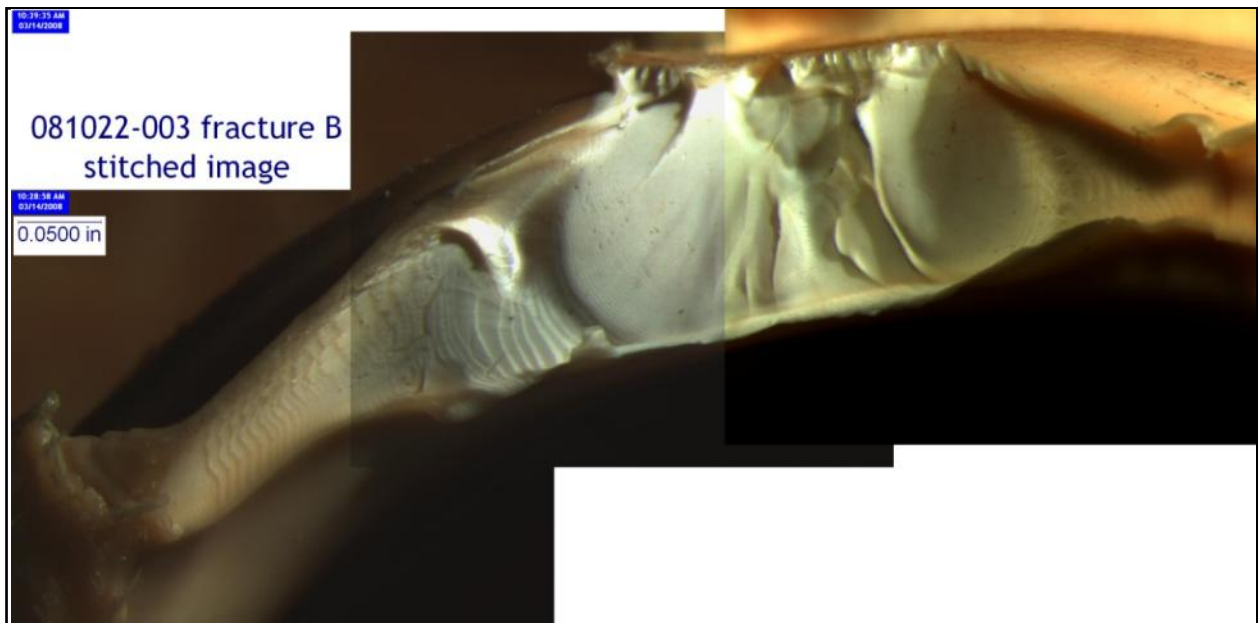


Figure 279. Opposing Fracture Face Microscopy

Density

The skeletal density of the pipe was determined to be 0.939g/cc using the helium pycnometer. This was consistent with medium density polyethylene gas pipe material from the time period sample 642909 was manufactured.

Melt Flow

Sections of the pipe were prepared and subjected to ASTM D1238 melt flow testing.

Table 68: Melt Flow Measurements

Sample ID	Trial #	Rate (g/10min)
642909-001	1	1.0246
642909-001	2	1.1580
642909-001	3	1.1660
Average		1.1162±0.0794

These results were consistent with medium density polyethylene gas pipe material.

Thermal Analysis

Specimens were prepared from the pipe section and subjected to ASTM D3418 differential scanning calorimetry. The resulting thermograms, seen in Figure 280, indicated a heat of fusion of 171.2J/g and no additional melting or exotherms were detected which would have suggested the presence of contamination. In addition, ASTM D3895 was performed on the prepared specimen and indicated an oxidative-induction time of 51.7 minutes as shown in Figure 281. This was consistent with the age of the PE considering it has absorbed organic materials from the gas supply over time. These organic compounds are relatively easily oxidized when compared to PE.

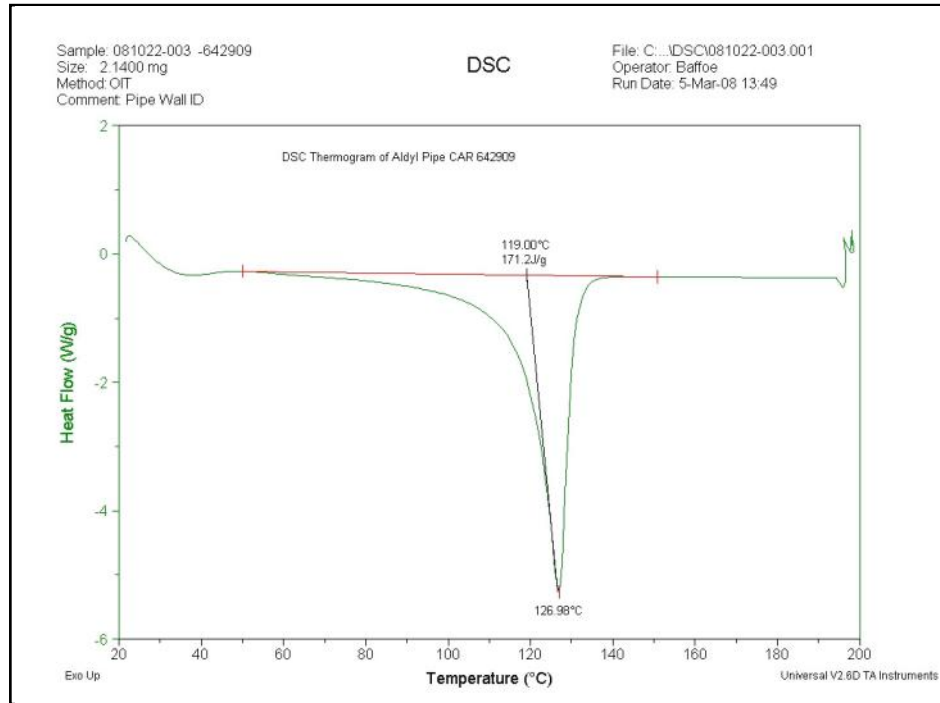


Figure 280. Differential Scanning Calorimetry

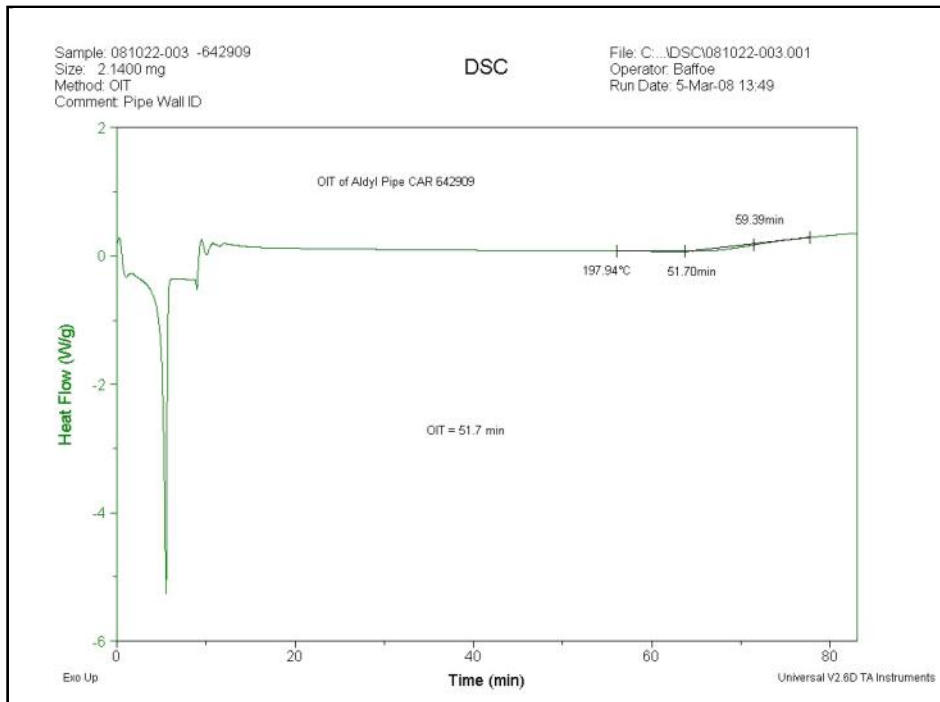


Figure 281. Oxidative Induction Time

Infrared Analysis

A comprehensive infrared analysis was performed to determine the condition of the pipe as it detects the presence of any organic materials not associated with the pipe material. The results did not indicate the presence of any foreign organic materials in the outer middle or inner pipe wall within the detectability of the instrument. Weak absorbencies detected in the 1650cm^{-1} to 1750cm^{-1} region of the spectra suggested minor oxidation of the pipe material had occurred.

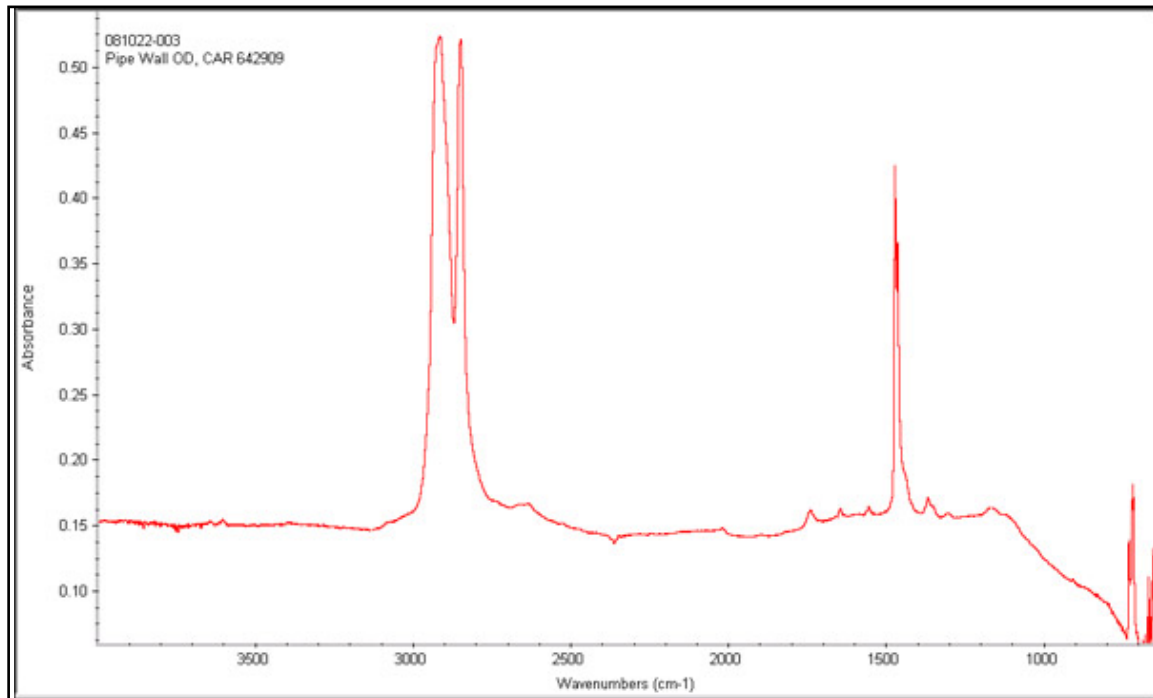


Figure 282. FT-IR - Outer Wall

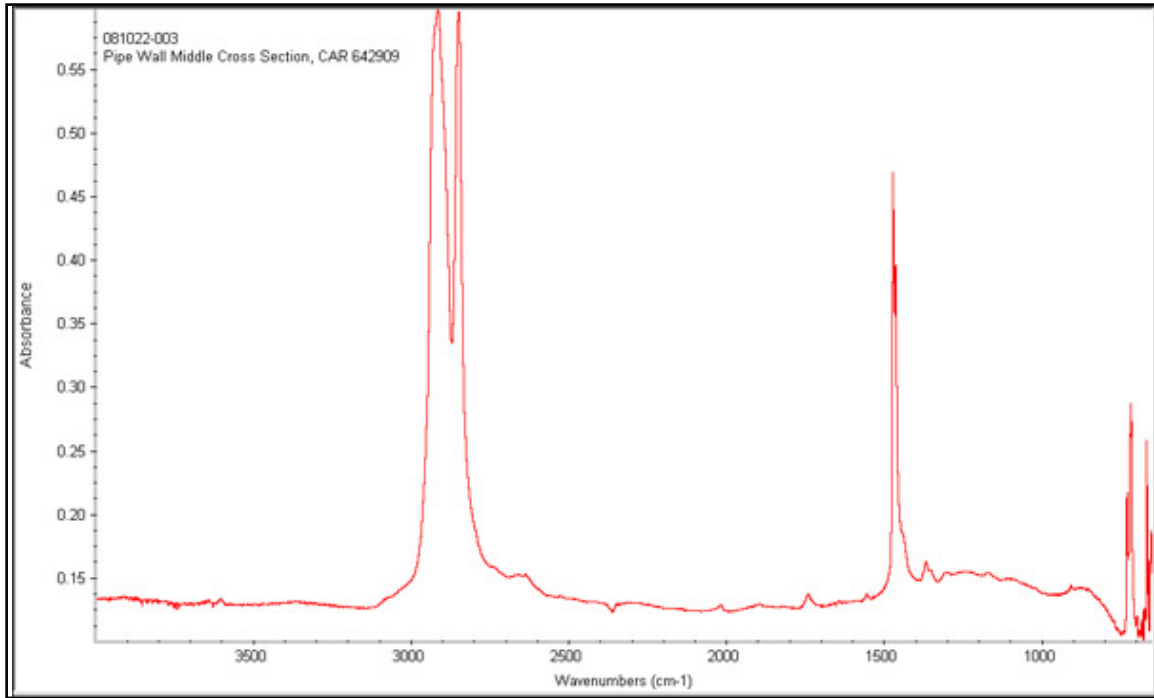


Figure 283. FT-IR - Middle Wall

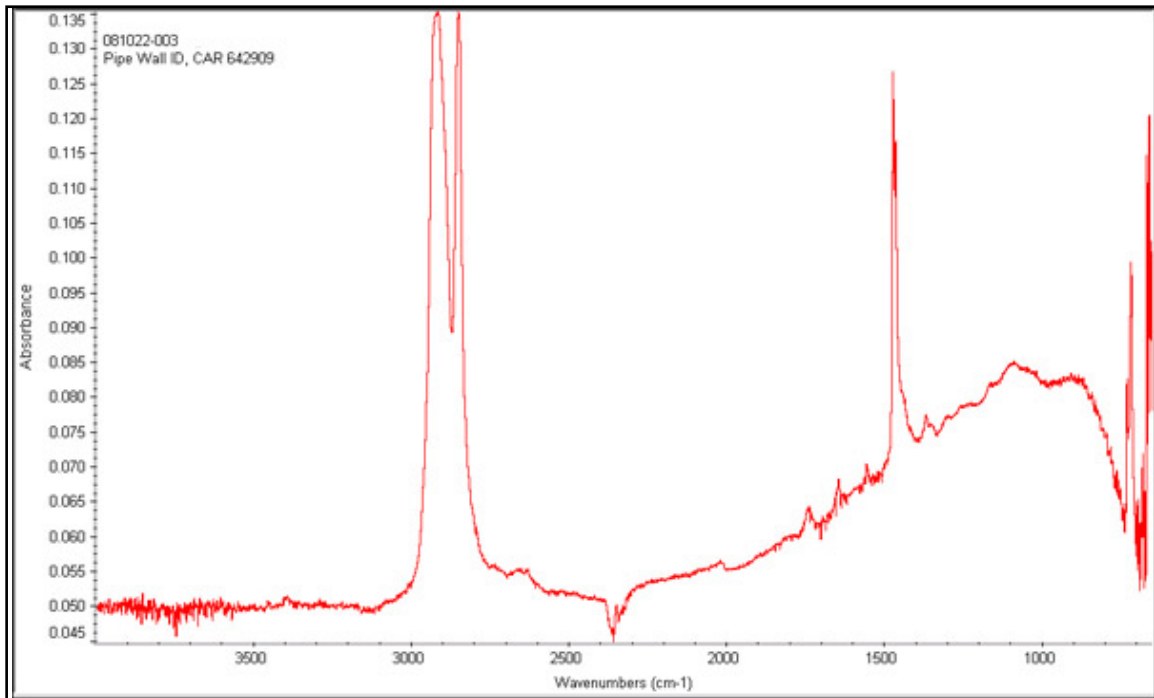


Figure 284. FT-IR - Inner Wall

Conclusions

Based on the tests performed, it was concluded that:

- 1) The saddle fusion surface tee exhibited a large area that was not properly fused. A good fusion would be stronger than the pipe wall itself and would result in tearing of the pipe wall before separation of the fusion.
- 2) The pipe segment was significantly deformed. The deformation was consistent with significantly high loads, possibly from digging equipment.
- 3) Examination of the fractured surfaces indicated ductile overload of the pipe wall material. No smaller fracture characteristics were observed which would have indicated a pre-existing crack prior to the ductile overload.
- 4) Excavation damage is the most likely the cause of failure.

Electrofusion Tee – #642430

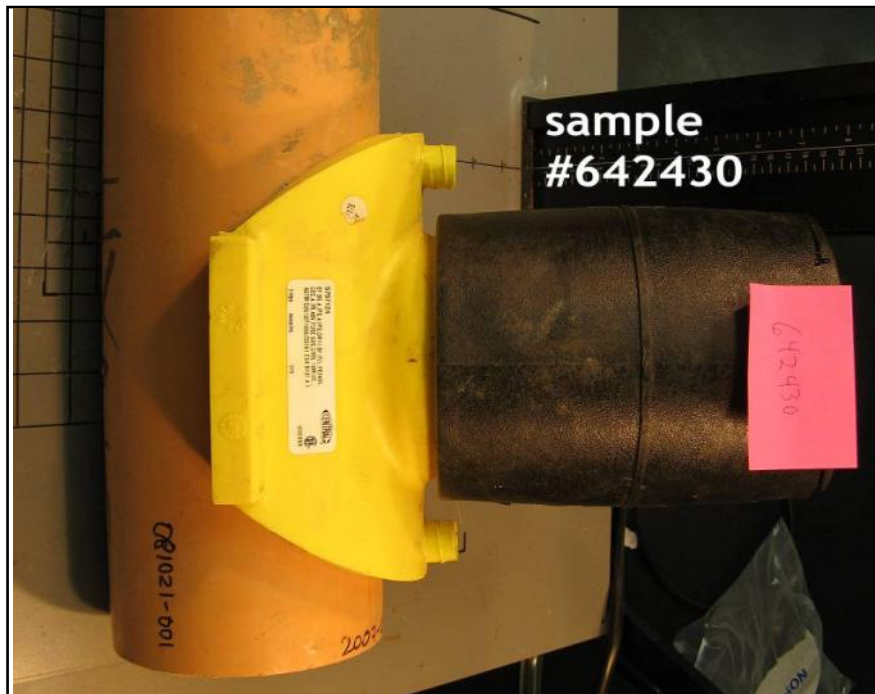


Figure 285. As Received Sample



Figure 286. Brittle Plastic Seepage from the Tee

Table 69. 4" x 4" Electrofusion Tee Background

Pipe Information	642430
Diameter	4"
SDR	11.5
Resin	PE 2306 or PE 2406
Manufacturer	DuPont
Design Pressure	60psig
Service Information	
Operating Pressure	~55 psig in summer / ~19 psig in winter
Service Temperature	60°F
Comments	NA
Timeline	
Placed in Service	November 1984
Installation Method	Direct Lay
Removed from Service	October 2007
Comments	Failed EF procedure
Environmental	
Soil Type	Rocky, sandy and silty
Evidence of 3rd Party Damage	No

Visual Examination

The pipe segment containing the electrofused saddle tee (Figure 285) was subjected to visual examination using the naked eye as well as high powered stereo optical microscopy. Results of this examination indicated a solidified area of material between the saddle fusion tee and the pipe that had seeped from the tee-pipe interface as seen in Figure 286.

Thermal Analysis

Specimens were prepared from the pipe section and companion electrofused tee as well as the seepage material and subjected to ASTM D3895. The resulting thermograms indicated oxidative induction times (OITs) of 27, 70, and 14 minutes for the pipe, tee, and seepage material respectively. See Figure 287, Figure 288, and Figure 289. The OIT of 27 minutes for the pipe material was considered on the low side of normal for an in service pipe. The OIT of 70 minutes for the tee material was considered normal. The OIT of 14 minutes for the seepage material was significantly low and suggested significant material degradation.

In addition, ASTM D3418 differential scanning calorimetry was performed on a set of specimens. The resulting thermograms (Figure 290, Figure 291, and Figure 292) indicated heats of fusion of 181J/g, 172 J/g, 232J/g for the pipe, tee, and seepage material respectively. No additional melting or exotherms were detected which would have suggested the presence of contamination. The significantly higher heat of fusion for the seepage material suggested material densification as the result of degradation and/or relatively slow cooling rate of the material.

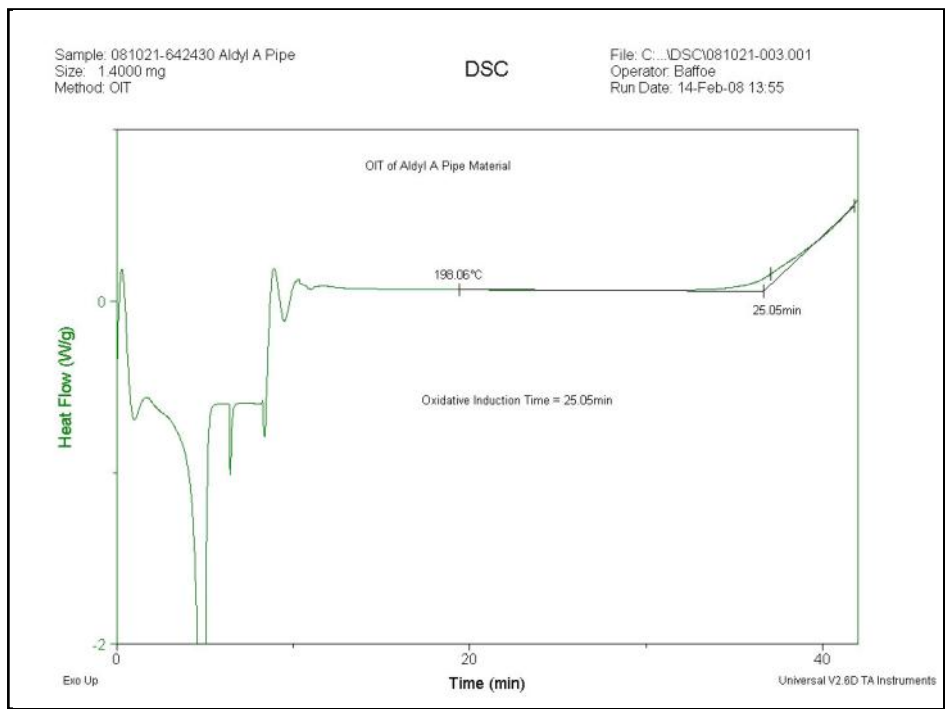


Figure 287. Oxidative Induction Time - Pipe

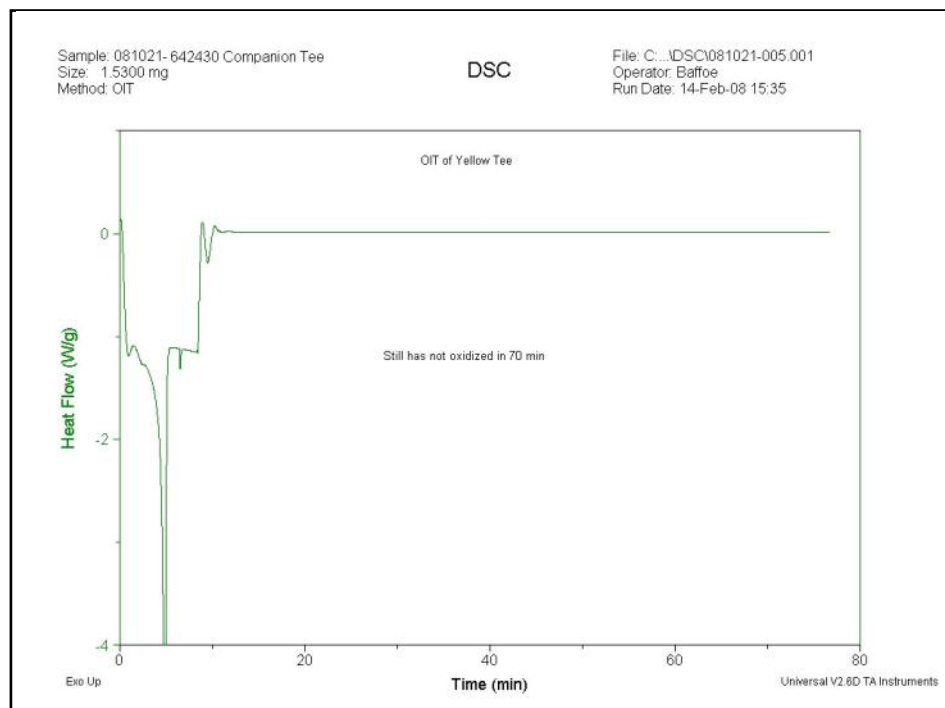


Figure 288. Oxidative Induction Time - Tee

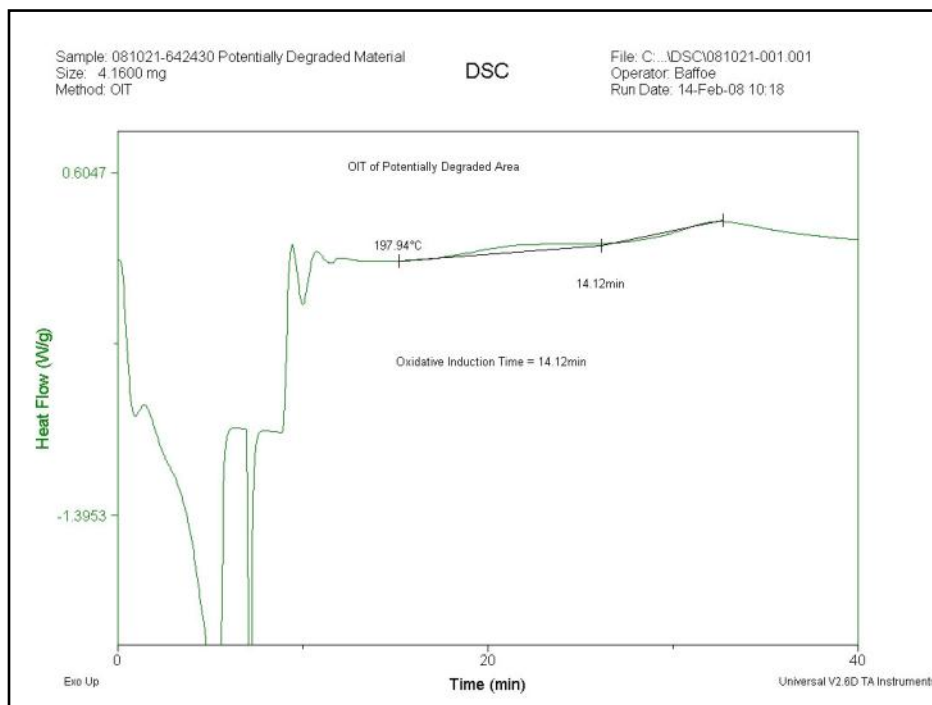


Figure 289. Oxidative Induction Time - Seepage Material

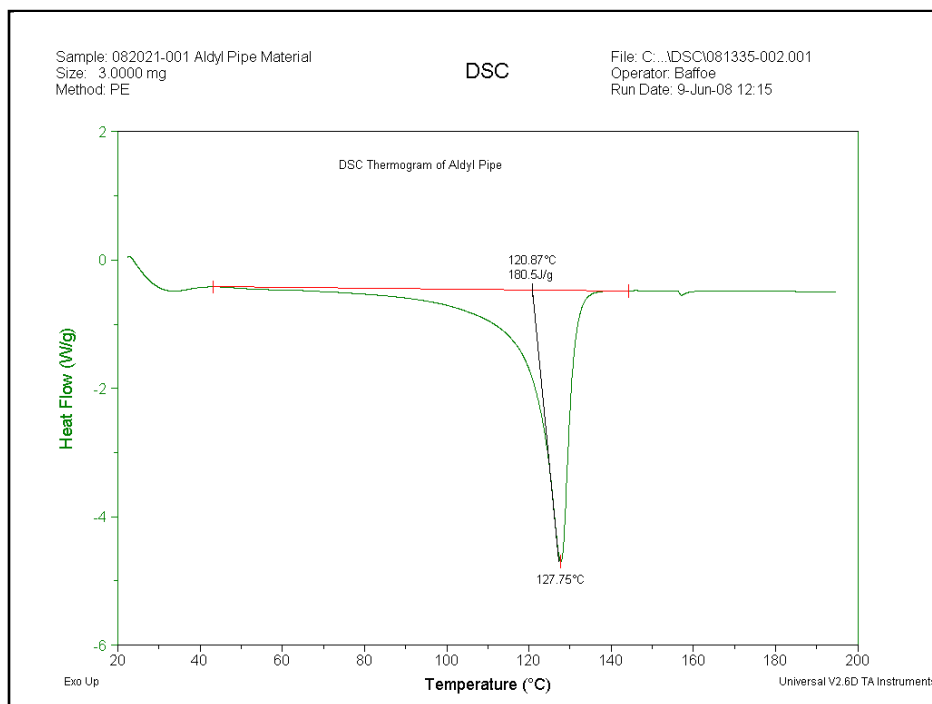


Figure 290. Differential Scanning Calorimetry – Pipe

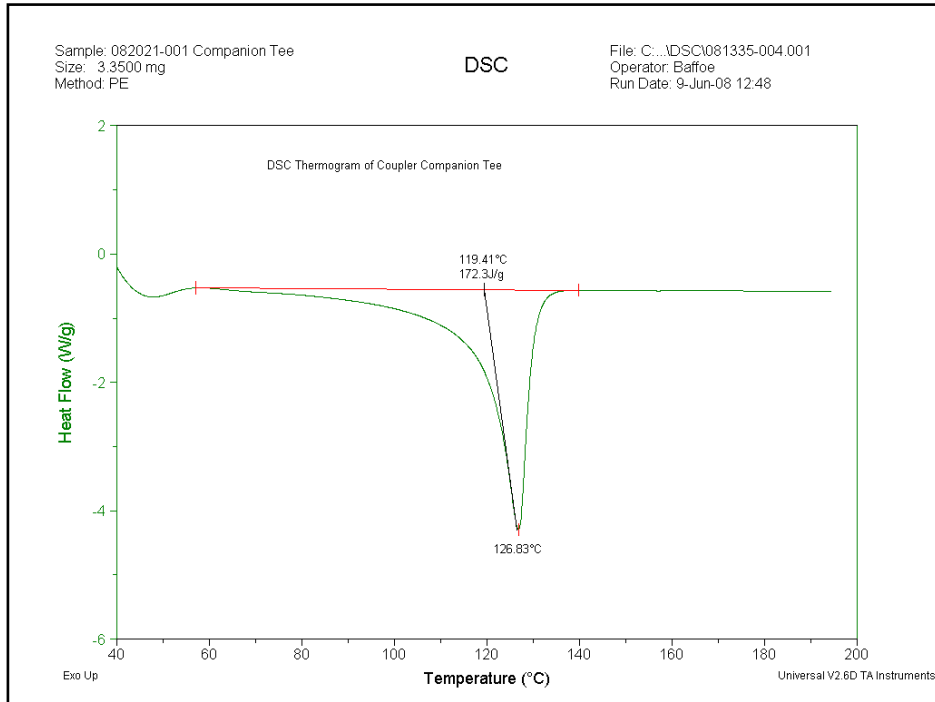


Figure 291. Differential Scanning Calorimetry – Tee

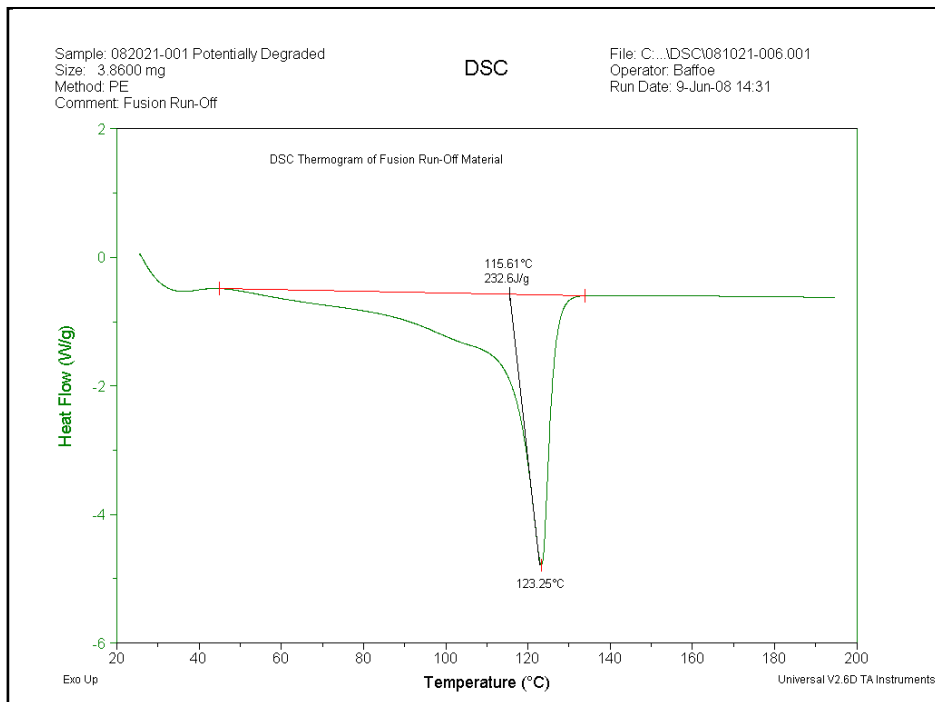


Figure 292. Differential Scanning Calorimetry – Seepage Material

Infrared Analysis

A comprehensive infrared analysis was performed to determine the condition of the pipe, tee, and seepage material and to detect the presence of any organic compounds not associated with the respective materials. The results did not indicate the presence of any foreign organic compounds in the material specimens. There were no detectable oxidation absorbencies in the pipe or tee material as shown in Figure 293 and Figure 294, respectively. An absorbance was detected at 1718cm^{-1} of the seepage material spectrum characteristic of a ketone compound consistent with oxidation products of polyethylene. The absorbance peak is noted in Figure 295. The peak height was measured and compared against the 1460cm^{-1} peak of the spectrum. The resulting quotient was 0.17 (carbonyl index, CI). Typical CI for non-aged samples is 0.01-0.05.

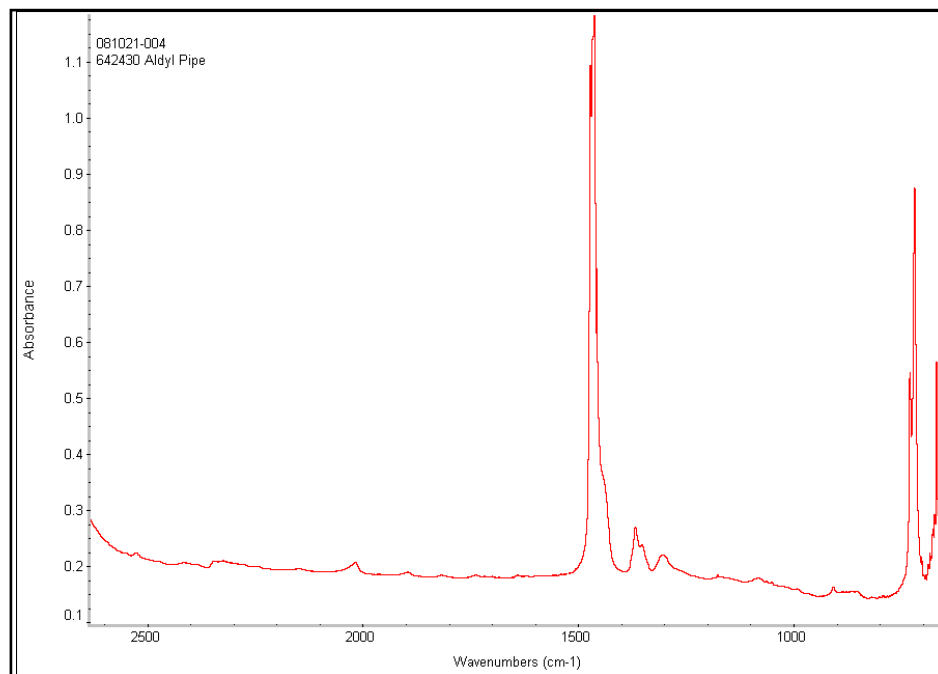


Figure 293. FT-IR Spectrum – Pipe Material

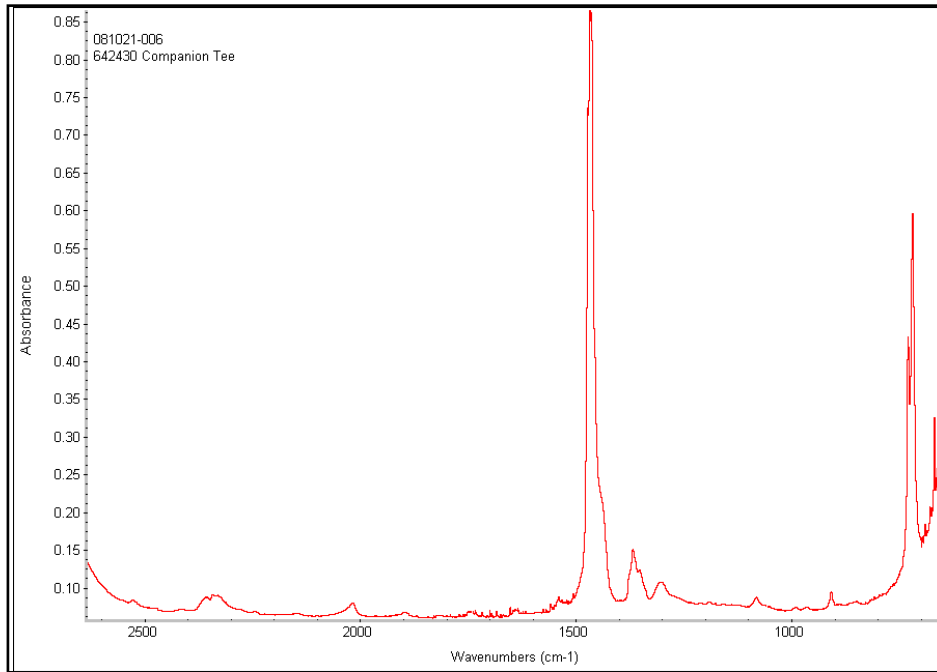


Figure 294. FT-IR Spectrum – Tee Material

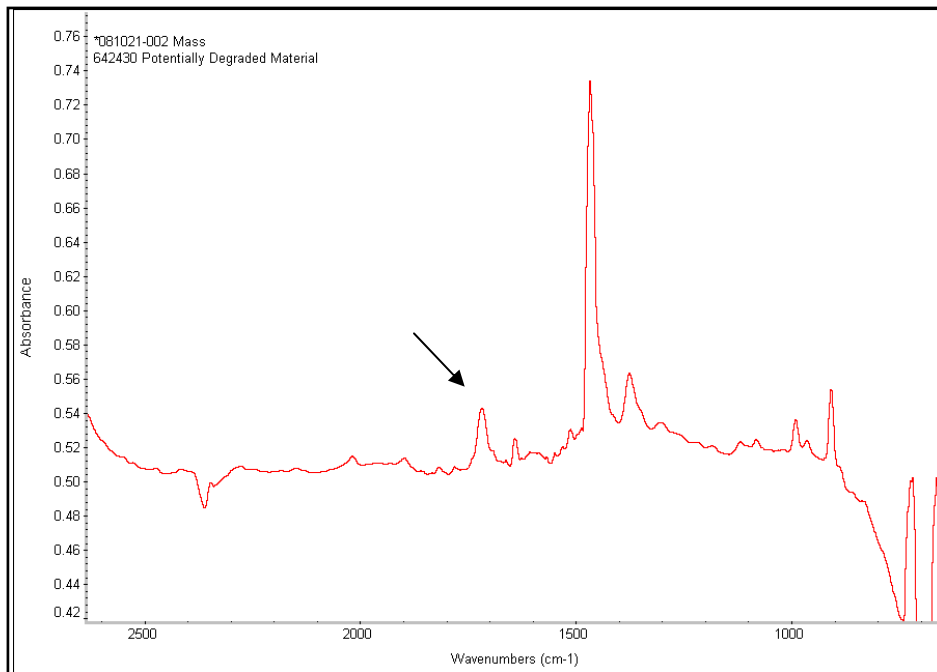


Figure 295. FT-IR Spectrum – Seepage Material: Note ketone absorbance

Conclusions

Based on the tests performed, it was concluded that:

- 1) The electrofusion saddle generated enough heat to degrade the pipe and tee material at the fusion interface. This degradation was detected by both DSC-OIT and FT-IR. The degradation was severe enough to cause a significant localized melt viscosity reduction or thinning of the material, facilitating the observed seepage. The effects of this degradation on the fusion longevity could not be determined and would require a more in depth study.
- 2) Some potential causes include equipment malfunction and/or electrofusion programming error(s).

Material / Quality

Compression Fitting - #17020701

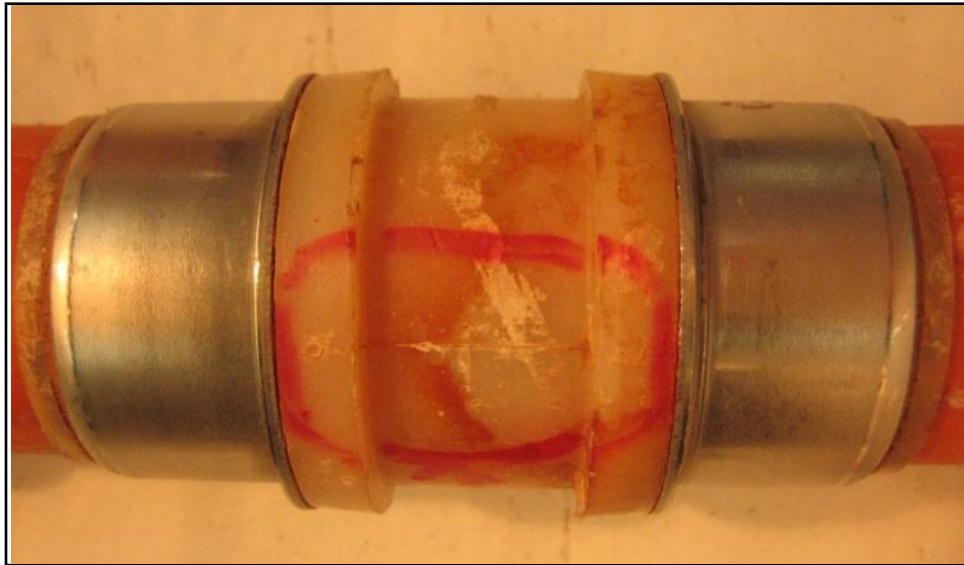


Figure 296. As Received Fitting

Table 70. 1 – ¼” Amp Fitting Background

Pipe Information	17020701
Color	Orange
Diameter	1 – ¼”
SDR	-
Resin	PE 2306
Manufacturer	-
Design Pressure	-
Service Information	
Operating Pressure	1-60 psig
Service Temperature	60°F
Comments	Pressure tested at 100 psig for 2 hours
Timeline	
Placed in Service	June 1977
Installation Method	Direct Burial; Bored
Removed from Service	January 2007
Comments	14” depth of cover
Environmental	
Soil Type	Clay
Evidence of 3rd Party Damage	No

Visual Examination

The fitting exhibited a slit failure at the mold seam/knit line as shown up close in Figure 297. All surfaces of the fitting show crazing.

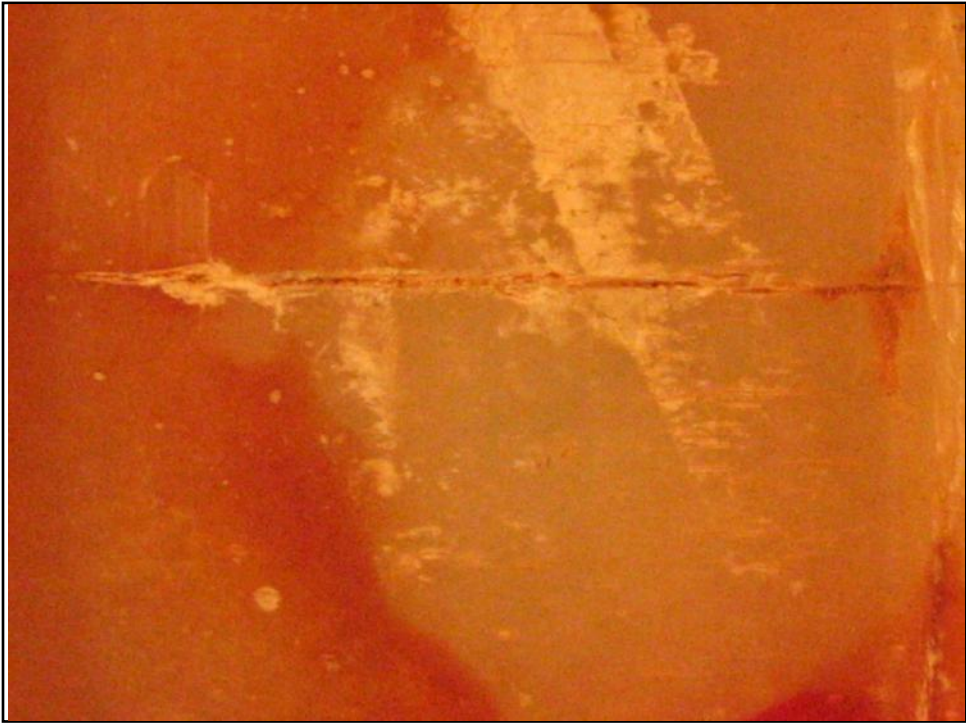


Figure 297. Slit at Knit Line

Procedural / Material

Mechanical Fitting - #41020409



Figure 298. As Received Sample

Table 71. 1 – ¼” x 1” Fitting Background

Pipe Information	41020409
Color	Yellow/White
Diameter	1 – ¼” x 1”
SDR	-
Resin	-
Manufacturer	AMP
Design Pressure	-
Service Information	
Operating Pressure	1-60 psig
Service Temperature	60°F
Comments	-
Timeline	
Placed in Service	-
Installation Method	-
Removed from Service	February 2004
Comments	-
Environmental	
Soil Type	Clay
Evidence of 3rd Party Damage	No

Visual Examination

The AMP fitting exhibited a partial pullout. The actual cause cannot be determined without dissecting the fitting.



Figure 299. Close up View of AMP Fitting

Tap Tee - #27020640

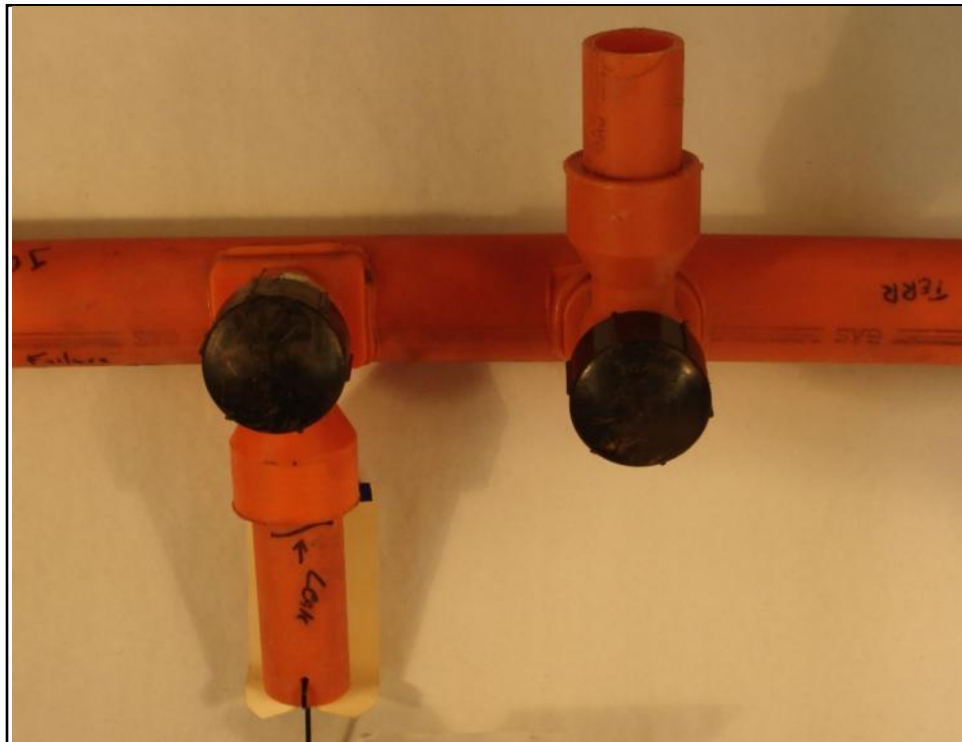


Figure 300. As Received Sample

Table 72. Tap Tee Background

Pipe Information	27020640
Color	Orange
Diameter	2" (main) 1 – ¼" (service)
SDR	11
Resin	PE 2306
Manufacturer	Driscopipe 6500 (main) Plexco (tee)
Design Pressure	-
Service Information	
Operating Pressure	1-60 psig
Service Temperature	60°F
Comments	Pressure tested at 100 psig for 15 minutes
Timeline	
Placed in Service	July 1983
Installation Method	-
Removed from Service	October 2006
Comments	48" depth of cover
Environmental	
Soil Type	Clay
Evidence of 3rd Party Damage	No

Visual Examination

A circumferential gap/crack was located between the ID of the socket and the OD of the pipe. The area containing the crack had less rollback than the remaining socket surface. Root cause determination would require sectioning of the fusion joint though poor workmanship is probable.



Figure 301. Socket Joint



Figure 302. Area Identified as Leaking

Bolt-on Tap Tee - #14020742



Figure 303. As Received Tee

Table 73. Bolt-on Tap Tee Background

Pipe Information	14020742
Color	Orange
Diameter	2"
SDR	11
Resin	PE 2306
Manufacturer	Driscopipe (pipe) Amp (fitting)
Design Pressure	-
Service Information	
Operating Pressure	1-60 psig
Service Temperature	60°F
Comments	Pressure tested at 100 psig for 15 minutes
Timeline	
Placed in Service	July 1979
Installation Method	-
Removed from Service	December 2007
Comments	24" depth of cover
Environmental	
Soil Type	Gravel
Evidence of 3rd Party Damage	No

Visual Examination

Leak markings were indicated on both sides of the fitting. The inner surface of the pipe did not show signs of cracking which would suggest that the leak was caused by the service tee seal. A definitive cause would require fitting disassembly.



Figure 304. Side View of Mechanical Tee

Root Cause Failure Results

Fifty-five samples were analyzed over the course of the project. Of these, 22 were classified as material failures, 24 as procedural failures/poor workmanship, 2 as quality control problems, 3 miscellaneous failures, and 4 were not classified. These results combined with a previous database account for 104 samples of which, 45 were classified as material failures, 36 as procedural failures, 12 as quality control problems, 7 miscellaneous failures, and 4 were not classified. These results have been placed into the following tables: Table 74. Material Failures, Table 75. Procedural Failures, Table 76. Quality Control Failures, Table 77. Miscellaneous Failures, and Table 78. Other Failures.

Table 74. Material Failures

Specimen Number	Description	Material	Pipe Size	Nature of Failure
F-83025	Bending/earth settlement	PE 2306	2" IPS SDR11	Circumferential slit
F-84014	Butt Joint	PE 2306	2" IPS SDR11	Joint misalignment
20020447	Cap	-	2" x ¾" Service Tee	Circumferential crack within threads
21020739	Cap	-	-	Circumferential crack within threads
22020733	Cap	-	-	Circumferential crack within threads
23020464	Cap	-	-	Circumferential crack within threads
24020499	Cap	-	-	Circumferential crack within threads
25020718	Cap	-	2"	Circumferential crack within threads
31020650	Cap	-	3 x 1- ¼" Tee	
49020718	Cap	-	-	Circumferential crack within threads
50020726	Cap	-	-	Circumferential crack within threads
26020806	External Loading	PE 2306	4"	Axial Slit
00590	Impingement	PE 2306	4"	Axial Slit
602533	Impingement	PE 2306	4"	Axial Slit
04020731	Impingement	PE 2306	2"	Axial Slit
F-82006	Insert Renewal	PE 2306	1-3/8" OD, .090" wall	Axial Slits
F-84005	Internal Pressure	PE 2306	½" IPS SDR11	Axial rupture in pipe wall
F-81001	Rock Impingement	PE 2306	2" IPS SDR11	Axial Slits
F-81002	Rock Impingement	PE 2306	2" IPS SDR11	Axial Slits
F-81003	Rock Impingement	PE 2306	2" IPS SDR11	Axial Slits
F-81004	Rock Impingement	PE 2306	2" IPS SDR11	Axial Slits
N/A	Rock Impingement	PE 2306	2" HDPE	Through-wall crack
F-84009	Saddle Joint	PE 2306	2" IPS x ½"	Circumferential crack through pipe
F-84011	Saddle Joint	PE 2306	3" IPS x ½"	Axial crack through pipe
F-85010	Saddle Joint	PE 2306	4" IPS SDR11	Circumferential crack through pipe

F-86002	Saddle Joint	PE 2306	2" IPS SDR11	Inadequate fusion
F-86003	Saddle Joint	HDPE	3" IPS SDR11	Circumferential slit failure at edge of saddle fusion
15020650	Service Tee Threads	PE 2306	2 x 1- 1/4" Tee	Circumferential crack within threads
29020510	Service Tee Threads	-	2"	Circumferential crack within threads
30020542	Socket Coupling	-	2"	Circumferential crack through coupling
35020485	Socket Coupling	PE 2306	1" Socket Fusion	Circumferential Slit
39020603	Socket Coupling	PE 2306	2" SDR 11	Circumferential Slit
F-81011	Socket Joint	PE 2306	2" IPS SDR11	Circumferential crack through pipe wall
F-84012	Socket Joint	PE 2306	1/2" CTS	Circumferential cracks through pipe
F-84018	Socket Joint	PE 2306	2" IPS SDR11	Socket misalignment
19020414	Socket Tee	PE 2306	4" 3 Way	Circumferential Slit
33020602	Socket Tee	PE 2306	2" SDR 11.5	Circumferential Slit
34020623	Socket Tee	PE 2306	2"	Circumferential Slit
F-81005	Squeeze-off	PE 2306	2" IPS SDR11	Axial Slits
F-83019	Squeeze-off	PE 2306	2" IPS SDR11	Axial Slits
F-83023	Squeeze-off	PE 2306	3" IPS SDR11	Axial Slits
678156	Tap Tee	PE 2306	2"	Circumferential Slit
F-84013	Tapping Tee	PE 2306	6" SDR17 w/ tapping tee	Axial stress
F-81006	Tapping Tee Cap	PE 2306	N/A	Circumferential crack within threads
F-84003	Tee	PE 2306	2" IPS SDR11 2x2x2 Tee	Circumferential crack through fitting

Table 75. Procedural Failures

Specimen Number	Description	Material	Pipe Size	Nature of Failures
07020714	Butt Fusion	PE 2306	4" SDR 11.5	Misalignment
08020601	Butt Fusion	PE 2306	3" SDR 11.5	Lack of bond
09020552	Butt Fusion	PE 2306	2"	Irregular Fusion Bead
10020477	Butt Fusion	PE 2306	4" SDR 11	Lack of bond
11020541	Butt Fusion	PE 2406	4" SDR 11.5	Foreign body
12020550	Butt Fusion	PE 2306	4"	Irregular Fusion Bead
13020706	Butt Fusion	PE 2306	4"	Lack of bond
45020551	Butt Fusion	PE 2406	6" SDR 11.5 (pipe) 11 (valve)	Lack of bond
060204100	Butt Fusion	PE 2306	2"	Overload
F-80004	Butt joint	PE 2306	4"IPS SDR11	Lack of bond
F-80005	Butt joint	PE 3406	6"IPS	Lack of bond
F-85001	Butt joint	PE 2306	3"IPS SDR11	Inadequate fusion
F-89005	Butt joint	PE 2406	2"IPS SDR11	Failed during plow-in
N/A	Butt joint	HDPE	8"SDR11 HDPE	Inadequate fusion
F-84008	Ell fitting	PE 2306	2"IPS SDR11	Lack of bond in 90° Ell due to misalignment
00632	High Volume Tapping Tee	-	4" x 2"	Inadequate fusion
N/A	Impact on a bolt	PE 3408	1 – ¼" DR11 HDPE	Through-wall crack
40020413	Multiple Fusion Joints	-	3" and 1 - ½"	Poor workmanship
F-90013	Saddle joint	PE 2306	2"IPS SDR11	Poor fusion practice
16020611	Socket Coupling	PE 2306	1" SDR 11	Poor workmanship
31020649	Socket Coupling	PE 2306	2 x 1- ¼" Tee	Poor workmanship
F-84006	Socket joint	PE 2306	4"IPS SDR11	Lack of bond in fusion joint
36020713	Socket Tee	-	1 – ¼"	Poor workmanship
47020565	Socket Tee	PE 2306, TR 418	4" SDR 11.5	Poor workmanship
02020717	Squeeze-off	PE 2306	4" SDR 11.5	Over squeezed
03020647	Squeeze-off	PE 2306	2"	Over squeezed
05020548	Squeeze-off	PE 2306	2" SDR 11	Misaligned in machine
28020502	Tap Tee	-	1 – ¼" x 1"	Poor workmanship
42020711	Tap Tee	PE 2306	2 x 3/4" SDR 11	Poor workmanship
43020555	Tap Tee	PE 2306	2" x ¾" IPS	Lack of bond
44020539	Tap Tee	PE 2306 (tee) TR 418 (pipe)	1 – ¼" x 1" (tee) 1 - ¼" SDR 10 (pipe)	Poor workmanship
32020543	Tap Tee - Socket Fusion	PE 2306	2" IPS x ½" CTS	Overload
F-86001	Tapping tee	PE 2306	2 x 5/8" tapping tee	Inadequate joint
N/A	Tapping tee	PE 2306	1 – ¼" w/ ½" tapping tee	Longitudinal cracks
18020538	Transition Fitting	TR 418	1 – ¼" SDR 11	Bending Stress
F-90005	Transition fitting	PE 2306	4"IPS SDR11.5	SCG driven by misalignment or external bending

Table 76. Quality Control Failures

Specimen Number	Description	Material	Pipe Size	Nature of Failures
642535	¾" Valve	PE 2306	¾"	Damaged O-ring
675540	3" Elbow	PE 2306	3"	Circumferential crack
N/A	Charred PE mass inside pipe		3" MDPE	Internal obstruction
F-82001	Dimensional tolerance	PE 2306	4" IPS SDR11.5	Out-of-roundness
F-80008	Melt irregularities	PE 3408	3" IPS SDR11	Irregular fusion bead
F-84001	Microscopic defects	PE 2306	5/8" CTS	Pinholes
N/A	Mold weld-line cracking	PE 2306	6" IPS Aldyl tee	Cracking through crotch
F-87003	Quality control: manufacturing defect	PE 3406	2" IPS SDR11	Inclusion extending through pipe wall
N/A	Saddle joint	PE 3408	4", 6"	Inadequate fusion
F-82004	Visible defects	PE 2306	2" IPS SDR11	Thin spots
062994-1	Weak lap due to polyamide film	PE 3408	4" SDR11	Axial crack
092394-1	Weak lap due to polyamide film	PE 3408	4" SDR11	Axial crack

Table 77. Miscellaneous Failures

Specimen Number	Description	Material	Pipe Size	Nature of Failures
01020436	Charred Pipe	PE 2406	¾"	Overheating of material
642909	Tap Tee	PE 2306	1 – ¼"	Lack of bond/Overload
642430	Electrofusion Tee	PE 2306	4" x 4"	Overheating of material
F-90010	Melted pipe	PE 2306	4" IPS	Overheated electric light cable laying on pipe
N/A	Pipe at compressor station	PE 3408	2"	Axial crack
N/A	Pipe at compressor station	PE 3408	2"	Axial crack
N/A	Plowed-in pipe	Philips 6500	2" SDR 11 MDPE	Circumferential crack

Table 78. Other Failures

Type of Failure	Specimen Number	Description	Material	Pipe Size	Nature of Failures
Material/Quality	17020701	Mechanical Coupling	PE 2306	1 – ¼"	Slit Failure
Procedural/Material	41020409	Mechanical Fitting	-	1 – ¼" x 1"	Pullout
Procedural/Material	27020640	Tap Tee	PE 2306	2 x ¼" Tee	Irregular Fusion Bead
Procedural/Material	14020742	Bolt-on Tap Tee	PE 2306	2" SDR 11	

Table 79. All Failures

Type of Failure	Specimen Number	Description	Mat'l	Pipe Size	Nature of Failure
Quality Control	642535	¾" Valve	PE 2306	¾"	Damaged O-ring
Quality Control	675540	3" Elbow	PE 2306	3"	Circumferential crack
Material	F-83025	Bending/earth settlement	PE 2306	2" IPS SDR11	Circumferential slit
Procedural/ Material	14020742	Bolt-on Tap Tee	PE 2306	2" SDR 11	
Procedural	07020714	Butt Fusion	PE 2306	4" SDR 11.5	Misalignment
Procedural	08020601	Butt Fusion	PE 2306	3" SDR 11.5	Lack of bond
Procedural	09020552	Butt Fusion	PE 2306	2"	Irregular Fusion Bead
Procedural	10020477	Butt Fusion	PE 2306	4" SDR 11	Lack of bond
Procedural	11020541	Butt Fusion	PE 2406	4" SDR 11.5	Foreign body
Procedural	12020550	Butt Fusion	PE 2306	4"	Irregular Fusion Bead
Procedural	13020706	Butt Fusion	PE 2306	4"	Lack of bond
Procedural	45020551	Butt Fusion	PE 2406	6" SDR 11.5 (pipe) 11 (valve)	Lack of bond
Procedural	060204100	Butt Fusion	PE 2306	2"	Overload
Material	F-84014	Butt Joint	PE 2306	2" IPS SDR11	Joint misalignment
Procedural	F-80004	Butt joint	PE 2306	4"IPS SDR11	Lack of bond
Procedural	F-80005	Butt joint	PE 3406	6"IPS	Lack of bond
Procedural	F-85001	Butt joint	PE 2306	3"IPS SDR11	Inadequate fusion
Procedural	F-89005	Butt joint	PE 2406	2"IPS SDR11	Failed during plow-in
Procedural	N/A	Butt joint	HDPE	8"SDR11 HDPE	Inadequate fusion
Material	20020447	Cap	-	2" x ¾" Service Tee	Circumferential crack within threads
Material	21020739	Cap	-	-	Circumferential crack within threads
Material	22020733	Cap	-	-	Circumferential crack within threads
Material	23020464	Cap	-	-	Circumferential crack within threads
Material	24020499	Cap	-	-	Circumferential crack within threads
Material	25020718	Cap	-	2"	Circumferential crack within threads
Material	31020650	Cap	-	3 x 1- ¼" Tee	
Material	49020718	Cap	-	-	Circumferential crack within threads
Material	50020726	Cap	-	-	Circumferential crack within threads
Quality Control	N/A	Charred PE mass inside pipe		3" MDPE	Internal obstruction
Miscellaneous	01020436	Charred Pipe	PE 2406	¾"	Overheating of material
Quality Control	F-82001	Dimensional tolerance	PE 2306	4" IPS SDR11.5	Out-of-roundness

Miscellaneous	642430	Electrofusion Tee	PE 2306	4" x 4"	Overheating of material
Procedural	F-84008	EII fitting	PE 2306	2" IPS SDR11	Lack of bond in 90° EII due to misalignment
Material	26020806	External Loading	PE 2306	4"	Axial Slit
Procedural	00632	High Volume Tapping Tee	-	4" x 2"	Inadequate fusion
Procedural	N/A	Impact on a bolt	PE 3408	1 - ¼" DR11 HDPE	Through-wall crack
Material	00590	Impingement	PE 2306	4"	Axial Slit
Material	602533	Impingement	PE 2306	4"	Axial Slit
Material	04020731	Impingement	PE 2306	2"	Axial Slit
Material	F-82006	Insert Renewal	PE 2306	1-3/8" OD, .090" wall	Axial Slits
Material	F-84005	Internal Pressure	PE 2306	½" IPS SDR11	Axial rupture in pipe wall
Material/ Quality	17020701	Mechanical Coupling	PE 2306	1 - ¼"	Slit Failure
Procedural/Ma terial	41020409	Mechanical Fitting		1 - ¼" x 1"	Pullout
Quality Control	F-80008	Melt irregularities	PE 3408	3" IPS SDR11	Irregular fusion bead
Miscellaneous	F-90010	Melted pipe	PE 2306	4" IPS	Overheated electric light cable laying on pipe
Quality Control	F-84001	Microscopic defects	PE 2306	5/8" CTS	Pinholes
Quality Control	N/A	Mold weld-line cracking	PE 2306	6" IPS Aldyl tee	Cracking through crotch
Procedural	40020413	Multiple Fusion Joints	-	3" and 1 - ½"	Poor workmanship
Miscellaneous	N/A	Pipe at compressor station	PE 3408	2"	Axial crack
Miscellaneous	N/A	Pipe at compressor station	PE 3408	2"	Axial crack
Miscellaneous	N/A	Plowed-in pipe	Philips 6500	2" SDR 11 MDPE	Circumferential crack
Quality Control	F-87003	Quality control: manufacturing defect	PE 3406	2" IPS SDR11	Inclusion extending through pipe wall
Material	F-81001	Rock Impingement	PE 2306	2" IPS SDR11	Axial Slits
Material	F-81002	Rock Impingement	PE 2306	2" IPS SDR11	Axial Slits
Material	F-81003	Rock Impingement	PE 2306	2" IPS SDR11	Axial Slits
Material	F-81004	Rock Impingement	PE 2306	2" IPS SDR11	Axial Slits
Material	N/A	Rock Impingement	PE 2306	2" HDPE	Through-wall crack
Material	F-84009	Saddle Joint	PE 2306	2" IPS x ½"	Circumferential crack

					through pipe
Material	F-84011	Saddle Joint	PE 2306	3" IPS x ½"	Axial crack through pipe
Material	F-85010	Saddle Joint	PE 2306	4" IPS SDR11	Circumferential crack through pipe
Material	F-86002	Saddle Joint	PE 2306	2" IPS SDR11	Inadequate fusion
Material	F-86003	Saddle Joint	HDPE	3" IPS SDR11	Circumferential slit failure at edge of saddle fusion
Procedural	F-90013	Saddle joint	PE 2306	2" IPS SDR11	Poor fusion practice
Quality Control	N/A	Saddle joint	PE 3408	4", 6"	Inadequate fusion
Material	15020650	Service Tee Threads	PE 2306	2 x 1- ¼" Tee	Circumferential crack within threads
Material	29020510	Service Tee Threads	-	2"	Circumferential crack within threads
Material	30020542	Socket Coupling	-	2"	Circumferential crack through coupling
Material	35020485	Socket Coupling	PE 2306	1" Socket Fusion	Circumferential Slit
Material	39020603	Socket Coupling	PE 2306	2" SDR 11	Circumferential Slit
Procedural	16020611	Socket Coupling	PE 2306	1" SDR 11	Poor workmanship
Procedural	31020649	Socket Coupling	PE 2306	2 x 1- ¼" Tee	Poor workmanship
Material	F-81011	Socket Joint	PE 2306	2" IPS SDR11	Circumferential crack through pipe wall
Material	F-84012	Socket Joint	PE 2306	½" CTS	Circumferential cracks through pipe
Material	F-84018	Socket Joint	PE 2306	2" IPS SDR11	Socket misalignment
Procedural	F-84006	Socket joint	PE 2306	4" IPS SDR11	Lack of bond in fusion joint
Material	19020414	Socket Tee	PE 2306	4" 3 Way	Circumferential Slit
Material	33020602	Socket Tee	PE 2306	2" SDR 11.5	Circumferential Slit
Material	34020623	Socket Tee	PE 2306	2"	Circumferential Slit
Procedural	36020713	Socket Tee	-	1 – ¼"	Poor workmanship
Procedural	47020565	Socket Tee	PE 2306, TR 418	4" SDR 11.5	Poor workmanship
Material	F-81005	Squeeze-off	PE 2306	2" IPS SDR11	Axial Slits
Material	F-83019	Squeeze-off	PE 2306	2" IPS SDR11	Axial Slits
Material	F-83023	Squeeze-off	PE 2306	3" IPS SDR11	Axial Slits
Procedural	02020717	Squeeze-off	PE 2306	4" SDR 11.5	Over squeezed
Procedural	03020647	Squeeze-off	PE 2306	2"	Over squeezed
Procedural	05020548	Squeeze-off	PE 2306	2" SDR 11	Misaligned in machine
Material	678156	Tap Tee	PE 2306	2"	Circumferential Slit
Miscellaneous	642909	Tap Tee	PE 2306	1 – ¼"	Lack of bond/Overload
Procedural	28020502	Tap Tee	-	1 – ¼" x 1"	Poor workmanship
Procedural	42020711	Tap Tee	PE 2306	2 x 3/4" SDR 11	Poor workmanship
Procedural	43020555	Tap Tee	PE 2306	2" x ¾" IPS	Lack of bond
Procedural	44020539	Tap Tee	PE 2306 (tee) TR 418 (pipe)	1 – ¼" x 1" (tee) 1 - ¼" SDR 10 (pipe)	Poor workmanship

Procedural/Material	27020640	Tap Tee	PE 2306	2 x ¼" Tee	Irregular Fusion Bead
Procedural	32020543	Tap Tee - Socket Fusion	PE 2306	2" IPS x ½" CTS	Overload
Material	F-84013	Tapping Tee	PE 2306	6" SDR17 w/ tapping tee	Axial stress
Procedural	F-86001	Tapping tee	PE 2306	2 x 5/8" tapping tee	Inadequate joint
Procedural	N/A	Tapping tee	PE 2306	1 – ¼" w/ ½" tapping tee	Longitudinal cracks
Material	F-81006	Tapping Tee Cap	PE 2306	N/A	Circumferential crack within threads
Material	F-84003	Tee	PE 2306	2" IPS SDR11 2x2x2 Tee	Circumferential crack through fitting
Procedural	18020538	Transition Fitting	TR 418	1 – ¼" SDR 11	Bending Stress
Procedural	F-90005	Transition fitting	PE 2306	4"IPS SDR11.5	SCG driven by misalignment or external bending
Quality Control	F-82004	Visible defects	PE 2306	2" IPS SDR11	Thin spots
Quality Control	062994-1	Weak lap due to polyamide film	PE 3408	4" SDR11	Axial crack
Quality Control	092394-1	Weak lap due to polyamide film	PE 3408	4" SDR11	Axial crack

The samples received by GTI under this project were also incorporated with a previous database of received field failures. They are included in Table 80. This group of failures shows the largest number of defects occurred at joints, particularly at saddles, sockets, butt, and tee joints.

Table 80. Received Failures

Failure Type	Number
Material Failures	
Pipe	
Rock Impingement	9
Squeeze-off	8
Insert Renewal	1
Bending/Settlement	3
Internal Pressure	1
Joints	
End Caps	8
Tapping Tee Caps	9
Tees and Ells	21
Sockets	74
Saddles	118
Fusion Failures in Joints	
Butt Fusion	29
Socket Fusion	7
Saddle Fusion	5
Quality Control Problems	6
Third Party	14
Other	8
Total	321

Characterizing the Resistance of PE to RCP through S-4 Testing

It is estimated that about 30% of all the new PE pipe installations are 4-inch and larger in size. Many gas distribution companies now routinely install PE pipes in 12- and 16-inch diameter sizes. Also, many of the newer high-density (HD) PE pipelines including those extruded from Bi-Modal materials are being subjected to pressures greater than 100psig.

RCP is a failure mode that is in complete contrast to SCG. RCP is characterized by a fast moving large-scale crack that can travel at high speeds over long spans of a PE pipeline. These types of failures are rare but reports of RCP field failure do exist. A PE gas system had a RCP failure in which a pipe crack propagated 700 meters before arresting. Other less severe RCP incidents have occurred in gas pipelines.(Vanspeybroeck, 2002) RCP failures may be very severe events due to the large volumes of gas that can be quickly released. It is critical that the phenomenon is well understood and pipelines are designed to minimize the susceptibility to RCP failures.

Rapid Crack Propagation

A RCP failure mode consists of two phases. First, there is an initiation phase where a critical crack is formed; this can be a pre-existing notch or generated under dynamic conditions that involve loads impacting the pipe at high speeds.(Kanninen, O'Donoghue, Cardinal, Green, Curr, & Williams, 1989) Investigations have shown that a pre-existing notch or crack is considered critical if it extends about 90% through the pipe wall.(Krishnaswamy, Maxey, Leis, & Mamoun, 1986) If the pipeline is free of any pre-existing critical defects or notches, then crack initiation may be induced by a sharp-edged object, such as a blade, that impacts the pipe line at a very high speed. In this case, the sharp-edged object or source impacting the pipe creates a notch in the pipe and causes a large amount of elastic strain energy to be stored in the pipe material and possibly released. Observations of numerous experiments have shown that a sharp-edged object that impacts a PE pipe causes an RCP critical notch when the notch depth is in the range of about 50 to 70% of the wall thickness and the notch axial length is about one pipe diameter.

The second phase involves the release of the stored elastic energy to sustain crack propagation. This phase is characterized by a steady state crack growth at speeds in excess of 200 m/s over a very long pipe span. To sustain RCP, the energy that drives the crack, denoted as (J), needs to be greater than the Dynamic Toughness of the PE pipe material, denoted as (J_c). Equation [9] mathematically expresses the necessary condition for the dynamic propagation of a crack.(Leis, 1989)

$$J > J_c \quad (9)$$

Where:

J = driving energy

J_c = dynamic toughness

If the driving energy (J) decreases or is less than J_c , the crack will stop propagating, i.e. the crack will arrest. The energy or force that drives the growth of a dynamic RCP crack, denoted as J , is given in equation [10].

$$J = \frac{11.25p^{2.5}D\left(\frac{D}{t-1}\right)^2}{E_D^{3/2}} \quad (10)$$

Where:

J = driving energy

P = pipe internal pressure

D = diameter

E_D = dynamic modulus

The expression for J is developed using numerical modeling techniques and principles of fracture mechanics. E_D is a materials property that is dependent on temperature. The dynamic toughness of a PE pipe material (E_D) decreases substantially and rapidly with decreasing temperatures. From equation [2], it should be noted that the RCP driving force is directly proportional to the pressure raised to a power of 2.5, the pipe diameter, and SDR. The energy that drives the growth of a dynamic RCP crack J is inversely related to the dynamic modulus. Thus, the RCP driving force increases substantially with increasing pressure, SDR and pipe diameter. The RCP driving force J is inversely proportional to the dynamic modulus.

Figure 305 depicts a schematic illustration of a RCP event in which the crack is traveling axially along the pipe. Typically, a RCP crack propagates in a sinusoidal pattern along the axial direction of the PE pipe. In some cases, the RCP crack bifurcates or rings around the pipe. (Leis, 1989)

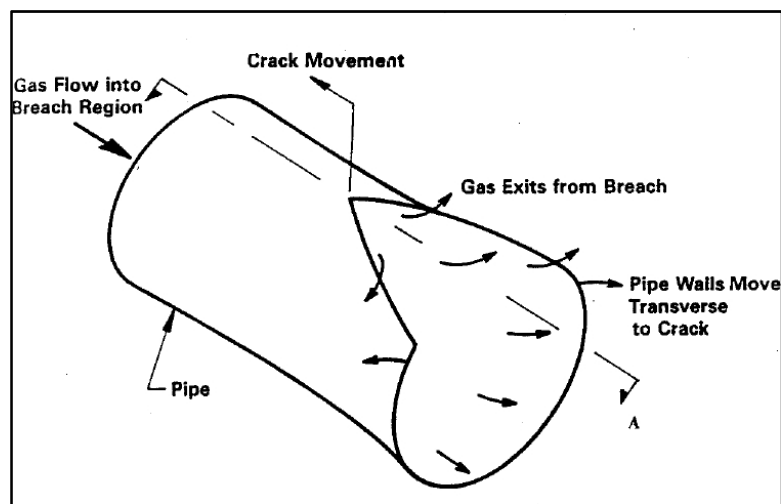


Figure 305: Schematic of Growing RCP Crack. (Kanninen, Et Al., 1997)

Equation [10] shows that a primary driving force for RCP is the internal pressure of the pipe. However, an initiated and growing crack allows for gas to rapidly escape the pipe leading to a pressure drop as shown in Figure 305. This sets a balance between how quickly the crack grows (crack propagation) and how quickly the internal pressure escapes from the pipe (decompression speed). The entire length of pipe in the field is pressurized; as the gas escapes through the crack it is replaced from the gas contained in the remaining section of the pipe. If the crack speed and decompression speed are matched, the pressure drop at the crack tip will remain static as there is insufficient time for it to drop further. In this situation, the crack can propagate over very long pipe spans. If the pipe decompression is sufficiently fast, the pressure driving the RCP crack will quickly dissipate thus causing the driving force to be less than J_c , causing crack arrest.

From equation [10] some general relations that lead to a greater chance of RCP are clear:

- Increasing pressure substantially increases RCP susceptibility
- Increasing pipe diameter increases RCP susceptibility
- Increasing SDR increases RCP susceptibility
- Decreasing dynamic modulus increases RCP susceptibility

In summary,

- If $J > J_c$ Then the RCP crack propagates.
- If $J < J_c$ Then the crack arrest occurs.

S-4 Background

Appropriate testing methodologies were developed to better understand the conditions that lead to RCP and what prevents it. Tests of all types were considered but due to the pipe size requirement in RCP, most testing methods focus on using full or longer-sized pipes for experimentation. GTI conducted numerous RCP full-scale field tests on different types of PE pipes materials and sizes. These full-scale field tests were performed on pipes having a length greater than 50 feet. To correlate the results of the full-scale field tests with a small-scale bench-top test, GTI conducted several tests using a modified version of the Charpy impact test. (Brown, Lu, & Mamoun, 2000) However, these correlations were inconclusive.

Test Requirements

A test method to evaluate a plastic pipe's resistance to RCP needs to fit a criteria (Wolters & Ketel, 1983):

- A sharp crack needs to be initiated at a high speed (greater than decompression speeds);
- Crack propagation and crack arrest need to be differentiated; and
- Sufficient gas pressure/supply to prevent too quick of a decompression of the pipe test sample.

Along with these requirements, any test would need to produce consistent and reproducible results that can be correlated to field conditions. This would help determine design and operating factors that the plastic pipeline industry can implement and use. Currently, to characterize the resistance of PE pipe materials to RCP, two tests are typically conducted. These are the Full-Scale field RCP tests and the laboratory small-scale steady-state (S-4) test.

Full-Scale RCP Field Tests

Full scale RCP testing mimics the conditions conducive to a RCP event that may occur in an installed PE gas pipe. In a full-scale field test, the length of the PE pipe test sample is typically in the range of 70 to 100 feet. The test temperature and pressure of the pipe are controlled and monitored throughout the test. A sharp crack is then initiated in a section of the pipe through either a pre-notched slit or a fast moving blade. This crack then grows through the pipe depending on the various test conditions. In many GTI full-scale field tests, the crack speed is monitored and recorded using timing wires; this information was needed to develop small-scale laboratory tests that could be accurately correlated with full-scale field tests.

Figure 306 is a photographic view of one of GTI full-scale tests that were conducted on a 100-ft long pipe sample. This view shows the possible catastrophic failure that can occur during a RCP event and also illustrates the RCP sinusoidal crack that propagated axially along the pipe length.

The full-scale RCP field tests involve substantial engineering design and planning costs. This cost makes the full-scale test less than ideal for parametric evaluations of the RCP phenomenon in plastic pipe materials.



Figure 306: Full Scale RCP Testing Result (Kanninen Et Al., 1997)

S-4 Testing

Due to the difficulty and costs involved in conducting experiments on full-scale pipe specimens, a small more compact version of the test was developed for laboratory evaluations: the small-scale steady-state (S-4) test.

The small-scale steady-state (S-4) test is conducted on short lengths of PE pipes. In an S-4 test, the length of the pipe test sample is between seven (7) and nine (9) times the pipe diameter. The pipe test sample is cooled to a uniform constant temperature, subjected to a constant internal pressure, and then impacted at one end with a sharp blade to produce an axial crack in the PE pipe test specimen. The S-4 test is performed in accordance with ISO 13477 test specification.

The objective of the S-4 test is to experimentally determine either the:

- Critical pressure $p_{c,S4}$ corresponding to a given constant temperature determined from a series of initiation tests; or
- Critical temperature $T_{c,S4}$ corresponding to a constant pressure of 5 bars (1 bar = 14.7psig).

In the S-4 test, the pipe test sample is conditioned and cooled to a specified test temperature determined from a series of initiation tests. Then, while the test specimen is at that temperature, the pipe is pressurized and impacted with a sharp-edge blade. A rapidly running crack is initiated in the pipe by the fast moving steel blade. The resultant crack can be measured, characterized, and categorized as either propagation or arrest. A key feature of the S-4 test apparatus is that internal baffles prevent rapid decompression of the sample. This feature allows for testing of a small pipe sections and at lower pressures than required for full scale testing. (Kanninen, Kuhlman, & Mamoun, Rupture-Prevention Design Procedure to Ensure PE Gas Pipe System Performance, 1993) A systematic series of tests can be carried out by varying a single condition at a time. This assists in performing extensive parametric evaluation of the important variables effecting RCP.

Using the S-4 test methodology, the critical temperature or critical pressure can be determined for any pipe material and size.

ISO Specification (ISO 13477)

ISO Specification 13477: Thermoplastics Pipes for the Conveyance of Fluids – Determination of Resistance to Rapid Crack Propagation (RCP) – Small-Scale Steady-State Test (S4 Test) describes in detail the physical dimensions of many components of an S-4 testing apparatus. The details and specifications on sample preparation and testing conditions are described in the ISO specification. The sections that follow briefly describe the testing procedure contained within the ISO 13477 specification; for full details please reference the specification directly.

The S-4 test procedure involves performing first the so-called initiation tests. The initiation tests are then followed by conducting a series of the S-4 full-scale arrest and propagation tests to determine either the critical pressure or the critical temperature for a PE pipe test material.

Initiation Tests

Before performing a full S-4 tests, initiation tests must be carried out. The initiation tests are to verify whether or not a fast moving sharp crack can be generated by the striking blade in a given pipe material and size. The test sections are cooled to 32 °F and struck with no internal pressure applied. A successful initiation consists of a crack that is at least 0.7 pipe diameters in length. In this way the energy needed to initiate the fast moving crack is determined for a given PE pipe material. Figure 307 shows a successful crack initiation test, in which the crack reached a length greater than 0.7 pipe diameters. If the initiation conditions are not met the blade speed can be modified but must remain within 5 m/s of 15 m/s. If initiation is not induced at 32°F, then the test temperature is reduced until the required crack initiation conditions are met. Alternatively, an internal notch can be introduced to facilitate crack initiation. (ISO 13477)



Figure 307: S-4 Crack Initiation Result

Critical Pressure Testing

In the standard S-4 procedure, the pipe test specimen is cooled to the required initiation temperature. Then, the pipe specimen is pressurized with a compressible fluid, usually air. The pipe is then struck with a sharp-edge blade to initiate a fast moving crack. To evaluate a pipe's critical pressure, a series of S-4 tests are performed while systematically varying the internal pipe pressure. This test method is incorporated into the ISO 13477 specification with the condition that the test temperature is held constant at a temperature of 32 °F. The crack that results is considered "propagation" if its length exceeds 4.7 times the pipe diameters. If a crack is initiated, by growing more than 0.7 pipe diameters and fails to propagate a length of 4.7 times the pipe diameters then it is considered an "arrest."(ISO 13477) After performing a series of S-4 tests at different pressures, the highest pressure at which crack arrest occurs is considered the critical pressure for that specific pipe material and size.

Correlation of the S-4 Critical Pressure to the Full-Scale Field Test

Several full-scale RCP field tests and S-4 were conducted on different PE pipe materials manufactured in Europe. On the basis of these tests, researchers developed an empirical correlation between the S-4 critical pressure and the pressure that caused RCP failures in the full-scale field tests. This correlation was developed by testing resins and pipe materials with substantial compounding and manufacturing differences than United States produced PE pipe materials. These differences may result in pipe materials having different RCP resistant properties. Therefore this correlation may not be valid for US gas grade pipe materials and

should serve as a guide. The empirically found correlation is given in Equation [11], (ISO 13477):

$$p_{c,FS} = 3.6(p_{c,S4} + p_{atm}) - p_{atm} \quad (11)$$

Where:

$p_{c,FS}$ = full scale critical pressure

$p_{c,S4}$ = S-4 critical pressure

p_{atm} = atmospheric pressure

In this Equation, it should be noted that $1 p_{atm} = 1 \text{ Bar} = 14.7 \text{ psig}$.

Critical Temperature Testing

To determine the critical temperature of a PE pipe material using the S-4 test, a series of tests are performed on a given PE pipe material of a specific size. The S-4 tests are conducted on pipe test specimens subjected to a constant pressure of 5 bars or 72.5 psi. In this series of tests, the pipe temperature is systematically varied until a temperature is determined above which crack arrest occurs. The coldest/lowest test temperature that results in a crack arrest is designated as the critical temperature. Above this temperature, no amount of pressure will sustain RCP. (Leevers, Venizelos, & Morgan, 1993) In some pipe materials it may be impossible to determine the critical temperature following the S-4 test procedure. (ISO 13477)

GTI S-4 Test Apparatus

The requirements of an S-4 test apparatus are described in detail in ISO 13477:2008(E). What follows is the description of GTI's implementation of the ISO specification. Figure 308 depicts the major components of the S-4 test apparatus:

1. Pipe Assembly: Metal Shaft, Anvil, and Baffles
2. External Containment Cage and Frame
3. Striking Blade Assembly.

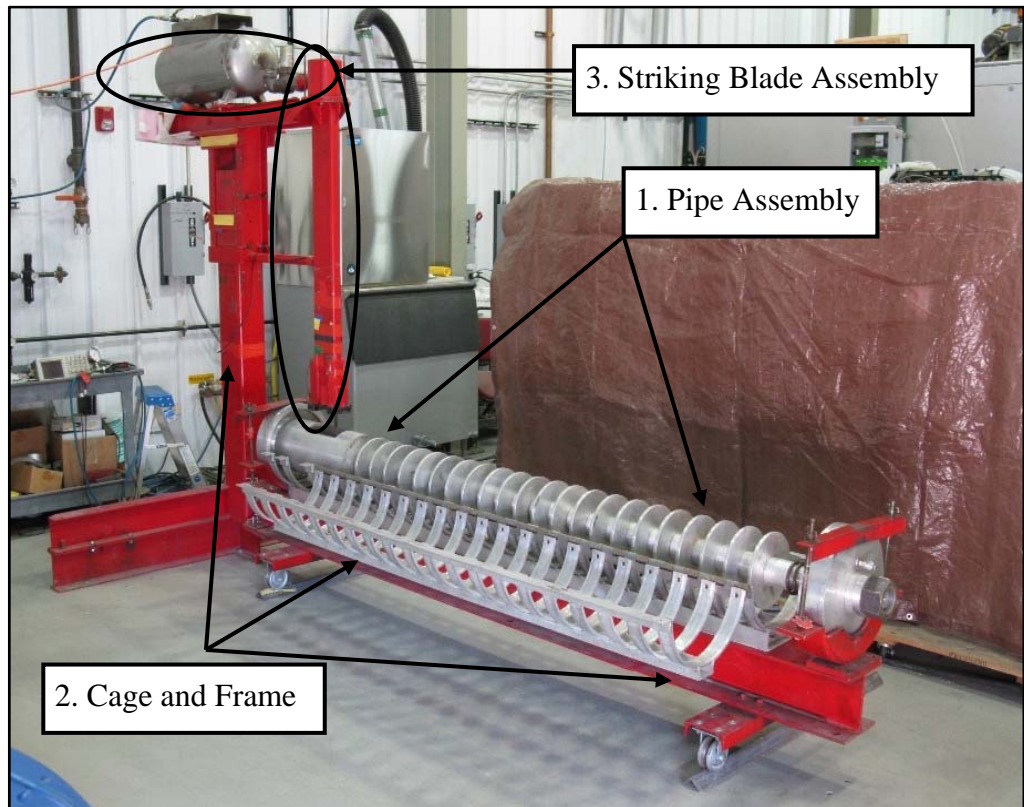


Figure 308: GTI's S-4 Testing Apparatus

Shaft, Anvil, Baffles and Pipe Assembly

The pipe assembly consists of a metal shaft, baffles, an external containment cage, and end caps. The shaft and end caps facilitate sealing the pipe air-tight and contain ports to allow for pressurization and pressure monitoring, see Figure 309. A metal anvil is inserted on the metal shaft preventing excessive pipe deformations; see

Figure 310, at the blade's point of impact. The metal baffles are cylindrical disks that are assembled on the pipe shaft and are equidistant apart by the insertion of metallic spacers. The

baffles as shown in Figure 312 are evenly spaced and sized according to the ISO specification. The baffles prevent quick decompression of the pressurized pipe sample after crack initiation.

The PE pipe test specimen is inserted over the anvil and the end-caps are tightly secured at the pipe ends. The entire pipe assembly consisting of the anvil, the baffles and the PE pipe with its end-caps can be removed from the test apparatus and placed into an environmental chamber to allow for pipe conditioning at the required test temperature. The entire pipe assembly is conditioned and cooled at the chosen temperature for a minimum of 24 hours before being removed for S-4 testing. GTI monitors the pipe's temperature with thermocouples and carries out the testing within the time period allowed by the ISO specification.



Figure 309: End Cap Contains a Port to Fill/Monitor Pipe Specimen.

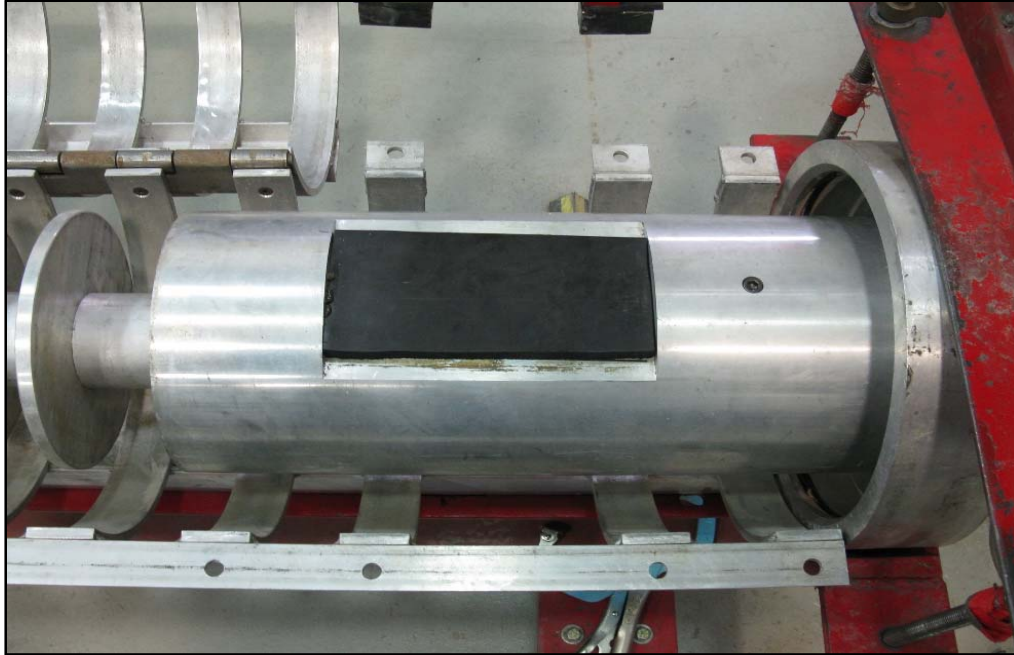


Figure 310: Assembly Anvil Prevents Excessive Pipe Wall Deformation during Impact

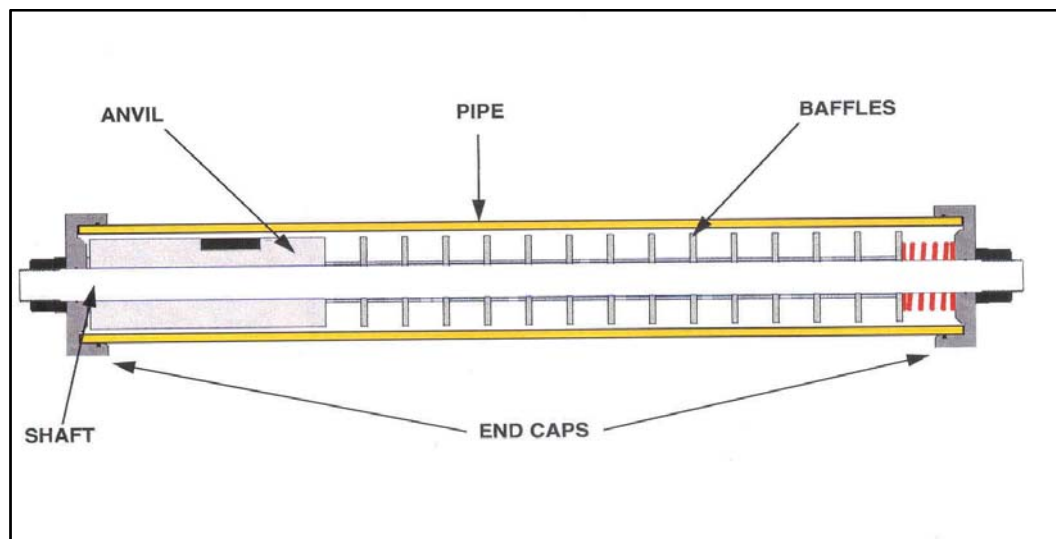


Figure 311: Schematic of Pipe Assembly Used at GTI



Figure 312: Baffles and Anvil That Are Contained Within the Pipe Specimen

External Containment Cage and Frame

The S-4 containment cage and frame are attached to the laboratory's floor and provide a stable base for the S-4 test. After cooling, the pipe assembly is quickly centered in the external cage which has spacing that matches the internal baffle system as specified in the ISO standard. The cage prevents excessive diametric deformations of the pipe as the crack propagates as shown in Figure 313. The frame attached to the cage is movable to allow for the insertion of the pipe assembly after which it is moved under the blade-impacting assembly. The exterior cage is then closed around the pipe assembly and locked in place, as pictured in Figure 314. The overall frame keeps the alignment between the pipe assembly and blade assembly.

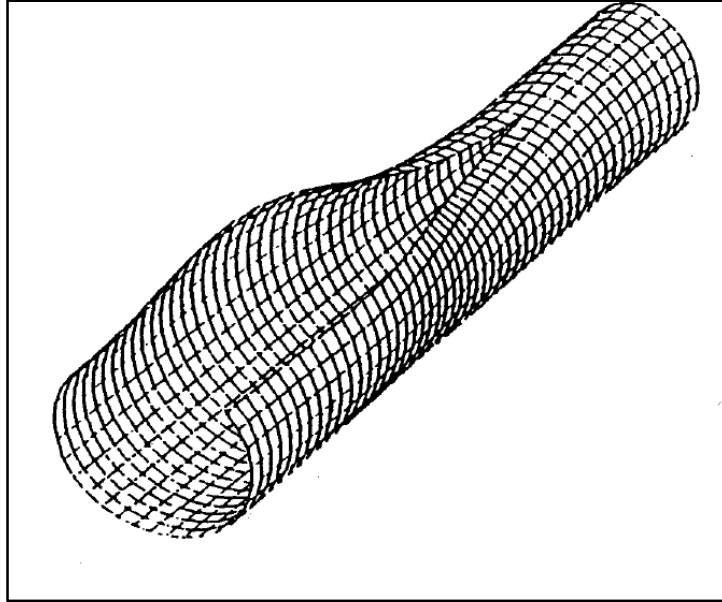


Figure 313: FET Analysis Showing the Extensive Deformation of a Pipe during RCP



Figure 314: External Cage

Striking Blade Assembly

This section of the S-4 apparatus propels a steel blade into the pipe surface to initiate the fast moving crack. The blade assembly is adjustable to different pipe diameters by moving it up and down and changing the size of the blade. A large pressurized air cylinder controlled by a solenoid valve provides the acceleration for the steel blade down the rectangular shaft pictured in Figure 308. When it strikes the pipe assembly, the blade speed is near 15 m/s. GTI monitors the blade's speed at impact by timing the blade's travel over a known distance. As the blade exits the shaft it strikes the pipe above the anvil initiating a crack as pictured in Figure 315.

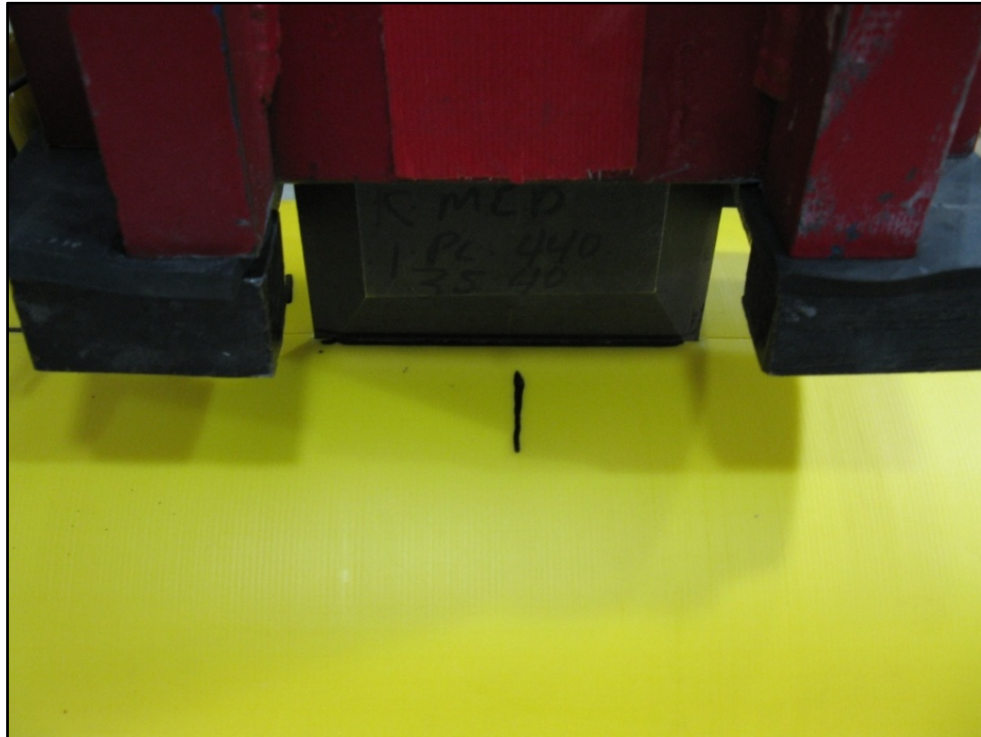


Figure 315: Blade Resting in the Crack It Initiated

PE Materials Subjected to S-4 Test s

In this project, S-4 tests were conducted on six (6) PE gas-grade pipe materials currently marketed in the U.S. These pipe materials were selected by the project Steering/Advisor committee.

The S-4 Critical Pressure was determined for each of the 6 PE pipe materials. In addition, the S-4 Critical Temperature was determined for the three 6-inch diameter pipe materials. To determine the Critical Pressure or the Critical temperature, a series of S-4 tests were. Table 81 lists the pipe materials used and the tests that were performed for each.

The S-4 test data from all the S-4 tests are listed in the following section. Table 82 through Table 90 present the S-4 test results. All the S-4 test results are also presented in graphical plots showing the crack length as a function of the pipe test pressure or the pipe test temperature. Photographs of typical PE pipe test specimens that were subjected to the S-4 tests are also presented.

Table 81: Pipe Materials Used For the S-4 Testing

Pipe Material	S- 4 Tests	Print Line
6" MDPE	Critical Pressure & Critical Temperature	6" IPS SDR11.0 DRISCOPEX 6500 GAS PE2406/2708 CEE ASTMD2513 K V18P 022608
6" HDPE	Critical Pressure & Critical Temperature	6" IPS SDR11.0 POLYPIPE GDB30 GAS PE3408 PE3608 CDE ASTMD2513 X30Q04 03APR08
6" PE100	Critical Pressure & Critical Temperature	6" IPS DR11 Yellow Stripe ® 8300 Gas PE 3408/4710 PE100 CEE ASTM D2513 WT012Y B2-075 15 JAN 08
8" MDPE	Critical Pressure	8"IPS DR11.0 DRISCOPEX 6500 GAS PE 2406/2708 CEE ASTM D2513 021508
8" PE100	Critical Pressure	8" IPS DR13.5 YELLOWSTRIPE 8300 GAS PE3408/4710 PE100 CEE ASTM D2513 WT009 Y B2-028 07FEB08
12" MDPE	Critical Pressure	12" IPS SDR11.0 DRISCOPEX 6500 PE2406/2708 CEE ASTMD2513 KV17 P K002 031108

6 Inch MDPE – Critical Pressure and Critical Temperature

Table 82: 6" MDPE Critical Pressure Test Results

Critical Pressure 6" MDPE						ISO 13477			
Test No.	CP Specimen No.	Test Temp.(°F) +/- 1°F	Pressure (psig) +/- 1psig	Blade Speed (m/s) +/- 0.1 m/s	Test Pipe Specimen Length (In)	Crack Length (In) from Blade Centerline As	Nominal Outer Pipe Diameter (In) De (avg.)	As/De	Event Propagation (P) or Arrest (A) As/De > 4.7 = (P) As/De ≤ 4.7 = (A)
Crack Initiation Tests									
1	2A	33.2	0.0	15.88	36.9	7 1/2	6.626		I
2	2B	32	0.0	15.875	36.9	8	6.629		I
3	2C	31.7	0.0	15.875	37.0	7 7/8	6.634		I
4	2D	32.7	0.0	15.6	36.9	6 1/4	6.631		I
5	224	32	0.0	15.875	36.9	8 1/2	6.633		I
S-4 Tests									
6	215	31.9	10.5	15.875	66.9	23 3/4	6.638	3.58	A
7	222	31.8	12.4	15.875	66.8	25 1/2	6.633	3.84	A
8	219	32.1	14.5	15.875	67.0	21 3/4	6.636	3.28	A
9	216	32.4	15.5	15.875	67.1	25 1/4	6.637	3.80	A
11	28	32.6	18.2	15.875	66.8	32 7/8	6.636	4.95	P
12	214	32.4	21.0	15.875	67.1	32 1/2	6.637	4.90	P
13	213	31.9	25.0	15.875	67.0	31 7/8	6.638	4.80	P
14	217	32.2	30.5	15.6	67.0	51 1/2	6.638	7.76	P

* Crack Length is the entire length of the pipe.

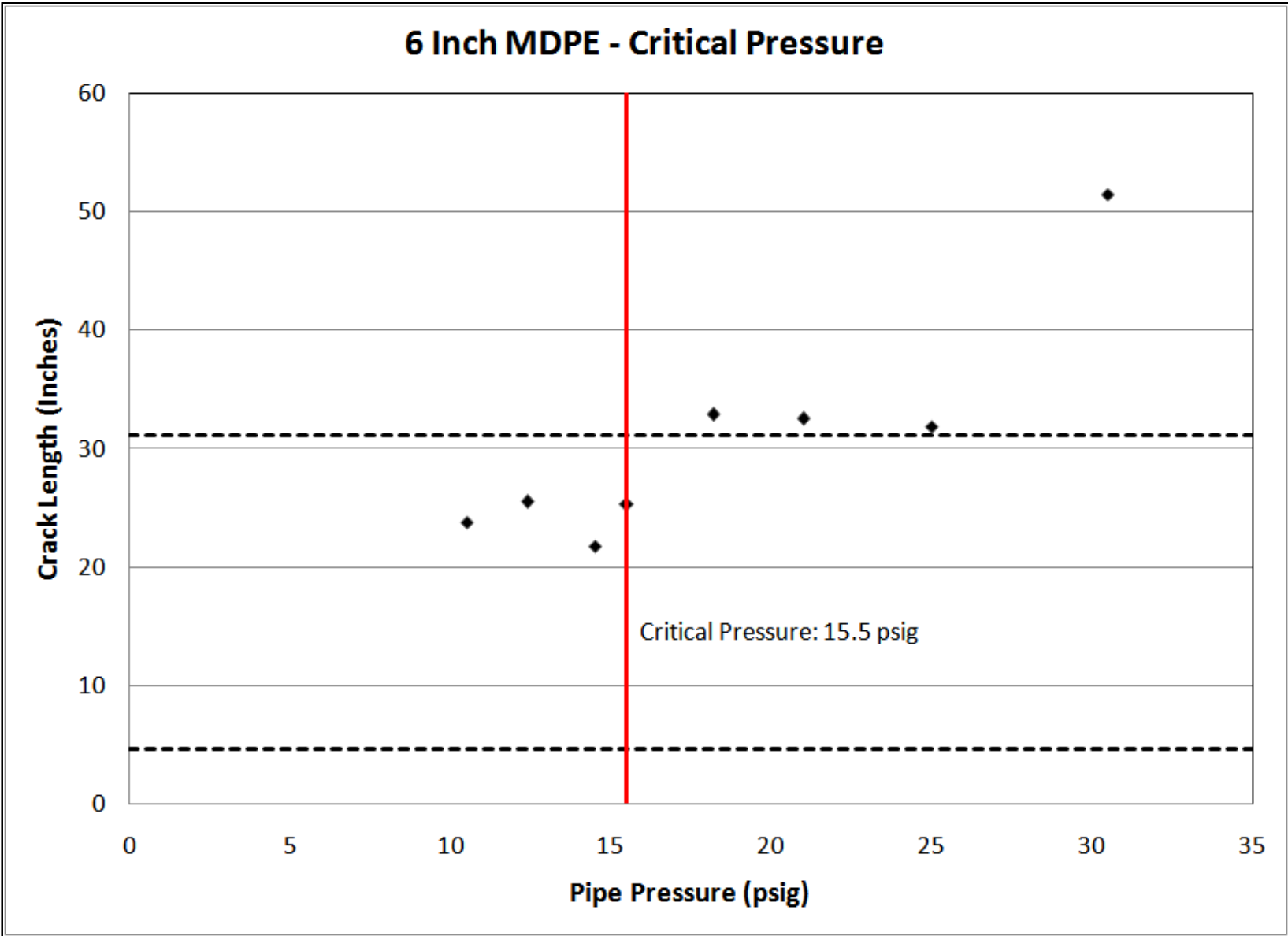


Figure 316: 6" MDPE Critical Pressure Test Results: Critical Pressure: 15.5 Psig

Table 83: 6" MDPE: Critical Temperature Test Results

Critical Temperature 6" MDPE						ISO 13477			
Test No.	CP Specimen No.	Test Temp.(°F) ± 1°F	Pressure (psig) ± 1psig	Blade Speed (m/s) ± 0.1 m/s	Test Pipe Specimen Length (In)	Crack Length (In) from Blade Centerline As	Nominal Outer Pipe Diameter (In) De (avg.)	As/De	Event Propagation (P) or Arrest (A) As/De > 4.7 = (P) As/De ≤ 4.7 = (A)
Crack Initiation Tests									
1	2A	33.2	0.0	15.88	36.9	7 1/2	6.626		I
2	2B	32	0.0	15.875	36.9	8	6.629		I
3	2C	31.7	0.0	15.875	37.0	7 7/8	6.634		I
4	2D	32.7	0.0	15.6	36.9	6 1/4	6.631		I
5	224	32	0.0	15.875	36.9	8 1/2	6.633		I
S-4 Tests									
6	218	67.2	72.5	15.6	67.3	13	6.637	1.96	A
7	25	65.5	72.5	15.6	67.3	13 3/4	6.633	2.07	A
8	27	64.1	72.5	15.6	67.3	46 1/4	6.632	6.97	P
9	210	59.0	72.5	15.6	67.3	59 1/2	6.633	8.97	P*
10	221	52.3	72.5	15.875	67.3	59 1/2	6.634	8.97	P*
11	212	48.2	72.5	15.875	67.3	59 1/2	6.634	8.97	P*
12	22	44.1	72.5	15.875	67.3	59 1/2	6.633	8.97	P*
13	220	39.2	72.5	15.875	67.3	59 1/2	6.636	8.97	P*
14	26	37.9	72.6	15.6	67.3	59 1/2	6.632	8.97	P*

* Crack Length is the entire length of the pipe.

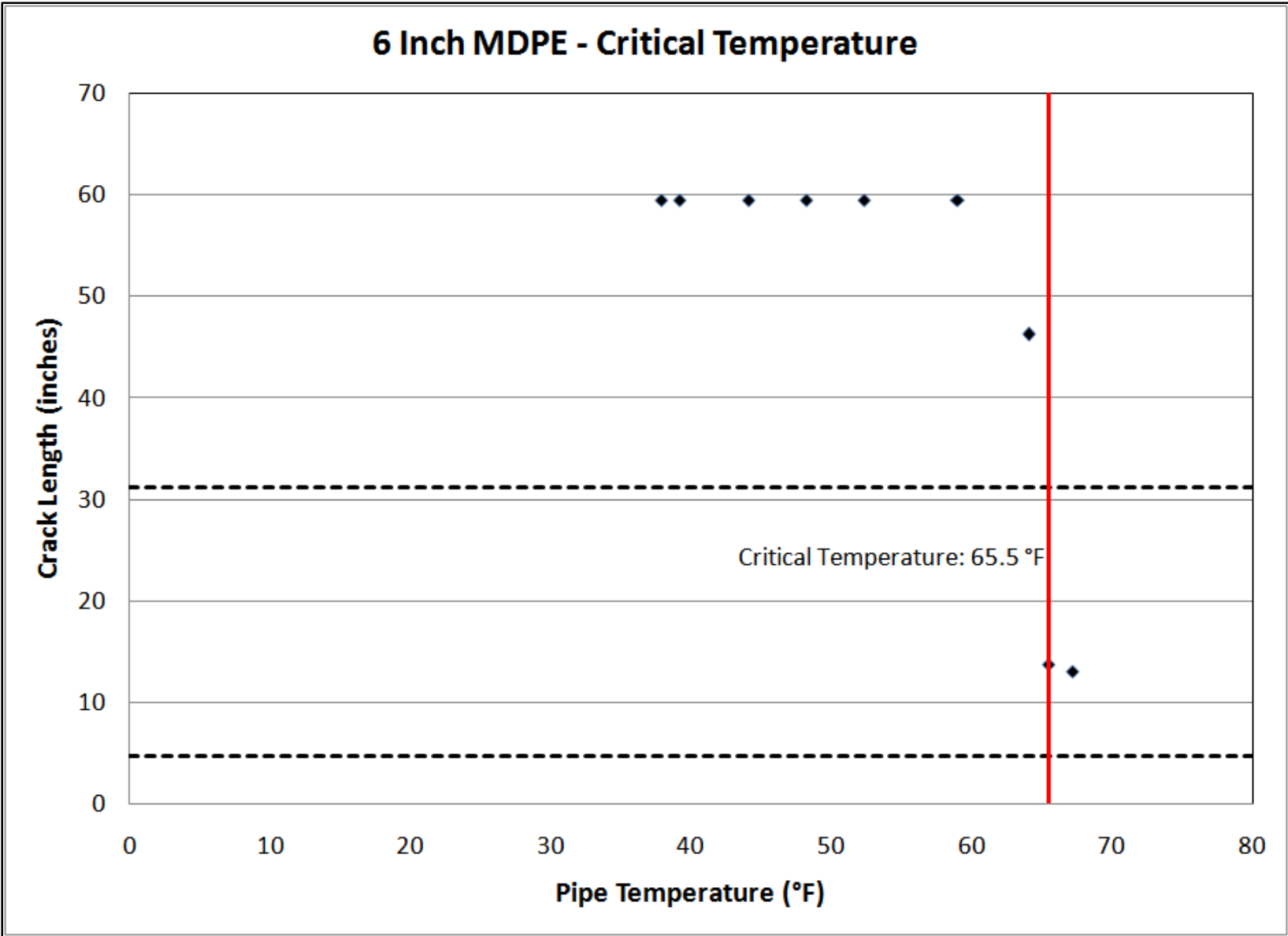


Figure 317: 6" MDPE Critical Temperature Test Results: Critical Temperature: 65.5 °F

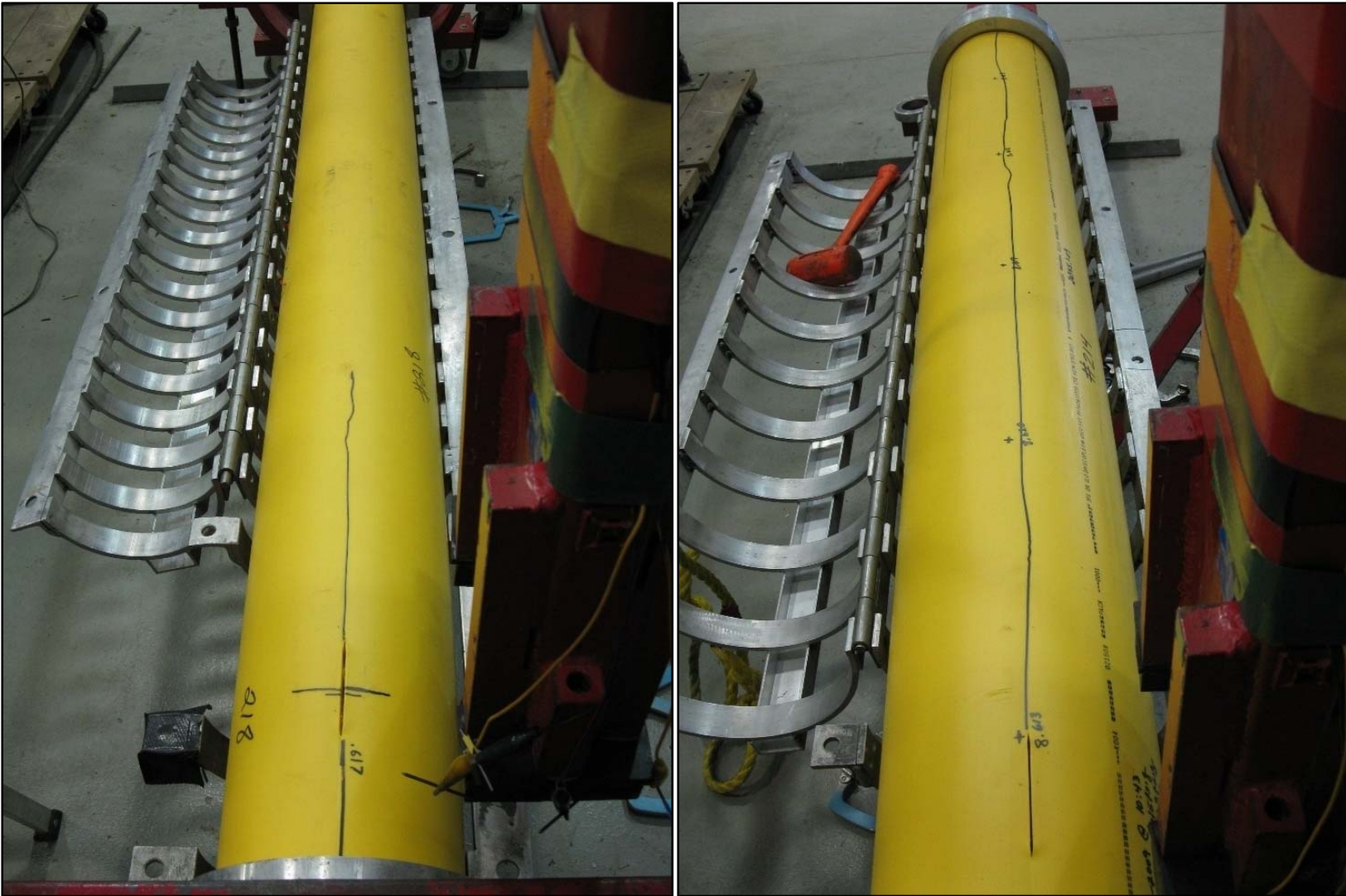


Figure 318: 6" MDPE S-4 Tests: Left, Crack Arrest; Right, Crack Propagation

6" Inch HDPE Critical Pressure and Critical Temperature

Table 84: 6" IPS HDPE Critical Pressure Test Results

Critical Pressure						ISO 13477			
Test No.	CP Specimen No.	Test Temp. (°F) ± 1°F	Pressure (psig) ± 1psig	Blade Speed (m/s) ± 0.1 m/s	Test Pipe Specimen Length (In)	Crack Length (In) from Blade Centerline As	Nominal Outer Pipe Diameter (In) De (avg.)	As/De	Event Propagation (P) or Arrest (A) As/De > 4.7 = (P) As/De ≤ 4.7 = (A)
Crack Initiation Tests									
1	3A	30.9	0.0	16.56	36.0	7 3/4	6.625		I
2	3C	31.4	0.0	16.56	36.0	11 1/8	6.624		I
3	3D	31.2	0.0	16.56	36.0	12	6.625		I
S-4 Tests									
4	35	31.4	12.5	16.56	67.3	13	6.627	1.96	A
5	327	31.6	15.0	16.56	67.3	19 1/2	6.630	2.94	A
6	33	31.6	16.5	16.56	67.3	19	6.625	2.87	A
7	326	30.2	17.0	16.56	67.3	14 1/2	6.630	2.19	A
8	32	31.4	20.0	16.56	67.3	59	6.626	8.90	P
9	325	31.8	21.0	16.56	67.3	54 3/4	6.629	8.26	P
10	324	33.8	25.0	16.56	67.3	59	6.629	8.90	P
11	322	31.4	26.8	16.56	67.3	59	6.630	8.90	P
12	328	31.7	32.0	16.56	67.3	60 1/4	6.624	9.10	P*
13	323	31.8	41.0	16.56	67.3	59 3/4	6.629	9.01	P

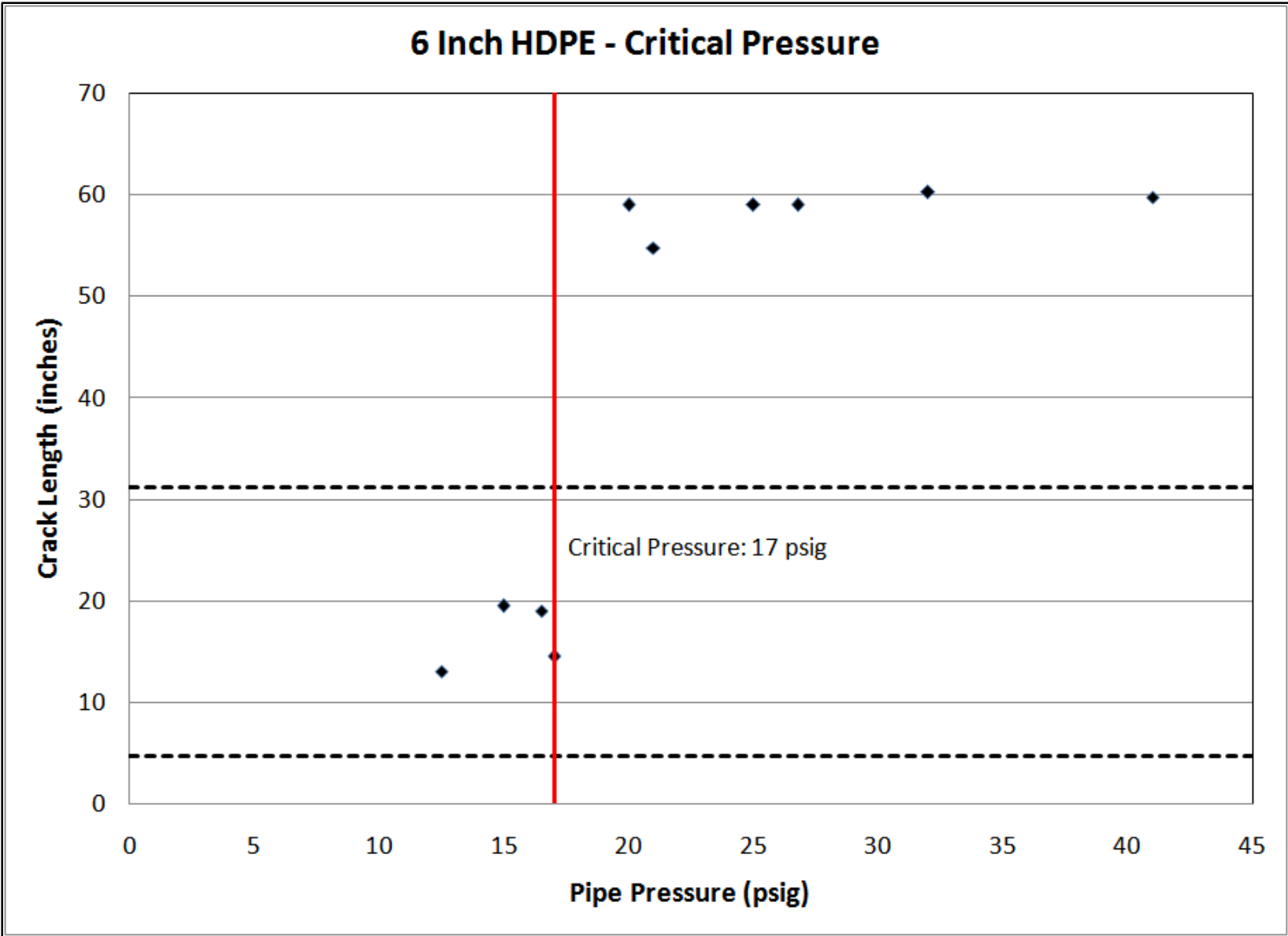


Figure 319: 6" HDPE Critical Pressure Test Results: Critical Pressure: 17.0 Psig

Table 85: 6" HDPE Critical Temperature Test Results

Critical Temperature						ISO 13477			
Test No.	CP Specimen No.	Test Temp.(°F) +- 1°F	Pressure (psig) +- 1psig	Blade Speed (m/s) +- 0.1 m/s	Test Pipe Specimen Length (In)	Crack Length (In) from Blade Centerline As	Nominal Outer Pipe Diameter (In) De (avg.)	As/De	Event Propagation (P) or Arrest (A) As/De > 4.7 = (P) As/De ≤ 4.7 = (A)
Crack Initiation Tests									
1	3A	30.9	0.0	16.56	36.0	7 3/4	6.625		I
2	3C	31.4	0.0	16.56	36.0	11 1/8	6.624		I
3	3D	31.2	0.0	16.56	36.0	12	6.625		I
S-4 Tests									
4	314	60.3	72.5	16.56	67.3	2 3/8	6.626	0.36	I.N.S.
5	318	55.0	72.5	16.56	67.3	1 3/8	6.624	0.21	I.N.S.
6	317	51.3	72.5	16.56	67.3	3	6.625	0.45	I.N.S.
7	312	51.0	72.5	16.56	67.3	1 3/8	6.627	0.21	I.N.S.
8	39	50.8	72.5	16.56	67.3	3 1/4	6.628	0.49	I.N.S.
9	316	50.2	72.5	16.56	67.3	59 1/2	6.625	8.98	P*
10	315	48.8	72.5	16.56	67.3	59 1/2	6.624	8.98	P*
11	38	47.9	72.5	16.56	67.3	59 1/2	6.630	8.97	P*
12	310	43.6	72.5	16.56	67.3	59 1/2	6.627	8.98	P*
13	313	34.3	72.5	16.56	67.3	59 1/2	6.625	8.98	P*
* Crack Length is the entire length of the pipe. I.N.S. = Initiation not satisfied.									

6 Inch HDPE - Critical Temperature

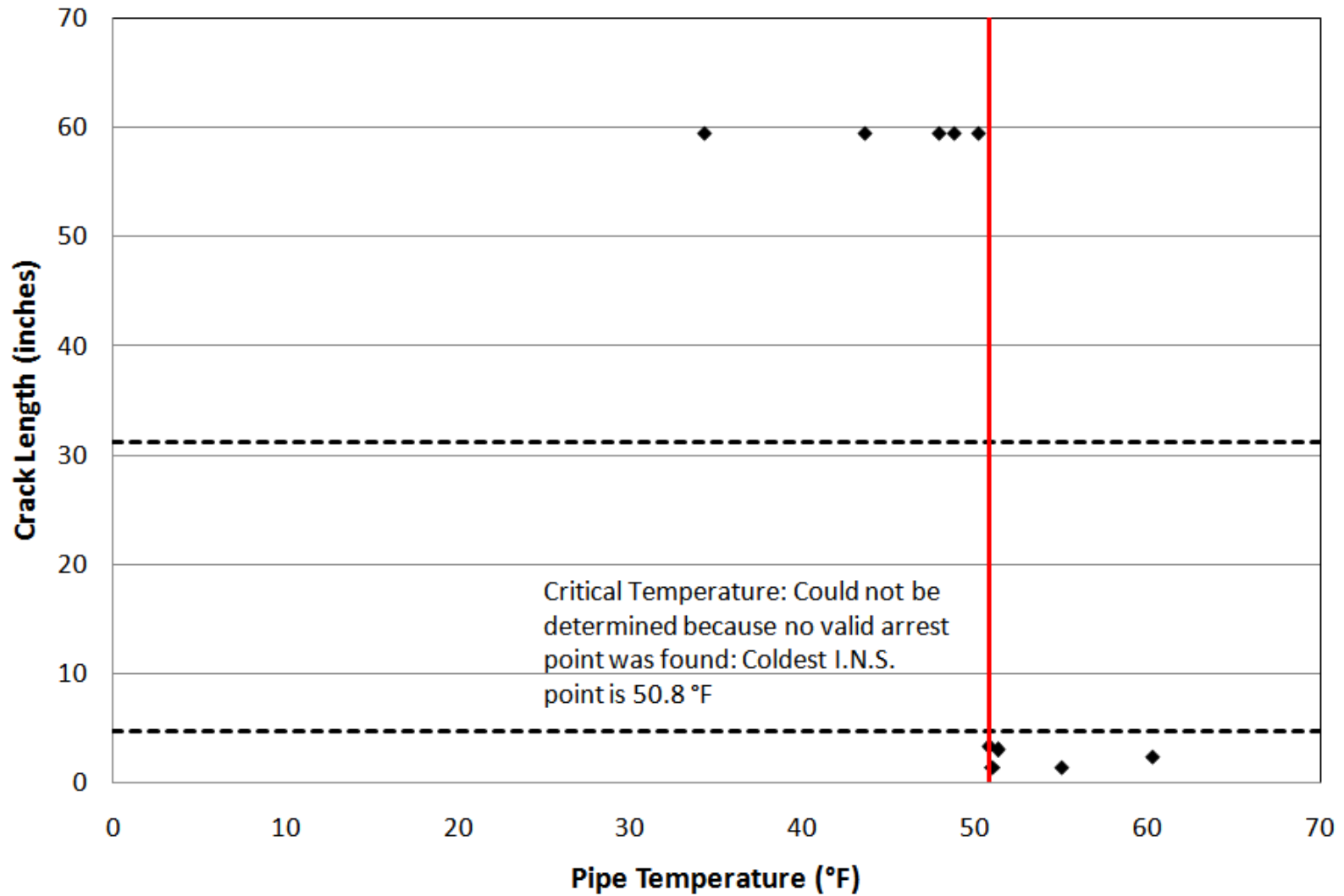


Figure 320: 6" HDPE Critical Temperature Test Results: Critical Temperature: 50.8 °F

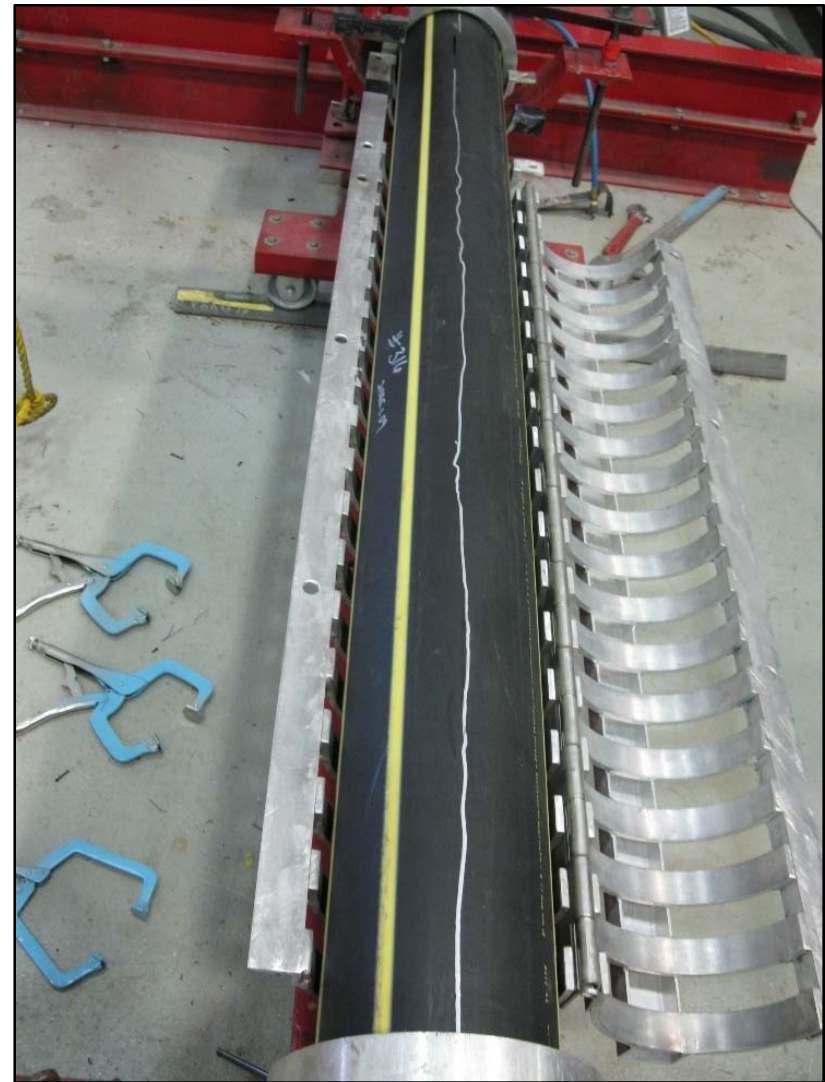
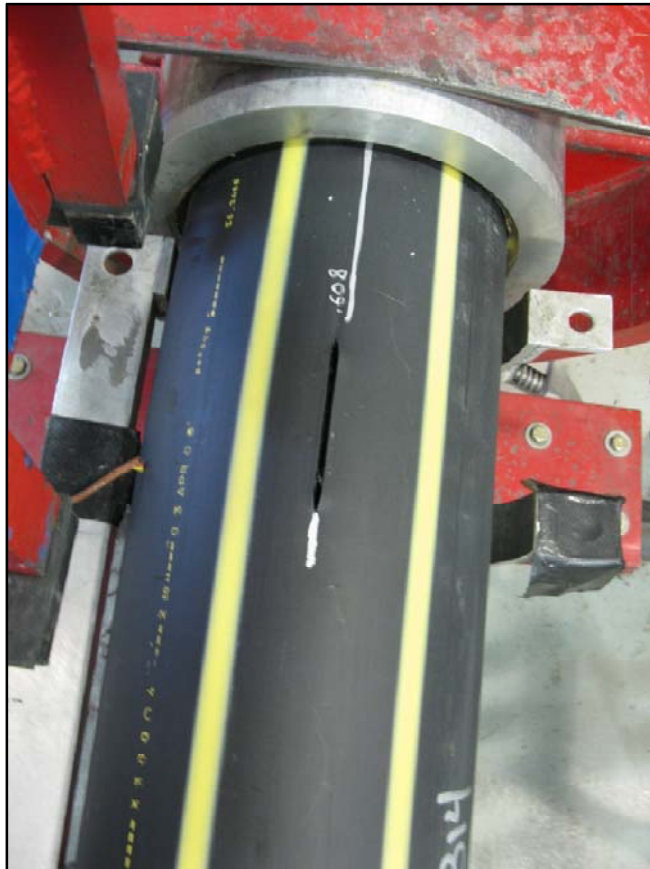


Figure 321: 6"HDPE S-4 Tests: Left, an Insufficient Crack Length; Right, Crack Propagation

6" PE100 Critical Pressure and Critical Temperature

Table 86: 6" PE100 Critical Pressure Test Results

Critical Pressure						ISO 13477			
Test No.	CP Specimen No.	Test Temp.(°F) +- 1°F	Pressure (psig) +- 1psig	Blade Speed (m/s) +- 0.1 m/s	Test Pipe Specimen Length (In)	Crack Length (In) from Blade Centerline As	Nominal Outer Pipe Diameter (In) De (avg.)	As/De	Event Propagation (P) or Arrest (A) As/De > 4.7 = (P) As/De ≤ 4.7 = (A)
Crack Initiation Tests									
1	4A	29.2	0.0	16.56	37.0	0	6.631		I
2	4B	23.9	0.0	16.56	36.5	0	6.631		I
3	4C	19.7	0.0	16.56	36.5	9	6.629		I
4	4D	23.5	0.0	16.9	36.8	8 1/8	6.630		I
5	415A	21.7	0.0	16.56	33.4	8 3/4	6.631		I
S-4 Tests									
6	47	22.6	22.0	16.56	67.0	14 1/2	6.634	2.19	A
7	48	24.2	24.7	16.56	67.3	18	6.631	2.71	A
8	45	23.3	25.0	16.56	67.3	12 3/4	6.632	1.92	A
9	410	24.9	27.5	16.56	67.3	18 1/2	6.633	2.79	A
10	49	23.0	27.6	16.56	67.3	23	6.632	3.47	A
11	44	23.1	30.0	16.56	66.5	59 1/2	6.630	8.97	P*
12	42	19.7	31.3	16.56	66.6	59 1/2	6.630	8.97	P*
13	43	24.1	34.0	16.56	66.8	59 1/2	6.634	8.97	P*
14	46	21.5	44.0	16.56	67.3	59 1/2	6.636	8.97	P*

* Crack Length is the entire length of the pipe.

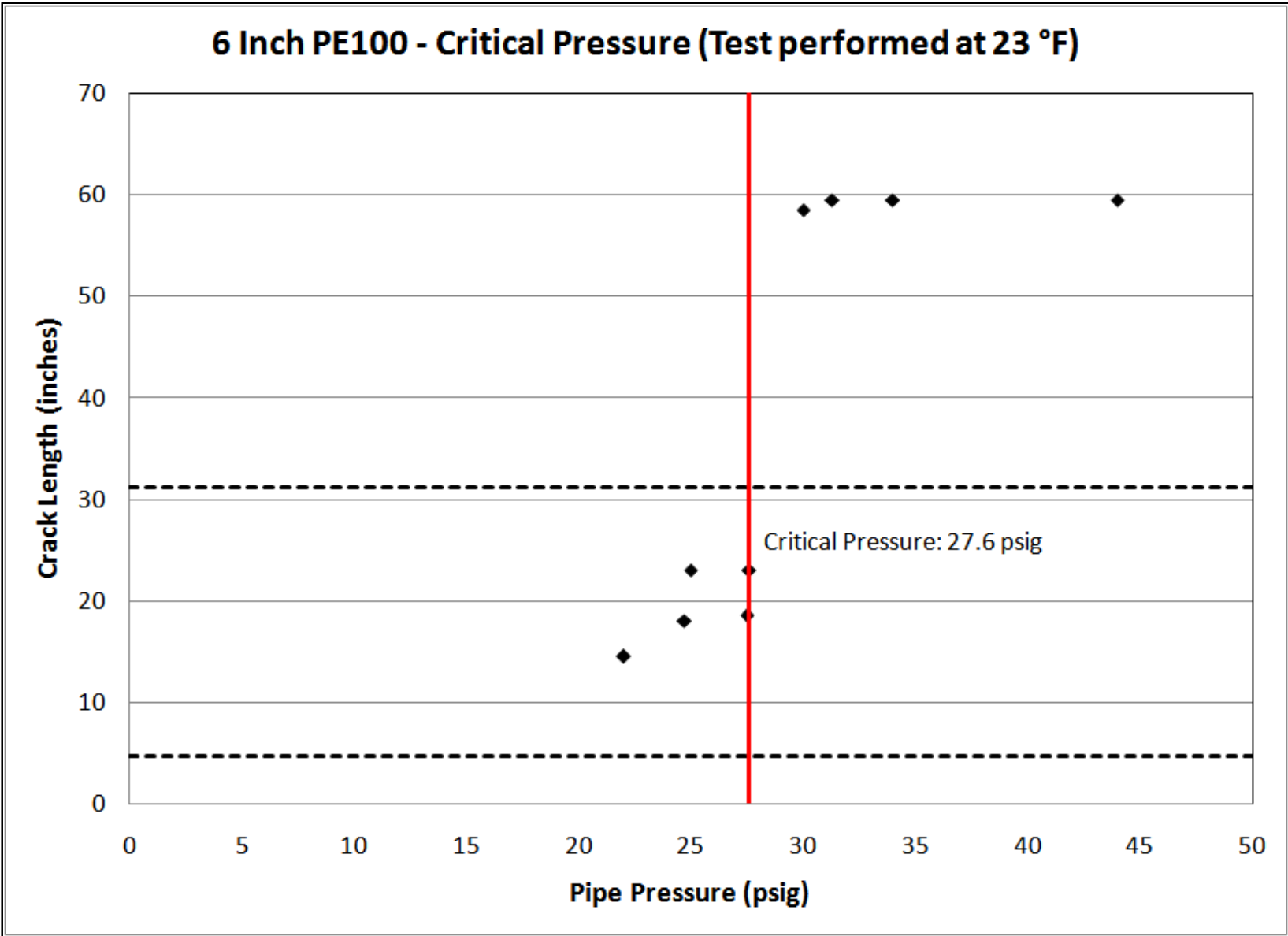


Figure 322: 6" PE100 Critical Pressure Test Results: Critical Pressure: 27.6 Psig

Table 87: 6" HDPE Critical Temperature Test Results

Critical Temperature						ISO 13477			
Test No.	CP Specimen No.	Test Temp.(°F) ± 1°F	Pressure (psig) ± 1psig	Blade Speed (m/s) ± 0.1 m/s	Test Pipe Specimen Length (In)	Crack Length (In) from Blade Centerline As	Nominal Outer Pipe Diameter (In) De (avg.)	As/De	Event Propagation (P) or Arrest (A) As/De > 4.7 = (P) As/De ≤ 4.7 = (A)
Crack Initiation Tests									
1	4A	29.2	0.0	16.56	37.0	0	6.631		I
2	4B	23.9	0.0	16.56	36.5	0	6.631		I
3	4C	19.7	0.0	16.56	36.5	9	6.629		I
4	4D	23.5	0.0	16.9	36.8	8 1/8	6.630		I
5	415A	21.7	0.0	16.56	33.4	8 3/4	6.631		I
S-4 Tests									
6	416	39.2	72.5	16.56	67.3	4 1/4	6.630	0.64	I.N.S.
7	413	38.3	72.5	16.56	67.3	7 5/8	6.624	1.15	A
8	412	36.9	72.5	16.56	67.3	6 3/4	6.625	1.02	A
9	411	36.9	72.5	16.56	67.3	16	6.628	2.41	A
10	420	35.3	72.5	16.56	67.3	59 1/2	6.627	8.98	P*
11	421	35.1	72.5	16.56	67.3	59 1/2	6.625	8.98	P*
12	419	31.4	72.4	16.56	67.3	59 1/2	6.624	8.98	P*
13	417	29.1	72.5	16.56	67.3	59 1/2	6.626	8.98	P*

* Crack Length is the entire length of the pipe.

I.N.S. = Initiation not satisfied.

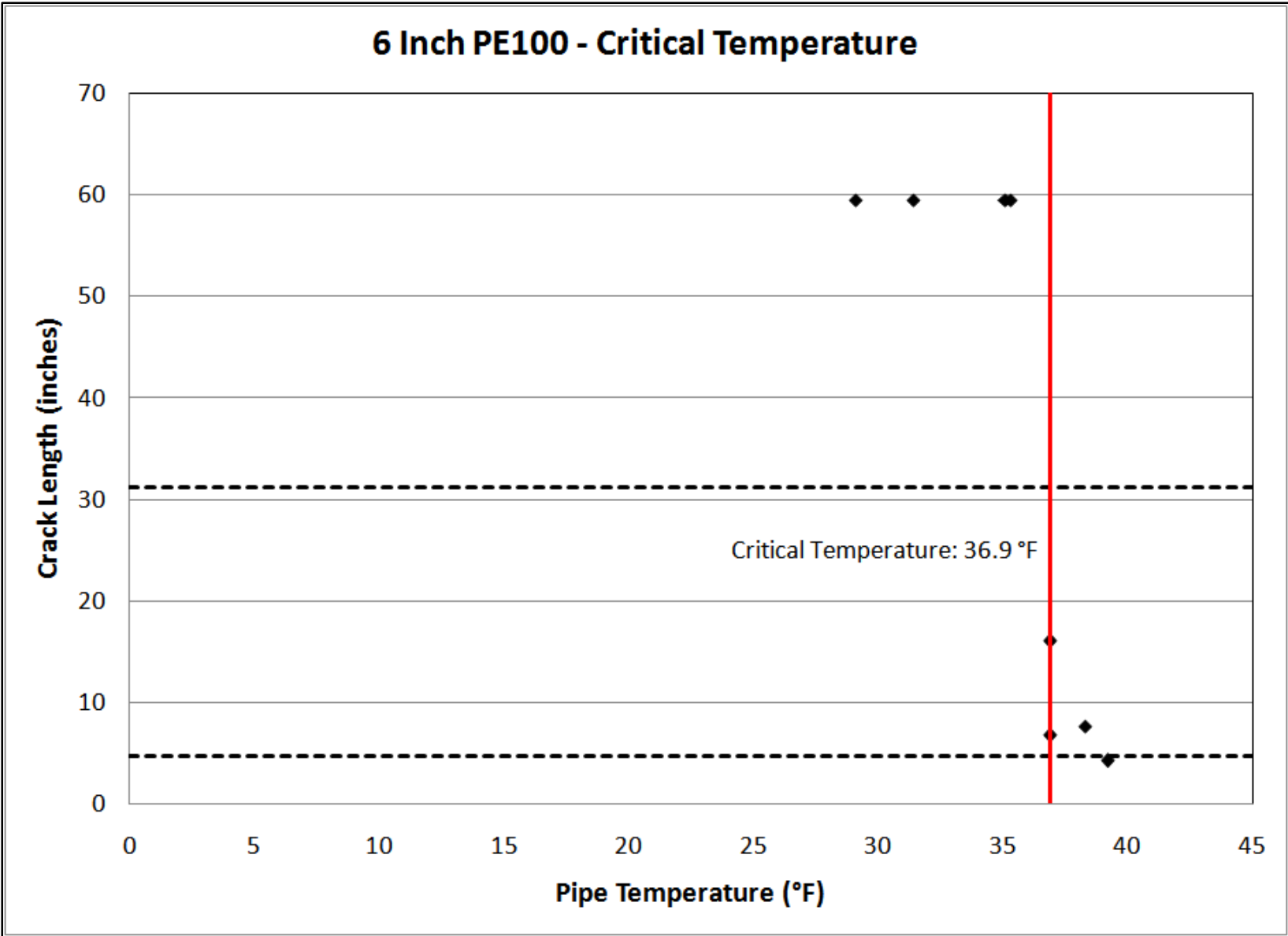


Figure 323: 6" PE 100 Critical Temperature Test Results: Critical Temperature: 36.9 °F



Figure 324: 6"PE100 S-4 Tests: Left, Initiation Test; Right, Crack Propagation

8" MDPE Critical Pressure

Table 88: 8' MDPE Critical Pressure Test Results

Critical Pressure 8" MDPE						ISO 13477			
Test No.	CP Specimen No.	Test Temp.(°F) +/- 1°F	Pressure (psig) +/- 1psig	Blade Speed (m/s) +/- 0.1 m/s	Test Pipe Specimen Length (In)	Crack Length (In) from Blade Centerline As	Nominal Outer Pipe Diameter (In) De (avg.)	As/De	Event Propagation (P) or Arrest (A) As/De > 4.7 = (P) As/De ≤ 4.7 = (A)
Crack Initiation Tests									
1	2A	32.6	0.0	15.60	45.0	12 1/2	8.617		I
2	2B	31.5	0.0	15.60	45.3	13 3/4	8.616		I
3	2C	32	0.0	15.60	45.4	10 1/2	8.616		I
S-4 Tests									
4	213	31.0	9.0	15.6	73.1	32 3/4	8.617	3.80	A
5	210	32.7	11.5	15.6	73.1	31 3/4	8.615	3.69	A
6	215	31.7	13.5	15.6	73.1	51 1/2	8.618	5.98	P
7	211	31.0	15.0	15.6	73.1	61 1/2	8.614	7.14	P*
8	214	31.1	20.3	15.6	73.1	61 1/2	8.617	7.14	P*
9	212	31.1	30.0	15.6	73.1	61 1/2	8.617	7.14	P*

* Crack Length is the entire length of the pipe.

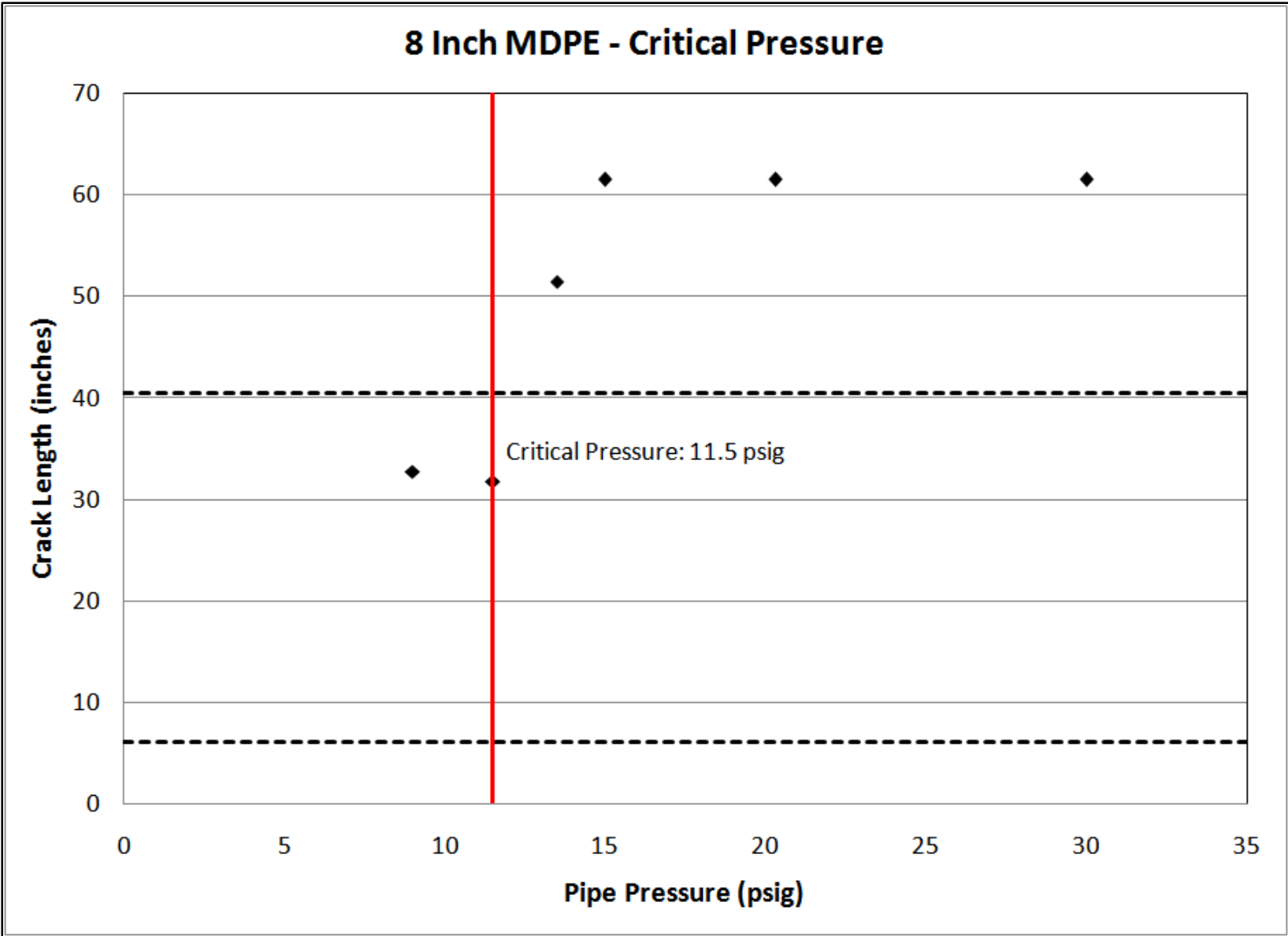


Figure 325: 8" MDPE Critical Pressure Test Results: Critical Pressure: 11.5 Psig



Figure 326: 8" MDPE S-4 Tests: Left, Crack Arrest; Right, Crack Propagation

8" PE100 Critical Pressure

Table 89: 8" PE 100 Critical Pressure Test Results

Critical Pressure						ISO 13477			
Test No.	CP Specimen No.	Test Temp.(°F) +- 1°F	Pressure (psig) +- 1psig	Blade Speed (m/s) +- 0.1 m/s	Test Pipe Specimen Length (In)	Crack Length (In) from Blade Centerline As	Nominal Outer Pipe Diameter (In) De (avg.)	As/De	Event Propagation (P) or Arrest (A) As/De > 4.7 = (P) As/De ≤ 4.7 = (A)
Crack Initiation Tests									
1	4A	32.0	0.0	15.9	43.0	9	8.625		I
2	4C	31.1	0.0	15.9	43.0	10 1/2	8.624		I
3	4D	31.5	0.0	16.2	43.0	11	8.620		I
S-4 Tests									
4	404	31.0	17.5	16.2	73.0	15 3/4	8.625	1.83	A
5	414	31.0	20.0	16.2	73.0	19 1/4	8.624	2.23	A
6	402	32.0	25.0	16.2	73.0	30	8.622	3.48	A
7	401	31.9	27.0	16.2	73.0	40 1/4	8.623	4.67	A
8	406	31.0	30.0	16.2	73.0	60 1/2	8.624	7.02	P*
9	408	33.0	31.5	16.2	73.3	60 1/2	8.625	7.01	P*
10	409	32.0	35.0	16.2	73.0	60	8.627	6.95	P*
11	407	31.0	40.0	16.6	73.0	60 1/2	8.626	7.01	P*

* Crack Length is the entire length of the pipe.

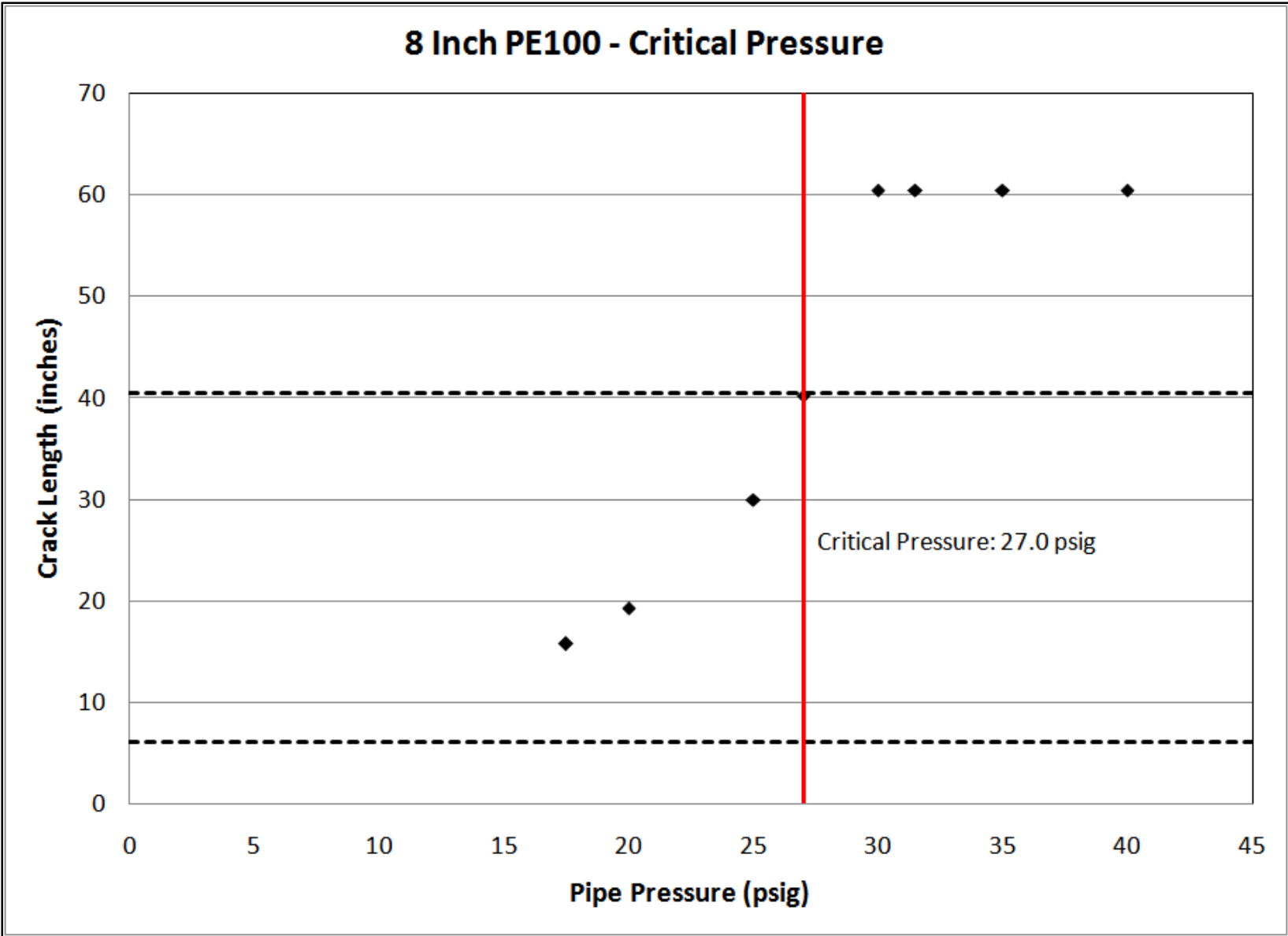


Figure 327: 8" PE 100 Critical Pressure Test Results: Critical Pressure: 27.0 Psig



Figure 328: 8" PE 100 S-4 Tests: Left, Crack Arrest; Right, Crack Propagation

12" MDPE Critical Pressure

Table 90: 12" MDPE Critical Pressure Test Results

Critical Pressure						ISO 13477			
Test No.	CP Specimen No.	Test Temp.(°F) +/- 1°F	Pressure (psig) +/- 1psig	Blade Speed (m/s) +/- 0.1 m/s	Test Pipe Specimen Length (In)	Crack Length (In) from Blade Centerline As	Nominal Outer Pipe Diameter (In) De (avg.)	As/De	Event Propagation (P) or Arrest (A) As/De > 4.7 = (P) As/De ≤ 4.7 = (A)
Crack Initiation Tests									
1	12B	31.5	0.0	15.24	60.5	17	12.730		I
2	12C	31.7	0.0	15.24	60.5	13 1/2	12.733		I
3	12D	31	0.0	15.24	60.5	17 7/8	12.733		I
S-4 Tests									
4	122	31.7	12.5	15.24	114.3	19 1/2	12.733	1.53	A
5	124	32.9	16.0	15.24	114.5	46 3/4	12.739	3.67	A
6	123	31.2	17.5	15.24	114.0	53 1/8	12.738	4.17	A
7	129	33.0	18.5	15.24	114.0	45 3/4	12.734	3.59	A
8	125	31.9	20.0	15.24	114.0	101 1/2	12.739	7.97	P*
9	127	31.2	22.5	15.24	114.0	90 1/4	12.735	7.09	P
10	128	31.4	28.5	15.24	114.3	102	12.735	8.01	P*

* Crack Length is the entire length of the pipe.

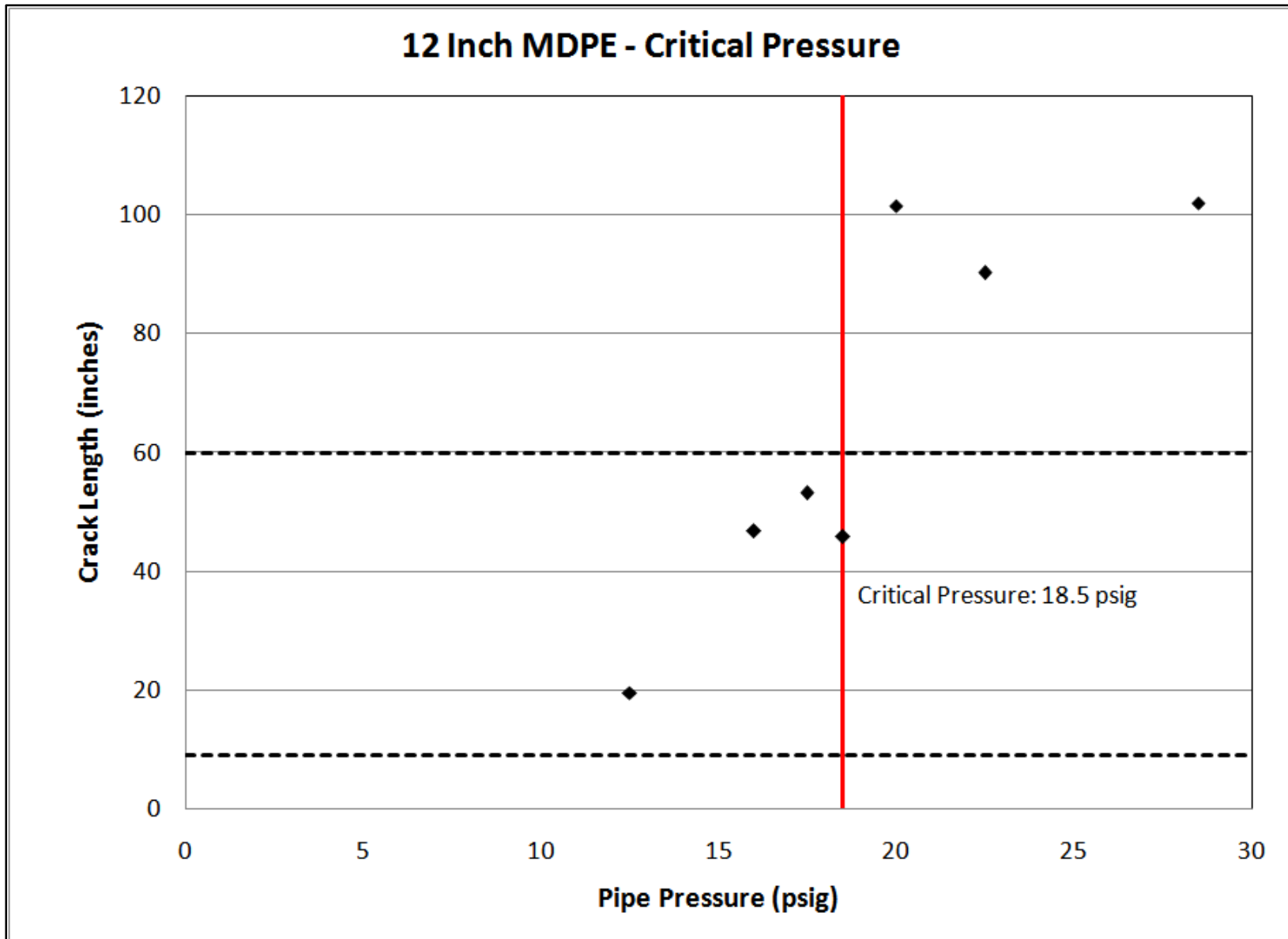


Figure 329: 12" MDPE Critical Pressure Test Results: Critical Pressure: 18.5 Psig

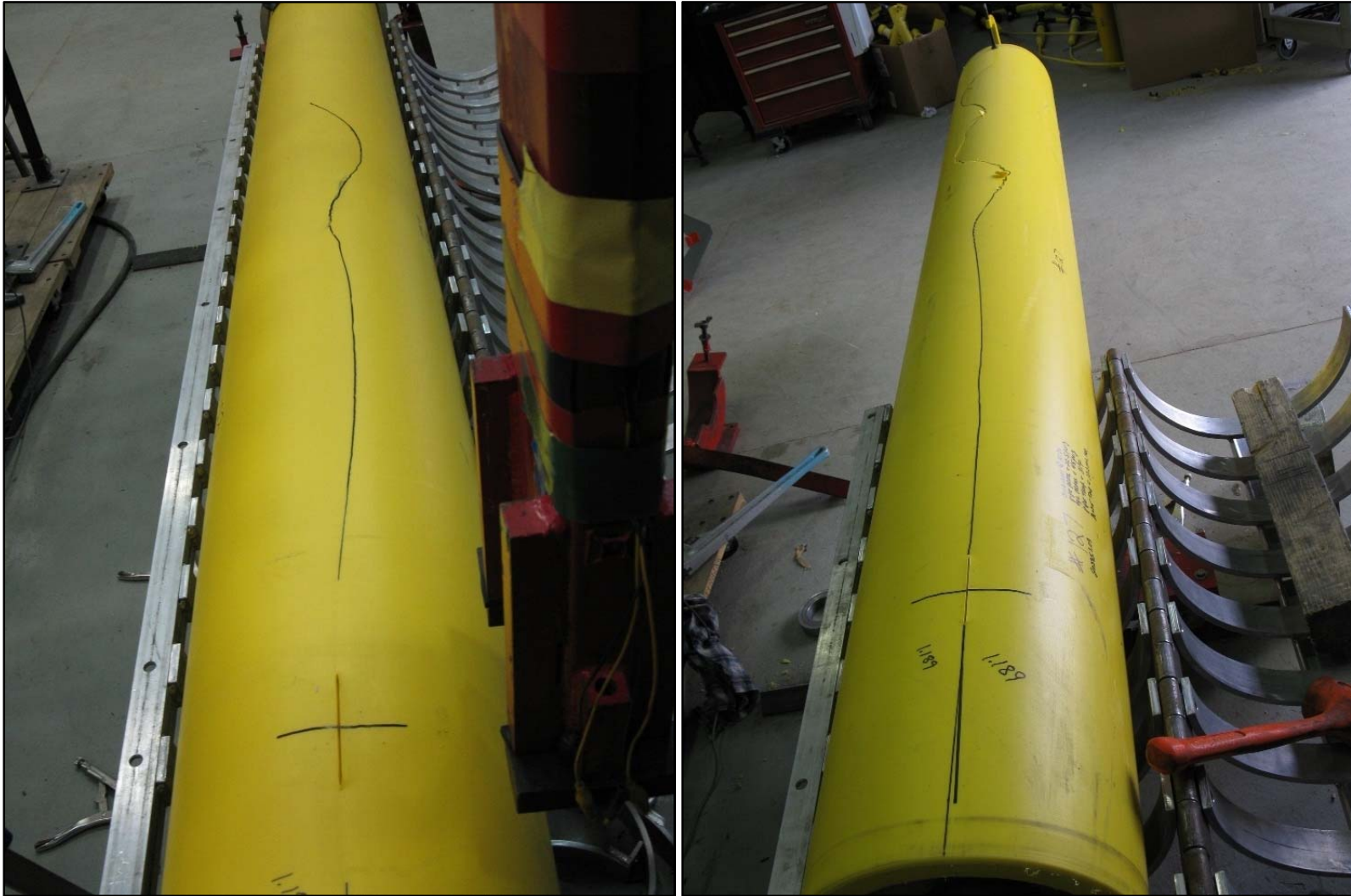


Figure 330: 12" MDPE S-4 Tests: Left, Crack Arrest; Right, Crack Propagation

RCP Results, Correlations, and Conclusions

The S-4 critical temperature and pressure values were determined for various pipe materials and sizes as shown in Table 91.

The critical pressure values corresponding to pipes subjected to full-scale field installations were calculated using equation [11] from the ISO standard. These values are listed in Table 91.

Table 91: Summary of S-4 Test Results

Pipe Material	Nominal Pipe Size Diameter(in)/SDR	Critical Pressure S-4 (psig)	Critical Temperature (°F(°C))	Correlated Critical Pressure** Full Scale (psig)
Driscoplex 6500 PE2406/2708	6" IPS/SDR 11.0	15.5	65.5 (18.6)	94.0
Polypipe PE3408/3608	6" IPS/SDR 11.0	17.0	50.8 (10.4)*	99.4
Yellowstripe 8300 PE100	6" IPS/SDR 11.0	27.6***	36.9 (2.7)	137.6
Driscoplex 6500 PE2406/2708	8" IPS/SDR 11.0	11.5		79.6
Yellowstripe 8300 PE100	8" IPS/SDR 13.5	27.0		135.4
Driscoplex 6500 PE2406/2708	12" IPS/SDR 11.0	18.5		104.8

* Note: No arrest point was found

** Correlated pressure calculated using equation 11: $p_{c,FS} = 3.6(p_{c,S4} + p_{atm}) - p_{atm}$

*** Critical pressure tests for 6" PE100 were carried out at a temperature of 23 °F

The S-4 Critical Pressure was determined for each of the 6 PE pipe materials. In addition, the S-4 Critical Temperature was determined for the three 6-inch diameter pipe materials. To determine the Critical Pressure or the Critical temperature, a series of S-4 tests were performed. For critical pressure determination, the test pressures were systematically varied while maintaining constant test temperature. For determining the critical temperature, the test temperatures were systematically varied while maintaining constant test pressure, 5 bars. If field conditions are well above a pipe's critical temperature, then it is very unlikely that RCP would occur. Assuming that the correlation is applicable and valid, the S-4 Critical Pressure was then combined with the model to determine the full-scale pipe pressure that may lead to a potential RCP field failure. The S-4 test results and correlations may be used to mitigate the potential for a RCP failure in the field through selection of proper PE pipe materials and sizes or by subjecting pipes to MAOP that would not exceed the field pressure calculated using the empirical correlating model.

Conclusion

The use of polyethylene (PE) piping has continuously increased. By 2006, the number of miles of plastic mains increased to 619,000 miles. The number of plastic services grew to over 39.6 million. In order to continue the delivery of safe and reliable energy, it is important to improve knowledge regarding the state of PE systems. The modes of failure and causes are well documented for plastic materials in general. The most common mode of field failures has been attributed to SCG. Many improvements have been made to make PE materials more resistant to SCG but no matter the material improvements, PE, as well as other piping materials, remains vulnerable to excavation damage. A review of the “Natural Gas Distribution Incident Data” from 1984 to 2006 showed that excavation damage especially by third parties was the number one contributor to the cost of damages, injuries, and fatalities in both plastic and steel. Eliminating excavation damage would cut the total number of reportable incidents by more than half.

Overall, the research performed as part of this report showed that there was very little data available in the public domain in regard to failures associated with plastic piping systems. GTI databases were evaluated to characterize SCG and identify susceptibility to premature SCG failures. Laboratory tests were evaluated to determine whether or not they can be used to provide information on SCG susceptibility. Additional data was generated through analysis of 55 field failures. Resistance of PE materials to RCP was investigated through laboratory S-4 testing. Critical pressure was determined for 6 pipe materials. Critical temperature was determined for 3 materials.

Recommendations

Under the Root Cause Analysis Task, GTI received fifty-five samples for analysis. Of these, nine were tapping tee caps. The prominent style of cap received contained the threads on the inside of the cap. There were eight of these caps and all fractures appeared to have started at the first thread root. Sample #50020726, which was examined in greater detail than the others, did not exhibit signs of over-tightening which may indicate a potential issue with this style or material. Consideration should be given to studying the remaining seven caps to determine if there is a systemic issue.

There is a need to develop a reliable technology that can be used to accurately locate underground plastic pipes. There is a critical need to develop a technology that can identify in real-time the presence of a third-party excavation activity and then promptly alert the pipeline operator.

References

A. Lustiger, M.J. Cassady, F.S. Uralil, and L.E. Hulbert, "Field Failure Reference Catalog for Polyethylene Gas Piping and Addendum," GRI-84/0235.1, 1984 GRI-84/0235.2, 1989 GRI-84/0235.3, 1991.

Allegro Energy Consulting, "Gas Distribution Incidents: Understanding the Hazards," December 2004.

Battelle Memorial Institute "Plastic Pipe Field Failures Catalog" GRI-98/0202. CD-ROM. Gas Research Institute, 1998.

Brown, N., "Microscopic Observations and Mechanics Analyses Long Term Fracture in Polyethylene Piping Materials," GRI-86/0071, 1986.

Brown, N., "Microscopic Observations and Mechanics Analyses of Long Term Fracture in Polyethylene Piping Materials," GRI-85/0037, 1985.

Brown, N., "Microscopic Observations and Mechanics Analyses of Long Term Fracture in Polyethylene Piping Materials," GRI-87/0087, 1987.

Brown, N., and X. Lu, "Impact Test for Predicting the Critical Temperature for Rapid Crack Propagation in PE Gas Pipes," GRI-00/0210, 2000.

Carr, S.H., and B. Crist, "Structural Basis for the Mechanical Properties of Polyethylene," GRI-87/0039, 1987.

Carr, S.H., B. Crist, and T.J. Marks, "Structural Basis for the Mechanical Properties of Polyethylene," GRI-84/0171, 1984.

Cassady, M., G. Derringer, J. Hassell, L. Hulbert, A. Lustiger, K. Prabhat, and F. Uralil, "The Development of Improved Plastic Piping Materials and Systems for Fuel Gas Distribution," GRI-84/0138, 1984.

Cassady, M., G. Derringer, N. Ghadiali, J. Hassell, L. Hulbert, A. Lustiger, R. Markham, V. Papaspyropoulos, R. Smith, K. Prabhat, and F. Uralil, "The Development of Improved Plastic Piping Materials and Systems for Fuel Gas Distribution, GRI-82/0101," 1982.

Cassady, M., L. Hulbert, P. Krishnaswamy, A. Lustiger, and F. Uralil, "Development of Short-Term Tests for Evaluating Plastic Gas Piping Materials," GRI-85/0251, 1985.

Cassady, M.J., G.C. Derringer, M.M. Epstein, J.A. Hassell, A. Lustiger, R.L. Markham, W.A. Maxey, F.S. Uralil, and W.M. Wong, "Development of Improved Plastic Piping Materials and Systems for Fuel Gas Distribution," GRI-80/0041, 1980.

Cassady, M.J., S.M. Pimputkar, M.A. Masood, and V.J. Brown, "Handbook of Hydrostatic Stress-Rupture Data for Plastic Pipe Materials Used for Gas Distribution," GRI-98/0355, 1998.

Chaoui, K., A. Chudnovsky, A. Moet, and J. Strebel, "Theory for Accelerated Slow Crack Propagation in Polyethylene Fuel Pipes," GRI-88/0220, 1988.

DOT/PHMSA, Distribution Annuals Reports, <http://ops.dot.gov/stats/DT98.htm>

DOT/PHMSA, Natural Gas Distribution Incident Data, <http://ops.dot.gov/stats/IA98.htm>

Forte, T., B. Leis, C. Cundiff, M. Wilson, R. Kurth, J. Ahmad, and D. Stephens, "Volume 3: User's Manual for the Slow Crack Growth Test Method for Polyethylene Gas Pipes," GRI-92/0481, 1992.

Hulbert, L.E., S.G. Sampath, D.M. Bigg, K. Prabhat, and F.S. Uralil, "Volume 1: A Review of Time-Dependent Deformation Models of Plastic Gas Piping," GRI-82/0101.1, 1982.

ISO 13477. (n.d.). Thermoplastics pipes for the conveyance of fluids - Determination of resistance to rapid crack propagation (RCP) - Small-scale steady-state test (S4 test).

Kanninen, M., C. Kuhlman, and M. Mamoun. (1993). Rupture-Prevention Design Procedure to Ensure PE Gas Pipe System Performance. *13th International Plastic Fuel Gas Pipe Symposium*. San Antonio: American Gas Association.

Kanninen, M., P. O'Donoghue, J. Cardinal, S. Green, R. Curr, and J. Williams. (1989). A Fracture Mechanics Analysis of Rapid Crack Propagation and Arrest in Polyethylene Gas Pipes. *11th Plastic Fuel Gas Pipe Symposium* (pp. 334-343). San Francisco: American Gas Association.

Kanninen, M.F., P.E. O'Donoghue, C.F. Popelar, C.H. Popelar, and V.H. Kenner, "Volume 1: Brief Guide for the Use of the Slow Crack Growth Test for Modeling and Predicting the Long-Term Performance of Polyethylene Gas Pipes," GRI-93/0105, 1993.

Kanninen, M.F., P.E. O'Donoghue, C.F. Popelar, C.H. Popelar, and V.H. Kenner, "Volume 2: Technical reference for the Use of the Slow Crack Growth Test for Modeling and Predicting the Long-Term Performance of Polyethylene Gas Pipes," GRI-93/0106, 1993.

Kanninen, M.F., P.E. O'Donoghue, S.C. Grigory, L.J. Kim, and H. Couque, "Design and Technical Reference to Mitigate Rapid Crack Propagation in Polyethylene Pipes for Gas Distribution," GRI-97/0166, 1997.

Kardos, J.L., R. Powell, and K.L. Jerina, "Structure and Properties of Polyethylene," GRI-81/0142, 1981.

Krishnaswamy, P., W. Maxey, B. Leis, and L. Hulbert, "A Design Procedure and Test Method to Prevent Rapid Crack Propagation in Polyethylene Gas Pipe, GRI-85/0010," 1985.

Krishnaswamy, P., W. Maxey, B. Leis, and L. Hulbert, "A Design Procedure and Test Method to Prevent Rapid Crack Propagation in Polyethylene Gas Pipe," GRI-85/0010, 1986.

Kuhlman, C. and G.G. Chell, "User's Manual PE LIFESPAN FORECASTING™ Plastic Piping Systems," GRI-98/0359, 1998.

Kuhlman, C., G.G. Chell, C.H. Popelar, D.A. McKee, and J.H. Feiger, "Guidelines and Methods for Service Life Estimation of Polyethylene Gas Piping," GRI-00/0138, 2000.

Leevers, P., G. Venizelos, and R. Morgan. (1993). Strategies for Avoiding RCP in Gas-Pressurized PE Pipe. *13th International Plastic Fuel Gas Pipe Symposium*. San Antonio: American Gas Association.

Leis, B. (1989). Rapid Crack Propagation in Polyethylene Gas Piping Distribution Systems. *11th Plastic Fuel Gas Pipe symposium* (pp. 354-359). San Francisco: American Gas Association.

Leis, B., J. Ahmad, T. Forte, L. Hulbert, M. Wilson, "Volume 1: Slow Crack Growth Test Method for Polyethylene Gas Pipes," GRI-92/0479, 1992.

Leis, B., T. Forte, J. Ahmad, M. Wilson, R. Kurth, P. Vieth, and C. Cundiff, "Volume 2: Applicability of the Slow Crack Growth Test Method for Polyethylene Gas Pipes," GRI-92/0480, 1992.

Mamoun, M., "Development of an Accelerated SCG Test Method for Plastic Pipe and Correlation with Hydrostatic Stress Rupture Test Method ASTM D 1598", July 2005.

Maupin, J., Plastic Pipe Failure Analysis. 7th International Pipeline Conference. Calgary, Alberta, Canada: ASME, 2008.

McKee, D.A., C.J. Kuhlman, and C.H. Popelar, "Service Performance of Polyethylene Pipes Containing Surface Notches Subjected to Internal Pressure," GRI-00/0137, 2000.

Moet, A. and A. Chudnovsky, "Theory for Accelerated Slow Crack Propagation in Polyethylene Fuel Pipes," GRI-86/0211, 1986.

Moet, A., A. Chudnovsky, and K. Sehanobish, "Fractographic Analysis of Field Failure in Polyethylene Pipe," GRI-84/0226, 1984.

Moet, A., A. Chudnovsky, K. Sehanobish, M.L. Kasakevich, and K. Chaoui, "A Theory for Accelerated Slow Crack Propagation in Polyethylene Fuel Pipes," GRI-85/0173, 1985.

National Transportation Safety Board, Special Investigation Report, "Brittle-like Cracking in Plastic Pipe for Gas Service," April 23, 1998.

Olson, R., T. Forte, D. Rider, and J. Stets "Field Loads Acting on Plastic Gas Pipes: Instrumentation and Data Acquisition," GRI-00/0239, 2000.

Papaspyropoulos, V. and L.E. Hulbert, "Volume 2: A Review of Time-Dependent Fracture Models of Plastic Gas Piping," GRI-82/0101.2, 1982.

Pimputkar, S. M., J. A. Stets, D. Mangaraj, G. Clark, and D. Rider, "Analysis of Microscopic Leaks in Polyethylene Gas Distribution Piping," GRI-96/0014, 1996.

Popelar, C.H., V.H. Kenner, and S.F. Popelar, "The Determination of the Performance Life of Heat Fusion Joints in Polyethylene Gas Pipe Materials," GRI-91/0032, 1991.

Popelar, C.H., V.H. Kenner, S.F. Popelar, and M.C. Pfeil, "Life Prediction of Butt Heat Fusion Joints in Polyethylene Gas Pipe Materials," GRI-91/0360, 1991.

Prabhat, K., W.A. Maxey, L. Hulbert, and M. Mamoun. (1983). The Use of Charpy and Robertson Tests in Predicting Rapid Crack Propagation in Polyethylene Pipes. *Proceedings of the 8th Plastics Fuel Gas Pipe Symposium*, (pp. 128-132). New Orleans.

Stewart, H.E., O. Bilgin, T.D. O'Rourke, and T.M. J. Keeney, "Technical Reference for Improved Design and Construction Practices to Account for Thermal Loads in Plastic Gas Pipelines," GRI-99/0192, 1999.

Uralil, F.S., and L.E. Hulbert, "The Slow Crack Growth Test for Comparing and Selecting Polyethylene Gas Pipe Materials," GRI-85/0045, 1985.

Uralil, F.S., C.S. Lee, R.L. Markham and M.M. Epstein, "Effects of Loads on the Structural and Fracture Behavior of Polyolefin Gas Piping," GRI-80/0045, 1980.

Vanspeybroeck, P. (2002). RCP, After 25 Years of Debates, Finally Mastered by Two ISO-Tests. *17th International Plastic Fuel Gas Pipe Symposium* (pp. 47-55). San Francisco: American Gas Association.

Wolters, M., and G. Ketel. (1983). Some Experiences with Modified Robertson Test Used for Study of Rapid Crack Propagation in PE Pipelines. *Proceedings of the 8th Plastics Fuel Gas Pipe Symposium*, (pp. 141-146). New Orleans.

Yuan, F.G., J. Lear, P.H. Geil, and S.S. Wang, "Theory and Experiment of Accelerated Testing for Polyethylene Piping Materials," GRI-88/0221, 1988.

"PE LIFESPAN FORECSATING: Plastic Piping Systems, (CD-ROM)," GRI-98/0358, 1998.

"Pipeline Accident Brief: Natural Gas Pipeline Leak, Explosion, and Fire in DuBois, Pennsylvania, August 21, 2004." PAB-06-01

"Pipeline Accident Report: Natural Gas Pipeline Explosion and Fire in South Riding, Virginia, July 7, 1998." PAB 01-01

"Pipeline Accident Report: Natural Gas Pipeline Rupture and Subsequent Explosion, St. Cloud, Minnesota, December 11, 1998." PAB 01-01

List of Acronyms

Acronym	Description
ABS	Acrylonitrile butadiene styrene
ASTM	American Society for Testing and Materials
BDSF	Bi-Directional Shift Functions
CTOD	Crack Tip Opening Displacement
DIMP	Distribution Integrity Management Plan
DOT	Department of Transportation
DSC	Differential Scanning Calorimetry
ED	Dynamic Modulus
FT-IR	Fourier Transform Infrared Spectroscopy
GRI	Gas Research Institute
GTI	Gas Technology Institute
HDB	Hydrostatic Design Basis
HDPE	High Density Polyethylene
HVTT	High Volume Tapping Tee
ID	Inner Diameter
ISO	International Organization for Standardization
LDIW	Low Ductile Inner Wall
LEFM	Linear Elastic Fracture Mechanics
LTHS	Long Term Hydrostatic Stress-Rupture
MDPE	Medium Density Polyethylene
MI	Melt Index
NTSB	National Transportation Safety Board
OD	Outer Diameter
OIT	Oxidative Induction Time
PE	Polyethylene
PENT	Pennsylvania Notch Test
PHMSA	Pipeline and Hazardous Materials Safety Administration
PPI	Plastics Pipe Institute
PVC	Polyvinyl chloride
QB	Quick Burst
RCP	Rapid Crack Propagation
RPM	Rate Process Method
S-4	Small Scale Steady State
SCG	Slow Crack Growth
SDR	Standard Dimension Ratio

END OF REPORT